UNIVERSITY OF LONDON THESIS

Degree phD Year 2007 Name of Author Miliyun CHIU

GALECTIN-3 AND THE DEVELOPMENT OF AUTOSOMAL RECESSIVE POLYCYSTIC KIDNEY DISEASE

by

Miliyun Chiu

A thesis submitted to the University of London in fulfilment of the requirement for the degree of Doctor of Philosophy

November 2006

Nephro-Urology Unit,
Institute of Child Health, UCL, 30 Guilford Street,
London, WC1N 1EH.

ProQuest LLC
789 East Eisenhower Parkway
P.O. Box 1346
Ann Arbor, MI 48106-1346

I, Miliyun Chiu, confirm that the work presented in this thesis is my own. Where information has been derived from other sources, I confirm that this has been indicated in the thesis.

To mum and dad:

Thank you

ABSTRACT

Galectin-3 is a β-galactoside-binding lectin implicated in renal collecting duct development and differentiation. Autosomal recessive polycystic kidney disease (ARPKD) affects 1 in 20,000 humans, and is characterised by cyst development from collecting ducts. Galectin-3 retards cystogenesis in at least 2 *in vitro* models. Hence, I hypothesised that endogenous galectin-3 may reduce cyst formation *in vivo*, and investigated this in the congenital polycystic kidney mouse (*cpk*), a well-characterised ARPKD model. Widespread galectin-3 expression was detected in *cpk* cyst epithelia in a distinct distribution compared to other developmental markers and renal galectins, and also in other cystic mice and human PKD, raising the possibility that galectin-3 may be a common part of a 'cystogenic' pathway.

Next, I investigated whether reduced galectin-3 accelerated cyst formation *in vivo* using *cpk* and *galectin-3* mutants to generate double *cpk/galectin-3* mutants. Initial results on a mixed genetic background demonstrated large variability, but still significantly increased cysts in mice lacking galectin-3. I then backcrossed onto a pure 129Sv background but offspring developed unexpected increased mortality and pancreatic cysts, which confounded this experiment. Hence, we imported different *galectin-3* mutants to reassess on the C57BL/6j background: cyst formation was less rapid than mixed/129Sv, but significantly more cortical cysts were again observed in *galectin-3* null mutants.

I detected galectin-3 in the primary cilium and centrosomes both *in vivo* and *in vitro* in normal and cystic samples for the first time. At least some of the galectin-3 appears on the outside of the cilia and paclitaxel, a therapy that retards PKD in *cpk* mice, caused increased extracellular galectin-3, a location where the lectin might interact with cilia. Preliminary experiments were also performed to investigate ciliary function using atomic force microscopy.

These data raise the possibility that galectin-3 may act as a 'natural' brake on cystogenesis in *cpk* mice, perhaps via ciliary roles.

ACKNOWLEDGEMENTS

Firstly, I would like to show my greatest appreciation to my supervisors, Dr. Paul Winyard and Prof. Adrian Woolf, for offering me this PhD studentship; for their continuous and unconditional support on my study and on my personal development; also to thank them for their dedication, enthusiasm and endless encouragement.

Next, I would like to thank my co-workers: David Gonzalez, Dagan Jenkins, Berk Bergu, David Long, Ambrose Gullett, Kate Hillman, Monica Banerjee, Marie-Klaire Farrugia, Claire Gannon, Leila Romio, Shung-Kai Chan, Simon Welham, Simon Waller, Karen Price, Vinny, Liam McCarthy, Margaret Godley, David Jackson, Stephen Marks, Eugenia Dahm-Vicker, Jolante Pitera, Hai-Tao Yuan, Jazz Dinza and Vanita Shah. You guys had provided me with a lot of help in the lab and a lot of fun in the Lamb.

Also, I would like to thank my collaborators, Dr. Colin Hughes and Suleman Bawumia from the NIMR for providing the galectin-3 protein and antibodies, and their great intellectual input in the project; Prof. Mike Horton and Dr. Belinda Haupt at University College London for helping me out with the atomic force microscope; Kerrie Venner for her help with the electron microscopy work; and Angie Wade for her help with the statistical analysis; and to my collaborator at the University of Alabama at Birmingham in the USA, Prof. Lisa Guay-Woodford, also her group: Kara, Zhihua Yang, Binli Tao, Kassie, Marie-Lou, Michal Mrug, Jigar for looking after me for 6 weeks.

I must also thank Kidney Research UK (previously known as National Kidney Research Fund) for funding my PhD and for organising those great annual meetings; and to University College London and Institute of Child Health for hosting my project.

On a personal note I would like to thank my family and friends for being there. Especially to mum and dad; thank you for providing so much for me and my sisters. I would not have started a PhD without your encouragement and would have found it impossible to finish if it wasn't for your unconditional support. You have inspired me to work hard and to achieve more than I thought I could.

INDEX

LIST OF FIGURES

LIST OF TABLES

ABBREVIATIONS

aa	amino acids
ABC	avidin-biotin peroxidase complex
ADPKD	autosomal dominant polycystic kidney disease
AFM	atomic force microscope
AGEs	advanced glycation end products
AGM	aorta-gonad-mesonephros
aq-2	aquaporin-2
ARPKD	autosomal recessive polycystic kidney disease
BBS	Bardet Biedl Syndrome
BCA	bicinchoninic acid
Bcl-2	B-cell leukaemia/lymphoma 2
BHK	baby-hamster-kidney
bp	base-pair
BSA	bovine serum albumin
cAMP	cyclic adenosine monophosphate
calb	calbindin
cDNA	complementary DNA
CHF	congenital hepatic fibrosis
ci	confidence interval
cpk	*congenital polycystic kidney*
CRD	carbohydrate recognition domain
DAB	diaminobenzidine tetrahydrochloride
DBA	dolichos bifloros agglutinin
DMEM	Dulbecco's modified Eagle's medium
DMSO	dimethyl sulfoxide
DNA	deoxyribonucleic acid
ECL	enhanced chemiluminescence
ECM	extracellular matrix
EDTA	ethylene-diamine tetra-acetic acid
EGF	epidermal growth factor
EM	electron microscopy
ER	endoplasmic reticulum
ESRD	end-stage renal disease
EST	expressed sequence tag
Et Br	ethidium bromide
FCS	fetal calf serum
FITC	fluoroscein isothiocyanate
gal-3	galectin-3
H&E	haematoxylin and eosin
HCl	hydrochloric acid
HGF	hepatocyte growth factor
HRP	horseradish peroxidase
IFT	intraflagellar transport
IGF	insulin-like growth factor
Ig	immunoglobulin
IMCD	inner medullary collecting duct

inv	inversin
ITS	Insulin transferrin selenium
JNK	c-Jun N-terminal kinases
kb	kilobase
kD	kilo Dalton
K/B ratio	kidney/body weight ratio
LacNAc	*N*-acetyllactosamine
LB	Lennox broth
LDL	low density lipoprotein
M	Molar ie. concentration in moles per litre
µg	microgram
µl	microlitre
MLwiN	Multilevel Modelling
MDCK	Madin Darby canine kidney
ml	millilitre
mg	milligram
Mgat5	β1,6 *N*-acetylglucosaminyl-transferase V
M-loop	microtubule loop
MM	mesonephric mesenchyme
MMP	matrix metalloproteinase
mRNA	messenger RNA
NaCL	sodium chloride
NE	nuclear extracts
nl	nanolitre
odf-2	outer dense fibre 2
OFD	oral-facial-digital
ORF	open reading frame
PAGE	polyacrylamide gel electrophoresis
PAS	periodic acid Schiff
PAX	paired box containing genes
PBS	phosphate buffered saline
PC-1	polycystin-1 protein
PC-2	polycystin-2 protein
PCNA	proliferating cell nuclear antigen
PCR	polymerase chain reaction
PFA	paraformaldehyde
PI	propidium iodide
PKD	polcystic kidney disease
PKHD1	*polycystic kidney and hepatic disease 1*
PMSF	phenyl methyl sulfonyl fluoride
PTP	permeability transition pore
RCC	renal cell carcinoma
RNA	ribonucleic acid
RNase	ribonuclease
RNP	ribonucleoprotein
rpm	revolutions per minute
RT-PCR	reverse transcription polymerase chain reaction
SD	standard deviation

SDS	sodium dodecyl sulphate
SE	standard error
T3	triiodothyronine
TAE	tris acetate EDTA electrophoresis buffer
TE	tris EDTA
TEMED	N,N,N',N' tetramethylethylenediamine
TESPA	3-aminopropyl-triethoxysaline
TGF	transforming growth factor
TM	transmembrane
TRIS	trizma base
TRITC	tetramethylrhodamine isothiocyanate
UV	ultra violet
VPV2R	vasopressin V2 receptor
x g	times gravity

OVERVIEW

Galectin-3 is an important molecule which has been implicated in renal development and cyst formation in human ARPKD (Winyard *et al.*, 1997; Bullock *et al.,* 2001). Preliminary evidence from a previous PhD student in my host laboratory (Dr Tanya Johnson) also suggested increased expression in the *cpk* mouse model of ARPKD, and that excess galectin-3 reduced *cpk* cyst formation *in vitro*.

I characterised galectin-3 expression in *cpk* mice, comparing it with other collecting duct markers and renal galectins and also investigated the effects of reduced galectin-3 *in vivo*, by crossing *cpk* mice with *galectin-3* mutant mice. Then I investigated galectin-3 in the primary cilium, and examined whether paclitaxel and galectin-3 might act via common ciliary mechanisms to reduce cyst formation. Finally, I began to investigate cilia using the atomic force microscope.

These studies generated considerable new insights into potential functional roles for galectin-3 in *cpk* mice, and parts of this work are included in a recently accepted paper "Galectin-3 associates with the primary cilium and modulates cyst growth in congenital polycystic kidney disease", to be published in the American Journal of Pathology in December 2006. These findings may also be applicable to other PKD, including human ARPKD, and future studies of this lectin are certainly warranted as galectin-3 must now be considered a potential therapy for this devastating condition.

INTRODUCTION

CHAPTER 1: AUTOSOMAL RECESSIVE POLYCYSTIC KIDNEY DISEASE

Autosomal recessive polycystic kidney disease (ARPKD) is a type of polycystic kidney disease (PKD) that mainly affects children. PKD is a genetic disorder of the kidneys and is characterised by the presence of multiple cysts in both kidneys which results in kidney enlargement and eventually kidney failure (see fig 1.1). ARPKD is distinguishable from other forms of PKDs by its specific mutation of the *PKHD1* gene (Ward *et al.*, 2002; Onuchic *et al.*, 2002), its early onset and the fact that most cysts in ARPKD are derived from the collecting tubules. Human ARPKD kidney histological samples are dominated by collecting duct cysts.

ARPKD affects approximately 1 in 20000 human live births (Zerres *et al.*, 1998). The disease manifests either *in utero* or at birth, though a small percentage of patients begin to develop renal cysts in adolescence or even adulthood. Prenatal diagnoses are made by fetal sonography or by serial monitoring in families with affected members. Affected fetuses characteristically have enlarged kidneys and oligohydramnios (reduced amniotic fluids) due to poor renal output *in utero* (Kemper *et al.*, 2001). As a result of the oligohydramnios, these infants develop the "Potter's sequence" (Potter, 1964), a syndrome consisting of pulmonary hypoplasia, characteristic facial appearance (sidely set eyes, a beaked nose, mild retraction of lower jaw, and large, low-lying ears with incomplete cartilaginous development) and deformaties of the spine and limbs.
Approximately 30% of ARPKD infants die at birth or shortly after that mainly due to malformation of the lungs and suppression of the diaphragm by the massive kidneys (Sharp *et al.*, 2005). However, infants that survive mechanical ventilation have a good chance of survival. For those who survive the first month of life, 92% were alive at 1 year and 87% were alive at 5 years (Guay-

Woodford and Desmond, 2003), but a third of ARPKD patients require dialysis or kidney transplantation by the age of 10.

In the kidney the disease is characterised by cyst growth in the collecting tubules. As much as 90 per cent of collecting tubules in affected neonates are dilated. The disease is often accompanied by congenital hepatic fibrosis (CHF), which is a disease of the liver caused by malformation of the ductal plate during liver development and abnormal portal vein branching. The outcomes of CHF are scarring and blood flow restriction, though liver function tests often remain normal even for symptomatic individuals. Other clinical features of ARPKD are hypertension, which can lead to cardiac hypertrophy and death; hyponatraemia resulting from the inability of patients to dilute their urine; and pyuria.

At the moment there are no effective therapeutic drugs against renal cystogensis. Treatment is based on dialysis and kidney transplantation.

Figure 1.1. Kidneys from ARPKD patients.

The kidneys are grossly enlarged and are filled with dilated tubules and cysts, A) a cross-section of the kidney. B) A histological section of the kidney shows the radially oriented, fusiform cysts that are characteristic of ARPKD. (Figure adapted from Coffman 2002).

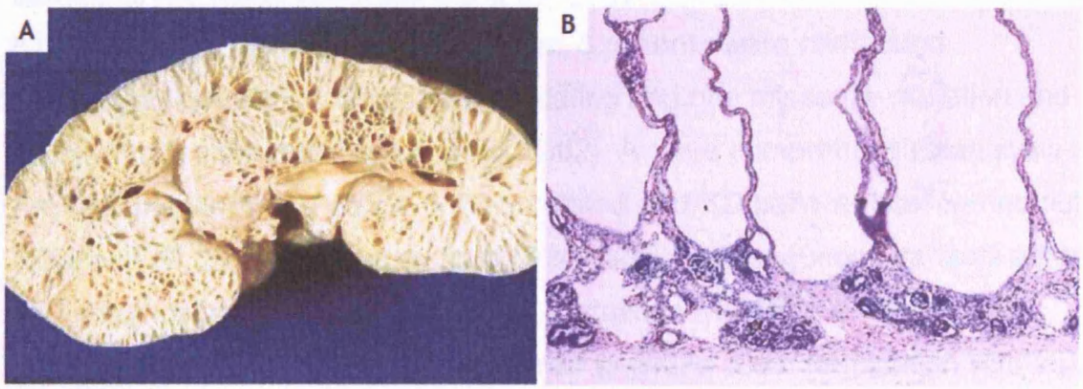

PKHD1 gene and its encoded protein

The gene mutated in ARPKD was initially identified and characterised by two different research groups using two different methods: a conventional positioning cloning approach and a comparative genomic approach (Ward *et al.*, 2002; Onuchic *et al.*, 2002). Both determined a mutation of a gene *PKHD1* (Polycystic Kidney and Hepatic Disease 1) at a single locus on chromosome 6p21.1-p12. *PKHD1* consists of at least 86 exons with a longest continuous open reading frame (ORF) of 67 exons, spanning ~472kb of genomic DNA. It encodes for a large protein called polyductin or fibrocystin.

For this thesis, the protein is referred to as fibrocystin. The protein is predicted to contain 4074 amino acids with an unglycosylated molecular weight of 447 kD. To date the best reported mutation detection rate of this gene associated with ARPKD is 82.7% (Sharp *et al.*, 2005), in an ethnically diverse population with a wide range of ARPKD associated phenotypes. The mutation detection rate is not an absolute reflection of the presence of a mutation in *PKHD1*, as it is a very large gene; the gene structure and its splice variants are not yet completely characterised. No other genes have been found to cause ARPKD, perhaps suggesting that *PKHD1* is the only gene that when mutated causes ARPKD.

Mutations are found scattered along the gene. Analysis of 14 families revealed 6 truncating and 13 missense mutations; 8 patients were compound heterozygotes in which 6 had one truncating and one missense mutation and 2 had two missense mutations (Harris, 2002). A more comprehensive analysis of *PKHD1* mutations in a cohort of 75 unrelated ARPKD patients was carried out (Sharp *et al.*, 2005). The study found 124 pathogenic sequence variants among 150 chromosomes, in other words 124 mutations were found. Among the putative mutant alleles, 22 were predicted to cause chain termination with 16 frameshift variants (deletions, insertions and duplications) and 6 nonsense mutations. Out of 56 patients analysed, homozygous mutations were detected in 12 patients and the remaining patients were compound heterozygotes. The wide range of mutations in different locations of the gene may explain the

variety of clinical presentation of ARPKD patients. A study on the genotype/phenotype correlations of these 56 patients suggested that neither the location nor the type of amino acid substitution correlates with disease severity. The finding disagrees with another report that milder presentation of ARPKD correlates with the presence of amino acid substitution mutations (Furu *et al.*, 2003). Clearly, more work has to be carried out to find out if there are any correlations between the types of mutation and the phenotype of the disease. Success in finding such correlations would aid the diagnosis of ARPKD patients.

Predicted structure of fibrocystin

Fibrocystin is predicted to have a single transmembrane domain (TM) near the carboxyl terminus. The protein contains several TIG/IPT domains, Ig-like fold shared by plexins and transcription factors near its carboxyl terminal; and Parallel β-Helix 1 (PbH1) repeats which can bind carbohydrates in its amino terminus (Ward *et al.*, 2002; Onuchic *et al.*, 2002), see figure 1.2. In addition there are 64 potential N-glycosylation sites and 2 potential phosphorylation sites can be found in the carboxyl terminus (Sweeney, Jr. and Avner, 2006). Northern blot analysis of *PKHD1* transcripts detects a smear of products, which may represent multiple splice forms (Ward *et al.*, 2002). Several splice variants are predicted to encode truncated products that lack the TM domain and may be secreted. Fibrocystin is a novel protein that share structural features with hepatocyte growth factor receptor and plexins, which are involved in the regulation of cellular adhesion and repulsion as well as cell proliferation (Guay-Woodford, 2002; Harris, 2002).

Figure 1.2. Predicted structure of fibrocystin.

Fibrocytsin consists of a large extracelluar portion that contains various different domains (signal peptide, TIG, TIG-like, TMEM homology). At the C-terminal, which is also the cytoplasm portion of the protein, there are four potential phosphorylation sites. Adapted from (Hogan *et al.*, 2003).

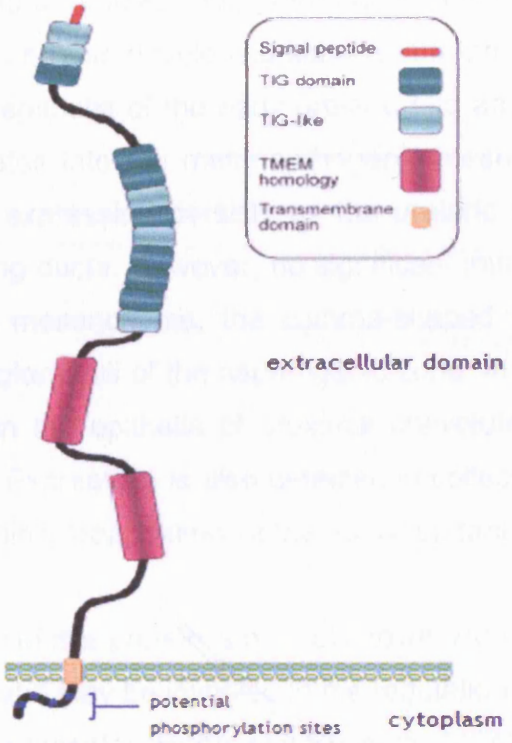

Expression of fibrocystin

Commercially acquired human adult and human fetal multiple-tissue northern blots analysis reveals that *PKHD1* is expressed in adult kidney and pancreas, with a lower level in liver. Moderate expression in fetal kidney is also detected (Onuchic *et al.*, 2002). RT-PCR analysis in mouse found that the gene is most strongly expressed in new born and adult kidney, with lower levels in liver, pancreas and lung, and no expression in brain, spleen, colon, thymus, heart and skeletal muscle (Ward *et al.*, 2002). *In situ* hybridisation studies of *Pkhd1* on mouse tissues shows a high level of expression in renal and biliary tubular structures at all time points between E12.5 to 3 month postnatal (Nagasawa *et al.*, 2002). The gene expression pattern is consistent with the ARPKD

phenotype, with the highest expression in renal collecting ducts, as well as in the ductal plate and bile ducts in the liver.

During embryogenesis, the gene is widely expressed in epithelial derivatives, including neural tubules, gut, pulmonary bronchi, and hepatic cells (Zhang *et al.*, 2004). In mouse developing kidneys, the protein is expressed at the apical surfaces of epithelia of the early ureteric bud and mesonephric tubules, as the bud penetrates into the metaneprhogenic mesenchyme (Zhang *et al.*, 2004). This apical expression persists as the ureteric buds branch and differentiate into collecting ducts. However, no significant immunostaining is detected in the condensing mesenchyme, the comma-shaped body, the S shaped body or developing glomeruli of the nephrogenic zone. In adult kidney, PKHD1 is widely expressed in the epithelia of proximal convoluted tubules with a cytoplasmic distribution. Expression is also detected in collecting ducts and thick ascending limbs of Henle's loop, mainly at the apical surface (Zhang *et al.*, 2004).

The function of this protein is not yet known. However, sequence analysis suggests that it may be involved in the regulation of cell adhesion or it may function as a receptor (Harris and Rossetti, 2004).

PKHD1 homolog

A *PKHD1* homolog, *PKHDL1* has been identified by Hogan *et al.,* 2003. The gene is in chromosome region 8q23 through analysis of human genomic sequence. *PKHDL1* contains 78 exons, covering a genomic region of 168kb; its transcript of 13081bp encodes for a large protein called fibrocystin-L. No mutation of this gene is found in ARPKD patients with no *PKHD1* mutations, suggesting that *PKHDL1* is not associated with ARPKD. Similar to fibrocystin, fibrocystin-L is predicted to be a large receptor protein (4243aa, 466kDa) with a signal peptide, a single transmembrane domain and a short cytoplasmic tail. The two proteins share an overall identity of 25.0% and similarity of 41.5%. RT-PCR studies reveal that *PKHDL1* is widely expressed in most tissues with the

most prominent expression is found in blood-derived cell-lines. Low level expression is detected in many primary immune cell subtypes but up-regulated specifically in activated T lymphocytes, suggesting a role in cellular immunity (Hogan *et al.*, 2003).

Other forms of polycystic kidney disease

Autosomal dominant PKD has a much higher incidence, 1:800 to 1000 (Nauli and Zhou, 2004; Wilson, 2004a), arguably being the most common genetic disease. Although it is somewhat similar to the recessive form of PKD, as both are characterised by cyst growth in kidneys, there are clear differences between them. ADPKD usually occurs later in life, at the fourth decade. Affected patients have cysts developed and dilated tubules at any point along the nephron and rapidly close off from the nephron of origin. In contrast, in ARPKD, initially the proximal tubules are dilated and later cysts arise from the collecting tubules, which remain connected to the nephron of orgin (Wilson, 1995). Due to the high frequency of human ADPKD, studies into kidney cystic diseases have most often been carried out in the ADPKD models. This gives important information into the mechanisms of cysts growth which in turn, if there is common mechanisms, and also enhances our potential understanding of the development of ARPKD.

Cystic kidneys are also common in other genetic diseases such as Nephronophthisis, Oral-facial-digital syndrome type I, Bardet Biedel syndrome and Fraser syndrome (Otto *et al.*, 2003; Ansley *et al.*, 2003; Romio *et al.*, 2003). Although they are classified as different diseases, there are many similarities in terms of the pathophysiology of renal epithelial cells which lead to cyst formation.

The following section describes the pathophysiologies that are common to all forms of PKD.

Pathophysiology of PKDs

The exact disease mechanism that results in cyst growth in the kidney is yet to be resolved. However, several common features are present in cystic kidneys.

Abnormal proliferation and apoptosis

Many investigators have found a significant increase in proliferation rate in renal cystic epithelia (Grantham, 1993; Nadasdy *et al.*, 1995; Ostrom *et al.*, 2000). Using immunohistochemistry to detect the presence of proliferating cell nuclear antigen, PCNA, a marker for cells undergoing proliferation, Nadasdy et al (Nadasdy *et al.*, 1995; Nadasdy *et al.*, 1998) calculated the proliferative index (PI – percentage of PCNA positive cell nuclei) among epithelial cells lining the renal tubule or cysts of developing kidney tubules, normal kidney tubules, and cystic epithelia of human ADPKD and ARPKD. They found that in normal developing kidneys, the PI decreases as the kidney matures and in adult kidneys, there are less than 0.5% of proliferating epithelial cells per tubule. However compared with that of developing kidneys which is between 5.9% and 12.4% in cystic kidneys, the PI value is significantly higher compared with normal (PI= 2.58% in ADPKD and 10.5% in ARPKD). This phenomenon occurs particularly in ARPKD where the level of proliferating cells is comparable to that of developing kidneys (Nadasdy *et al.*, 1995; Nadasdy *et al.*, 1998).

Increased levels of apoptosis are also common in cystic kidneys, both in the cystic epithelia and in the surrounding tissues (Woo, 1995; Winyard *et al.*, 1996; Ostrom *et al.*, 2000). The latter may contribute to cyst growth by allowing cysts to expand. The importance of apoptosis in cystogenesis is highlighted in the knockout experiments where *Bcl-2* (B-cell leukaemia/lymphoma 2) was inactivated (Veis *et al.*, 1993). Bcl-2 protects cells from apoptosis by modulating the permeability of the mitochondrial membrane. It induces the release of cytochrome c which then activates caspase-9 and caspase-3, leading to apoptosis (Gross *et al.,* 1999). During early kidney development, the protein is highly expressed in the ureteric bud and metanephric mesenchyme and the

level gradually declines to low levels as the kidney matures. It is thought that tight regulation of apoptosis, hence *Bcl-2* expression, is essential for normal kidney development (Novack and Korsmeyer, 1994). Mice lacking functional Bcl-2 develop polycystic kidney disease (Nakayama *et al.*, 1994). In the polycystic kidneys there is widespread apoptosis in the interstitium around undilated tubules distant from cysts, in undilated tubules between cysts and in cystic epithelia (Winyard *et al.*, 1996). Another study on caspase activity in the Han:Sprague-Dawley-cy (Han:SPRD-cy) rat, a phenotypic ADPKD model, shows an increase in caspase activity and apoptosis in affected rats. Moreover, treatment with the caspase inhibitor IDN-8050 significantly reduces tubular apoptosis and proliferation and slows disease progression in this animal model (Tao *et al.*, 2005). These studies emphasise the importance of the regulation of apoptosis in renal cytogenesis.

Polarity and fluid secretion

Polarity of epithelial cells refers to the specific localisation of characterised proteins at the cell surface. Common epithelial cells differentiate in a uniform way which produces a defined protein composition in each surface domain of the cells: apical and basolateral surfaces. The two domains are separated by tight junctions, which act as semi-permeable seals around the cells. During epithelial cell differentiation, microtubules align along the apico-basal polarity axis of the cell (Musch, 2004). In renal epithelial cells, microtubules create asymmetry by orienting their minus-ends toward the apical domain and their plus-ends towards the basal surfaces.

Maturation of murine nephrons relies on intense proliferation during postnatal development which drives the lengthening of tubules (Fischer *et al.,* 2006). The direction of cell growth is goverened by planar cell polarisation. In normal mouse kidneys, the mitotic spindle alignment is parallel with the tubule axis; whereas the alignment is distorted in *HNF1β*-deficient mice and in *pck* rats, both develop renal cysts. The mitotic angles in these mutant animals are between 30° and 90° to the tubular axis (Fischer *et al.,* 2006). Defective planar

cell polarisation in these animals leads to cell growth in the wrong direction, resulting in dilation of tubules instead of elongation.

The specific ends of the microtubules aid the transport of vesicles to their destined surface domains (Musch, 2004). These vesicles contain specific proteins that dock and fuse with either the apical or the basolateral domains. The distribution of enzymes, ion transporters, channels, pores, growth factors and matrix receptors are tightly regulated. In renal cystic epithelia, some of these proteins are mis-located to the opposite domain. In cystic epithelial cells, epidermal growth factor receptor (EGFR), Na^+/K^+-ATPase are expressed in the apical cell membrane instead of their normal location at the basolateral site (Sweeney and Avner, 1998; Avner *et al.,* 1992). Aquaporin 2 which is normally expressed at the apical site is found to be mis-localised to the basolateral site in cystic epithelial cells of 3 weeks old cystic *cpk* mice. At this stage the kidneys are mostly composed of collecting duct cysts (Gattone *et al.*, 1999). In contrast, studies of human ADPKD uninephrectomy samples showed that both aquaporin 2 and 3 are expressed in the correct domain even in cystic epithelia, but only two samples were examined (Hayashi *et al.*, 1997).

Importantly, the mislocalisation of Na^+/K^+-ATPase and aquaporin-2 may partly be responsible for the fluid accumulation in renal cysts (Avner *et al.*, 1992; Rohatgi *et al.*, 2003). Fluid reabsorption in the normal kidney is controlled by sodium ion gradients established by Na^+/K^+-ATPase in the basolateral domain and the presence of aquaporin-2 at the apical site and aquaporin-3 at the basolateral sites which allow water to permeate through the cell from the luminal to the basolateral compartments. Compared with control age-matched collecting tubules, ARPKD cells absorb Na^+ at a rate approximately 50% greater. The expression of aquaporin-2 is upregulated and partially mislocated in cystic kidneys (Gattone *et al.*, 1999; Rohatgi *et al.*, 2003). This may result in a reversal of fluid transport.

Adhesion

In cystic kidneys, the abnormal expression of adhesion molecules and altered extracellular matrix (ECM) biology leads to atypical cell-matrix interactions, thickened basement membranes, alterations in matrix composition and abnormal numbers of integrin receptors are frequent in PKD (Joly *et al.,* 2003; van Adelsberg, 1994; Nakamura *et al.,* 2000). ECM structure is altered by increased activity of fibroblasts (Murcia *et al.*, 1999) and matrix metalloproteinases (MMPs) (Obermuller *et al.*, 2001). Fibroblasts from cystic kidneys exhibit increased proliferation *in vitro* and increase ECM deposition *in vivo*, which may participate in the formation of abnormal cystic tubular microenvironment. MMPs are responsible for ECM degradation, and their expression in *cpk* kidneys is upregulated, which contributes to the restructuring of the tubular basement membrane (Rankin *et al.*, 1996).

Studies on PC-1 reveal that the protein is expressed on several different sites in renal cells including the cell-cell junctions and at focal adhesions (Huan and van Adelsberg, 1999). PC-1 colocalises with cell adhesion molecules E-cadherin and catenin, it coprecipates with these proteins and comigrates with them on sucrose density gradients. Hence, PC-1 is part of a complex with these adhesion molecules (Huan and van Adelsberg, 1999). Furthermore, PC-1 colocalised with $\alpha 2\beta 1$-intergrin in focal clusters in adherent renal epithelia (Wilson *et al.,*1999). These findings suggest that PC-1 may function as a modulator in cell adhesion. The composition of PC-1/E-cadherin/catenin complexes can be modulated by Ca^{2+} (Geng *et al.,* 2000). High calcium treatment of human renal collecting tubules cells increases PC-1-E-cadherin interactions.

Bcl-2 null mice, which develop polycystic kidneys, have abnormal intergrin subunits expression in tubular epithelial cells, with an increased level of $\alpha 3$-, $\alpha 5$- and $\alpha 6$-integrin in cystic kidneys as well as a slight decrease in $\beta 1$-integrin compared with their wild-type counterparts (Ziehr et al 04). PC-1 contains cysteine-flanked leucine-rich repeats (LRR), which interact with a number of

ECM components including fibronectin, laminin and collagen I (Malhas *et al.*, 2002). All these point towards the importance in regulating adhesion in kidney epithelial cells, which when disrupted may cause cystogenesis.

Defective primary cilia

Primary cilia are cellular organelles expressed singly in most vertebrate cells except bone marrow-derived cells and the intercalated cells of the kidney collecting duct (Praetorius *et al.*, 2004). Ciliary dysfunction is associated with the development of PKD (Ong and Wheatley, 2003; Pazour, 2004; Praetorius and Spring, 2005). Many proteins mutated in PKD are expressed in the primary cilia, either in the shaft of the cilia or at the basal body. Examples of such proteins in human are PC-1, PC-2, fibrocystin, OFD, nephrocystin, Bardet-Biedl syndrome proteins; and in mouse are inversin, polaris, cystin, bicaudal C (Yoder *et al.*, 2002a; Guay-Woodford, 2003; Ward *et al.*, 2003; Otto *et al.*, 2003; Ansley *et al.*, 2003; Romio *et al.*, 2004; Wolf *et al.*, 2005). Several studies have shown that structural or functional defects in primary cilium result in development of tubular cysts (Calvet, 2003; Lin *et al.*, 2003; Ong and Wheatley, 2003; Nauli and Zhou, 2004). Detailed description of this organelle can be found in Chapter 2.

Molecular mechanisms of PKD protein

Fibrocystin

To date, not much is known about the cellular functions of fibrocystin, the protein mutated in ARPKD. Fibrocystin was identified just before this project began. It belongs to a new class of protein therefore not much is known about its possible role in cells. It is implicated in tubulogenesis of IMCD cells (Mai *et al.,* 2005). Yeast two-hybrid system identifies that intracellular C-terminus of fibrocystin interacts with calcium modulating cyclophilin ligand, a protein involved in Ca^{2+} signalling (Nagano *et al.,* 2005).

More investigations have been done on polycystin-1 (PC-1, *Pkd1*) and polycystin-2 (PC-2, *Pkd2*).

Polycystin-1 and polycystin-2

PC-1 is a large protein of 4302 amino acids; it contains 11 transmembrane domains, a short cytoplasmic tail and a large extracellular region (Hughes *et al.*, 1995). The extracellular part of the protein has homology to many recognised domains which are usually involved in protein-protein or protein-carbohydrate interactions. The large portion of the protein is a homolog to a group of sea-urchin proteins that are involved in sperm-egg interactions (Moy *et al.,* 1996). The overall structure of PC-1 suggests that it is involved in cell-cell and/or cell-matrix interactions. The large extracellular region comprises a unique combination of potential adhesion and protein-protein interaction domains. The amino-terminus of PC-1 contains a leucine-rich repeat, a low-density-lipoprotein-A domain, a Receptor-for-Egg-Jelly domain and a calcium-dependent lectin domain (Hughes *et al.*, 1995). The carboxy-terminus of PC-1 contains several phosphorylation sites and a putative coiled-coil domain which interacts with the carboxy-terminus of PC-2 (Qian *et al.*, 1997). Its features suggest that PC-1 is a large, multifunctional protein that is involved in carbohydrate motif recognition, ligand binding and Ca^{2+} regulation. PC-1 also interacts with a variety of other proteins, such as G proteins. The interaction with G protein may activate $G_{i/o}$-type proteins. This interaction is antagonised by PC-2 binding, indicating that the two proteins may compete for binding position (Delmas *et al.*, 2002).

PC-2 is an ion channel of 968 amino acids. It is predicted to have cytoplasmic N- and C- termini and 6 transmembrane domains with a homology to voltage-activated calcium and sodium channels (Mochizuki *et al.*, 1996). The transmembrane region is homologous to PC-1 and also to voltage activated and transient receptor potential channel subunits. There are strong suggestions from various studies that PC-2 is a calcium channel and that its action may partly be triggered by its interaction with PC-1 (Hanaoka *et al.,* 2000).

PC-1 and PC-2 have been shown to assemble at the plasma membrane to regulate Ca^{2+} entry (Hanaoka *et al.*, 2000). It appears that PC-1 and PC-2 act together to regulate intracellular levels of calcium, where PC-1 acts as a receptor by binding to extracellular ligands which then in turn triggers the action of PC-2 (Harris, 2002; Nauli *et al.*, 2003). One of the expression sites of these two proteins is on the primary cilia. Calcium influx is triggered by the bending of this organelle, a process that requires the functions of both PC-1 and PC-2 (Nauli *et al.*, 2003); see chapter 2.

The functions of PC-1 and PC-2 do not completely depend on each other. Immunohistochemistry shows that PC-1 and PC-2 are expressed in different locations in the kidneys and in different sub-cellular location (Foggensteiner *et al.,* 2000). PC-1 is found highly expressed in human fetal kidney tissue in developing glomeruli, epithelia of ureter-derived structures and the comma and S-shaped bodies (Geng *et al.,* 1996; Ward *et al.,* 1996; Foggensteiner *et al.,* 2000). Whereas PC-2 is expressed in the primitive tubules later in gestation at week 30 compared to week 17 for PC-1 expression. PC-2 is not found in the comma and S-shaped bodies (Foggensteiner *et al.,* 2000). In human adult kidney, colocolisation of the two proteins is only found in a subset of cortical tubules. PC-1 is more widely expressed than PC-2. PC-1 can be found in the Bowman's capsules, proximal tubules and the collecting tubules. Whereas PC-2 is expressed in the medullary thick ascending limbs of the loop of Henle and cortical distal tubules where PC-1 is also expressed (Geng *et al.,* 1996; Foggensteiner *et al.,* 2000). Subcellularly, PC-2 is mainly expressed in the basolateral domain whereas PC-1 is predominantly found in the lateral location of the basolateral domain, overlapping with E-cadherin (Foggensteiner *et al.,* 2000). The differences in localisation of the two proteins suggest that they can function independently of each other.

Calcium and PKD

Studies into the function of primary cilia suggest that calcium influx is impaired in PKD cells at least *in vitro*. Defects in either PC-1 or PC-2 in renal epithelial cells disrupt intracellular Ca^{2+} homeostasis or Ca^{2+} signalling leading to cyst growth (Murcia *et al.*, 1998; Gonzalez-Perrett *et al.*, 2001; Nauli and Zhou, 2004).

Primary culture of ARPKD cystic cells have a reduced intercellular Ca^{2+} level (Yamaguchi *et al.*, 2006), indicating that fibrocystin may also be involved in regulating calcium concentration. All these point toward the importance of Ca^{2+} homeostasis in the initiation and/or the progression of cyst growth. But how does calcium level affect cyst growth in PKD epithelial cells but not in normal cells? The most convincing evidence came from studies on cAMP.

cAMP

Adenosine-3',5'-cyclic monophosphate, commonly known as cAMP or cyclic AMP, is important in many biological processes. It is a second messenger used for intracellular signal transduction, for example transferring the effects of hormones such as glycagon and adrenaline, which cannot pass through the cell membrane. Its main purpose is the activation of protein kinases, though it is also used to regulate the passage of Ca^{2+} through ion channels. The concentration of cAMP depends on the rate of synthesis from ATP by adenylate cyclase and its rate of breakdown to cAMP by a specific phosphodiesterase, see figure 1.3 below.

Figure 1.3. Synthesis and breakdown of cAMP.

cAMP is found to stimulate both fluid secretion and proliferation of cyst epithelial cells (Belibi *et al.*, 2004; Yamaguchi *et al.*, 2004). *In vitro* studies show that cAMP accelerates proliferation of PKD cells by stimulating the B-Raf/MEK/ERK pathway (Yamaguchi *et al.*, 2006). In contrast, cAMP inhibits proliferation of normal human kidney (NHK) cells (Yamaguchi *et al.*, 2006). One physiological difference between PKD cells and NHK cells is that the former (cells derived from either ADPKD or ARPKD) have a lower intracellular level of Ca^{2+} (Yamaguchi *et al.*, 2006). Experimentally impairing Ca^{2+} concentration in NHK cells, using Ca^{2+} entry blockers, transformed the cells to take up the phenotype of PKD cells. These cells then respond to cAMP by stimulating proliferation, in the same way as PKD cells (Yamaguchi *et al.*, 2004). Additionally, when Ca^{2+} levels are restored in PKD cells, the mitogenic response to cAMP is completely reversed (Yamaguchi *et al.*, 2006). Thus, the response of epithelial cells to cAMP can be modulated by intracellular Ca^{2+} concentration.

Animal models for the study of ARPKD – *cpk* mouse

Animal models are employed to study the development of PKD, these include genotypic animals (*pck* rat – *Pkhd1* gene in human; *pkd1* and *pkd2* mice – genotypic animals to the same genes, genetically engineered animals; *inv* mouse, genotypic model of Nephronophthisis type II), phenotypic animals (*cpk*, *bpk*, *jck, orpk* mice) and chemically induced renal cystic disease using glucocorticoids.

Cpk (congenital polycystic kidney) mice were used in these studies. This model arises from a spontaneous mutation on the C57BL/6j background (Russell and McFarland, 1977). It is a good model for the study, although it is not a genotypic model, it exhibits very similar kidney pathology to the human ARPKD. In addition, it is genetically and phenotypically well characterised and can be easily genotyped by polymerase chain reaction; its rapid progression to end stage renal failure allows researchers to progress quickly. Dilated tubules first

appear at approximately embryonic day 16 and are localised primarily in the proximal tubules. Cyst growth gradually changes to be derived predominantly from the collecting ducts. Affected animals usually reach end stage renal failure and death by 3 to 4 weeks of age. At this stage, the kidneys are massively enlarged, and can be seen distending at the back of the animal (Guay-Woodford, 2003). Histological examination shows that kidneys of 3 weeks old *cpk* mice were mostly filled with collecting duct cysts.

The *cpk* mouse does not exhibit liver lesions at least not on the C57BL/6j background. The study carried out in this thesis concentrated on kidney cystogenesis, therefore the lack of phenotype in the liver did not affect this study.

The *cpk* gene

The *cpk* locus maps to mouse chromosome 12 (Guay-Woodford, 2003); the human orthologue is located to chromosome 2p25.1 (Fliegauf *et al.*, 2003). Although mutations in *cpk* mice causes severe cystic kidney disease, no *cpk* mutations have been detected in human using mutation analysis of eight families affected by humans cystic kidney disease through autosomal recessive transmission (Fliegauf *et al.*, 2003). However, one can argue that analysis of only 8 families was not an extensive study given that we know there are many different mutations that cause mouse PKD. Protein sequence comparison of the human cystin (CYS1, 158 aa) and murine cystin (Cys1 145 aa) shows 57% identity and 64% similarity.

The mouse *cpk* gene is encoded by 5 exons spanning 14.4 kb of genomic DNA. The ATG start codon sits in exon I. The 435bp open reading frame extends into exon III; exon IV and V are untranslated. A putative cryptic splice site (gaacagCTG) within exon V appears to account for the 1,856bp and 1,786bp splice variants (Hou *et al.*, 2002). An atypical polyadenylation signal (ATTAAA) lies 22 nucleotides upstream of the poly-A tail. In *cpk* mice, PCR

amplification and direct sequence analysis identified tandem 12bp and 19bp deletions in exon 1 of the *cpk* gene. The resulting frameshift truncates the predicted protein leading to a nonsense mutation of the protein, see figure 1.4 for a schematic view of the mutant gene (Hou *et al.*, 2002).

Characterisation of *cpk* mutations allowed accurate genotyping of each sample using specific primers that flanks the two tandem deletions (see fig 1.4). Polymerase Chain Reaction (PCR) is used to amplify the DNA fragment flanked by the primers and the genotype is determined by the size of the fragment: the mutant allele produces a smaller fragment - 320bp, whereas the wildtype allele gives a fragment of 351bp. Heterozygotes, which do not develop cystic kidneys, would have one of each allele.

Figure 1.4. The organisation of *cpk* gene.

The five exons of *cpk* are shown at the top of the figure as boxes with roman numbers below them. Untranslated regions are in white, translated regions in black and the grey box represents the splice variant due to the cryptic splice site (gaacagCTG) within exon V. *cpk* mutation is caused by the two deletion (12bp and 19bp, in red) within exon I, just after the start codon (ATG, highlighted in red). The primers used for genotyping are shown as blue arrows. They sit within exon 1 and flank the two deletions. (Adapted from Hou et al 2002).

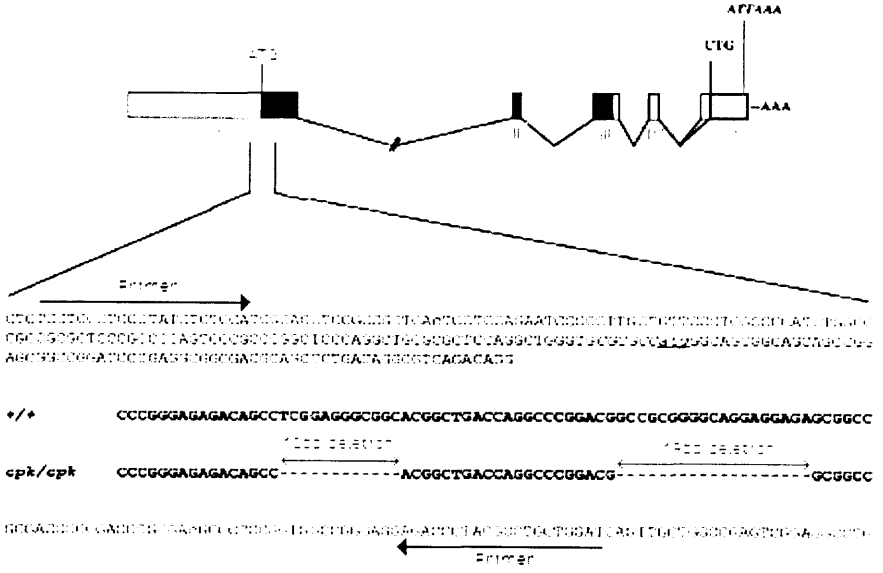

Characterisation of *cpk* encoded protein, cystin

The *cpk* gene encodes a novel, hydrophilic protein, named cystin. Motif searches have identified two potential myristoylation sites (AA 2-7 and AA 43-48), the former is coupled to a polybasic domain (AA 12-16). A potential PEST – polypeptide enriched in proline (P), glutamic acid (E), serine (S), and threonine (T) – sequence is predicted at position 101-118 (Hou *et al.*, 2002). Other identified domains include a cAMP phosphorylation site, several putative phosphorylation sites and a possible tyrosine sulfation site. There are no predicted N-glycosylation sites. The highly conserved middle portion of the protein and the C-terminal end do not share any predictable protein motifs. There is no evidence for specific DNA-binding motifs, but the protein is proline rich (10%) and is predicted to have at least two potential nuclear localisation signals (Hou *et al.*, 2002; Fliegauf *et al.*, 2003).

Protein expression studies of human fetal tissue using western immuno-blot analysis indicates that cystin is expressed in the kidney, but not in the liver, brain and lung. This result is consistent with the finding in mouse, where high cystin expression is detected in the kidney but not in the liver, brain and lung (Hou *et al.*, 2002). Pancreatic expression of human cystin is also reported (Fliegauf *et al.*, 2003). Subcellular localisation of cystin as analysed in mouse collecting duct cells shows that the protein is mainly expressed in the primary cilia, both at the basal body and the ciliary axoneme. In addition, the protein is found in the lipid raft compartment, after physical fractionation of kidney cells on a sucrose density gradient (Prof. Guay-Woodford, personal communication). The molecular function and biological processes of the protein are currently being investigated.

The N-terminal myristoylation site plays an important role in membrane targeting of the protein such as Rous sarcoma oncogene (c-SRC) and proto-ocogene protein c-Ki-*ras,* and its polybasic domain suggests that the cystin is associated with the plasma membrane and/or membranes of intracellular organelles (Hou *et al.*, 2002; Resh, 2004). More importantly, mutation analysis

of the myristoylation site in cystin retards the transport of cystin to the membrane (Yang *et al.,* 2004). It is unknown how the protein is transported and anchored to the membrane but it may involve the lipid raft.

CHAPTER 2: PRIMARY CILIA ASSOCIATION WITH PKD

During my PhD study, an organelle called the primary cilium became the centre of attention for much research into PKD.
Primary cilia are cellular organelles expressed singly in most vertebrate cells except bone marrow-derived cells and the intercalated cells of the kidney collecting duct (Praetorius and Spring, 2005). Ciliary dysfunction is associated with the development of PKD (Ong and Wheatley, 2003; Pazour, 2004; Praetorius and Spring, 2005). Many proteins mutated in PKD are expressed in the primary cilia (Table 2.1 and Fig 2.1). Several studies have shown that structural or functional defects in the primary cilium results in development of tubular cysts (Lin *et al.*, 2003; Ong and Wheatley, 2003; Nauli *et al.*, 2003).

What is the primary cilium?

The primary cilium has a 9 + 0 axoneme, which refers to its nine peripherally located doublet microtubules and the absence of the central microtubule pair seen in motile cilia or 9 + 2 cilia (Praetorius and Spring, 2005).

The primary cilium is formed in many G1/G0 cells in culture and *in vivo.* It is often reabsorbed very late in the cell cycle as cells enter prophase prior to cell division (Wheatley *et al.*, 1996). In proliferating cells, the cilium appears several hours after mitosis; in fibroblasts, it takes 2 to 4 hours after cell division for the cilium to be fully formed and in pig kidney epithelial cells, the cilium is only found during S phase (Alieva and Vorobjev, 2004).

The primary cilium is derived from the mother centriole, also known as the mature centriole (see fig 2.1). During cell differentiation, the centrosome migrates to the plasma membrane. The mother centriole is then attached to the plasma membranes at its distal end, a process which involves the appendages of the mother centriole (Ishikawa *et al.*, 2005). The centrosome sits at the bottom of the cilium forming the basal body. Not all cultured cells develop

primary cilia, those where the mature centrioles had no satellites and appendages (e.g. Chinese Hamster kidney cells) never develop the organelle even in the fully differentiated state (Alieva and Vorabjew 2004). This finding is further supported by investigations into the function of a protein called outer dense fibre 2 (Odf2, also known as cenexin). Odf2 is a scaffold protein that is specifically localised at the distal/subdistal appendages of mother centrioles and not in the daughter centrioles because the latter do not have the appendages. *In vitro* studies reveal that mutant cells with no functional Odf2 lose their centriolar appendages. Although these cells are able to undertake the normal cell cycle, they have lost the ability to develop primary cilia. The loss of primary cilia in *Odf2* $^{-/-}$ cells can be rescued by exogenous Odf2 administration. Odf deficiency appears to affect the docking of centrioles to membranes, which may explain the lack of primary cilia (Ishikawa *et al.*, 2005).

The close relationship between the cilium and the centrosome leads to speculation that the cilium acts as a regulator of cell cycle (Quarmby and Parker, 2005). Though some cell lines that have gone through many passages do not express primary cilia, but they do divide, therefore primary cilia do not govern cell division completely. However one can argue that in their absence, the regulation of division rate may be disturbed (Wheatley *et al.*, 1996).

Table 2.1. Human PKD diseases and murine models of PKD and the expression of mutated proteins in renal cilia.

Below are a list of diseases that result in polycystic kidney disease in human and a list of murine models of PKD. Most of the proteins are expressed on the renal cilia.

Human PKD	**Protein mutated**	**Ciliary expression (Shaft or basal body)**
ADPKD	PC-1	Yes, shaft
ADPKD	PC-2	Yes, shaft
ARPKD	Fibrocystin	Yes, shaft
*Nephronophthisis	Nephrocystin	Yes, shaft
*Bardet-Biedl syndrome	BBS1-11	Yes, not all BBS proteins are identified to be located in the primary cilia, but the majority are found in the basal body.
Oral-Facial-Digital syndrome	OFD1	Yes, basal body
Fraser syndrome	FRAS-1, FREM-1, FREM-2	Not yet determined.
Tuberose Sclerosis	Tuberin	Not yet determined.
Von Hippel-Lindau	VHL	Not yet determined. However, the expression of VHL correlates to ciliogenesis (Lutz and Burk, 2006).
Murine models	**Protein mutated**	**Ciliary expression (Shaft or basal body)**
Cpk	Cystin	Yes, Shaft
Bpk	Bicaudal C	Yes, not stated
Orpk	Polaris	Yes, Shaft
Inv	Inversin	Yes, Shaft
Jck	Nek-8	Yes, Shaft
Kat	Nek-1	Yes, Shaft
Pcy	NPHP3**	Not yet determined
Han:SPRD-cy	SamCystin	Not yet determined
Pck	Fibrocystin	Yes, Shaft
BCL-2 null	BCL-2	Not yet determined
Congenital cystic kidney disease and diabetes	Hepatocyte nuclear factor -1 beta (HNF-1β)	Not yet determined, although human homologue of the mouse HNF-3 is expressed in the cilia.

* Ciliary disfunction disorders (Fliegauf *et al.,* 2006; Yen *et al.,* 2006; Badano *et al.,* 2006). ** Not confirmed (Olbrich *et al.,* 2003).

Figure 2.1. Diagrammatic illustration of selected PKD proteins express in the primary cilium.

Various PKD associated proteins are depicted, all of which when mutated lead to the development of kidney cysts. Ciliary microtubules (long grey bar inside the cilium) are derived from the mother centriole, which sits at the bottom of the cilia as basal bodies. Kinesin-2 and dynein1B are motors that run along the ciliary axoneme in the direction shown. These motors are responsible for transporting intraflagellar transport (IFT) proteins up and down the cilia in order to assemble and maintain the cilium.

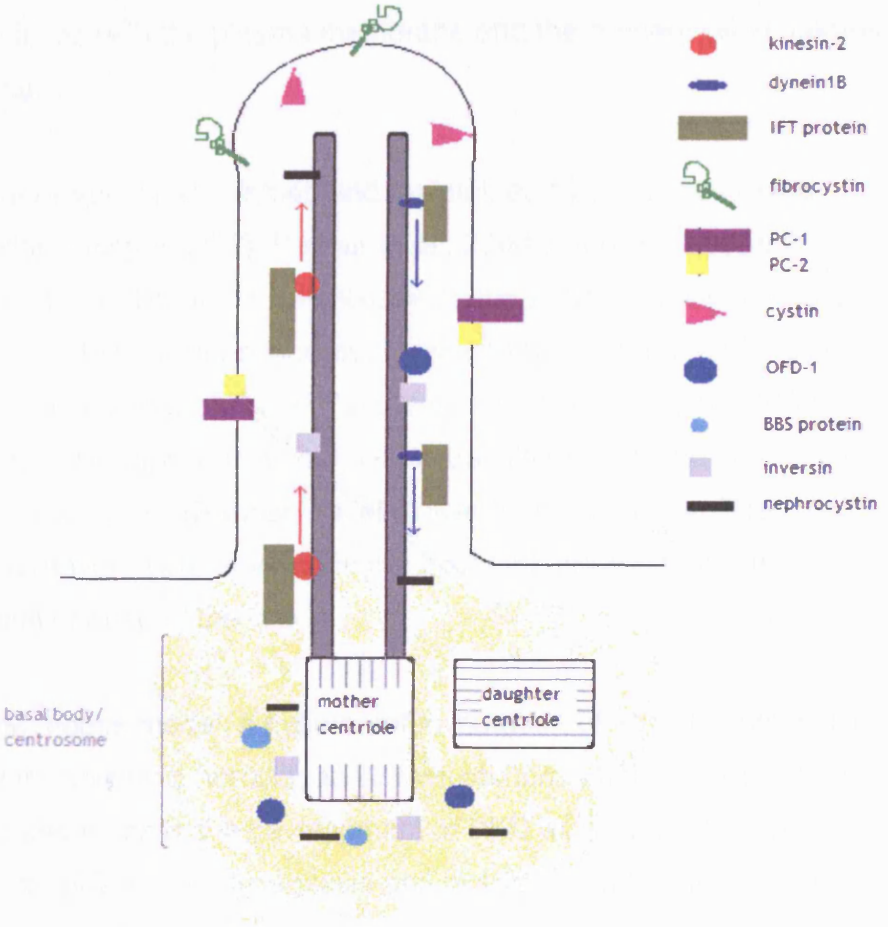

The formation of primary cilia

The formation of the primary cilium has been observed in cultured cells using serial sectioning at different time points (Alieva and Vorobjev, 2004). At the end of mitosis, the centrosome migrates to near the apical surface of epithelial cells, which then engages with the membrane. The triplet microtubules from the distal end of the mother-centriole then extend to form the doublet microtubules of the primary cilium. The next step is the elongation of the axoneme that requires growth of the membrane vesicle. Later on the membrane vesicles surrounding axoneme fuses with the plasma membrane and the primary cilium comes to the cell surface.

The primary cilium is assembled and maintained by a process called intraflagellar transport (IFT) (Pazour *et al.,* 2000; Lin *et al.,* 2003). IFT is a bi-directional movement of non-membrane bound proteins along the doublet microtubules of the ciliary axoneme, between the axoneme and the plasma membrane. The movement of IFT proteins is carried out by two different motors, the anterograde kinesin-2, which travels towards the tip of the cilia; and the retrograde dynein1B which travels towards the cell body. There is a constant turnover of proteins within the axoneme, therefore the IFT is important for the maintenance of the cilia.

In the *orpk* mouse model, a hypomorphic mutation of an IFT protein, *Tg737* (encodes for polaris, a homolog to *Chlamydomonas* IFT88) blocks ciliary assembly and leads to the development of PKD as well as other organ defects such as liver biliary duct hyperplasia and dysplasia and pancreatic cysts; all three organs contain duct lined with ciliated epithelium. Work on IFT proteins in other organisms (*Chlamydomonas, Caenorhabditis, Tetrahymena,* sea urchins) all shows that disruption of the expression of IFT proteins: IFT172, kinesin-2 or dynein1B, block ciliary assembly (Pazour, 2004). Mutations in the IFT88 and IFT172 leads to phenotypic changes similar to those when hedgehog signalling

is defective, suggesting that IFT88 and IFT172 are part of the signalling pathway (Huangfu *et al.*, 2003).

Structural or functional defects in the renal cilium lead to PKD

Studies have shown that structural defects of the primary cilium are associated with the development of cyst in kidneys. Inhibition of renal ciliogenesis leads to the development of cysts in kidneys (Lin *et al.*, 2003; Yoder *et al.,* 2002b). Tissue-specific inactivation of KIF3A, a subunit of kinesin-II that is essential for cilia formation, in renal tubular epithelial cells results in viable offspring with normal-appearing kidneys at birth, but with renal cysts appearing at postnatal day 5 and renal failure by postnatal day 21 (Lin *et al.*, 2003).

The earliest observed phenotype in *orpk* mutant embryos is the loss of cilia expression on ventral node cells leading to malformation of neural tubes (Murcia *et al.* 2000). Other phenotypes include polydactyly (containing more than the normal number of digits on the hands and/or feet), hydrocephalus (an accumulation of cerebrospinal fluid in the ventricles of the brain), abnomalities in the photoreceptor rod cell outer segment and retinal degeneration, hypogonadism (smaller than normal testis), male sterility and left-right asymmetry defects (Murcia *et al.*, 2000; Taulman *et al.*, 2001; Yoder *et al.,* 2002b; Zang *et al.,* 2003). Motile cilia in the trachea appear normal when examined under transmission or scanning electron microscopy in these mutant mice. *In vivo* analysis of renal ciliary structure showed the majority of cystic cells in *orpk* mice either lack the expression of primary cilium or express a shortened cilium (Pazour *et al.*, 2000; Brown and Murcia, 2003).

Functional defects of the primary cilium are linked to cystogenesis. Many proteins responsible for causing PKD when mutated are expressed on the primary cilium; PC-1, PC-2, fibrocystin, OFD, nephrocystin, BBS and cystin. They may act as channels or receptors on the cilium and that defects in ciliary signalling pathway are important to the cause of the disease.

Bending of the primary cilium leads to calcium influx

Cytoplasmic calcium concentration modulates various cellular functions, such as gene expression, metabolism, proliferation, secretion, neural excitation and fertilisation (Gomes *et al.*, 2006). It is certain that calcium influx is important to the primary cilia in regulating the normal functions of the kidney epithelial cell and how it leads to cystogenesis. Recent work has shown that disruption of calcium influx plays a big role in the development of renal cysts.

Several studies reveal that the cilium is involved in the initiation of calcium influx in response to fluid flow (Praetorius and Spring, 2001; Nauli *et al.*, 2003; Shiba *et al.*, 2005; Liu *et al.*, 2005). *In vitro* experiments using Madine Darby Canine Kidney cells, MDCK, show that primary cilia develop in confluent monolayer culture. Experiments by Praetorius and Spring (2001) showed that by physically bending the cilium, either by suction with a micropipette or by increasing the flow rate of perfusate, causes an increase in intracellular calcium concentration. They further demonstrate that the calcium increase in one cell can spread to adjacent cells by diffusion of a second messenger through gap junctions. Removal of extracellular calcium after the initial response does not significantly alter the magnitude or time course of the increase and spread to adjacent cells. This shows that the widespread calcium influx is caused by the release from intracellular storage of the ion (Praetorius and Spring, 2001). This study suggests that at least in MDCK cells, the primary cilium is mechanically sensitive and responds to flow by greatly increasing intracellular calcium, although it does not address the mechanism behind the initial calcium influx nor suggest how ciliary dysfunction results in cyst formation.

Further studies on the mechanosensation in the cilium have been carried out in cell lines with disruption in the functions of PC-1 and PC-2. Using these *in vitro* models, Nauli et al (2003) assessed the function of PC-1 and PC-2 in response to fluid flow in mouse embryonic kidney epithelial cells. Wild-type cells respond

to fluid shear stimulation with an increase in intracellular calcium throughout the cell population. Compared to experiments in MDCK cells (Praetorius and Spring, 2001), these embryonic kidney epithelial cells give the same calcium influx response but quicker. Cells with mutations in PC-1 do not activate flow-induced Ca^{2+} signalling. Various antibodies directed against extracellular domains of PC-1 and PC-2 block the calcium influx response of wild-type cells to flow stimulation. In addition, using medium depleted of Ca^{2+}, Nauli et al proved that Ca^{2+} entry is required to initiate flow-induced Ca^{2+} signalling and that PC-1 and PC-2 play an important role in initiating Ca^{2+} entry through the primary cilia, presumably through the PC-2, which is an ion channel (Nauli *et al.*, 2003). Furthermore, isolated renal tubules in *Tg737* mutants, which express a reduced number and size of primary cilia, display blunted increases in intracellular Ca^{2+} concentration in response to fluid stress compared to normal tubules (Liu *et al.*, 2005).

By contrast, *inv* (encodes for inversin, which is found at the base of primary cilia) mutant epithelial cells respond to fluid flow by inducing Ca^{2+} influx at the same rate compared to normal cells. *inv* mutant mice also produce cystic kidneys (Shiba *et al.*, 2005). This suggests that not all PKD mutations disrupt Ca^{2+} influx in response to flow. Experiments in zebrafish show that Inversin is involved in the Wnt-β-caterin signalling pathway (Simons *et al.* 2005). It acts as a molecular switch between different Wnt signalling cascades by inhibiting the canonical Wnt pathway by targeting cytoplasmic dishevelled for degradation (Simons *et al.* 2005). It is unclear whether the functions of inversin take place in the primary cilium but further experiments in zebrafish link primary cilia to Wnt signalling (Oishi *et al.,* 2006). Knockdown of dub in zebrafish enbryos results in defects in primary cilia. The function of dub is regulated by phosphorylation, which in turn depends on Frizzled-2-mediated non-canonical Wnt signalling.

PC-1 has a number of large extracellular putative binding domains that may act as mechanosensors. If that is the case, these domains must be rigid enough to withstand the physiological force of bending. Hence, the domains must be able

to resist unfolding when placed under mechanical forces. Atomic force microscopy (AFM) can be used to measure the mechanical properties of proteins. It has been used to assess the stability of PC-1 under mechanical stress. The experiment concluded that the first four extracellular domains of PC-1 were exceptionally stable, similar to that of immunoglobulin domains in the giant muscle protein titin. The results suggest that these domains in PC-1 will remain folded under external force (Forman *et al.*, 2005), supporting the hypothesis that PC-1 in the primary cilia acts as a mechanosensor and transfers the physical force to a signal that induces calcium entry through the opening of PC-2.

Nodal cilia

Loss of left-right axis determination (or *situs inversus*) are found in several forms of cystic diseases and animal models, e.g. *inv* mutant, *Tg737* (*orpk*) mutant and *pkd2* mutant (Pennekamp *et al.*, 2002; Morgan *et al.*, 2002; Brown and Murcia, 2003); as well as in human PKD: Bardet-Biedl syndrome, Nephronophthisis type 2 (Otto *et al.*, 2003; Ansley *et al.*, 2003). The association between PKD and defects in left-right determination prompted studies on the nodal cilium, which is structurally very similar to the renal primary cilium. Nodal cilium is a motile form of the 9 + 0 cilium. It does not beat from side to side as does the 9 + 2 cilium, but exhibits a characteristic twirling movement that generates the nodal flow which is crucial for the development of left-right symmetry in the developing embryo (Nonaka *et al.*, 1998). Mutation in *KIF3B* disrupts the formation of nodal cilia; mutation in *inv* leads to a weaker twirling movement of the nodal cilia thus insufficient nodal flow; or mutation in *Pkd2*, all result in defects in left-right axis determination (Nonaka *et al.*, 1998; Okada *et al.*, 1999; Pennekamp *et al.*, 2002). These findings support the link between PKD and *situs inversus* through the functions of cilia.

CHAPTER 3: THE GALECTIN FAMILY

Galectins are involved in many important biological functions: such as cancer, immunity, and organogenesis. With regard to this study, several galectins (-1, -3 and -9) are implicated in kidney development. Studies of galectin-3 in renal cyst development were initiated by work on kidney collecting ducts cells, MDCK. Addition of exogenous galectin-3 suppresses the growth of MDCK cysts in 3D collagen culture, an *in vitro* cytogenesis model (Bao and Hughes, 1995). Galectin-3 is expressed during human nephrogenesis and childhood cystic diseases (Winyard *et al.*, 1997). Details of galectin-3 and its role in cystogenesis can be found in chapters 4 and 5. In this chapter, brief summaries of all mammalian galectins are described.

The galectin family is part of a super-family of proteins called lectins. By definition, lectins are protein or glycoprotein substances of non-immunoglobulin nature, capable of specific recognition of and reversible binding to carbohydrate moieties of complex glycoconjugates, without altering the covalent structure of any of the recognised glycosyl ligands. Some antibodies and enzymes also bind to carbohydrates, however they are not considered to be lectins.

Specific interactions between carbohydrate moieties and lectins play a critical role in various developmental, physiological, and pathological processes. Mammalian lectins are classified into five major categories: C-type lectins, I-type lectins, P-type lectins (mannose-binding lectins), pentraxins, and galectins (also called S-Type lectins); see figure 3.1 for summary. They are classified based on their saccharide-specificity and consensus sequence.

Table 3.1. Summary of the five types of lectin.

The five different types of lectin each with different defining features in protein sequence, calcium dependency and their specific carbohydrate recognition.

Lectin groups	Defining features in protein sequence	Calcium dependence	Carbohydrate recognition
C-type	Consensus sequence in CRD*	Yes (most)	Variable
I-type	Immunoglobulin-like domains	No	Sialic Acids
P-type	Unique repeating motif	Variable	Mannose-6-Phosphate
Pentraxins	Multimeric binding motifs	Yes (most)	Variable
Galectins	Consensus sequence in CRD* and binding affinity to β–Galactosides	No	β-Galactosides

* CRD = carbohydrate-recognition domain

Characteristics of galectins

The galectin family was formally identified in 1994. It was initially defined by their calcium independent binding affinity for β-Galactosides and by conserved sequence elements in the carbohydrate recognition domain, CRD (Barondes *et al.*, 1994). The sequence of each CRD has been shown to be mainly encoded by 3 exons. Most of the conserved residues are found in the sequence encoded by the middle one of these three exons. This sequence includes four adjacent β-strands and intervening loops in the structure. All residues that interact directly with a carbohydrate ligand are conserved among galectins. The importance of some of these residues for carbohydrate binding activity is supported by site-directed mutagenesis (Barondes *et al.*, 1994).

Another shared feature between the galectins is that although they are found in the cytoplasm and in the extracellular domain, none of them have a known

secretion signal peptide. Hughes and his colleagues have shown however that some galectins can be secreted through a novel mechanism in transfected baby hamster kidney (BHK) cells overexpressing galectin-3; immunofluorescence visualisation showed galectin-3 positive vesicles blebbing from the cell surface (Hughes, 1999). This suggests that the proteins may be secreted through a non-classical vesicle based mechanism.

To date, there are 15 mammalian galectins, named numerically from galectin-1 to -15. Galectins are also found in many non-mammalian species including birds, amphibians, insects, worms, sponges, fungi and possibly in plants and viruses (Cooper and Barondes, 1999; Gray *et al.*, 2004; Chiariotti *et al.*, 2004).

Galectins are classified into three groups, based on the content and organisation of the domains. The majority of galectins belong to the prototype, group containing galectin-1, -2, -5, -7, -10, -11, -13, -14, -15 and three of the 6 isoforms of galectin-8. These galectins contain only one CRD and their molecular weights are approximately 14kDa. The second group is the tandem repeat galectins, which includes galectin-4, -6, -8, -9 and –12. They contain two CRDs within a single polypeptide chain, with molecular weight of around 36kDa. The third group is the chimera galectin; there is only one galectin in this group: galectin-3. It contains one CRD, a N-terminal domain and an intervening proline-, glycine- and tyrosine-rich repeating domain of roughly 100 residues. The latter domain varies between species in the number of repeats; 8 in human, 11 in rat and 14 in dog, giving rise to various sizes of galectin-3 from 29kDa in murine to 30.3kDa in dog (Herrmann *et al.*, 1993; Bidon-Wagner and Le Pennec, 2004).

Galectins and kidney

Galectin-1, -2, -3, -7, -8, -9 and the two avian galectins has been found to be expressed in the kidneys (Hadari *et al.,* 1995; Saussez *et al.,* 2006; Stierstorfer *et al.,* 2000; Wada *et al.,* 1997; Wasano *et al.,* 1990; Winyard *et al.,* 1997).

Although their expression pattern during nephrogenesis and in mature kidneys vary from each other. The most studied galectins in the kidneys are galectin-1, galectin-3 and galectin-9, perhaps due to their strict regulation during development.

Galectin-1 is most widely expressed in mesodermally-derived cells during mouse embryogenesis, including the kidney (Poirier *et al.,* 1992). In the kidney, these cells form the mesodermal mesenchyme which gives rise to the non-tubular epithelia. As the kidney develops, the expression of galectin-1 is down-regulated (Wasno *et al.,* 1990).

The expression of galectin-3 in the kidney is also developmentally regulated. It is most widely expressed in the derivative of the ureteric bud in human (Winyard *et al.,* 1997) and in mouse (Bullock *et al.,* 2001). Similar to galectin-1, the expression of galectin-3 is developmentaly regulated and it is down-regulated in adult kidney although expression can be found in the collecting tubules (Winyard *et al.,* 1997; Hikita *et al.,* 1999). A detailed description of the role of galectin-3 in the kidney can be found later in Chapter 5.

In the kidney, galectin-9 functions as a sugar-regulated urate channel/transporter (Lipkowitz *et al.*, 2004), expressed mainly in the apical domain of proximal tubules and in collecting tubules of the cortex, with a lower level of expression in the medulla. In mice, galectin-9 expression is developmentally regulated. It is expressed at a low level beginning at E12, increased through embryonic development and postnatally, and reaches high and constant levels in the adult kidney (Hughes, 2004).

Galectin-2 mRNA is expressed in adult rat kidneys, although its expression is at least 6 times lower than in stomach and intestine. Galectin-7 is found in hamster kidney. It is expressed in the Bowman's capsule, perivascular tissue around arcuate artery and vein and extracellular matrix of the outer and inner stripes of the outer medulla (Saussez *et al.*, 2006). Galectin-8 mRNA is found in

adult rat kidney (Hadari *et al.,* 1995). The expression of galectin-2, -7 and -8 has only been reported in mature kidneys, therefore it is unknown whether their expressions in the kidney is developmentally regulated.

Expression studies of the two galectins in chicken kidneys have been carried out using histochemical analysis and electron microscopy. The two avian galectins, CG-14 and CG-16, are expressed in the epithelial cells of the mesonephric proximal tubules and of the metanephric collecting ducts. In addition, CG-16 is detected in early glomerular podocytes. CG-14 exhibits a diffuse cytoplasmic expression whereas CG-16 is mainly observed in mitochondria (Stierstorfer *et al.*, 2000).

Individual summary of each galectin

In this section, the expression and known functions of all 15 mammalian galectins are described as well as two avian galectins. A detailed description of galectin-3 can be found in chapter 4.

The following table gives a summary of the expression sites of all mammalian galectins as well as the two avian galectins.

Table 3.2. Summary of expression sites of all known mammalian and avian galectins.

Galectins are widely expressed in many different part of the body. Some members are expressed in the same organ, and some even in the same cell type; hence, overlapping expression of two different galectins is possible.

Galectin	Structural type	Major expression site
1	Prototype	Smooth muscle, skeletal muscle, nerves tissues and kidneys
2	Prototype	Epithelial cells of gastrointestinal tract (also a low level in kidneys)
3	Chimera	Notochord; developing bone, skin and kidney; macrophages
4	Tandem repeat	Epithelial cells of gastrointestinal tract
5	Prototype	Erythrocytes
6	Tandem repeat	Epithelial cells of gastrointestinal tract
7	Prototype	Skin and mature kidney
8	Prototype/ Tandem repeat	Highly expressed in lung and to lesser extend in liver, kidney, spleen, hind-limb and cardiac muscle
9	Tandem repeat	Kidney; also detected in liver, heart, brain and lung
10	Prototype	Eosinophilic and basophilic leukocytes
11	Prototype	Ovine stomach
12	Tandem repeat	Adipose tissue
13	Prototype	Placenta
14	Prototype	Eosinophils
15	Prototype	Ovine uterus
CG-14	Prototype	Avian galectin. Intestine, also found in kidney
CG-16	Prototype	Avian galectin. Liver, also found in kidney

Galectin-1

There may be at least 3 variants of galectin-1 in human tissues. It is found abundantly in smooth muscle, skeletal muscle, and the nervous tissues and less abundantly in many other tissues including the kidneys. This galectin is synthesized on free ribosomes. Amino acid sequence analysis reveals that the N-terminal of this polypeptide is acetylated. Both these pieces of evidence suggest that galectin-1 is a cytosolic protein. Indeed, immunofluorescence staining shows that the galectin-1 is found predominantly in the cytoplasm, with a diffuse distribution (Liu *et al.*, 2002). Nuclear localisation was not found in mouse C2 myoblasts and in Chinese hamster ovary cells. However, immunofluorescence of cryostat sections of adult chicken kidney and calf pancreas show that galectin-1 is located in both nuclei and cytoplasm (Liu *et al.*, 2002). The functions of galectin-1 include modulation of cell-matrix interactions and in regulating apoptosis (Horiguchi *et al.*, 2003). Both galectin-1 and galectin-3 are found in the nuclear extracts (NE), which is capable of carrying out pre-mRNA splicing. NE depleted of these two galectins concomitantly lose their splicing activity, suggesting that these galectins function as redundant splicing factors in the nucleus (Patterson *et al.*, 2004).

Galectin-2

Human galectin-2 was first isolated in HepG2 hepatoma cells (Gitt *et al.*, 1992). Studies of galectin-2 using Northern and Western blot analysis in various rat tissues indicate that this galectin is highly expressed in the stomach and intestine. A significantly reduced expression is found in the kidney, less than 1/6 of that of stomach (Oka *et al.*, 1999). RT-PCR/immunohistochemistry examination of human tissue revealed that this galectin is expressed in most epithelial cells of various organs, with overlapping expression with galectin-1 and -7 in certain organs. Expression is observed in cytoplasm and nucleus (Saal *et al.*, 2005). *In vitro* studies found that galectin-2 can induce apoptosis in activated T-cells (Sturm *et al.*, 2004).

Galectin-3

Galectin-3 is one of the most extensively studied galectins. The expression pattern of galectin-3 has been examined in the developing mouse embryo by *in situ* hybridisation and immunohistochemistry. The lectin is first detected in notochord and later found in developing bone and skin in mouse embryo (Fowlis *et al.*, 1995). In adults, it is normally expressed in activated macrophages and gut epithelia and the epithelial cells of the collecting ducts in kidneys. Their functions include the regulation of cell-matrix interaction, proliferation, pre-mRNA splicing and inflammation. It is also implicated in the development of several cancers. A complete review of galectin-3 will be given in Chapter 4.

Galectin-4

Galectin-4 expression has been examined using *in situ* hybridisation. In both mouse embryos and adults, the expression of galectin-4 is found only in the epithelial cells of the gastrointestinal tract. The lectin is expressed at about equal levels in colon and small intestine but much less in stomach (Gitt *et al.*, 1998). Galectin-4 is very closely related to galectin-6, which exhibits a very similar expression pattern.

Studies on lipid rafts (glycosphingolipid/ cholesterol-enriched membrane microdomains) in intestinal epithelia reveal galectin-4 to be enriched in these compartments of the cell membrane. Lipid rafts are commonly defined as membrane complexes insoluble in non-ionic detergents. They are rich in glycospingolipids, which contain a high degree of acyl chains that raise the melting temperature of the lipid, resulting in a more stablised and ordered lipid phase (Brown and London, 1998). Their discoveries have changed the perception of the role of membrane lipids, which have been promoted from a passive barrier function to molecular players of equal importance to proteins. There are several types of lipid rafts, identified by their solubility in different detergents at variable temperature. Their functions include signal transduction,

pathogen invasion, drug targeting and cholesterol transport (Danielsen and Hansen, 2003).

Galectin-4 is the most prominent protein in a type of intestinal microvillar rafts called superafts. It appears that galectin-4 acts as a stabiliser/organiser for other more loosely raft-associated proteins. Its affinity towards β-galactosyl residues and its ability to form lattices results in a "gluing" effect which keeps the glycolipids and glycoproteins in place (Braccia *et al.*, 2003). One suggested function of galectin-4 is to salvage the digestive enzymes at the brush border that would otherwise have been lost to the gut lumen by the proteolytic/ lipolytic actions of the pancreatic secretions during the digestive process (Danielsen and van Deurs, 1997; Danielsen and Hansen, 2003).

Galectin-5

Galectin-5 was first isolated in extracts of rat tissues. Further analysis revealed that the galectin was localised in the erythrocytes, and the cDNA sequence has been isolated from a rat reticulocyte cDNA library. Galectin-5 is a weak agglutinin of rat erythrocytes in comparison with galectin-1 and -3 (Gitt *et al.*, 1995). This galectin is also reported in the bone marrow (Lensch *et al.*, 2006).

Galectin-6

Galectin-6 was isolated while studying mouse colon mRNA for galectin-4. Compared with galectin-4, galectin-6 lacks the 24-amino acid stretch in the link region between the two CRDs. Otherwise, these two galectins have 83% amino acid identity. The expression of galectin-6 is very similar to that of galectin-4: both of them are confined to the epithelial cells of the embryonic and adult gastrointestinal tract. Unlike galectin-4, which has a reduced expressed in stomach, galectin-6 is expressed at about equal levels throughout the gastrointestinal tract. The two genes are clustered on proximal mouse chromosome 7, the syntenic human region is 19q13.1-13.3 (Gitt *et al.*, 1998).

Galectin-7

Galectin-7 is a keratinocyte protein. It is excreted in the medium by differentiated keratinocytes although it does not contain a known secretion peptide signal. Localisation studies using mouse tissue reveal that galectin-7 is mostly expressed in skin (both fetal and adult) and can also be detected in oesophagus, stomach, anus and tongue (Sato *et al.*, 2002). The production of this galectin coincides with the degree of stratification of the epithelia (Timmons *et al.*, 1999). In fact, galectin-7 is reported to be a marker of all types of stratified epithelia (Magnaldo *et al.*, 1998).

The suggested functions of galectin-7 include regulation of cell-cell and/or cell-matrix interactions, regulation of apoptosis and corneal epithelial cell migration in response to damage. Galectin-7 is remarkably down regulated in SV40 transformed K14 keratinocytes that are anchorage independent and unable to differentiate. These cells lack strong adhesion to the surrounding cells, they attach and detach with ease from other cells as they move. This evidence together with the localisation of galectin-7 in areas of cell-to-cell contact, suggests that galectin-7 may be involved in the regulation of cell-cell interaction (Madsen *et al.*, 1995). Studies on transfectants of HeLa and DLD-1 cells found that cells ectopically expressing galectin-7 are more susceptible to apoptosis than control transfectants. Further analyses demonstrate that galectin-7 functions intracellularly upstream of c-Jun N-terminal kinases activation and mitochondrial cytochrome c release (Kuwabara *et al.*, 2002). *In vivo* assessment of the role of galectin-7 in re-epithelialisation of corneal wounds reveals that expression of its mRNA and protein is markedly up-regulated in the corneal epithelium after injury. *In vitro* studies show that exogenous galectin-7 stimulates re-epithelialisation of corneal wounds (Cao *et al.*, 2003). Assessment of hamster adult kidneys using immunohistochemistry shows that galectin-7 is expressed in the Bowman's capsule and in perivascular tissue surrounding the arcuate artery and vein (Saussez *et al.*, 2006).

Galectin-8

Galectin-8 was first cloned from a rat liver cDNA expression library. Northern blot analysis using mRNA extracted from rat tissues reveals that galectin-8 is widely expressed. It is highly expressed in lung; and in lower level in liver, kidney, cardiac muscle, hind-limb and brain. There are six isoforms of galectin-8; three of which contains 2 CRDs, whereas the other three contain only 1 CRD (Hadari *et al.*, 1995). Adhesion studies of different cell types cultured in serum-free medium on immobilised galectin-8 suggest that it is a physiological modulator of cell adhesion. At maximum dosage, the galectin is equipotent to fibronectin in promoting cell adhesion and spreading. Truncation of one of the CRDs abolishes its ability to modulate cell adhesion; therefore, both CRDs are essential for the adhesion property of galectin-8. In constrast, excess soluble galectin-8 (like fibronectin) forms a complex with integrins that negatively regulate cell adhesion (Levy *et al.*, 2001). Various studies show that galectin-8 is widely expressed in tumour tissues. Its level of expression may correlate with the malignancy of human colon cancer and the degree of differentiation of lung sequamous cell carcinomas and neuro-endocrine tumours (Bidon-Wagner and Le Pennec, 2004).

Galectin-9

The biological functions and expression of galectin-9 have been investigated in embryonic, newborn and adult mice tissues. Northern blot analyses illustrate that this galectin is widely distributed and its expression is developmentally regulated. The transcript is seen in various fetal tissues (i.e. heart, brain, lung, liver and kidney) and its expression increases with successive stages of embryonic development extending into the postnatal period. In adult tissue, the transcript is highly expressed in thymus, small intestine and liver, and to a lesser extent in lung, kidney, spleen, cardiac and skeletal muscle. Galectin-9 induces apoptosis in T cell lines and thymocytes but not hepatocytes (Wada *et al.*, 1997; Kashio *et al.*, 2003). The galectin may induce apoptosis via the Ca(2+)-calpain-caspase-1 pathway at least in CD4(+) and CD8(+) T cells and it

may play a role in immunomodulation of T cell-mediated immune responses (Kashio *et al.*, 2003).

In situ hybridisation has been performed on sections of adult kidney. Galectin-9 mRNA expression is seen in glomerular and tubular cells of the renal cortex, whereas its expression in the renal medullary tubules is low (Wada *et al.*, 1997). Galectin-9 is a urate channel/ transporter and it plays an important role in renal and gastrointestinal urate excretion (Leal-Pinto *et al.,* 1997). Glucose significantly increases the opening of the urate channel but only when it is added to the extracellular face, suggesting a role for extracellular glucose in regulating the channel activity (Leal-Pinto *et al.,* 2002).

Galectin-10

Galectin-10, also known as Charcot-Leyden crystal protein, is expressed uniquely in eosinopilic and basophilic leukocytes (Dyer and Rosenberg, 2001). A study carried out an assessment of the expression of various galectins in myeloid cell differentiation. It demonstrates that galectin-10 mRNA expression is increased during eosinophilic and neutrophilic differentiation. It has been proposed that the changes in galectin-10 expression together with changes in galectin-3 and -9 expression are important in myeloid cell differentiation into specific lineages (Abedin *et al.*, 2003).

Galectin-11

Galectin-11 was isolated in sheep stomach tissue infected with the nematode parasite, *Haemonchus contortus* (Dunphy *et al.*, 2000). The mRNA is greatly up-regulated in helminth larval infected gastrointestinal tissue subject to inflammation and eosinophil infiltration. Immunohistochemistry reveals that the protein is expressed in the cytoplasm and nucleus of upper epithelial cells of the gastrointestinal tract. The protein is also detected in mucus samples collected from abomasum of infected sheep; the abomasum is the fourth and last stomach that is most similar to the monogastric stomach. These results

imply that galectin-11 may be involved in gastrointestinal immune/inflammatory responses (Dunphy *et al.*, 2000).

Galectin-12

Galectin-12 was identified separately by two different groups simultaneously (Hotta *et al.*, 2001; Yang *et al.*, 2001). The first group isolated the galectin from EST clones from a G1 phase Jurkat T-cells V cDNA. Cell cycle synchronisation of Jurkat cells revealed that galectin-12 is up-regulated in cells synchronised at the G(1) phase or the G(1)/S boundary of the cell cycle. Ectopic expression of galectin-12 in cancer cells causes cell cycle arrest at the G(1) phase and cell growth suppression. These results suggest that galectin-12 is a novel regulator of cellular homeostasis (Yang *et al.*, 2001).

Another group successfully identified galectin-12 in a human adipose tissue cDNA library. Galectin-12 mRNA is predominantly expressed in adipose tissue of human and mouse and in differentiated 3T3-L1 adipocytes. Immunocytochemistry revealed a nuclear localisation of the galectin in adipocytes. Like some other galectins, galectin-12 is present in the cytoplasm in a dotted pattern. Ultracentrifugation-fractionation studies demonstrate that this galectin is detected in the nuclear and mitochondrial fraction but not in the cytosolic fraction (Hotta *et al.*, 2001). Immunoblot analysis fails to show the presence of the protein in the culture media of 3T3-L1 adipocytes therefore this galectin may not be secreted. Transfection with galectin-12 cDNA induces apoptosis of cos-1 cells, suggesting that galectin-12 may participate in the regulation of the cell cycle, possibly by inducing apoptosis (Hotta *et al.*, 2001).

Lastly, studies on the involvement of galectin-12 in the development of insulin resistance using 3T3-L1 cells illustrate that the galectin is down-regulated by various insulin resistance-inducing hormones. Thus suggests a role of galectin-12 in the pathogenesis of insulin resistance (Fasshauer *et al.*, 2002).

Galectin-13

Galectin-13 was first isolated from human placental tissue (Bohn *et al.*, 1983) Almost two decades later, this protein was demonstrated in human fetal tissue, predominantly expressed in placenta. cos-7 cells transfected with the cDNA of galectin-13 sequester the protein in nuclei (Yang *et al.*, 2002). Using affinity chromatography, PAGE, MALDI-TOF mass spectrometry and post source decay, annexin II and β/γ actin have been identified as proteins specifically bound to galectin-13 in the placenta and fetal hepatic cells. Immunocytochemistry of syncytiotrophoblasts, outer layer of trophoblasts that actively invade the uterine wall, reveals galectin-13 expression in the perinuclear and in the membrane of brush border, which implies the secretion of the protein to the outer cell surface, possibly by ectocytosis in microvesicles containing actin and annexin II (Than *et al.*, 2004).

Galectin-14

Galectin-14 was first cloned from ovine eosinophil-rich leukocytes. It is most closely related to galectin-9, a potent eosinophil chemoattractant. Northern blot and western blot analyses indicate that galectin-14 is mostly expressed in eosinophil and not in other leukocytes. Flow cytometry and cytospot staining demonstrate that the protein localises to the cytoplasm of eosinophils. Western blot analysis of bronchoalveolar lavage fluid reveals that upon challenge with house dust mite allergen, galectin-14 is released from eosinophils into the lumen of the lungs. Galectin-14 may play an important role in eosinophil function and allergic inflammation (Dunphy *et al.*, 2002).

Galectin-15

Galectin-15 is a 14kDa lectin that contains a separate putative integrin binding domain. It is found in sheep uterus (Gray *et al.*, 2005) and has been proposed to function extracellularly to mediate implantation of blastocysts and intracellularly to regulate trophectoderm (the outer cell layer of the blastocyst). In addition the galectin is found in gastrointestinal tissue and secreted into the

intestinal lumen in response to inflammation and eosinophil infiltration after infection. Galectin-15 is most similar to human galectin-10 and human galectin-13 (Gray *et al.*, 2004).

Avian galectin-14 and galectin-16

Two avian galectins have been found, chicken galectin-14 (CG-14) and chicken galectin-16 (CG-16). They are mainly found in the intestine and the liver respectively and they are both expressed in the kidney (Stierstorfer *et al.*, 2000). Similar to mammalian galectins, their expression is developmentally regulated. The numbers given to the name of these galectins apply to the size of the protein: CG-14 is 14kDa and CG-16 is 16kDa. Therefore they do not imply correlation with mammalian galectins. Comparison of the primary structures of the avian galectins to vertebrate ones suggests that CG-14 and CG-16 are produced by gene duplication of an ancestral lectin gene at a time close to the divergence of birds and mammals (Sakakura *et al.*, 1990). The nearest equivalent of CG16 is mammalian galectin-1 (Hughes, 2004).

CHAPTER 4: GALECTIN-3

Galectin-3 is the most studied galectin due to its wide expression and particularly its role in cancer progression. Its involvement in kidney development and cystogenesis lead us to its investigation here. During development the lectin was first detected in notochord and was later found in developing kidneys, bone and skin. In adults, it is normally expressed in activated macrophages, gut epithelia and the epithelial cells of collecting ducts in kidney. In this chapter, the general properties and functions of galectin-3 are depicted. The specific roles of galectin-3 in kidney development and renal diseases are described in chapter 5.

Identification of galectin-3

The name galectin-3 was given in 1994 when the galectin family was formally recognized (Barondes *et al.*, 1994). Before then, the protein was identified separately by different groups with different names (e.g. Mac-2, CBP35 and L-34). Sequenced alignment analysis confirmed that these proteins are indeed the same (Cherayil *et al.*, 1990).

Galectin-3 was first identified in mice by Ho and Springer in 1982 using monoclonal antibodies: a macrophage antigen named Mac-2 was found on the surface of macrophages in response to specific differentiating signals (Ho and Springer, 1982). A year later, a separate group isolated a protein which they named carbohydrate-binding protein CBP35, from extracts of cultured 3T3 fibroblasts. It was shown that the protein recognised galactose-containing glycoconjugates and showed agglutination activity when assayed with rabbit erythrocytes (Roff and Wang, 1983). Another group had also successfully isolated galectin-3 from cDNA libraries of the murine UV-2237-IP3 fibrosarcoma cell line. A 34 kDa endogenous galactoside-specific lectin was identified and it was named L-34 (Raz *et al.*, 1987). Elevated levels of the protein was found in a wide variety of neoplastic cells and correlative evidence suggested that it is

involved in tumour metastasis *in vivo* and in galectin-3 transformed cells *in vitro* (Raz *et al.*, 1990).

Galectin-3 characterisation

Galectin-3 gene structure

The human *LGALS3* gene was mapped to chromosome 14q21-q22 by fluorescence *in situ* hybridisation and the location was confirmed by isotopic hybridisation with a tritium-labelled probe (Raimond *et al.*, 1997). The gene structure was characterised by screening the genomic library. Comparison of the genomic sequence with the published human galectin-3 cDNA sequences revealed that the gene consists of six exons and five introns, spanning a total of approximately 17kb (fig. 4.1). The translation start site is in exon II. The proline-glycine-tyrosine repeat motif is found entirely within exon III and the carbohydrate-recognition sequence is found entirely within exon V. The open reading frame of *LGALS3* in human is 750bp corresponding to a deduced polypeptide of 250 amino acids (Kadrofske *et al.*, 1998).

Figure 4.1. Genomic organisation of the human *LGALS3* gene.

The Roman numerals indicate the positions of exons. The dark boxes indicate exon sequences corresponding to the open reading frame. The hatched box represents the 3' untranslated region (UTR). The white boxes represents the 5'-UTR, and the white ovals represent Alu-family middle repetitive sequences (figure adapted from Karofske et al 1998).

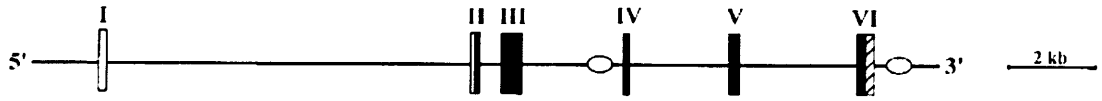

The galectin-3 gene is highly conserved across species. Sequence alignment indicates a 82% to 88% identity between human galectin-3 mRNA sequence and that of other species. However, differences were observed. Comparison of the genomic sequence between human and mouse galectin-3 revealed that the mouse galectin-3 gene has an alternative mRNA transcript (Rosenberg *et al.*,

1993). Mouse galectin-3 gene has two transcription initiation sites (α and δ), each of which is specifically associated with the use of alternative donor splice sites, resulting in two distinct mRNA transcripts, type I and type II messages. The former being 27bp longer. The human transcriptional start site corresponds to a position similar to the mouse δ initiation sites, but not to the α sites. Therefore humans lack the corresponding type I messages (Kadrofske *et al.*, 1998). Analysis of mRNA isolated from mouse 3T3 fibroblasts indicated that type II message level varies only a little over the first 20 hours after serum stimulation, whereas the type I message peaks at 16 hour post mitogen addition (Voss *et al.*, 1994).

Galectin-3 protein structure

The major difference between galectin-3 and other galectins is that it contains a unique proline, glysine, tyrosine-rich tandem repeat at the N-terminal domain. The number of repeats varies between species, giving rise to differences in the protein size. There are 8 such repeats in human, 11 in rat and mouse and 14 in dog. (Cherayil *et al.*, 1990; Herrmann *et al.*, 1993; Mehul *et al.*, 1994; Kadrofske *et al.*, 1998).

Figure 4.2. Galectin-3 protein structure.

Secondary structure of galectin-3. The dark box indicates the CRD and the hatched box represents the proline, glysine and tyrosine-rich tandem repeat (figure adapted from Moriki et al 1999).

Galectin-3 protein consists of two domains: the C-terminal domain containing the CRD (carbohydrate-recognition domain) and the N-terminal domain consisting of the proline, glysine, tyrosine-rich (YPGXXXPGA) repeat and a number of recognition sites for collagenase cleavage. The two domains appear to be structurally independent. However, studies indicate that the N-terminal

interacts with the CRD and participates in carbohydrate binding and self-association of the protein (Moriki *et al.*, 1999; Barboni *et al.*, 2000; Birdsall *et al.*, 2001)

The CRD domain contains sequence shared by other galectins' CRDs. It is highly conserved between species. Sequence alignment indicates that the human galectin-3 CRD is 97% identical to that of mice in a stretch of over 70 amino acids. Overall, the human galectin-3 protein sequence is 84% and 82% similar to that of murine and rat galectin-3 respectively. CRD of galectin-3 has a high affinity to lactose with dissociation constants ranging from 10^{-3} to 10^{-5} M depending on experimental conditions (Hsu *et al.*, 1992; Moriki *et al.*, 1999). The sugar is often used to inhibit the functions of CRD.

The N-terminal domain is unique to galectin-3 among the galectin family. This domain can be acetylated and phosphorylated (Herrmann *et al.*, 1993). Experiments using truncated galectin-3 that has no or a truncated N-terminal domain revealed the roles of the N-terminal domain in carbohydrate binding and in secretion. Within the N-terminal domain, proline to alanine mutagenesis of the sequence YP(90)SAP(93)GAY greatly reduced secretion. Similar mutagenesis of proline pairings present elsewhere in the N-terminal segment had no effect (Menon and Hughes, 1999). Cross linking studies indicate that N-terminal fragment of hamster galectin-3 can efficiently self-assemble into oligomers (Mehul *et al.*, 1994). It also has structural features seen in certain polypeptides from ribonucleoprotein (RNP) complexes (Kadrofske *et al.*, 1998).

Galectin-3 binding to glycoligands

A signature of all galectins is their ability to interact with β-galactoside via their CRDs. The CRD which encompasses 135 amino acid residues, is composed of 5 stranded (F1-F5) and 6 stranded (S1-S6a/6b) β-sheets, which associate in β-sandwich arrangement. Galectin-3, like all galectins, has a relatively high binding affinity to lactose. More specifically to galectin-3, when the hydroxyl

group in lactose is exchanged for a more hydrophobic acetamide group to make *N*-acetyllactosamine (LacNAc), the binding affinity is increased by over six fold; while the addition of a hydrophilic Gal residue to the 3-hydroxyl group of LacNAc futher enhances the affinity for galectin-3 by over 23 fold in comparison to lactose (Ochieng *et al.*, 2004). Moreover, galectins binds to poly-*N*-acetyllactosamine (branched or repeated units of LacNAc) with higher affinity (Hirabayashi *et al.*, 2002). Galectin-3 can be phosphorylated at N-termial Ser^6; it was shown that phosphorylation of galectin-3 significantly reduced its saturation binding to its ligands by greater than 85%, and the ligand binding can be fully restored by dephosphorylation with protein phosphatise type 1 (Mazurek *et al.*, 2000).

In cells, the preferred ligands for all galectins are generated in the Golgi by Mgat5 (β1,6 *N*-acetylglucosaminyl-transferase V), which catalyses the addition of β1,6GlcNAc to complex type N-glycans, leading to elongation with poly *N*-acetyllactosamine (Lagana *et al.*, 2006).

Self-association of galectin-3 involving the CRD and the N-terminal domain

Galectin-3 possesses many biological activities that are based on its multivalent binding of carbohydrate moieties. Since galectin-3 has only one CRD, it must be able to dimerise or polymerise in order to give some of its polyvalent functions.

Dimerisation and oligomerisation of galectin-3 was first suggested by Hsu et al in 1992 when they studied the binding capacity of the protein and its C-terminal domain to solid phase IgE. It has been found that the C-terminal domain alone is able to bind lactose and IgE. More importantly, addition of unlabelled galectin-3 increases the binding of labelled galectin-3 to IgE; however the binding is blocked by the addition of the C-terminal domain (Hsu *et al.*, 1992). Similar observation is shown using immobilised galectin-3. In addition it has

been determined that the C-domain alone does not self-associate, suggesting the involvement of the N-terminal in self-association (Kuklinski and Probstmeier, 1998).

The C-terminal domain of galectin-3 can bind to a C-terminal domain of another galectin-3 in the absence of its saccharide ligands. This interaction is inhibited by lactose and various saccharide ligands of the lectin. A galectin-3 mutant generated with a tryptophan to leucine replacement (W181L) in the C-terminus CRD exhibited diminished carbohydrate-binding activity and it does not bind to galectin-3C-Sepharose 4B. However, it retains its binding affinity towards the whole galectin, suggesting the involvement of N-terminal domains in self-association (Yang *et al.*, 1998).

The N-terminal of galectin-3 interacts with the CRD engaging in carbohydrate binding. Molecular modelling predicts that the N-terminal domain can lie across the carbohydrate-binding pocket of the CRD where it could participate in sugar-binding. Binding studies showed that tyrosine 102 and adjacent residues are important in the participation of carbohydrate recognition (Barboni *et al.*, 2000). Monoclonal antibodies against N-terminus domain epitopes reduced the binding affinity of galectin-3 to IgE and its haemagglutination activity (Liu *et al.*, 1996). It was also shown that the N-terminus fragment could self-assemble into oligomers (Mehul *et al.*, 1994). Also the N-terminal domain mediates pentamer formation in the presence of multivalent ligands, thereby cross-linking glycoproteins in proportion to ligand concentration. The resulting superstructure of galectins and glycoproteins generates a molecular lattice (Partridge *et al.*, 2004).

Figure 4.3. Schematic models for galectin-3 self-association.

Galectin-3 self-associates in the absence of saccharide ligands, predominantly through the C-terminal domains and possibly by the N-terminal interaction as well. In the presence of ligands, the C-terminal domain interaction is interrupted, but the protein can still self-associate through the N-terminal. N = N-terminal domain; R = tandem repeats; C = C-terminal domain (figure adapted from Yang et al 1998).

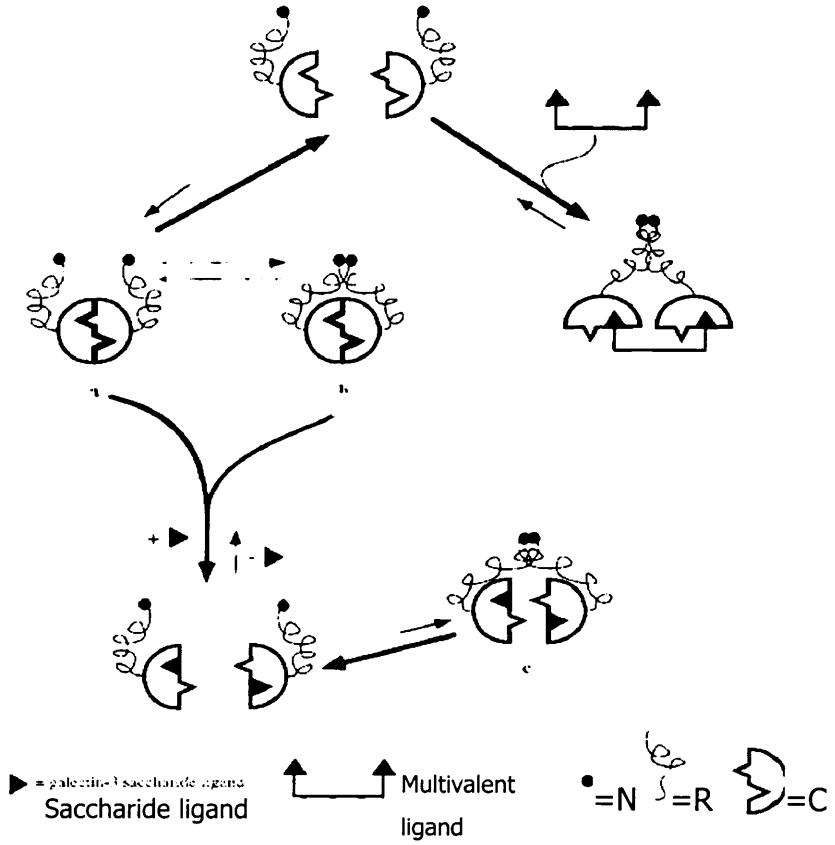

Localisation of galectin-3

Galectin-3 has been found in the nucleus and the cytoplasm within cells and is also secreted into the extracellular space. Its localisation correlates to its various functions due to the variety of ligands present in these different cellular compartments. Immunolocalisation and immunoblotting analysis of 3T3 fibroblasts revealed that galectin-3 is localised to the nucleus of proliferating cells, whereas in quiescent culture the protein expression is down-regulated, most cells lose their nuclear staining and acquire a cytoplasmic expression of galectin-3 (Moutsatsos *et al.*, 1987). Immunoblotting analysis of proteins extracted from mitochondria, isolated from human breast cell line BT549, showed that galectin-3 is also localised to this organelle (Yu *et al.*, 2002).

Galectin-3 can be externalised by various cell types including macrophages, kidney epithelial cells, polarised MDCK cells grown within collagen gels and BHK cells (Hughes, 1999; Hikita *et al.*, 2000; Sano *et al.*, 2003). Several other galectins have been found to be secreted even though they are not glycosylated and do not contain any signalling sequences that direct them to the ER-Golgi network. This indicates that they are not secreted through the classical pathway. In addition, non-classical pathways cannot account for the rapid rate of galectin-3 secretion from tumour cells. Hence an alternative pathway may take place. Immunocytochemical data illustrated that galectin-3 was released from BHK cells as vesicle blebbing from the cell surface Cells transfected with truncated galectin-3C that has no N-terminal could not be secreted, indicating the involvement of the N-terminal in galectin-3 secretion (Hughes, 1999). Galectin-3 can be rapidly internalised by breast carcinoma cells via a cavaleolae-like pathway of endocytosis and the internalisation is inhibited by lactose. More interestingly, the study demonstrated that extracellular galectin-3 at a concentration approaching 100 μg/ml could effectively mediate endocytosis of β-1 integrins (Furtak *et al.*, 2001).

The functions of galectin-3

There are several functions displayed by galectin-3. All of them depend on its particular cellular location, its phosphorylation state and sometimes on the cell cycle. The four most studied functions are its regulatory role in cell adhesion, proliferation, apoptosis and cancer.

Galectin-3 as a modulator in cell adhesion

Many extracellular ligands were identified to interact with galectin-3, which triggers different activities in different cell types. Figure 4.4 shows a summary of some of these ligands, as seen, most of the associated functions are related to the modulation of adhesion to cells or to the extracellular matrix (ECM).

Galectin-3 has a high affinity towards different glycoligands. Its implication in cancer metastasis has sparked much research into its role in cell-cell and cell-matrix interactions. The lectin binds to various major ECM proteins such as collagen IV, laminin, elastin, fibronectin and vitronectin. It also binds various matrix receptors such as $\alpha 1\beta 1$ integrins (Iacobini *et al.*, 2003; Ochieng *et al.*, 2004). Overexpression of galectin-3 in several transfected tumour cell lines enhanced the attachment of cells to ECM components by direct interaction and via increased expression of specific integrins (Matarrese *et al.*, 2000; O'Driscoll *et al.*, 2002). In contrast, incubation of tumour cells with galectin-3 reduced adhesion to ECM proteins such as laminin, collagen IV and fibronectin in a dose dependent manner. It was reported that pre-incubation of a variety of tumour cells with 0.8 to 3.33 μM of galectin-3 resulted in internalisation of β-1 integrins, which are principle receptor subunit for ECM proteins. The reduction of extracellular β-1 intergrins leads to a decrease in adhesion to ECM protein (Ochieng *et al.*, 1998; Furtak *et al.*, 2001). These results suggest that galectin-3, like galectin-8 (Warfield *et al.*, 1997) acts as both pro-adhesion and anti-adhesion.

Table 4.1. Extracellular ligands for galectin-3 and the associated functions

(modified from Ochieng et al 2004)

Ligand	Function associated with galectin-3 binding
Laminin	Modulates cell/ECM adhesion
Collagen IV	Modulates cell/ECM adhesion
Fibronectin vitronecin	Modulates cell/ECM adhesion
Hensin	Maintains terminal differentiation of renal epithelial cells
Elastin	Promotes adhesion of cells to elastin
Mac-2BP (gp90)	Promotes cell/cell and cell/ECM adhesion
Advanced glycosilation end products (AGE)	Mediates endocytosis of AGE
$\alpha 1\beta 1$ integrins	Modulates cell/ECM adhesion
$\alpha M\beta 1$ (CD11/18, Mac-1 antigen)	Modulates cell/ECM adhesion
CD66a/CD66b (human neutrophils)	Induces activation NADH oxidase and adhesion of cells to ECM
CD98 (Jurkat cells)	Induces uptake of extracellular Ca^{2+} and modulates cell/ECM adhesion
CD4+/CD8+ (T lymphocytes)	Inhibits apoptosis and modulates cell/ECM adhesion
NCA-160 (human neutrophils)	Induces an oxidative burst in neutrophils
Neural cell adhesion molecules (NCAM) MAG, L1	Modulates cell/ECM adhesion
IgE	Triggers degranulation and serotonin release
Lamp-1, Lamp-2 (tumour cells)	Modulates cell/cell, cell/ECM adhesion
Lipopolysaccharides (LPS) – bacteria	Adhesion of pathogen organisms to host ECM and cells

Galectin-3 roles in proliferation

Nuclear galectin-3 is associated with the regulation of proliferation. Several *in vitro* studies showed that galectin-3 stimulates cell proliferation. Incubation of normal human lung fibroblast IMR-90, mesangial cells from rat glomeruli or isolated hepatic stellate cells with recombinant galectin-3 leads to an increase in cell proliferation (Inohara *et al.*, 1998; Sasaki *et al.*, 1999; Maeda *et al.*, 2003). Overexpression of galectin-3 in a human breast carcinoma cells BT549 also enhances proliferation (Lin *et al.*, 2002). Experiments in thyroid cells using gel-retardation and transient transfection assays, it demonstrated that galectin-3 stimulates the DNA-binding and the transcriptional activity of TTF-1, a transcriptional factor that plays an important role in the proliferation of thyroid cells (Paron *et al.*, 2003). The study on hepatic stellate cells found that both galectin-1 and galectin-3 activate MAPK pathways, which are key signalling pathways involved in the growth factor-induced stimulation of these cells. More importantly, it was found that galectin-3 untilises protein kinase C and A to induce MEK1/2-ERK1/2 signalling pathway whereas galectin-1 does not. It was suggested that galectin-3 cross-links with target molecules through their β-galactoside-containing glycoconjugates, which triggers proliferation (Maeda *et al.*, 2003).

Galectin-3 roles in apoptosis

Over-expression of galectin-3 in T-cells, epithelial cells, macrophages and in breast carcinoma cells protects them from apoptosis induced by various apoptotic stimuli. Macrophages derived from galectin-3 null mutants were more susceptible to apoptosis (Hsu *et al.*, 2000). There are two pathways of apoptosis, the intrinsic and the extrinsic pathway. Galectin-3 was thought to work by preventing the initiation of the former pathway. Confocal and biochemical analyses revealed that galectin-3 is enriched in mitochondria of apoptotic cells. Upon apoptotic stimuli, the protein translocates to the perinuclear membrane of mitochondria consequently blocking the release of

cytochrome c (Yu *et al.*, 2002). Galectin-3 contains a BH1 (NWGR) domain of the Bcl-2 family, a group of anti-apoptotic proteins. Mutation of this domain abolished the anti-apoptotic function of galectin-3 in breast carcinoma BT 549 cells (Akahani *et al.*, 1997). In addition, galectin-3 can directly interact with Bcl-2 protein in the cytoplasm (Wang *et al.*, 2004). Also, p53-dependent apoptosis causes repression of galectin-3, indicating a new apoptotic pathway (Cecchinelli *et al.*, 2006).

Galectin-3 roles in cancer

Galectin-3 has been widely studied in various types of cancer: kidney, breast, gastrointestinal, lung, ovarian, thyroid etc. Its level in the sera of some cancer patients is elevated approximately 5 times compared with healthy normal individuals (Iurisci *et al.*, 2000). It is also expressed in some affected tissues which often correlate with tumour progression positively (head and neck squamous cell carcinoma, thyroid carcinoma) or negatively (breast carcinoma, prostate carcinoma) depending on the types of tissue involved (Takenaka *et al.*, 2004). These observations lead to the recognition of galectin-3 as a diagnostic/prognostic marker for specific cancer types (Califice *et al.*, 2004). In the case of renal cell cancer, galectin-3 is overexpressed (Young *et al.*, 2001); also galectin-3 together with other makers such as cimentin, CD74 and parvalbumin, can be used to define individual histologic subtypes of renal cancer (Kopper and Timar, 2006). Further details on the role of galectin-3 on renal cell cancer can be found in Chapter 5.

Galectin-3 may have various roles in tumour progression: it may act as an adhesion molecule in aid of angiogenesis and cell-matrix interaction during metastasis. Its regulatory role in apoptosis may contribute to anoikis by preventing tumour cells from under going programmed cell death. On the other hand, secreted galectin-3 induces apoptosis of human T leukaemia cells line, thus participating in the immune escape mechanism during tumour progression (Fukumori *et al.*, 2003).

Galectin-3 null mutant mice

Two types of *Galectin-3* null mutant mice were used in this thesis: one on the 129Sv background and the other on C57BL/6j. The former was engineered by Dr. Poirier from the ICGM (Institut Cochin de Génétique Moléculaire) in France; and the latter was created by Prof. Liu and was obtained from the Consortium for Funtional Glycomics. Both were created by homologous recombination

Galectin-3 mutant on 129Sv

The *galectin-3* gene was disrupted by deleting 3.7 kb of genomic DNA which removes exons II, III and IV, including the initiating codon in exon II. A replacement vector was prepared, it contains the mutated *galectin-3* gene structure, a neo cassette flanked by 1.5 kb of 5' homology corresponding to the BamHI-HindIII fragment from exon I and by 6 kb of 3' homology corresponding to the EcoRI-EcoRI fragment including exon V and VI. A pMC1-TK cassette was added to aid negative selection with gancyclovir. See figure 4.5 for a schematic explanation. The vector was introduced into WW6 ES cells by electroporation. WW6 ES cells were derived from a mixed genetic background (C57BL/6J,129/Sv and SJL). Transformed cell clones were selected and injected into blastocysts to generate chimeric animals. The animals carrying the mutated gene were selected based on the different gene structure using southern blotting; they were bred with 129 c/c females. *Galectin-3* heterozygotes were selected and inter-crossed to yield null mutant animals (Colnot *et al.*, 1998). These animals were maintained on the 129Sv background, with four years of inbreeding prior to shipment to my lab.

Galectin-3 mutant can easily be screened by genotyping using two primer pairs, each corresponds to either the wildtype or the mutant alleles, giving a specific size of DNA fragment. The primers that are probed against the wildtype allele amplify a 305bp fragment from the deleted region in intron I (just before exon

II); whereas the primers against the null mutant allele amplify a 577bp DNA fragment from the Neo cassette.

Figure 4.4. Galectin-3 mutant gene construct.

The figure shows the physical map of *galectin-3* in genomic DNA. The six exons are represented by vertical bars (black or red) with roman numbers I to VI below them. Exons II (containing start codon ATG – in red), III and IV in red were deleted in mutant *galectin-3*. The region disrupted which was 3.7 kb was replaces with a neo cassette. The vector contained the neo cassette flanked by the 1.5 kb and 6 kb (in blue). Other labels: E, B and H represent restriction enzyme sites (EcoRI, BamHI and HindIII). Adapted from Colnot et al 1998.

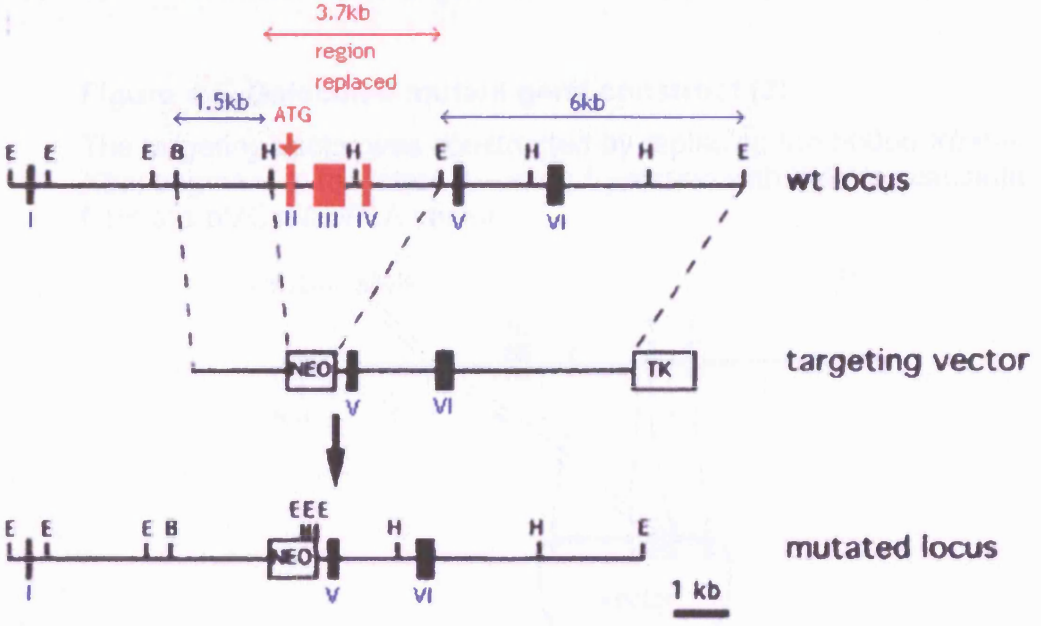

Galectin-3 mutant on C57BL/6j

Similar to the other *galectin-3* mutant, a Neo cassette was used to disrupt the galectin-3 gene. A replacement vector consisted of a *Neo gene* flanked by a segment from exon 4 and 5 of the *galectin-3* gene and another segment from exon 5 and 6. Therefore, exon 5 was interrupted by the *Neo* gene (see fig 4.6). Murine stem cells, D3, were electroporated with this vector. Transformed cells were selected and injected into 3.5 day old blastocysts from C57BL/6j mice and the injected blastocysts were implanted into pseudo-pregnant CD1 mothers. Male chimeric mice were bred to C57BL/6j females to produce heterozygotes, which were then intercrossed to generate homozygotes (Hsu *et al.*, 2000).

Figure 4.5. Galectin-3 mutant gene construct (2).

The targeting vector was constructed by replacing the 500bp *Xba*I – *Xba*I segment at the intron 4 – exon 5 junction with the *Neo* cassette from the pMC1NeoPLA vector.

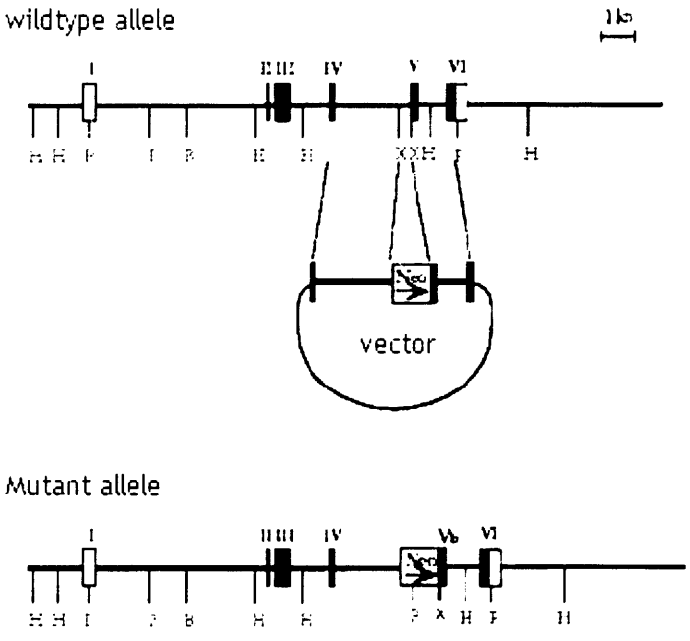

Both galectin-3 null mutants are viable and fertile. The mutant animals appear generally healthy and had a normal life span, suggesting that the roles of galectin-3 in normal development may be redundant or that they are replaced by other galectins. Interestingly, double mutant *galectin-1/galectin-3* null animals are also healthy and fertile although they were both implicated in embryo implantation (Colnot *et al.*, 1998). In kidneys; galectin-3 null mutant animals have normal kidney function although they have 11% fewer glomeruli compared with wildtypes, associated with kidney hypertrophy. In clearance experiments, urinary chloride excretion was found to be higher in the mutants, but there was no difference in urinary bicarbonate excretion, in glomerular filtration or urinary flow rates (Bichara *et al.*, 2006).

CHAPTER 5: THE ROLE OF GALECTIN-3 IN KIDNEY DEVELOPMENT AND CYSTOGENESIS

Galectin-3 is expressed in a tightly regulated manner during kidney development in humans and mice; as well as in an *in vitro* model of tubulogenesis of kidney epithelial cells, MDCK (Bao and Hughes, 1995; Winyard *et al.*, 1997; Bao and Hughes, 1999; Bullock *et al.*, 2001). It is also found to regulate cyst growth in an *in vitro* model, suspension culture from digested *cpk* kidneys.

Kidney development

In mammals and birds, the kidney develops in three stages: pronephros, mesonephros and metanephros.

Figure 5.1. Human embryogenesis illustrates early kidney development.

A) The mesonephric ducts appear adjacent to pronephric tubules and grow caudally. B) Pronephric tubules regress and mesonephric glomeruli and tubules are formed. C) The ureteric bud branches from the caudal mesonephric duct and enters the metanephric mesenchyme. Adapted from Winyard 1998.

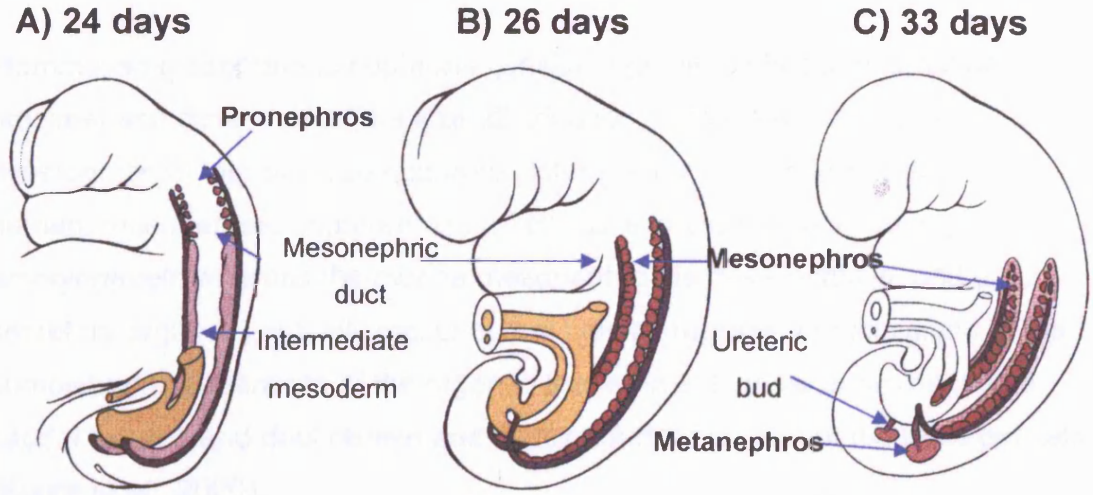

Pronephros

The pronephros is formed early in development, embryonic day 22 in human and embryonic day 8 in mouse. The structure and number of nephrons varies between species. In mammals most of the pronephric duct degenerates but the caudal portion becomes part of the excretory system and is referred to the Wolffian duct, which later gives rise to the ureteric bud (Kuure *et al.*, 2000).

Mesonephros

The mammalian mesonephros develops from a mesodernal region called the aorta-gonad-mesonephros (AGM) zone. As suggested by its name, the AGM region also contributes to the development of the aorta, gonads, mesonephoros as well as haematopoietic stem cells. Organogenesis of the mesonephros is based on the interaction between the mesonephric mesenchyme (MM) and the Wolffian/pronephric duct. It is initiated when the pronephric duct reaches the MM and induces adjacent mesenchymal cells to condense. The condensate contributes to the formation and branching of the ureteric buds that develop into nephrons. This takes place around E10.5 in mouse (Kuure *et al.*, 2000; Bard, 2002). The interaction between MM and Wolffian duct is governed by signalling and adhesion molecules such as WNT-11, GDNF (glial-cell-line-derived neurotrophic factor), integrins and proteoglycans that are heavily glycosylated with chains of long, linear carbohydrate polymers (Muller and Brandli, 1999).

Mammalian mesonephric nephrons consist of glomeruli-like structures and proximal and distal ducts. The size, distribution, functional maturity and developmental fate of these nephrons differ greatly between species. In human, mesonephric nephrons are functional excretory organs during embryogeneis whereas the murine mesonephros is more primitive and a non-secretory organ. Eventually mesonephric tubules regress and this leads to the complete disappearance of the organ in the female. In male embryos, some caudal tubules and duct remain and develop further as part of the male genitals (Kuure *et al.*, 2000).

Metanephros and the development of nephron

Nephrogenesis is very similar in the meso- and metanephros. However, it should be noted that in the mesonephros the tubules are formed along side the Wolffian duct whereas in the metanephric kidney they are organized around the branching ureteric tree. The metanephros starts to develop at embryonic day 11 in mouse when the metanephric blastema appears. Similar to organogenesis of mesonephros, metanephros development depends on the reciprocal inductive interactions between mesenchymal cells and ureteric bud. It is thought that signals from the mesenchyme initiate kidney development by inducing formation of the ureteric bud from the Wolffian duct. Subsequently, the growing ureteric bud starts to branch as a response to the mesenchymal signals and in return transmits signals to the mesenchymal cells, causing them to condense and generate pretubular aggregates around branches of the ureter tree.

The second stage (embryonic day 13.5 – after birth in mouse) is the formation and differentiation of nephron from disorganised mesenchymal cells to highly organised epithelial tubule. This process can be divided into four stages: 1) condensation, in which groups of about 100 cells condense tightly around the ureteric bud to from a distinct mass. 2) Epithelialisation, in which condensed cells lose their mesenchymal characteristics and gain epithelial ones. At the end of this stage the mesenchymal cells form a small epithelial cyst complete with a basement membrane, cell-cell junctions and a defined cellular apical-basal polarity. 3) Early morphogenesis, in which the epithelial cysts invaginate twice to form comma and then an S-shaped bodies, one of these invagination sites later becoming the glomerular cleft. At about this time, blood vessel progenitors invade the cleft to begin construction of the vascular component of the glomerulus. 4) Tubule maturation, in which the specialised segments of the nephron differentiate.

By about embryonic day 13 in mice, the extending ducts have reached the periphery of the metanephros, and the mesenchymal cells spread out over the

surface to give a rim of stem cells that both maintain duct development and support new nephron formation at the periphery. As time proceeds, existing, internal nephrons start to extend into the medulla forming the loop of Henle, mature and start functioning, while new, more peripheral nephrons continue to be induced by the ducts. 2 weeks after birth in mice and at approximately 34 weeks of gestation in humans, the populations of blast and stromal cells disappear, leaving a stable functioning kidney (Bard, 1992; Lechner and Dressler, 1997; Kuure *et al.*, 2000; Bard, 2002).

Galectin-3 expression in human kidney

During human kidney development, galectin-3 was detected in all stages. Using western blot and immunohistochemistry, galectin-3 protein was found, mainly apically, in mesonephric ducts and also in the distal mesonephric tubules from 5 weeks gestation age. In the metanephros, the lectin was detected in the apical domains of ureteric bud branches, and there was intense expression in fetal medullary and papillary collecting ducts in both the cytoplasm and plasma membranes. Low levels of galectin-3 were detected in the cytoplasm of a subset of cells in adult collecting ducts; the expression overlaps that of basal band 3 protein, which is a marker for α-intercalated cells (Winyard *et al.*, 1997).

Galectin-3 expression in mouse kidney

RT-PCR revealed that in mice kidneys the first *galectin-3* transcripts appear around embryonic day 12; the expression is maximal around E16 and then reduced sharply after birth and is barely detectable in adult kidney. In E17, galectin-3 is expressed at the stems of ureteric bud branches but not at their growing tips. Deep in the E17 cortex, collecting ducts expressed galectin-3 with various subcellular locations: some with cytoplasmic or weak basal expression, as detected by immunohistochemistry, others with a subset of cells with intense cytoplasmic immunostaining. Large medullary collecting ducts displayed intense galectin-3 staining basally. Proximal tubules that were confirmed with a

brush border marker – periodic acid schiff's reagent (PAS), had no galectin-3 expression. And no immunostaining was detected in glomeruli. Postnatally, galectin-3 protein was detected in a uniform apical distribution in cortical tubules that were PAS negative. These galectin-3 expressing tubules are often adjacent to the glomeruli in the cortex, suggesting that they are distal convoluted tubules. Galectin-3 is also found in deep medullary collecting ducts and the urothelium of the renal papilla (Bullock *et al.*, 2001; Nio *et al.*, 2006). Studies carried out by my predecessor, Dr Johnson, established that galectin-3 is widely expressed in the collecting tubules in the cortex and the medullary collecting tubules and in the urothelia in adult mice.

These findings suggest that galectin-3 may be involved in the early development of collecting tubules. Its precise functions in these tubules are unclear, it may play a role in regulating cell adhesion. Organ cultures where E11/E12 metanephroi were cultured in the presence of exogenous galectin-3 provided evidence that galectin-3 can modulate ureteric bud branching. Addition of galectin-3 to these whole organ cultures inhibited ureteric bud branching. The effect is reversible by withdrawal of galectin-3 in the medium. The addition of galectin-1 or mutant galectin-3, that lacks the high-affinity binding to extended oligosaccharides, did not perturb branching morphogenesis of the ureteric bud/collecting duct lineage. Moreover, the addition of a blocking antiserum to galectin-3 caused dilation and distortion of developing epithelia in E12 metanephroi cultures (Bullock *et al.*, 2001).

Galectin-3 expression in MDCK cells

Galectin-3 is expressed in immortalised kidney epithelial cells such as mouse inner medullary collecting duct cells (mIMCD), baby hamster kidney cells (BHK) and in Madin-Darby canine kidney epithelial cells (MDCK) (Bao and Hughes, 1995; Hughes, 1999). Studies of kidney epithelial tubulogeneis was carried out using MDCK cells in 3-D collagen gel cultures. In 3-D culture, MDCK cells develop into a cyst-like structure containing a polarised epithelium surrounding

a central lumen. These cysts can be induced to form tubules with hepatocyte growth factor (HGF). Shortly after induction, sprouting of the cysts occur and these processes develop into multicellular arms which branched and eventually formed tubular structures with a central lumen.
Prior to the induction of tubulogenesis, galectin-3 is expressed in the basolateral domain of the cyst-like structure, with little cytoplasmic expression. After the addition of HGF, galectin-3 expression in the main body of the sprouting cysts remains similar to that found in simple cysts developing in the absence of HGF: strong basolateral expression. Although the sites initiating extension of the multicellular tubules and the progressing tips clearly lack galectin-3. Additionally, galectin-3 is secreted by MDCK, BHK and IMCD cells via a non-classical pathway. These results support the organ culture study, further suggesting that galectin-3 play an important role in tubulogenesis during kidney development (Bao and Hughes, 1995).

The protein also exhibits an effect on the development of MDCK cysts in collagen gel. Galectin-3 added exogenously to the cultures exerted an inhibitory effect on cyst enlargement of MDCK cells in 3-D gel matrix; whereas anti-galectin-3 antibodies promote cyst growth (Bao and Hughes 1995).

Role of galectin-3 in terminal differentiation of intercalated cells and acidosis

Galectin-3 is involved in the terminal differentiation of rabbit renal intercalated cells, a type of kidney epithelial cell in the collecting tubules (Hikita *et al.*, 2000). The cortical collecting duct of the kidney is made up of principal cells, which are involved in salt, water and potassium transport; and the intercalated cells, which made up of a third of the cells in this segment and mediate acid-base transport (Al Awqati and Oliver, 2002). Two functionally distinct sub-types of renal intercalated cells have been identified: bicarbonate (HCO_3^-) absorbing α-intercalated cells and the HCO_3^- secreting β-intercalated cells. The former expresses Cl^-:HCO_3^- exchange at the baso-domain and apical H^+ ATPase,

thus it also secretes proton (H^+). Whereas the β-intercalated cells express these markers at opposite domains. β cells can convert to the α form both *in vivo* and *in vitro* (Al Awqati, 2003). Conversion takes place under the influence of acidification of the medium or acid diet *in vivo*. The seeding density of intercalated cells also influences the phenotype: subconfluent seeding results in the formation of β cells whereas high density seeding results in the α phenotype. In both cases, the conversion requires the deposition of a protein called hensin at the extracellular matrix. Galectin-3 was found to be associated with hensin in the extracellular matrix. Purified recombinant galectin-3 is able to bind to hensin and polymerise it *in vitro*. Seeding cells at high density induces secretion of galectin-3 to the extracellular matrix where it bundles hensin, which in turn signal the cell to change its phenotype.

Galectin-3 expression in rabbit kidney is altered under metabolic acidosis. Under normal diet, galectin-3 expression is restricted to the α-intercalated cells and the principal cells, however, under acid diet, the protein expression is dramatically increased in the cortical collecting duct cells, particularly in β-intercalated cells. This result further supports the role of galectin-3 in the β cells adaptation (Hikita *et al.*, 2000; Al Awqati and Oliver, 2002; Schwaderer *et al.*, 2006).

All these studies were carried out in rabbit, which may not represent human and mouse kidneys due to differences in kidney physiology and the diet of the animal.

Role of galectin-3 in diabetic nephropathy

Nonenzymatic glycation is implicated in the pathogenesis of the dysregulated tissue remodelling that characterises diabetic glomerulophaty, via the formation of advanced glycation end products (AGEs) and their binding to cell surface receptors. Galectin-3 is one of such receptors. In diabetic rats, galectin-3 can be detected in the glomeruli but not in the non-diabetic population. Its role in

the development of diabetic nephropathy was further studied using galectin-3 knockout mice that were rendered diabetic with streptozotocin. Galectin-3-deficient mice develop accelerated glomerulopathy compared with wild-type, as evidenced by more pronounced increase in proteinuria, which is associated with the higher AGE accumulation in kidneys (Pugliese *et al.*, 2000; Pugliese *et al.*, 2001).

Galectin-3 exhibits a high binding affinity towards AGE, in addition, it was shown to play a role in endocytosis of AGE and modified (acetylated or oxidised) low density lipoproteins, LDL. The lectin appears to play a functional role in the removal of these harmful compounds. It was suggested that the upregulation of galectin-3 in diabetic *milieu* was due to its participation in the pathogenesis of diabetic nephropathy by enhancing AGE removal. Hence galectin-3 protects kidneys from AGE-induced tissue injury (Zhu *et al.*, 2001; Iacobini *et al.*, 2003).

Galectin-3 and renal cell carcinoma

As mentioned in the Chapter 4, galectin-3 is overexpressed in renal cell carcinoma (RCC) (Francois *et al.*, 1999). There are different subtypes of RCC, conventional RCC which is the commonest form, oncocytoma and chromophobe RCC. Conventional RCCs were distinguished from oncocytoma and chromophobe RCCs based on large scale gene expression patterns. The latter two displayed similar expression profiles, consistent with the mitochondrion-rich morphology of these tumours and the theory that both lesions are related histogenetically to distal nephron epithelium. On the other hand, conventional RCCs underexpressed mitochondrial and distal nephron genes. Galectin-3 expression is predominantly found in low-grade conventional RCCs, indolent chromophobe RCCs and benign oncocytomas. Although microarray study reveals that galectin-3 mRNA overexpression is specific to oncocytoma and chromophobe RCCs (Young *et al.*, 2001). These results do not suggest the role of the galectin in RCC, however they open up a possibility

of using galectin-3 as a marker to define individual histologic subtypes of RCC (Kopper and Timar, 2006).

Galectin-1 and galectin-9 in kidney.

In addition to galectin-3, both galectin-1 and galectin-9 are expressed in the kidney. Galectin-1 is expressed widely in the mesodemally derived cells in the developing mouse embryo, including kidney, where these cells are responsible for the development of the mesodermal mesenchyme that in turn gives rise to the non-ureteric tubular epithelia. No expression was detected in ureteric epithelia (Hughes, 2004). Experiments involving two-dimensional gel electrophoresis combined with mass spectrometry on juvenile cystic kidney (*jck*) mice kidneys, galectin-1 protein expressed was found to be 9-fold higher compared with wildtype (Valkova *et al.*, 2005).

Galectin-9 expression in kidney, like galectin-3, is also developmentally regulated although in a different manner. Galectin-9 expression increases steadily from E12 through late embryonic development and postnatally, and reaches its highest and constant levels in adult kidney, whereas galectin-3 expression is highest during development and decreases as the kidney matures. Galectin-9 is most prominently found in the apical domain of the proximal tubules. Here, the galectin act as an urate transporter/channel that is incorporated into the lipid bilayer. It was suggested that the opening of the channel may in part be regulated by extracellular glucose binding to the CRD domain of the galectin (Leal-Pinto *et al.*, 2002; Hughes, 2004).

CHAPTER 6: THE EFFECT OF PACLITAXEL ON THE DEVELOPMENT OF POLYCYSTIC KIDNEYS

Currently, there are no treatments for human PKD patients. The disease leads to renal failure and patients at the end stage of PKD require dialysis or kidney transplantation. Investigators have tested various reagents in mice in the hopes of finding a treatment for PKD. One of these successful treatments in animals is paclitaxel (Taxol®) (Woo *et al.*, 1994). Paclitaxel is a poison produced by endophytic fungi that reside in a variety of plants (Amos and Lowe, 1999). It is isolated from Taxus brevifolia (Pacific yew tree) and Taxus yannanensis. Semisynthesis, cellular culture production, chemical synthesis and total synthesis of the molecule have been reported (Nicolaou *et al.*, 1994). It was first approved by the Federal Drug Administrator in the US in 1992 for treatment of ovarian cancer. It is now often used as chemotherapy against breast, ovarian and non-small lung cancer. Although it increases the toxicity profile of patients under treatment, it is the only reagent that on its own exhibits a relatively high response rate. It is often used in combination with different reagents such as doxorubin or cisplatin to increase the response rate in breast carcinoma (Maiche *et al.*, 2000).

In this thesis, paclitaxel treatment was investigated because preliminary results showed that it affects the expression pattern of galectin-3 in treated *cpk* cysts *in vitro* and *in vivo*. The location of galectin-3 expression appeared to be altered in paclitaxel treated cells from cytoplasmic staining in untreated cystic kidney epithelial cells to prominent apical expression.

How does paclitaxel work?

Paclitaxel targets the microtubules although the precise mechanism of how it works is not yet resolved (Amos and Lowe, 1999). It is often described as a microtubule-stabilising drug which inhibits the completion of mitosis by disrupting the spindle microtubule dynamics, thus blocking cell cycle progress

at the metaphase/anaphase transition. Cell death is caused by either aberrant mitosis resulting in an aneuploid G1 cell population: multinucleated cells of up to 11 micronuclei was found with PtK_1 cells under paclitaxel treatment (Jensen *et al.*, 1987); or by mitotic arrest at higher concentration (Torres and Horwitz, 1998; Yvon *et al.*, 1999; Alexandre *et al.*, 2006).

It was suggested that the microtubule damage caused by paclitaxel induces apoptosis through a JNK-dependent pathway in the early phase followed by a JNK-independent pathway, perhaps related to the activation of protein kinase A or of Raf-1 kinase, that results in phosphorylation of Bcl-2 (Blagosklonny *et al.*, 1999). Accumulation of hydrogen peroxide is also important in paclitaxel induced cell death, at least in cancer cells (Alexandre *et al.*, 2006).

Paclitaxel stabilizes microtubules

In order to understand how paclitaxel works, we must first examine the structure of microtubules. Microtubules are hollow cylindrical tubes formed primarily by self-association of α,β-tubulin heterodimers into polymers. Each polymer, called protofilament, is arranged in a polar fashion and these protofilaments interact laterally to form microtubules. The number of protofilaments in each microtubule ranges from 10 to 15 (Nogales, 2000; Orr *et al.*, 2003b). Microtubules are highly dynamic structures that depend on the balanced exchange between tubulin molecules associated with microtubules and a free cytoplasmic pool of tubulin (Jensen *et al.*, 1987). In differentiated cells microtubules are polarised with the fast growing plus-ends, which points towards the basolateral surface of epithelial cells, and the slow-growing minus-ends, which points towards microtubule-organising centre (MTOC) located near the apical surface of epithelial cells (Musch, 2004).

Paclitaxel reversibly binds to the hydrophobic pocket in the central domain of β tubulin, close to the microtubule loops (M-loop), which is the major lateral contact between adjacent protofilaments. It is believed that the binding to this

site causes a conformational change in the M-loop that strengthens the lateral contacts between protofilaments and enhances microtubules stability (Amos and Lowe, 1999; Nogales, 2000; Orr *et al.*, 2003).

Paclitaxel causes apoptosis

The disruption of microtubules caused by paclitaxel initiates apoptosis. Apoptosis can be induced via different transduction pathways: c-Jun N-terminal kinase (JNK) pathway and the caspase cascade triggered by the release of cytochrome c from the mitochondria.

Paclitaxel activates the JNK signalling pathway in a variety of human cells, and the activation is dependent on the interaction of the drug with microtubules (Wang *et al.*, 1998).

Paclitaxel also acts directly on isolated mitochondria, causing them to release cytochrome *c* which can potentially initiate caspase activity leading to apoptosis (Andre *et al.*, 2000). It was demonstrated that tubulin is localised in the mitochondrial membranes and that the mitochondrial tubulin interacts with the permeablility transition pore (PTP), which is responsible for mitochondrial permeabilisation. Therefore, it is possible that paclitaxel can bind to mitochondrial tubulin thus altering the PTP activity (Carre *et al.*, 2002). Furthermore, paclitaxel induces Bcl-2 phosphorylation and degradation, which in turn regulates its function to control cytochrome *c* release (Basu and Haldar, 1998; Brichese *et al.*, 2002).

Paclitaxel treatment in PKD animal models

Woo et al (1994) found that at least in the primary suspension culture of *cpk* kidneys, inhibition of DNA, RNA and protein synthesis with methotrexate (10 μg/ml), cytosine arabinoside (20 μg/ml), α-amanitin (100 ng/ml) or

cyclohexamide (40 μg/ml) does not prevent *in vitro* cyst formation. Whereas cultures in the presence of microtubule-specific agents colchicine, vinblastine or paclitaxel significantly reduced cyst formed *in vitro*. Further, the investigators found that a single treatment of *cpk* mice with 150 μg of paclitaxel between postnatal day ten and twelve prolongs the lifespan of these animals to 40-50 days old, compared with untreated animals which die between 25 and 28 days. Weekly paclitaxel treatment in *cpk* animals further prolongs their lifespan to over 200 days. Histological examination of paclitaxel-treated polycystic kidneys at up to 200 days revealed the presence of normal to slightly dilated renal tubules and normal glomeruli, which are absent in untreated end-stage cystic kidneys. Although cysts were present, they were less numerous and smaller in size compared with untreated 21-day-old polycystic kidneys.

The effect of other microtubule-specific agents *in vivo* could not be determined as treatment with the minimum doses of colchicine (250 nM), colcemid (200 nM) and vinblastine (200 nM) required to disaggregate microtubules *in vitro* are lethal to 10-12 day-old polycystic cpk mice. Sub-lethal doses of these compounds were ineffective in prolonging the survival of *cpk* mice. The results indicate that the microtubule cytoskeleton has a central role in the pathogenesis of PKD in *cpk* mice.

The treatment was repeated in different animal models. *In vitro* cultures derived from cystic kidneys of Han:SPRD (cy/+) rats. It was found that human cysts fluid and epidermal growth factor both stimulated the formation of cysts whereas paclitaxel inhibited cystogenesis (Pey *et al.*, 1999). However, contradictory outcomes were found when the same treatment was carried in different animals models *in vivo*. No beneficial effects were observed in *orpk* (Sommardahl *et al.*, 1997), *pcy* mice and Han:SPRD-*cy* rats (Martinez *et al.*, 1997), suggesting that the paclitaxel effect may be specific to the *cpk* model.

A close examination of the published data revealed that the dosage used for each experiment differed greatly. The dosage used by Woo et al in the original

cpk paper was a single dose of 30 μg/g at day 10, Sommardahl et al used 10 μg/g/week on the *orpk* mice model beginning at Day 7; Martinez et al treated 2- to 10-week-old *pcy* mice with approximately 15 μg/g/week, assuming that the animal weigh on average 6g at week 2; and treated 7- to 10-day-old Han:SPRD (cy/+) rats with 0.1 to 15 μg/g/week. A summary of the dosage used is in figure 6.1, which shows that all other models used a dosage that was at most, half the dosage used in the *cpk* mice. Hence, the inefficiency observed could be due to the reduced dosage used.

Table 6.1. Comparison of paclitaxel treatment in different PKD animals.

Studies on the effect of paclitaxel treatment against cyst growth suggested that paclitaxel only worked in *cpk* mice. However, close examination revealed that there is a great variation the dosage and the method of administration used. In particular the dosages for treating other animals are reduced, which may contribute to the lack of positive effect by paclitaxel.

PKD model	* Cyst development	Concentration used, μg/g	Method of administration	Reduce cystogenesis
Cpk, mice	AR, fast	30	Single dose at Day 10	Yes
Orpk, mice	AR, fast	10	Weekly from Day 7	No
Pcy, mice	AR, slow	~15	Weekly from week 2 to 10	No
Han:SPRD-cy, rat	AD, fast	0.1 to 15	Weekly from day 7 to 10	No

* AR = autosomal recessive, AD = autosomal dominant

Mechanisms of paclitaxel resistance

Paclitaxel resistance is a significant problem in cancer therapy. Several factors contribute to this effect and they may also contribute to paclitaxel resistance in some polycystic kidney disease models. Studies on several paclitaxel resistance cell lines such as A549 human non-small lung carcinoma, K562

erythroleukeukemia cell line, DU-145 prostate carcinoma cell line and KPTA5 cells revealed that alteration of the β-tubulin gene expression contributes to the drug resistance. In particular mutation around or within the M-loop domain that results in weaker interaction between protofilaments and mutation in the paclitaxel binding sites in β-tubulin is responsible for the drug resistance (Giannakakou *et al.*, 1997). Also the upregulation of the isotype β III-tubulin expression correlates to increase paclitaxel resistance (Jaffrezou *et al.*, 1995; Kavallaris *et al.*, 1997; Ranganathan *et al.*, 1998; Orr *et al.*, 2003). It was shown that microtubules consisting of only β III-tubulin are more unstable (Panda *et al.*, 1994) and this instability is linked to paclitaxel resistance. It may be possible that some PKD models exhibit these traits, in particular reduced stability of microtubules.

Further work on *cpk* mice found that only certain taxanes that are able to promote microtubule assembly, in contrast to those that are microtubule inactive, can significantly prolong the life of affect animals (Woo *et al.*, 1997). Paclitaxel may alter cystogenesis by suppressing proliferation of cystic epithelia which is up-regulated in cystic kidneys; it may also act directly on the primary cilia, which consist of acetylated tubulin. The disruption if microtubule caused by paclitaxel may affect the structure of the primary cilia.

Other potential therapies

Researchers have been trying to find potential therapeutic treatments using different animal models. These treatments include vasopressin V2 receptor (VPV2R) antagonist, epidermal growth factor receptor (EGFR) tyrosine kinase inhibitors, purinergic receptor P2X(7), base treatment and dietary modulation; all have shown to be effective in specific PKD models. For most of them, their effects have not yet proven to be effective to all PKD models and their mode of action are still unclear. Nonetheless they provided important clues into the mechanisms of the disease and potential treatment.

Vasopressin V2 receptor (VPV2R) antagonist OPC31260

OPC31260, an antagonist of VPV2R, the major cAMP agonist in the collecting duct, has recently been shown to be an effective therapy in three animal models: *pck* rat (orthologous to human ARPKD), *pcy* mouse (orthologous to human nephronophthisis and *Pkd*$^{-/tm1Som}$ (an orthologous to human *PKD2*) (Gattone *et al.*, 2003; Torres *et al.*, 2004a). cAMP levels was increased in cystic animals and it is present in cysts fluid. It stimulates fluid secretion in normal collecting ducts and isolated ADPKD cysts; it also increases proliferation of ADPKD cells while poses an opposite effect on normal kidney epithelial cells(Torres *et al.*, 2004a). The mechanisms responsible for these changes are unclear, however, these results showed that by inhibiting cAMP signalling pathways, it is possible to delay cystogenesis.

Epidermal growth factor receptor (EGFR)

Increased level of EGFR-specific tyrosine kinase activity is observed in affected kidneys of several different ARPKD animal models. The activity can be blocked by introducing a mutant EGFR (*wa2* mutation) into an ARPKD models (*orpk mice*), which exhibit a decrease EGFR tyrosine kinase activity and these double mutants have reduced cytogenesis (Richards *et al.*, 1998). Experiments showed that administration of tyrosine kinase inhibitor, EKI-785, markedly reduced collecting duct cyst formation in *bpk* mice (Sweeney *et al.*, 1999) although the same treatment did not yield any positive effects in *pck* rat (Torres *et al.*, 2004a). Specific inhibition of EGFR binding partner HER-2, which is the preferred dimerisation partner, to PKD1 null heterozygous mice significantly inhibited the development of renal cysts (Wilson *et al.*, 2006).

P2X(7)

P2X(7), a purinergic receptor, is expressed in the cystic epithelia in *cpk* mice. *In vitro* culture generated by dissociated *cpk* kidney in suspension culture reveals that a P2X(7) agonist, BzATP, reduces cystogenesis. The effect is P2X(7) specific as other purinergic agonists, ATP and UTP, had lesser effects; and the

P2X(7) inhibitor, oxidised ATP abolished the BzATP-mediated effect on cystogenesis (Hillman *et al.*, 2004).

Base treatment

Sodium/potassium bicarbonate or citrate markedly attenuates the development of kidney cysts in Han:SPRD-*cy* rat although it has no effect in *pcy* mice and actually accelerated PKD progression in *pck* rats. These conflicting results reflect the complexity of this disease. Different segments of the nephron may undergo different cystic changes in each model. The Han:SPRD-*cy* rat have cysts derived primarily from proximal tubules where as *pcy* mouse and *pck* rats have cysts originated in the distal tubules and collecting ducts (Tanner and Tanner, 2000; Guay-Woodford, 2003).

Dietary modulation

High protein diet was associated with accelerated renal cystogenesis whereas low protein diet was shown to attenuate disease progression in the slow progressive form of PKD models, *pcy* mouse and Han:SPRD-*cy*. Specific components within the protein diets appear to modulate PKD. Soy protein and flaxseed, were both shown to attenuate the development of renal cysts. In particular substances such as phytoestrogens, soy-derived isflavones were demonstrated to attribute to the beneficial effect (Tomobe *et al.*, 1994; Ogborn *et al.*, 1998; Aukema and Housini, 2001; Guay-Woodford, 2003).

CHAPTER 7: HYPOTHESES, AIMS AND EXPERIMENTAL STRATEGIES

Hypotheses

My main hypothesis was that galectin-3 is an endogenous, negative-regulator, of renal cyst growth in the *cpk* mouse model of ARPKD.

Subsidiary hypotheses were that:

I. Galectin-3 is implicated in other PKD.
II. Galectin-3 associates with the primary cilium.
III. Galectin-3 may have a role in paclitaxel-mediated restriction of cyst growth in *cpk* mice.

Aims

There were several primary aims in this thesis:

1. Fully characterise galectin-3 expression in the *cpk* mouse model of ARPKD, and determine whether expression is also increased in other PKD.
2. Determine whether lack of galectin-3 alters cyst formation in *cpk/galectin-3* mutants.
3. Investigate galectin-3 in the primary cilium.
4. Investigate whether paclitaxel and galectin-3 modulate cystogenesis via common mechanisms.

Experimental strategies

Four major groups of experiments were performed:

1. Expression analysis. The expression pattern of galectin-3 was examined in *cpk* mice, and compared to other collecting duct developmental markers

and renal galectins. Galectin-3 expression was also sought in other PKD including *bpk, orpk,* and *pkd2* mutant mice, plus human ADPKD and ARPKD kidney tissues.

2. Breeding experiments. *Galectin-3* and *cpk* mutants were bred to generate compound offspring with which to assess the effects of reduced galectin-3 on cyst formation. The level of cystogenesis was measured by kidney/body weight ratio and histological analysis, and compared to determine if the lack of galectin-3 resulted in enhanced cyst growth.
3. Galectin-3 and primary cilia. Immuno-cyto and -histochemistry was performed on primary cultures of kidney epithelia from *cpk* mice and inner medullary collecting duct (IMCD) cells, c*pk* and normal mouse kidney sections, and human ARPKD and ADPKD samples. Double labelling for galectin-3 and either α-acetylated or γ-tubulin was examined using a confocal microscope.
4. Paclitaxel and galectin-3. New *in vivo* experiments were performed to assess early effects of paclitaxel on general and cilial galectin-3 expression. Further *in vitro cpk* cyst culture experiments were used to determine whether paclitaxel and galectin-3 might act in the same or distinct pathways to reduce cyst formation.

Preliminary experiments were also conducted using the atomic force microscope as a novel technique to assess ciliary structure and function.

CHAPTER 8: MATERIALS

Animal husbandry

I studied normal mouse strains, C57BL/6j and 129Sv (Charles River mouse Farms, UK). Known heterozygous *cpk*/+ mice on C57BL/6j were obtained from the Jackson Laboratories (Bar Harbor, Maine, USA). Initially *galectin-3* null mutant mice on 129Sv were obtained from Dr. Poirier from the ICGM (Institut Cochin de Génétique Moléculaire) in France. Later, *galectin-3* null mutant mice on C57BL/6j were obtained from the Consortium for Functional Glycomics (http://www.functionalglycomics.org/static/consortium).

ARPKD affected mice are homozygous recessive (*cpk/cpk*), and hence are the F1 progeny from mating two heterozygotes. Statistically half of the litter from parents that carry the mutation, will be heterozygotes, one quarter will be affected homozygotes and one quarter, wildtype mice that do not carry the mutation. Mice were kept with their mothers until they were weaned at 21 days old. Both the Home Office, and the Institute of Child Health, Animal Welfare Committee, approved all studies involving animals.

Kidneys were collected, via micro-dissection, from *cpk* homozygous offspring and their littermates at 1 or 3 weeks of age, as well as from normal mouse strains at the same ages. All homozygous *cpk* mice were culled before week 4 at which point they became severely ill. The *cpk* allele was also bred onto the 129Sv background for 10 generation to yield *cpk* animals on a virtually pure 129Sv background.

Galectin-3 null mutants on 129Sv (from Dr. Poirier) were bred with *cpk* heterozygotes to yield double mutants. They were also inter-bred to maintain the null allele on 129Sv background. *Galectin-3* null mutant on C57BL/6j (from the Consortium for Functional Glycomics) were also bred with *cpk*

heterozygotes to yield double mutants on the C57BL/6j backgroud. Details of these two mutants are in chapter 4.

Following micro dissection tissues for immunohistochemistry were placed into 4% paraformaldehyde (PFA); tissues for protein and DNA analysis were placed into liquid nitrogen, tissues for cell culture were placed into L15 medium at 4^0C and tissues for electron microscopy were placed into 3% gluteraldehyde.

Kidney samples of various PKD models

Kidneys from different PKD mouse models were obtained to assess galectin-3 expression. 3 weeks old *cpk* mutants on Balb/c and DBA backgrounds, 3 weeks old *bpk* and 1 week old *orpk* mutant kidneys were obtained from Prof. Guay-Woodford and Dr. Yoder from the University of Alabama in Birmingham; adult *pkd2* mutant samples were kindly provided by Dr. Somlo. Human samples were obtained from Histopathology Department in the Institute of Child Health. Due to the limitation of resources, only one kidney was obtained per sample. All mice samples were obtained in wax block and the human samples were provided as histology sections.

Bpk model arose from a spontaneous mutation in an inbred colony of Balb/c mice and the disease is transmitted in an autosomal recessive fashion (Nauta *et al.*, 1993). Renal cystogenesis in this model is very similar to that of *cpk* mice. The three-week old *bpk* kidney samples has severe cystic lesion, similar to *cpk* mice. Renal cysts were also presented in adult *pkd-2* mutant mice (autosomal dominant inheritance, renal cysts develop in affected adults), with 40% of cysts derived from the collecting tubules (Wu *et al.,* 1998). *Orpk* model, which is another autosomal recessive PKD model, was developed as part of a large-scale insertional mutagenesis programme (Moyer *et al.* 1994). The *TgN737* gene codes for polaris is disrupted. Most mutants die at first week of age therefore 1 week old *orpk* kidney samples were examined. Similar to *cpk* model, the severity of cystic lesion depends on the genetic background. The

orpk samples obtained was on the FVB background, and at one week it did not have a gross renal cystic presentation.

Tissue culture

Cells

mIMCD-3 cells were obtained from ATTC (Middlesex, UK), a global bioresource centre with catalogue number CRL-2123. These cells were derived from the inner medullary collecting duct from a transgenic mouse (Rauchman *et al.*, 1993). These cells are commonly used an *in vitro* model of renal collecting tubules.

Media

Dulbecco's Modified Eagle Medium F12 mix (DMEM/F12) was supplied by Gibco BRL (Paisley, UK).

Media supplements

Sigma-Aldrich Corporation (Poole, Dorset, UK) supplied: insulin transferrin selenium (ITS), dimethyl sulfoxide (DMSO), human recombinant Epidermal Growth factor (EGF), antibiotics solution, hydrocortisone, triiodothyronine (T3) and paclitaxel. Gibco BRL (Paisley, UK) supplied the heat inactivated fetal calf serum.

Galectin-3 recombinant protein

Proteins used include: Recombinant hamster galectin-3 protein, Δ1-93, containing the C-terminal domain but lacking most of the N-terminal domain of full length galectin-3. A mutant protein, named SS, similar to full length galectin-3, except for a mutation, where residue Arg139 has been changed to serine (Mehul *et al.*, 1994). The recombinant protein was generously supplied by Dr

Colin Hughes and Suleman Bawumia, National Institute for Medical Research, Mill Hill, London, throughout the duration of this study.

Tissue culture plasticwares

Nunc (Roskilde, Denmark) supplied the petri dishes (30mm and 90mm), 6 well and 96 well plates.

Genotyping

cpk mice and *galectin-3* null mutant mice were genotyped by DNA amplification followed by polymerase chain reaction (PCR) using specific primers. Different genotypes were identified by the size and pattern of DNA bands in electrophoretic gel.

DNA extraction

Tail tips were collected from animals to be genotyped and DNA was extracted from them using the DNeasy kit (Qiagen, West Sussex, UK), which consists of DNeasy Mini Spin Columns, two washing buffers and an elution buffer. Procedures were carried out in accordance with the manufacturer's manual. The DNeasy kit uses advanced silica-gel-membrane technology for rapid and efficient isolation of total cellular DNA without phenol, chloroform, or ethanol precipitation. In the presence of ethanol, DNA binds to the DNeasy membrane, while contaminants such as protein and polysaccharides are efficiently removed by two wash steps. Pure DNA is then eluted in a small volume of low-salt buffer (provided with kit).

Polymerase chain reaction

Polymerase chain reaction were carried using HotstarTaq (Qiagen, West Sussex, UK) which includes buffer solution, solution Q* and magnesium chloride; dNTP PCR nucleotide mix (Promega, Southampton, UK), DMSO

(Sigma-Aldrich, Poole, Dorset, UK), MilliQ water and primers (MWG-Biotech AG, London, UK). Further information on primers as followed). Reactions were performed on DNA Engine DYAD^{TM} (GRI, Essex, UK).
* Solution Q is a PCR additive that facilitates amplification of difficult templates by modifying the melting behaviour of DNA, particular for those with a high degree of secondary structure or that are GC-rich.

Primers

Primers (MWG-Biotech AG, London, UK) were used for polymerase chain reaction to genotype *cpk* mice and galectin-3 mutant mice.
cpk primers were 5' TCCTCCCTCCCTATCTCTCCAT 3' and 5' ATCCAGCAGGCGTAGGGTCTC 3'(Hou *et al.*, 2002). These flank the 31bp deletion in exon 1 of cystin, and generate 351 or 320bp products from wildtype and mutant alleles respectively. Sequence provided by Prof. Guay-Woodford.

Galectin-3 genotyping for samples on the 129Sv and mixed background utilised two PCR reactions concurrently: galectin-3 primers were 5' CACGAACGTCTTTTGCTCTCTGG 3' and 5' TGAAATACTTACCGAAAAGCTGTCTGC 3' which produced a 305bp fragment only from wildtype alleles; neomycin primers were 5' CAAGATGGATTGCACGCAGG 3' and 5' TATTCGGCAAGCAGGCATCGCCA 3' which generated a 577bp product only from the mutant, neomycin-containing allele. Sequence provided by Dr. Francoise Poirier.

C57BL/6j Galectin-3 genotyping utilised two individual primers, with a common downstream primer of 5' CACTCTCAAAGGGGAAGGCTGACTGTC 3'; wildtype allele - 5' GTAGGTGAGAGTCACAAGCTGGAGGCC 3' which produced a 490bp fragment; mutant allele - 5' GGCTGACCGCTTCCTCGTGCTTTACGG 3' which amplified a 300bp segment from the Neomycin gene. Sequence provided by Prof. FT Liu.

DNA gel electrophoresis

Agarose gel electrophoresis was used to separate DNA fragments according to size. Electrophoretic graded agarose was provided by Gibco (Paisley, UK). Tris-Acetate-EDTA (TAE) buffer was prepared by making up a 50x stock (242g Tris base, 57.1ml Acetic acid and 100ml of 0.5M EDTA, all from Sigma, made up to 1 litre by adding ddH_2O and adjust pH to 8.5). DNA samples were loaded on to the gel using a 6x Type 1 gel loading solution (Sigma-Aldrich, Poole, Dorset, UK).

Electrophoretic gels were prepared using a gel tray and the process was performed using a Gel tank. 1 Kilobase (Kb) DNA marker was purchased from Gibco BRL.

Ethidium Bromide (Sigma-Aldrich, Poole, Dorset, UK) was used to visualise DNA bands in electrophoresis. It binds to DNA and fluoresces readily when exposed to ultraviolet light.

Molecular size markers

1 Kilobase (Kb) DNA marker was purchased from Gibco (Paisley, UK).

Protein extraction and quantification

RIPA buffer plus protease inhibitors were used to extract proteins from cells and tissue. RIPA buffer was made up of 150mM of sodium chloride, 1% nonident P-40 (NP-40), 0.5% sodium deoxycholate, 1% sodium dodecyl sulphate (SDS) and 50mM of Tris buffer. Protein inhibitors: Aprotinin, PMSF and sodium orthovanadate were used together with RIPA buffer. All reagents provided by Sigma-Aldrich (Poole, Dorset, UK). Eppendorf vial-shaped homogeniser was used to homogenise cultured cells. Sonicator was used to lyse cell membrane further.

BCA protein assay kit was purchased from Pierce (Northumberland, UK) and was used to quantify protein concentration. The BCA Protein Assay is based on bicinchoninic acid for the colorimetric detection and quantitation of total protein.

This method combines the well-established reduction of Cu^{2+} to Cu^{1+} by protein in an alkaline medium (the biuret reaction) with the highly sensitive and selective colorimetric detection of the cuprous cation (Cu^{1+}) using a reagent containing bicinchoninic acid. The purple-coloured reaction product of this assay is formed by the chelation of two molecules of BCA with one cuprous ion. The water-soluble complex exhibits a strong absorbance at 562 nm that is nearly linear with increasing protein concentration over a broad working range (20-2000 μg/ml). The macromolecular structure of protein, the number of peptide bonds and the presence of four particular amino acids (cysteine, cystine, tryptophan and tyrosine) are reported to be responsible for colour formation with BCA. Protein concentrations were determined with reference to standards of a common protein such as bovine serum albumin (BSA).

Lipid raft extraction

Lipid raft extraction was carried out using IMCD cells. Reagents used were 0.1% Triton X-100 (ice-cold), buffer B (50mM Tris/HCL, pH 7.4; 150mM NaCl; 5mM sodium vanadate; 1mM PMSF; and protease inhibitor cocktail (Roche, East Sussex, UK), Optiprep (Axis-Shield, Norway), which is a density gradient medium. It is a ready made, sterile and endotoxin tested solution of iodixanol, 5,5'-[(2-hydroxy-1-3 propanediyl)-bis(acetylamino)] bis [N,N'-bis(2,3dihydroxypropyl-2,4,6-triiodo-1,3-benzenecarboxamide], designed for the *in vitro* isolation of biological particles.

Other equipments used were tight-fitting Dounce homogenizer, 27-gauge needle, SW 50Ti centrifudge tube and L8-M ultracentrifudge (Beckman, High Wycombe, UK).

Mouse monoclonal anti-caveolin-1 (BD Transduction laboratories, Oxford, UK) was used as a marker for lipid raft.

Western Immunoblotting

Western blotting equipment

Mini-Protean II cell gel electrophoresis tank system (including glass plates and metal strips), trans-blot SD semi-dry transfer cell and Polyvinylidene diflouride membrane (PVDF) were purchased from Bio-Rad (Hemel Hempstead, UK), supplied by Gibco (Paisley, UK).

Gel electrophoresis

Gibco (Paisley, UK) supplied electrophoresis graded agarose. Sigma-Aldrich (Poole, Dorset, UK) supplied: 30% acrylamide, ammonium persulfate, TEMED, and X-ray film: Kodak X-OMAT AR. 3MM chromatography paper was supplied by Whatmann Ltd (Maidstone, Kent, UK). Amersham Pharmacia (Chalfont St.Giles, Bucks, UK) supplied nitrocellulse membrane: Hybond-N.

Buffers and reagent

SDS gel-loading buffer: 2x was prepared, it consisted of 1M Tris-HCL (pH 6.8), 4% SDS, 20% glycerol, 0.2%bromophenol blue and 200mM dithiothreitol. The SDS in the loading dye surrounds the protein with a negative charge and the β-marcaptoethanol prevents the reformation of disulfide bonds. It was used to denature protein samples prior to electrophoresis.

Running buffer: It was prepared in 5x the working concentration. The 5x solution consisted of 25mM Tris, 250mM glycine (pH 8.3) and 0.1% SDS made up to 1 litre with distilled water.

Transfer buffer: It consisted of 48 mM Tris, 39 mM glycine, 0.037% SDS, 20% methanol.

Ponceau S (Sigma-Aldrich, Poole, Dorset, UK) was used to detect protein bands on the nitrocellulose membrane. It is a sodium salt of a diazo dye that is

used to prepare a reversible stain of protein bands on nitrocellulose membranes. It stains protein bands pink which can be readily washed out with water.

Immunohisto/cyto-chemistry

Tissues samples were fixed, embedded and sectioned for immunohistochemistry; whereas cells grown on monolayer or in suspension culture were fixed and used for immunocytochemistry.

Equipment and chemicals

The following equipment was used: microtome, water bath, hot plates, microscope slides, coverslips. Reagents used were all provided by Sigma-Alrich: 3-aminopropyltreithoxysailane (TESPA), fluorescence mounting medium (DAKO), paraformaldehyde, bovine serum albumin, ethanol and histoclear.

Antibodies

Specific antibodies were used to detect antigens on tissue or cell samples. All antibodes were purchased from commercial companies, except anti-galectin-3 antibodies which was produced by Dr. Hughes and Suleman Bawumia, National Institute for Medical Research, Mill Hill, London.
The specific anti-galectin antibodies do not cross-react with other galectins, e.g. anti-galectin-1 antibodies do not react with galectin-3. The primary antibodies used during this thesis were raised against the following molecules, dilutions used for immunohisto/cyto-chemistry are listed:

Anti-galectin-1 goat polyclonal antibody (Cat#: AF1245, R & D Systems, UK). It was raised against *E.coli*-derived, recombinant mouse galectin-1. Galectin-1 specific IgG was purified by affinity chromatography. This antibody was tested to cross-react with human galectin-1. Dilution used for immunohisto/cyto-chemistry 1:100

Anti-galectin-3 rabbit polyclonal affinity purified antibody was kindly provided by Dr Colin Hughes and Suleman Bawumia, National Institute for Medical Research, Mill Hill, London, throughout the duration of this study.
This antibody was produced in rabbit and was raised against a full length hamster galectin-3 protein. The protein sequence of hamster galectin-3 is 89% identical to that of mouse and 83% identical to that of human. This antibody was previously shown to detect human and mouse galectin-3 (Bao and Hughes, 1995; Winyard *et al.*, 1997; Bullock *et al.,* 2001). Dilution used for immunohisto/cyto-chemistry 1:100; dilution used for western immunoblotting 1:250

Anti-galectin-4 goat polyclonal antibody (Cat#: sc-19286, Santa Cruz Biotechnology). It was raised against a peptide mapping within an internal region of human galectin-4. It cross-reacts with mouse and rat galectin-4. Dilution used for immunohisto/cyto-chemistry 1:100

Anti-galectin-9 goat polyclonal antibody (Cat#: sc-19294, Santa Cruz Biotechnology). It was raised against a peptide mapping at the carboxy terminus of mouse galectin-9. it cross-reacted with human and rat galectin-9. Dilution used for immunohisto/cyto-chemistry 1:100

Anti-acetylated tubulin monoclonal mouse antibody, (Cat#: 6-11B-1, Sigma-Aldrich). It was derived from the hybridoma produced by the fusion of mouse myeloma cells and splenocytes from an immunized mouse. Acetylated tubulin from the outer arm of Strongylocentrotus purpuratus (sea urchin) was used as the immunogen. The antibody cross-reacted with human, mouse, pig, bovine, rat, hamster, monkey, chicken and frog; as well as non-vertebrates protista and plants. Dilution used for immunohisto/cyto-chemistry 1:1000

Anti-γ tubulin monoclonal mouse antibody (Cat#: GTU-88, Sigma-Aldrich). It was derived from the GTU-88 hybridoma produced by the fusion of mouse

myeloma cells and splenocytes from an immunized mouse. A synthetic γ-tubulin peptide (N-terminal amino acids 38-53) conjugated to KLH was used as the immunogen. The antibody cross-reacted with human, bovine, dog, hamster, rat, mouse, chicken and Xenopus γ-tubulin. Dilution used for immunohisto/cyto-chemistry 1:1000

Anti-aquaporin 2 polyclonal rabbit antibody (Cat#: 22110201, Chemicon International, USA). This antibody was raised against highly purified peptide corresponding to residues 254-271 of rat or mouse Aquaporin-2 with an additional N-terminal lysine and tyrosine. The antibody was shown to react with human, rat and mouse aquaporin-2. Dilution used for immunohisto/cyto-chemistry 1:300

Anti-calbindin D-28K polyclonal rabbit antibody (Cat#: 22090345, Chemicon International, USA). It was raised against recombinant calbindin. Immunoglobulin was affinity purified and recognises human, rat and mouse calbindin. Dilution used for immunohisto/cyto-chemistry 1:100

Anti-ret polyclonal rabbit affinity purified antibody (Cat#: R787, Immuno-Biological Laboratories Co, Japan). It was raised against synthetic peptide for C-terminal of human c-Ret. It also cross-reacts with mouse and rat. Dilution used for immunohisto/cyto-chemistry 1:100

PCNA (proliferating cell nuclear antigen): (Cat#: 555566, Oncogene Science, Massachusetts, USA): mouse monoclonal antibody (IgG2) to the PCNA that is expressed at high levels during S phase. The antibody is conjugated with biotin. Dilution used for immunohisto/cyto-chemistry 1:100.

Pre-immune serum (Sigma-Aldrich). Rabbit IgG was used as negative control.

Secondary antibodies: Secondary biotinylated antibodies which combined anti mouse / anti rabbit IgG were included in the ABC kit (DAKO) and secondary

goat anti-rabbit horseradish-peroxidase (HRP) were purchased from DAKO. Fluorescent FITC (fluoroscein isothiocyanate) and TRITC (tetramethylrhodamine isothiocyanate) conjugated antibodies raised against rabbit and mouse IgG were purchased from Boehringer-Mannheim (Mannheim, Germany). Alexa Fluor Dye Series anti-rabbit, anti-mouse and anti-goat secondary antibodies were purchased from Molecular Probes, USA.

Specific Markers

Lectins; biotin conjugated lectins were obtained from Sigma-Aldrich. Lectins are proteins or glycoproteins, often derived from natural sources such as plants, which bind to specific carbohydrate residues. The specificities of lectins used in this thesis were: *Arachis hypogaea* (peanut) – β-gal(1-3)galNAc and *Dolichos biflorus* – α-galNAc. In the kidney, lectins can be used to identify different parts of the mature nephron. *Arachis hypogaea* specifically detects the collecting ducts and *Dolichos biflorus* specifically detects the ureteric bud and its derivatives (Holthofer, 1981 and 1984; Verani et al., 1989).

Periodic Acid- Schiff's (PAS) reagent (Sigma-Aldrich) was used to detect proximal tubules in kidneys. It labels brush border of proximal tubules pink.

In situ Cell Death Detection Kit, Fluorescein (Roche) was used to detect cells that underwent apoptosis. This kit detects cell death base on the TUNEL-reaction (Terminal deoxynucleotidyl Transferase Biotin-dUTP Nick End Labeling). Cleavage of genomic DNA during apoptosis may yield double-stranded, low molecular weight DNA fragments as well as single stand breaks, which can be identified by labelling free 3'-OH termini with modified nucleotides. This reaction is catalyzed by Terminal deoxynucleotidyl transerase (Tdt).

Haematoxylin and eosin (Sigma-Aldrich) were used to immunostain nucleus and cytoplasm respectively under light microscopy.

Propidium iodide (Sigma-Aldrich) was used to label the nucleus under fluorescent microscopy. It intercalates in the nucleic acid helix (both DNA and RNA) with a resultant increase in the fluorescence.

Detection reagents

ABComplex/HRP kit (DAKO). The avidin-biotin complex (ABC) was used to amplify the signal. It has proven to be an excellent and sensitive immunoassay technique. Avidin (reagent A), a protein found in egg white and certain bacteria, has an extraordinarily high binding affinity to biotin. It is a 68 kDa tetrameric glycoprotein composed of four identical subunits. Each subunit is glycosylated, and contains one binding site for biotin. Peroxidase (Reagent B) has been biotinylated with activated biotin. The reagent A and B were mixed together to increased the signal produced by the secondary antibodies; the avidin molecule that binds to the biotinylated secondary would have more then one peroxidase attached to it. And hence the signal is amplified. Peroxidase activity is then detected by colorimetric changes in DAB. Usage of the kit is in accordance to the manufacturer's guide.

3,3-diaminobenzidine tetrahydrocholride (DAB) buffer (DAKO) was used to indicate positive reaction under light microscopy. DAB is suitable for use in peroxidase-based immunohistochemistry. Upon oxidation, it forms an insoluble brown end product at the site of the target antigen.

Microscopy

Light and fluorescent microscopy was performed on a Zeiss Axiophot microscope (Carl Zeiss, Oberkochen, Germany) using objective lenses of 5x, 10x, 20x, 40x and 63x (oil immersion) magnification. Specimens were taken digitally using an Olympus Camedia C-3030Zoom Digital camera.

Confocal fluorescent microscopy was performed on a Leica Aristoplan microscope and computer confocal laser scanning system (Aristoplan-Leica, Heidleberg, Germany) with oil immersion objective lenses of 16x, 25x, 40x, 63x and 100x and software interpolation of intermediate magnifications. Images were saved as tagged image format (TIF) files and imported, for labelling, into Adobe Photoshop (Version 7.0, Adobe Systems Europe, Edinburgh, UK) or Microsoft Powerpoint 2000 (Microsoft Corporation, Seattle, USA). A dual-channel confocal instrument was used which was able to produce a single image of expression of two different proteins.

Dr Kerrie Venner prepared cystic kidney samples for scanning electron microscopy in the Electron Microscopy Department, Institute of Neurology (UCL, London). They were then examined on a Joel 100 CX transmission electron microscope.

Atomic force microscope, AFM (JPK Instruments AG, Germany) was housed in the Bone and Mineral Centre at UCL and operated under the supervision of Prof. Mike Horton and Dr. Belinda Haupt. AFM detects the surface of a sample with such a discriminating touch that it can sometimes even distinguish individual atoms on the surface of a crystal such as gold (Dufrene 2001; Charras *et al.,* 2001). It does this by raster-scanning a small tip back and forth over the sample surface. The tip is on the end of a cantilever, which deflects when the tip encounters features on the sample surface. This deflection is sensed with an optical lever: a laser beam reflecting off the end of the cantilever onto a detector that magnifies small cantilever deflections into large changes in the relative intensity of the laser light on the two segments of the

photodiode. In this way, the AFM generates a topographic map of the sample surface. See figure 8.1.

Figure 8.1. Simple diagram illustrating the principle of AFM.

The diagram below simply illustrates the components of an AFM. A cantilever is set to be in contact with the sample on the sample stage and it scans through the sample to give a topograph. A laser beam is adjusted to direct to the back of the cantilever and the beam is reflected to a detector. The movement of the cantilever can therefore be detected and measured as the beam reaches different points on the detector.

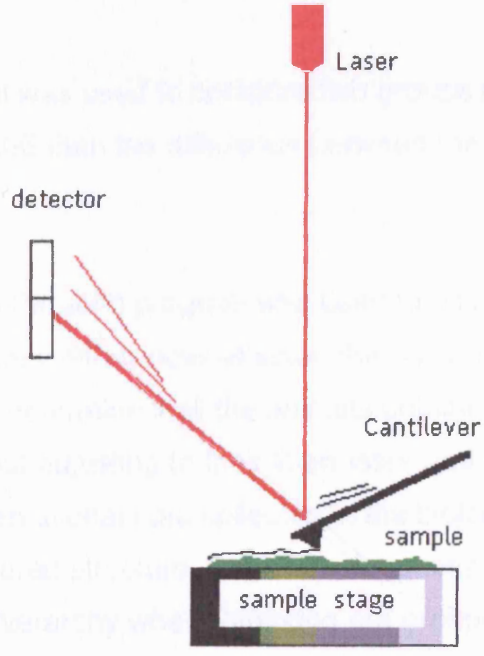

Statistical analysis

Microsoft Excel 2003, SPSS (Illinois, US) and MLwiN (Multilevel Modelling – Bristol, UK) were used to analyse data.

Chi-squared from MS Excel was used to see if the offspring followed Mendelian's Law of Inheritance, by comparing observed ratio of genotypes to the expected ratio (e.g. 1:2:1 ratio when assessing one locus). If the chi-square value is less than 0.05, than the outcome does not follow Mendel's Law of Inheritance.

t-test from MS Excel was used to compare two groups of samples. If the p-value is less than 0.05 than the difference between the two groups was significant.

Multilevel Modelling (MLwiN) program was used to assess inter-and intra-litter differences and if these differences affected the outcome of the results; and more importantly to determine if all the animals obtained could be analysed as one big group without adjusting to their littermates and parents. Many kinds of data, including observational data collected in the biological sciences, have a hierarchical or clustered structure. For example, animal studies of inheritance deal with a natural hierarchy where offspring are grouped within families. Offspring from the same parents tend to be more alike in their physical and mental characteristics than individuals chosen at random from the population at large.

CHAPTER 9: METHODS

Generation of *cpk*, galectin-3 double null mutants

Initially, *galectin-3* null mutants were obtained from our collaborator Dr. Poirier. These mutants were on the 129Sv background. They were crossed with *cpk* heterozygotes (on C57BL/6j background) to yield F1; from which double heterozygotes (*cpk* +/- *galectin-3* +/-) were selected by genotyping and intercrossed to yield offspring, some of which were cystic with various *galectin-3* genotypes. To obtain double mutants on a pure background, *cpk* allele was backcrossed 10 times to 129Sv animals, to give a genetic background difference of less than less than 0.2%. Double heterozygotes on the 129Sv background were intercrossed to yield double mutants. Because of confounders described later, *galectin-3* mutants on the C57BL/6j were imported and they were bred with *cpk* heterozygotes; as above, double heterozygotes were selected and intercrossed to yield double mutants on the pure C57BL/6j background. For the study of cystogenesis in animal with different *galectin-3* genotypes, all animals were sacrificed at 1 week because we predicted that *galectin-3* null mutant would have accelerated cyst growth. Their body and kidney weights recorded. The kidney/body weigh ratio was use as an indicator of cytogenesis. For each sample, the body weight was recorded before cervical dislocation; a tail tip was saved for DNA extraction and genotyping; the left kidney was carefully dissected out and stored on ice before weighing then stored at -70°C; the right kidney was dissected out and placed immediately in 4% paraformaldehyde (PFA – supplemented with calcium chloride and magnesium chloride) to preserve the kidney morphology structure, prior to sample embedment.

Cystic index of cortical cysts in kidneys.

A cystic index score was developed to quantify the cortical cystic level of each sample and to compare subtle differences in cystogenesis between cystic mice with different *galectin-3* genotype. This scheme grades cortical cysts as follows:

0 - no cysts; 1 - mildly dilated tubules/ducts only; 2 - occasional moderately dilated ducts and cysts; 3 – more frequent or larger cysts, or cysts extending to the edge of the cortex but with relatively well preserved architecture; 4 - frequent large cysts disrupting cortical architecture. Three sections were prepared from the mid section and outer quarters of each kidney and reacted with DBA, counterstained with PAS (see later on methods for immunhistochemistry); these were then photographed by a blinded observer, and scored by three blinded observers to generate a mean cortical cyst score for each sample.

Cell culture

Inner Medullary Collecting Ducts cells (IMCD3)

IMCD3 were used to assess the localisation of galectin-3 and other proteins such as acetylated tubulin. This immortalised cell line is derived from adult mouse kidney. They were preserved as frozen stock in liquid nitrogen. Prior to experiment these cells were thawed and plated into fresh medium.

Maintenance of cell culture

Aseptic technique was employed to ensure no contamination. All procedures were carried out in a sterile laminar flow hood. IMCD3 cells were grown in tissue culture flask in a 37°C incubator. Medium and PBS were warmed up to 37°C before use. To feed these cells, first the old medium was extracted carefully, and then the cells were washed three times with room temperature PBS by adding 3 to 5ml then gently shake the flask from side to side. The PBS was then discarded and fresh medium was added.

IMCD3 cells have to be split once they reach confluent growth, which took 2 to 3 days. The cells were split into 2 or 3 portions and each portion was plated into a new flask. Before splitting, the cells were washed with PBS three times as described above, and then they were dislodged by adding trypsin-EDTA

solution, 1 ml to a 25 cm^2 flask and 3 ml to a 75 cm^2 flask. The flask was then shaken gently sideways for no more then 30 seconds, followed by removal of all trypsin-EDTA solution and incubation at 37°C until cells are floating. This usually takes around 5 minutes. After checking that all the cells were dislodged under a microscope, they were collected in fresh medium into a falcon tube, and then centrifuged at 2000 rpm for 5 minutes. The supernatant was discarded and the cells were resuspended in 30 or 45 ml of fresh medium, this volume depends on the size of culture flask used. One third of the medium with suspended cells was plated into a culture flask.

Freezing and thawing cells

Immortalised cells can be preserved in liquid nitrogen. It is best to freeze cells when they were growing rapidly and just before reaching confluence. For monolayer culture, the cells were always fed a day before freezing. The cells were washed with PBS twice, followed by removal of the solution. Then they were dislodged using trypsin-EDTA as described above and then resuspended in 1 ml of 10 % DMSO in fetal calf serum. The cells were frozen down slowly by putting in a polystyrene box in -70°C overnight. Finally the frozen cells were transferred into liquid nitrogen.

To thaw the stock, the frozen cells were warmed up quickly by putting into a 37°C water bath. The thawed stock was then added dropwise to 10 ml of warm medium in a 25 cm^2 culture flask. The cells were added slowly to avoid osmotic shock. The cells were allowed to adhere for approximately 8 hours then the medium was changed to get rid of all DMSO which is toxic to cells.

Primary culture

Primary cultures of kidneys from *cpk* mice were carried out to grow collecting duct epithelial cells, as an *in vitro* model of *cpk* epithelial cells. In suspension, these cells form cysts within 24 hours (Woo *et al.* 1994). Whereas cultures from non-cystic kidneys did not form cysts after 24 hours. Primary cultures of normal kidney were also carried out in order to grow normal epithelial cells *in vitro*.

Three-dimensional suspension culture of *cpk* cyst

Suspension cultures were used to grow cysts *in vitro*. These cells came from 3-week old *cpk* -/- kidneys. The pair of kidneys was dissociated to give partially digested kidney cells, which were then cultured in suspension. The cultures were incubated for 24 hours (Woo *et al.*, 1994). For experiments involving the addition of taxol and/or galectin-3, these reagents were added before incubation. After 24 hours, the plate was assessed and at least 12 random fields were photographed. The photos were then evaluated for cyst number and size using computer software, Scion or ImageJ.
Details of experimental procedures are as follows.

Kidney dissociation:
3 week old *cpk* cystic animals were sacrificed and their kidneys were dissected and placed into ice-cold L15 medium with antibiotics. All subsequent procedures were performed in a tissue culture hood using aseptic techniques. The kidneys were gently cut by scalpels to release cyst fluid which was discarded. Then the tissue were cut into small pieces <2mm^3, which were transferred into 7ml of DMEM:F12 supplemented medium (see material), with 10mg/ml collagenase, 200mg/ml of dispase and 10mg/ml of DNase I. These enzymes dissociate cells to virtually a single cell dispersion and degrade released DNA, which contributes to cell clumping. The mixture was left for 30 minutes in a 37°C water bath with occasional shaking. Afterward, the suspension was spun at 2000 rpm for 5 minutes, and the supernatant discarded.

Plating cells:
The pellet was resuspended in 14ml of fresh DMEM:F12 supplemented medium by pipetting up and down. It was then left to settle for 2 minutes to allow large aggregates and tubules to settle to the bottom, afterward the top 12 ml containing single cells, small aggregates and tubule fragments was removed to a fresh tube. Next the number of viable cells was counted under a

haemacytometer. Viable cells were determined by mixing 10μl of tryphan blue with 10μl of cell suspension. Dead cells are permeable to the tryphan blue, and hence appear blue. The optimal plating cell density was 5 x 10^5 cells per ml. When required, the cell suspension was diluted to obtain the plating density. 2ml of cell suspension was plated on each well of a 6 well plate that was coated with 1% agar in cultured medium; the agar gel was used to stop cells from adhering to the plastic surface of the cultured plates. The cultures were incubated at 37°C in a moisture saturated incubator in 5% CO_2 and air for 24 hours (Woo *et al.,* 1994; Hillman *et al.,* 2004). The supplements added to the medium encouraged the growth of epithelial cells.

Culture assessment:

After incubation, cell growth was terminated by addition of 1ml of 4% paraformaldehyde in PBS with 1mM $CaCl_2$ and 1.5mM of $MgCl_2$. Calcium and magnesium prevent microtubule depolymerisation, which was useful when assessing microtubule organisation (e.g. acetylated tubulin in primary cilia). This step also fixed the cells for immunocytochemistry.

The plates were gently shaken to disperse the cells evenly across each well. After the cells had settled to the bottom, twelve random fields per wells were photographed using a digital camera attached to the microscope. The pictures were analysed using computer software, Scion or ImageJ, to determine the mean number and size of cysts per well.

Epithelial monolayer using *cpk* cells

Monolayers of *cpk* mutant cells were extracted from cystic kidneys and *cpk* wildtype and heterozygotes kidney cells were extracted from the medulla of non-cystic kidneys. These cells were grown to assess the localisation of galectin-3 and other protein (such as acetylated tubulin) by immunocytochemistry. The procedure employed here was very similar to that used in 3-D cyst culture. Instead of plating the cell on agar-coated plates, the dissociated cells were plated on glass cover slips or chamber slides to form

monolayers. For the growth of non-cystic kidney epithelia, only the medulla was cultured. The cortex was carefully cut out before partial digestion of the medulla. Due to the smaller size of these samples, they were incubated in the dissociation enzymes (collagenase, dispase and Dnase 1) for 20 minutes only instead of 30 minutes. The plating density of cells was 5×10^5 cells/ml.

Culture assessment:

The assessment of these monolayers are different to the 3-D cyst cultures: All monolayers were plated using DMEM/F12 medium with 5% serum and supplements until cells were adhered to the bottom. This usually took 24 hours, then the medium was changed to serum-free to discourage the growth of fibroblasts. Once islands of epithelial cells were grown, the serum free medium was changed everyday. Prior to the addition of fresh serum-free medium with supplements, the cells were washed twice with PBS to get rid of all the non-adherent cells and allow the continuous growth of the epithelial monolayer. Relatively big colonies of epithelial cells appeared after five days in culture, which at that stage they were fixed and immuno-stained. The cultures were kept for no more then 10 days as by that stage, a mixed population of cultures were seen and were beginning to be overgrown by fibroblasts.

Genotyping

The *cpk* and *galectin-3* genotypes of animals were determined. It was carried out by Polymerase Chain Reaction (PCR) using specific primers flanking the locus of interest. DNA was extracted from samples. After PCR, the genotype of an individual was determined by the size of the fragment and/or the presence or absence of fragments showed on an electrophoretic gel (see figure 9.1).

Figure 9.1. Patterns of DNA bands on electrophoretic gel indicating different genotypes.

Genotyping were carried out by PCR and the genotype of samples was distinguished by the size of DNA fragment obtained. Below pictures of two electrophorectic gels show the correlation between the size of DNA fragment and the *cpk* genotypes and *galectin-3* genotypes from the129Sv mutant.

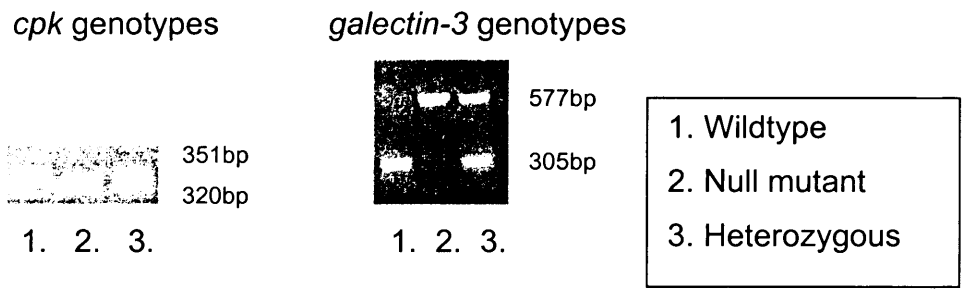

DNA extraction

DNA was extracted from the tail tip of the animals, around 0.3 mm tail tip of 4 weeks old mice or 0.5 mm tail tip of culled, pre-weaned mice were cut and stored in -20°C. All extractions were carried out using the DNeasy kit (Qiagen) and based on the protocol supplied with the kit. In some cases where tail tips were not available, ~ 25 mg of animal tissues were used instead.

Polymerase Chain Reaction

PCR was used to amplify DNA fragments that were size-specific to a particular sub-type of the *cpk* or *galectin-3* loci. The primers used were specifically designed (see Materials for sequence).

Both *cpk* genotyping and *galectin-3* genotyping were optimised by varying the primer concentration and dNTP concentration to determine maximum yield. Also the annealing temperature was optimised by running the reaction in a temperature gradient. The PCR reaction was initiated by incubating at 95°C for 15 minutes to activate the HotstartTaq polymerase.

For *cpk* genotyping, the reaction mix consisted of 41.6 μl of MilliQ water, 0.4 μl of dNTP, 0.4 μl of each primer, 100-500 ng of DNA, 1 unit of HotstartTaq polymerase, 1 μl of DMSO, 5 μl of buffer solution provided with the enzyme. And for *galectin*-3 genotype, the reaction mix was made up of 13.6 μl of milliQ water, 0.6 μl of dNTP, 0.4 μl of each primer, 100-500ng of DNA, 1 unit of HotstartTaq polymerase, 5 μl of solution Q provided with the enzyme kit, extra 1 mM of $MgCl_2$, 2.5 μl of buffer solution provided.

The first step of the cycle was DNA denaturing at 94°C for 30 seconds; followed by annealing for 30 seconds at 64°C for *cpk* genotyping and 57°C for *galectin-3* genotyping; then DNA replication was carried out at 72°C for 5 minutes. This cycle was repeated 30 times and was terminated by incubating at 72°C for 7 minutes to allow complete elongation of DNA fragments, followed by incubation at 4°C for storage.

DNA Electrophoresis

Agarose gel electrophoresis was used to separate DNA fragments according to size. This method is based on the fact that DNA molecules are negatively charged and that fragments of linear DNA migrate through agarose gels with a mobility that is inversely proportional to the $\log_{10}$ of their molecular weight.

Therefore the shorter the DNA fragment the further it runs through the gel. For this experiment, 1.5% agarose gel was used to separate DNA fragments produced by *cpk* genotyping and 1% agarose gel was used to separate DNA fragments yielded by *galectin-3* genotyping. The higher concentration used for *cpk* genotyping was due to the smaller difference between the two DNA fragments produced by the wildtype and null allele.

To make up a 1.5% gel or 1%, 1.5 g or 1g of agarose was dissolved in 100 ml of TAE buffer by microwaving at full power, 0.5 μg/ml of ethidium bromide solution was added as the agarose cooled to reduce the risk of ethidium bromide, which is an active carcinogen, from vaporising. It was then poured into a casting tray and the comb was inserted. The gel was allowed to set for around 30 minutes. Once set, the comb was carefully removed and the tray was placed in an electrophoresis apparatus, which was filled with enough TAE buffer to cover the gel. 7 to 10 μl of the DNA sample containing 1x blue loading dye was loaded into the wells. The gel was run at up to 100 volts and required a minimum of 45 minutes running time, according to the size of the fragment. The DNA fragments were visualised and photographed under UV light.

Protein extraction

Protein was extracted from cultured cells and kidneys for immunoblotting. RIPA buffer (150 mM sodium chloride, 1% nonident P-40, 0.5% sodium deoxycholate, 1% sodium dodecyl sulphate and 50 mM Tris buffer pH 8.0) plus protease inhibitors (66 μg/ml of aprotinin, 100 μg/ml of PMSF and 1 mM of sodium orthovanadate) were use to lyse cells and prevent protein degradation. RIPA buffer was stored at 4°C and protease inhibitors were added fresh to the buffer just before use.

Cell homogenisation

Cultured cells

Medium was aspirated from culture flasks and the culture was washed twice with PBS. 500 μl of ice cold RIPA buffer with protease inhibitors was added to the culture flask, using a cell scraper, cells were scraped off the flask and were transferred to a 1.5 ml eppendorf tube on ice. The cells, still on ice, were treated with intermittent sonication.

Kidney samples

Proteins were extracted from one or three weeks old normal and cystic kidneys. For three weeks old cystic kidneys, cyst fluid was first removed by gently pressing the kidneys with a scalpel. The fluid was collected and stored at -70°C for later use. Using two scalpels the kidneys were diced on a sterile plastic Petri dish in RIPA buffer with protease inhibitors; 700 μl was used for normal and one week old cystic kidneys, 1.5 ml was used for three weeks old cystic kidneys. The kidneys were cut into small pieces <2mm^3 and together with RIPA buffer was transferred into either a 1.5 ml eppendorf tube or a 2 ml eppendorf tube. The samples were placed on ice and were homogenised using a plastic homogenator specifically used with eppendorf to break the tissues down further, followed by sonication.

Sonication

Homogenised samples were sonicated to ensure all cell membranes were lysed. The probe was washed with distilled water before use. Samples were placed on ice during the process and were sonicated by placing the probe in solution. The samples were intermittently sonicated for no more than 5 seconds per stroke to avoid overheating which leads to the breakdown of the protein. Approximately 5 strokes were applied for each sample or until the solution went frothy.

Protein collection

The samples were certrifuged at 13000 rpm at 4°C for 30 minutes. Supernatant which contained protein was transferred to a fresh eppendorf and stored at -70 °C.

Protein quantification

Protein was quantified using a BCA (bicinchoninic acid) protein assay kit. Procedures carried out following the manufacturer guide. Protein samples were quantified using a 96 well ELISA plate

Preparation of BSA standards and working reagent

2 mg/ml of BSA was provided with the kit and was used to prepare a standard curve of known dilution: 2000 μg/ml, 1000 μg/ml, 500 μg/ml, 250 μg/ml, 125 μg/ml, 25 μg/ml and 0 μg/ml. BSA protein was diluted with PBS. Working reagents were prepared by mixing the two reagents provided (50 parts of A plus 1 part of B). 200 μl of working reagent was required for each sample, hence the total volume of working reagent required was calculated by multiplying 200 μl the number of tester samples plus 7 (the number of standard) plus 2 (spare).

Sample incubation and detection

Two hundred μl per sample or standard of working reagent was added into a 96-well plate. 25 μl of each sample or standard was added to the working reagent. The order and position of the samples was recorded for later reference. The plate was covered and mixed gently before incubation at 37°C for 30 minutes. After which the plate was cooled and the absorbance was measured at 560 nm on a plate reader.

Determination of protein concentration

First the standard concentration was plotted with MS Excel, with the absorbance (y-axis) versus the know protein concentration (x-axis). Using MS Excel, equation that showed the slope of the graph and the y-intercept was shown, e.g. y = 0.0003x + 0.0589. Using the equation, the protein concentration (value x) of each unknown samples was determined by substituting y with the absorbance.

Lipid raft extraction

Lipid raft extraction and fractionation was carried out in IMCD cells in order to assess the presence of galectin-3 in lipid rafts.
Lipid raft is a more ordered domain within the lipid bilayer, containing a high degree of tightly packed lipid acyl side chains. It is insoluble in cold detergent (1% Triton) thus making it feasible to be isolated. Due to its high lipid content, it floats to the top of a sucrose gradient during ultracentrifugation. In this thesis, commercially available Optiprep was used instead of sucrose.

Confluent IMCD cells were harvested in cold PBS with a cell scrapper and pelleted by centrifugation at 3000rpm for 5 minutes. The cell pellet was resuspended in 1% triton X-100 in cold buffer B (see Material for constituents) and incubated for 30 minutes on ice. The cells were then homogenised with 10 strokes of a tight-fitting Dounce homogenizer followed by 3 passages through a 27-gauge needle. The homogenates were adjusted to 35% Optiprep and 600μl the solution was placed at the bottom of a SW 50Ti centrifudge tube beneath a discontinuous gradient (0% to 35%) of Optiprep. There were a total of three layers: the bottom layer was the cell homogenates/ 35% Optiprep, the middle layer was 2400 μl of 30% Optiprep and the top layer was 700 μl of buffer B. Each layer was added slowly along the side of the tube to avoid mixing. Dilution was made with buffer B. The tube was then weighed and a second centrifuge tube was adjusted to the same weight. It was very important to have the two tube to the exact same weights as they have to balance each other during the

ultracentrifugation. The two tubes were carefully placed into the appropriate tube holders which were then securely placed into a Beckmann SW 50Ti rotor. The samples were centrifuged at 200,000 x g for four hours at 4°C. Afterward, the content in the tube was divided into ten fractions; starting from the top 370 μl was carefully pipetted out. The interface between the top and the middle layer (fraction 3) contained lipid raft proteins. The ten fractions were then used for western blot analysis (see below), a marker was loaded to the first fraction due to space limitation on the gel, which only contains 10 wells. Western blotting was carried out using antibodies against galectin-3 to determine which fractions the protein could be found; and anti-caveolin-1 as a marker for lipid raft.

Western Immunoblotting

Western blot analysis was used to detect the presence of a particular protein in a mixture of any number of proteins while giving information on the size of the protein. This method depends on the use of a specific antibody directed against a desired protein. Process in brief: proteins were extracted from tissue or cultured cells; the proteins were then separated using SDS-polyacrylamide gel electrophoresis, which separates the proteins by size; protein bands were transferred to a nitrocellulose membrane; specific proteins were detected by incubating the membrane with specific antibodies and detection reagents.

Details of procedures are as follows:

Setting up gel apparatus

For this equipment, two gels need to be run together whether they contain any samples or not, therefore two sets of glass plates are needed.
Electrophoresis glass plates and racks were washed in distilled water then with 70% ethanol and dried completely. The glass plates and metal strips were assembled in the rack in the correct orientation (large glass first, then metal strips on each side and the smaller glass placed on top). The metal strips were

pushed to the side and bottom and the rack were tightened. The racks were then clicked into apparatus stand. 70% ethanol were poured in between the glass slides to ensure no leakage, after that, all solution were poured out and the glass slides were dried with 3MM paper.

Preparation of gels

Resolving gel

Twelve % resolving gels were used in this study. Fifteen ml of resolving gels were prepared each time to make up two gels. It consisted of 4.9 ml of distilled water, 6 ml of 30% acrylamide mix, 3.8 ml of 1.5M Tris pH 8.8, 0.15ml of 10% SDS 0.15 ml of 10% ammonium persulfate (made up fresh) and 6µl of TEMED (added last as it caused polymerisation). Using a pipette, 7 ml of resolving gel was poured slowly in between each set of the glass plates. On top of resolving gel water-saturated butanol (50% butanol and 50% distilled water, left overnight to separate into two distinct layers) was added, which removed any air bubbles which inhibits polymerisation and will ensure a flat gel meniscus. It took approximately 40 minutes to an hour for the gel to set; this was checked by observing the remaining gel which was not used. Once set, butanol was poured off and the area above the gel was washed with distilled watered and dried with 3MM paper, being careful not to damage the resolving gel.

Stacking gel and combs

Ten ml of 5% stacking gel was prepared for each set-up. It consisted of 6.8 ml of distilled water, 1.7 ml of 30% acrylamide mix, 1.25 ml of 1.0 M Tris pH 6.8, 0.1 ml of 10% SDS 0.1 ml of 10% ammonium persulfate and 10 µl of TEMED. Stacking gel was carefully pipetted on top of the resolving gel to the top of the glass plate. Combs were placed into the stacking gel by first putting one side over the metal strip at the side and then gently glided the comb into the gel. Care was taken to ensure no trapped air bubbles. It took approximately 1 hour for the stacking gel to set, this again was checked by observing the unused

stacking gel. The gel was either prepared for immediate use or made up the night before, wrapped in cling film and stored at 4°C.
Combs were removed from the gels, which together with the racks were transferred into a holder and were placed vertically into an electrophoresis tank. Running buffer (see chapter 7: Materials for details) was poured into the centre of the holder, in the area between the two gels and outside the holder in the tank. Checks were carried out to ensure that there were no leaks and no air bubbles in wells.

Protein denaturing

Forty to 50 μg of protein sample was loaded into 1.5 ml eppendorf tube and an equal volume of 2x electrophoresis buffer was added to each sample. The samples were then heated to 95°C for 5 minutes to denature the proteins and unfold them completely and were placed on ice afterward for another 5 minutes. Denatured protein samples were stored in -70°C for future use or kept on ice for loading in the same day.

Sample loading and electrophoresis

Twenty to 40 μl of denatured protein samples were loaded into the wells. Care was taken to ensure no spillage of samples into adjacent wells. The dense sample solution will sink in buffer solution and sits onto the gel surface, forming a sharply defined layer. 12 μl of marker was loaded to allow comparison of protein bands later. Unused wells were filled with an equivalent volume of blank sample buffer.
The electrophoresis apparatus was connected to the power pack in the correct orientation. 140 mV was applied to the apparatus for 40 minutes for detecting galectin-3: by this point the protein travelled to the middle of the stacking gel.

Electroblotting

Semi-dry electroblotting was used to transfer proteins from the gel to a nitrocellulose membrane. The electrophoretic apparatus was carefully dismantled and the two glass plates were separated carefully without breaking the gel, which was transferred to distilled water for a quick rinse before immersing it in transfer buffer (see chapter 7: Materials for details). 6 pieces of 3MM paper and a protein transfer nitrocellulose membrane (Hybond C) were cut to slightly bigger than the gel. They were all placed in transfer buffer before use. On the semi-dry transfer apparatus, three pieces of 3MM paper were placed first, followed by the membrane and the gel. Before a new layer was put on top of the last one, air bubbles were removed by rolling a pipette over the papers/ membrane. This was done because air bubbles would stop the current from going across the gel. Sellafilm was placed around the outside of the gel so that electric current was run efficiently through the gel to the membrane. On top of the gel, three more layers of 3MM papers, again using a pipette to eliminate air bubbles. The lid was placed on securely and the transfer took place at 12V for 60 minutes. After this step the apparatus was dissembled, the membrane was inspected for adequate transfer by checking the transfer of marker. No component of the marker should be left on the gel. Experimental details and marker bands were marked on the membrane. The membrane was placed in PBS.

Staining with Ponceau S solution

The membrane was immersed in Ponceau S solution for 1 minute, then washed with distilled water. For most cases, a smear of protein bands were observed. These band patterns were photographed for later reference. The membrane was then washed with distilled water using a rotating platform until all Ponceau S staining was washed off. After that, the membrane was carefully placed into a 50 ml falcon tube with PBS.

Blocking non-specific binding directly to the membrane

Some antibodies can directly bind to the membrane, therefore available site was blocked to eliminate non-specific false positive reaction. This was done using a blocking solution (5% skim milk, 0.3% Bovine Serum Albumin and 0.2% Tween-20), which was usually prepared fresh and can be kept at 4°C for 3 days. The membrane was immersed in blocking solution and was placed on a rotating mixer for a minimum of 30 minutes at room temperature, although membranes were often blocked for overnight at 4°C because of time-limit.

Incubation with antibodies

Primary antibody was diluted in blocking solution, the dilution used for each antibody is listed in chapter 7: Materials. 5 ml of this solution was prepared per membrane. Blocking solution was poured out of the falcon tube and primary antibody was added. For the detection of galectin-3, anti-galectin-3 antibody was incubated at room temperature for 2 hours. After the reaction, the membrane was washed three times in PBS-0.2% Tween for 15 minutes each then incubated with blocking solution again for 20 minutes in room temperature. Secondary antibody (again diluted in blocking solution) was incubated for 30 minutes at room temperature. After that, the membrane was washed three times with PBS-0.2% Tween for 15 minutes each and once in PBS for 15 minutes.

Signal detection

Luminol ECL reagent was used to detect signal. The two solutions (A+B) were mixed by adding an equal volume of each into a 15 ml falcon tube. Prepare 2 ml of working solution for each blot. The membrane was carefully removed from the tube and was placed face up to dry. ECL was added directly onto the membrane and was incubated for 1 minute. ECL solution was poured off and the membrane was placed in a developing cassette in between two clear plastic sheets. The following steps were carried out in the dark room to avoid exposing the X-ray films. In the dark, an X-ray film was placed in the cassette

on top of the membrane. One corner of the film was cut to mark the orientation of the film and the film was place to the edges of the cassette so that the film and membrane could be aligned after development. The film was exposed to the membrane for various length of time, usually starting with 30 seconds. And based on that initial result, exposure time was adjusted to increase or decrease the signals. The HRP reaction only lasts for 1 hour maximum. After exposure, the film was developed then it was aligned to the membrane and the marker bands were marked on the film.

Immunohisto/cyto-chemistry

Immunohistochemistry and immunocytochemistry were carried out to detect the presence of specific antigens in tissues. In brief, fixed tissue or cells on a microscope slide reacted with a primary antibody specific to the protein of interest. The preparation was then treated with a secondary antibody that was coupled to the enzyme, horseradish perosidase (HRP) and was directed against the primary antibody. It was then treated with a chromogenic substrate (DAB) which reacted to HRP. A positive reaction was indicated by the development of a colour which signified the presence of the protein. Alternatively, the secondary antibody was directly coupled to a fluorofluor which was visualised under a fluorescent microscope or a confocal microscope. Microscopic examination revealed the presence of labelling, and hence of the specific protein to be detected.
Immunohistochemistry was carried out on mouse tissues unless otherwise stated.
Details of experimental procedures are as followed:

Repetition of samples

For most samples examined, at least 3 individuals from the same group were examined unless otherwise stated.

Tissue fixation

Kidneys and sometimes other tissues were harvested and were put immediately into 4% paraformaldehyde (PFA) for 1 to 24 hours to preserve the tissue morphology and to confer chemical stability on the tissue by covalently cross-linking adjacent amino acids. For immunocytochemistry, cells grow in monolayer or in suspension were fixed with 4% PFA with calcium and magnesium for 20 minutes. The ions were added to maintain microtubule stability especially when detecting primary cilia.

Tissue embedment

Tissues were embedded in wax in order to preserve them permanently as specimen blocks and to obtain sections for immunohistochemistry. Fixed samples were washed twice with PBS. They were then dehydrated through an increasing ethanol gradient at room temperature: 30%, 50%, 70%, 85%, 95% and 100% twice. The solutions were changed every 30 minutes. Next the samples were immersed in Histoclear, twice for 30 minutes each, followed by a 1:1 Histoclear:wax at 60°C for 1 hour. The samples were then submerged into wax three times for 30 minutes each at 60°C. Samples were then transferred to a mould, where they were oriented and the wax was allowed to set.

Sectioning

Sections of 3 – 5μm in thickness were cut using a microtome. These sections were floated on a 45°C water bath to allow the tissue to un-crease. The sections were then picked up on either electrostatic glass slides or on glass slides that were treated with TESPA (aminopropyltriethoxysilane), which form a strong adhesion to the tissue. Slides were dried at 37°C overnight and stored at room temperature.

Rehydration and pre-treatment

Sections were first dewaxed and rehydrated. The slides were placed in a rack and sequentially passed through Histoclear twice for 5 minutes each to fully dewax the tissues. Then the sections were passed through a graded ethanol series of 100% twice, 90%, 80%, 70% and 50% either for 5 minutes each or several seconds with agitation, followed by washing in running tap water.
The next step was to permeablise the cells to improve antibody penetration. This was achieved by microwaving the sections, which was reported to cause antigen unmasking (Shi *et al.* 1991). A pressure cooker was filled with citric buffer (2.1g Citric Acid in 1 litre milliRo water, adjusted to pH 6.0 with sodium hydroxide). The buffer was heated up by microwaving in full power for 5 minutes. Then the hydrated slides were transferred into the buffer and microwaved at full power for another 5 to 6 minutes depending on the number and type of specimens. Slides were then left to cool by adding running tap water before washing in two short dips of MilliRo water followed by immersing in PBS/Tween, twice, for 5 minutes each. A wax ring was drawn surrounding each section to prevent spillage of solution in subsequent steps.

Blocking steps

The following two steps were designed to reduce background caused by endogenous peroxidase and non-specific binding. Before using horseradish peroxidise (HRP) in immunohistochemistry it was necessary to quench any endogenous peroxidase that was present in the tissue sections. In particular in kidney proximal tubules where a detectable level of peroxidase was present. Quenching was achieved by immersing slides in 3% hydrogen peroxide(H_2O_2) in PBS-0.1% tween-20 for 15 minutes in room temperature and then washed three times in PBS for 5 minutes each.
Non-specific binding was eliminated by incubating the slides in 5% fetal calf serum in PBS or 1% bovine serum albumin for 30 minutes in room temperature. At the same time, a humid chamber was prepared with PBS-soaked tissues. Blocking solution was tapped off prior to the addition of primary antibodies.

Primary antibodies

The dilution of the primary antibodies differ from 1:50 to 1:1000 in blocking solution depending on the antibodies used, optimum concentration was determined in preliminary experiment where varying concentrations (1:50, 1:100, 1:200, 1:500 and 1:1000) were used. This reaction took place in a humid chamber either overnight at 4°C or at 37°C for 1 hour. After incubation, the slides were washed three times with PBS-Tween, 5 minutes each. The concentration of each antibodies used can be found in chapter 7: Materials.

Secondary antibodies

For light microscopy analysis, the signal was amplified with the commercial avidin-biotin conjugate (ABC) kit. The biotinylated secondary antibodies were applied in 1:100 or 1:200 dilution depending on the antibodies and samples, for 30 minutes at room temperature. Followed by washing with PBS/Tween for three times 5 minutes each.

For fluorescent immunohistochemistry, fluorescent secondary antibodies were added directly onto primary antibodies, usually in 1:100 dilution for 1 hour room temperature or at 4°C overnight. These slides were then washed three times in PBS/Tween for 5 minutes each and were ready for mounting.

Avidin Biotin Complex/ ABComplex-HRP kit

ABComplex/HRP (mixture of reagent A and B) is applied to the samples after excess secondary antibodies were washed off. The samples were incubated with the ABComplex/HRP for 20-30 minutes, followed by washing with PBS/Tween 3 times.

Detection

3,3-diaminobenzidine tetrahydrocholride (DAB) solution was used to produce a coloured end product. It was directly applied onto the sections. Colour development was monitored either microscopically or directly by naked eye. Development was terminated when a brown colour developed by placing the slides in running water for 5 mintues. The time for colour development was kept constant when assessing different samples with the same antibodies, so immunostaining intensities can be directly compared.

Counterstaining

Counterstaining was performed to define the anatomy/histology of samples and help identify cells that expressed the antigen of interest and its location. Dolichos bilforus agglutinin (DBA) was commonly used to identify collecting tubule or the origin from it in kidney samples. Haematoxylin and/or eosin were usually used; the former stains nuclei dark purple and the latter stains cytoplasm pink. And for some kidney samples, periodic acid – Schiff's (PAS) reagent was performed before haematoxylin, it stains brush border of kidney proximal tubules pink. For samples that were counterstained with PAS, no eosin staining was carried. For fluorescent staining, some samples were counterstained with propidium iodide, which stains the nucleus red. Following describe the procedures involved in carrying out these counterstainings.

Dolichos bilforus agglutinin (DBA), lectin

For staining collecting ducts, the slides were incubated in 1:100 dilution of biotinylated *Dolichos bilforus* agglutinin (DBA) for 30 minutes in room temperature or in 4°C overnight. Wash the samples 3 times in PBS for 5 minutes. The biotin was detected by incubation in streptavidin-peroxidase mix (A/B solution from the ABC kit) for 30 minutes in room temperature, followed by washing in PBS for 5 minutes. The samples were again washed 3 time in PBS followed by immersing in DAB solution, which produces a brown precipitate

through reacting with the A/B mixture and this reaction can be monitor by the naked eye or microscopically. The colour was usually developed between 1 and 5 minutes, after that the slides were washed in running tap water. The time for colour development was kept constant when assessing different samples, therefore immunostaining intensities could be directly compared.

Haematoxylin/ eosin

The slides were submerged in reagent for 30 seconds to 2 minutes in room temperature, depending on the concentration of the reagent. Then washed in running for 10 minutes.

Periodic Acid Schiff's (PAS) reagent

PAS reagents were stored at 4°C. They were allowed to warm up to room temperature before use. The staining was carried in a fume hood at room temperature. Slides were immersed in periodic acid solution for 5 minutes. They were then rinsed several times in distilled water, followed by immersing in Schiff's reagent for 15 minutes and washing in running tap water for 5 minutes.

Propidium Iodide

Propidium iodide is commonly used as a red-fluorescent marker that binds to DNA. It is applied onto section in 1:5000 dilutions for 5 minutes at room temperature. Followed by washing with PBS/Tween 3 times for 5 minutes each.

Dehydration and mounting

Slides were dehydrated by passing through solutions of increasing ethanol concentrations from 50%, 70%, 80%, 90% and 100% twice either 1 minutes each or several seconds with vigorous agitation, then the slides were submerged in Histoclear twice for 5 minutes each. After drying the slides were

mounted in DPX solution and covered with glass coverslips. They were stored away and were observed using a light microscope.
Slides stained with fluorescent antibodies did not require to be dehydrated. These slides were mounted using fluorescence mounting medium and the glass coverslips were sealed with nail vanish, which held the coverslips and avoided mixing of the glycerol and the oil when used oiled lens. They were then stored in the dark at 4°C and were examined within three to five days.

Negative control

Negative controls were used to evaluate non-specific immunostaining and allow better interpretation of specific immunostaining at the antigen site. All slides had a section that was not reacted with any primary antibodies, instead PBS-Tween was used. This allowed assessment of background levels. In some cases, primary antibody was preabsorbed with an excess (10:1 weight/weight) of immunising peptide before applying to sections; that pre-immune antibodies were applied. This allowed assessment of the specificity of each antibody.

Double staining using fluorescent antibodies

In most fluorescent immunochemistry, two different isotopes were stained together, i.e. in looking at the localisation of galectin-3 and γ-tubulin and determine whether the two proteins are expressed at the same location. In this case, the two primary antibodies used were derived from two different types of animal, hence, rabbit anti-galectin-3 antibodies and mouse anti-γ-tubulin antibodies. And the two secondary antibodies were conjugated to different fluorescent marker, goat anti-rabbit-FITC (green) and goat anti-mouse-TRITC (red). These slides were examined using the confocal microscopy and the images were processed with a computer programme called Leica Confocal Software (LCS).

Determination of proliferative index on histological samples

A PCNA antibody was used as a marker for proliferating cells.
Kidney histological samples were immunostained with antibodies against PCNA for 1 hour at 37 °C and they were counter-stained with haematoxylin. After mounting, they were examined and counted blind using light microscopy. For each sample 20 cysts, approximately 600 cystic epithelial cells were counted per sample. Proliferative Index (PI) was measured as a percentage of PCNA positive cells over the total number of cystic epithelial cells. All samples were processed at the same time to ensure consistency in signal intensity.

Determination of apoptotic index on histological samples

Apoptotic cells were detected using the *In Situ* Cell Death Detection kit, Fluorescein, which is based on the TUNEL technology. Reaction was carried out according to manufacturer's protocol. The kidney sections were treated with trypsin (30 minutes at 37°C) before the labelling with TUNEL reaction mixture (1 hour at 37°C), then the samples were counterstained with propidium iodide. Each sample was photographed using a confocal microscopy with a 40X lens. At least 10 fields were taken for each kidney, for which the number of positive apoptotic cystic epithelial cells and the total number of cystic epithelial cells in each data point were counted. Approximately 700 cystic epithelial cells were counted per sample. Apoptotic index was expressed as a percentage of apoptotic bodies over the total number of cystic epithelial cells counted.

Immuno-staining for the presence of extracellular galectin-3 in primary cilia.

The sub-cellular localisation of galectin-3, in particular in primary cilia, was assessed by immunocytochemistry of non-permeablised IMCD cells. The primary antibodies (anti-galectin-3) were incubated to live cells, as fixation caused a slight permeablisation (as previously tested). IMCD cells were grown to confluency in 4 wells chamber slides and were allowed to ciliate. Prior to

immunoreaction with anti-galectin-3 antibodies, the cells were gently washed with room temperature PBS three times then they were cooled to 4°C. Primary antibodies were added to the samples and were incubated at 4°C for two hours. The samples were then washed five times with PBS and fluorescent secondary antibodies (anti-rabbit) were added and incubated at 4°C for one hour; followed by 5 washes with PBS. The samples which were immunostained for extracellular galectin-3 were then fixed using 4% PFA for 20 minutes. The purpose of this experiment was to detect extracellular galectin-3 on the primary cilia, therefore the organelle were marked out using anti-acetylated tubulin antibodies. For this, the cells were permeablised with 0.5% Triton for 10 minutes so that the antibodies could gain assess to the tubulin structure of the primary cilia. The samples were then incubated with anti-acetylated tubulin antibody for 1 hour at room temperature, followed by three washes with PBS-Tween and incubation with fluorescent secondary antibodies (anti-mouse). The samples were then washed three times with PBS-Tween. Excess solution was poured off and the samples were mounted with fluorescence mounting medium; covered with glass coverslips and sealed with nail vanish. The samples were then examined under a confocal microscope.

Quantification of galectin-3 expression in renal epithelial cells

The expression of galectin-3 in normal collecting tubules and in cystic epithelial cells were compared, in order to determine any difference in the level of expression. The expression level was reflected by the immunostaining intensity following immunofluorescence staining. The intensity was quantified using the Leica Confocal Software (LCS). Cystic and normal kidney samples were immunostained for galectin-3 at the same time using the same concentration to ensure consistency. At least 10 frames per samples were recorded using the same intensity of laser beams under the confocal microscope. The intensity of galectin-3 expression was measured by tracing the epithelia; the expression profile of the trace, which represented cystic epithelia or normal tubule, was automatically generated by the LCS.

The profile showed the mean, maximum and minimum amplitude of a given trace. The amplitude reflected the immunostaining intensity, thus mean amplitude was a measurement of the mean galectin-3 expression among a group of cells marked out by the trace and the maximum amplitude was the level of expression of the most intensely stained point. The trace line (ROI in figure 9.2) was manually drawn on the computer image by tracing a tubule or cyst. The mean and maximum amplitude was use to compare the level of galectin-3 expression.

It is worth noting that this is a very crude method for determining the level of expression and that it did not take into account the amount of secreted protein.

Figure 9.2. Illustration of staining quantification using Leica Lite software.

A) shows the traces of immuno-stained cysts for measurement. The five traces were represented as RO1 to RO5, in different colour. B) is a graphic representation of the immunostaining intensity of the five traces in A. Each trace was represented by a colour. C) shows the measurements of the traces in A. The amplitude reflected the immunostaining intensity, thus mean amplitude was a measurement of the mean galectin-3 expression among a group of cells marked out by the trace and the maximum amplitude was the level of expression of the most intensely stained point. The mean and maximum amplitude was use to compare the level of galectin-3 expression.

A

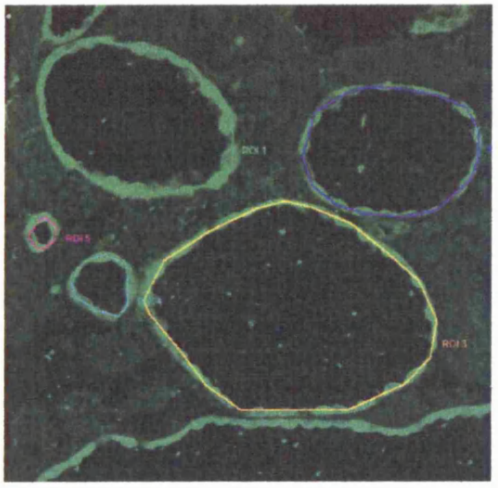

B

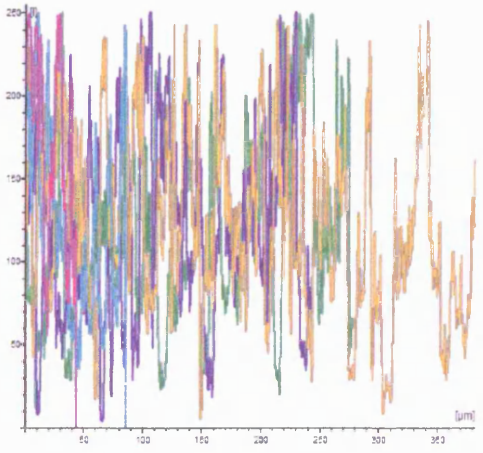

C

	ROI 1	ROI 2	ROI 3	ROI 4	ROI 5
Length	277.20 µm	243.31 µm	381.45 µm	86.00 µm	43.39 µm
Mean Amplitude	121.47	124.77	125.45	125.19	172.73
Max. Amplitude	255	255	250	255	254
Min. Amplitude	12	4	5	0	0
Average Deviation	43.53	47.69	44.98	48.28	54.42
Standard Deviation	54.58	58.01	54.44	58.03	61.59
Variance	2979.36	3364.82	2963.91	3367.74	3792.83

Microscopy

Atomic force microscopy

Atomic force microscope (AFM) works were carried out in this thesis in order to find a novel approach to study primary cilium in culture.
The works were carried out in collaboration with Prof. Mike Horton and Dr. Belinda Haupt at the Bone and Mineral Centre at UCL. IMCD cells were cultured to confluency and were fixed with 4% PFA. For the examination of dried samples, the cells were washed three times with distilled water after fixation to avoid the build up of salt crystals, which can be detected by the cantilever of the AFM and interfere with the image outcome. For wet examination, the samples were incubated in PBS after fixation. A wax ring was drawn around the samples to hold the PBS while the cantilever scanned across the cells.
Topographs were obtained that showed the size and shape of primary cilia on the surface of the cells.

Scanning electron microscopy

Scanning electron microscopy, SEM, was used to observe primary cilia in cystic kidneys. The work was carried out in collaboration with Dr. Kerrie Venner. 3 weeks old *cpk* kidneys were dissected and immediately placed in 3% glutaraldehyde/0.1M sodium cacodylate/5mM calcium chloride and were given to Dr. Venner for further processing. The samples were manually chipped into 2-3mm pieces under liquid nitrogen and then passed through distilled water, and 1% Osmium Tetroxide to 100% ethanol. Critical point drying was then performed and samples mounted on aluminium stubs before overnight vacuum drying. They were then gold coated and imaged with a Jeol JSM-35CF scanning electron microscope

Statistical analysis

For the *in vivo* study of cystogenesis in animals with various *galectin-3* genotypes, large amounts of data were obtained (approximately 200 per group of experiment). Data recording, sorting, analyses and graph preparations were all carried out using MS Excel. Multilevel Modelling (MLwiN) program was used to assess inter- and intra-litter differences.

Error bars presented in results represent standard error (SE).

CHAPTER 10: RESULTS

The results of this thesis are organised into four groups: expression of galectin-3 in kidneys of *cpk* and other PKD models; effects of *galectin-3* mutations on cystogenesis *in vivo*; expression of galectin-3 on the primary cilium of renal epithelial cells and the effect of paclitaxel on the cystogenesis of *cpk* mice. All these results support the hypothesis that galectin-3 is important to the development of renal cysts, and more importantly these results suggest that galectin-3 suppresses cystogenesis and may act via the primary cilium.

EXPRESSION OF GALECTIN-3 IN *CPK* KIDNEYS

Galectin-3 is normally expressed in the collecting tubules of the kidneys. It was previously reported to be up-regulated in human renal cystic disease. The protein is also implicated in renal development in a strictly regulated fashion (Winyard et al 1997, Bullock et al 2001). Here the expression of galectin-3 in a PKD model, *cpk* mouse, is investigated.

Persistent expression of galectin-3 in the renal cystic epithelia of *cpk* mice

Examination of several (n > 5) normal adult kidney tissue showed that galectin-3 expression occured in the collecting tubules in the cortex (fig. 10.1A). These expression patterns overlapped with that of DBA (black arrows fig. 10.1B) and not with PAS (pink arrows in fig. 10.1A), which indicated that galectin-3 was expressed in the collecting tubules and not proximal tubules. The protein was also expressed in the urothelium of the renal pelvis (* in fig. 10.1C). Cystic kidney samples of *cpk* mutant on B57BL/6j background at 1 week and 3 weeks were examined. In both age, galectin-3 was found in almost all cystic epithelia (fig. 10.1D, 1F, 3A –3D) derived from the collecting tubules as confirmed by DBA staining (fig. 10.1E). These results agree with those previously observed, confirming the expression of galectin-3 in collecting tubules of normal kidney

and in human cystic epithelia (Winyard *et al.*, 1997; Bullock *et al.*, 2001). As a negative control, the antibody staining was performed on *galectin-3* null mutant samples which showed no positive signal (fig. 10.1G).

Galectin-3 exhibited a predominantly cytoplasmic expression in both normal and cystic samples.

Intracellular expression of the galectin-3 in normal and cystic samples was carried out by immunoflorescent staining and confocal microscopy. Examination revealed that galectin-3 was expressed in the cytoplasm of the epithelial cells, with a small proportion of cells expressing the protein apically in both normal and cystic samples (white arrows in fig. 10.2C and 10.3C). The intensity of cytoplasmic staining varied between cells and was barely detectable in a small number of cells (fig. 10.3B). Negative control was performed using pre-immune rabbit IgG on cystic kidney sample (fig. 10.3E) which gave no positive signal.

Using western blot analysis, secreted galectin-3 was detected in the cyst fluid of 3 weeks old *cpk* kidneys of 2 samples taken from different animals. Both galectin-3 monomer (30kD) and dimer (60kD) were detected. Cysts fluid was obtained by cutting the kidney in half and gently squeezing the samples, a process that released approximately 1 ml of cyst fluid per kidney. The cyst fluid was used undiluted and untreated as samples for immuno-blotting for the detection of galectin-3. Negative control of western blot analysis was performed using preabsorbed antibodies and postive control was used where recombinant galectin-3 was used (fig. 10.3F).

Figure 10.1. Expression of galectin-3 in 3 week old normal and *cpk* kidneys.

Galectin-3 expression in kidney samples. In normal kidneys, galectin-3 was expressed in the collecting tubules in the cortex (A, black arrows), in the medulla (C) and in the urothelium (* in C). In cystic kidneys, galectin-3 is expressed in the cystic epithelia (D and F). Immunostaining on *gal-3* null mutant samples confirmed the specificity of the antibodies (G). Collecting tubule origin was confirmed by Dolichos bilforus agglutinin (DBA) (B and E). Pink arrows in A indicate proximal tubules stained with periodic acid Schiff's reagent (PAS), which gave a pink signal and they did not express galectin-3. F shows that galectin-3 was expressed cytoplasmically. Scale bars = 50 mm

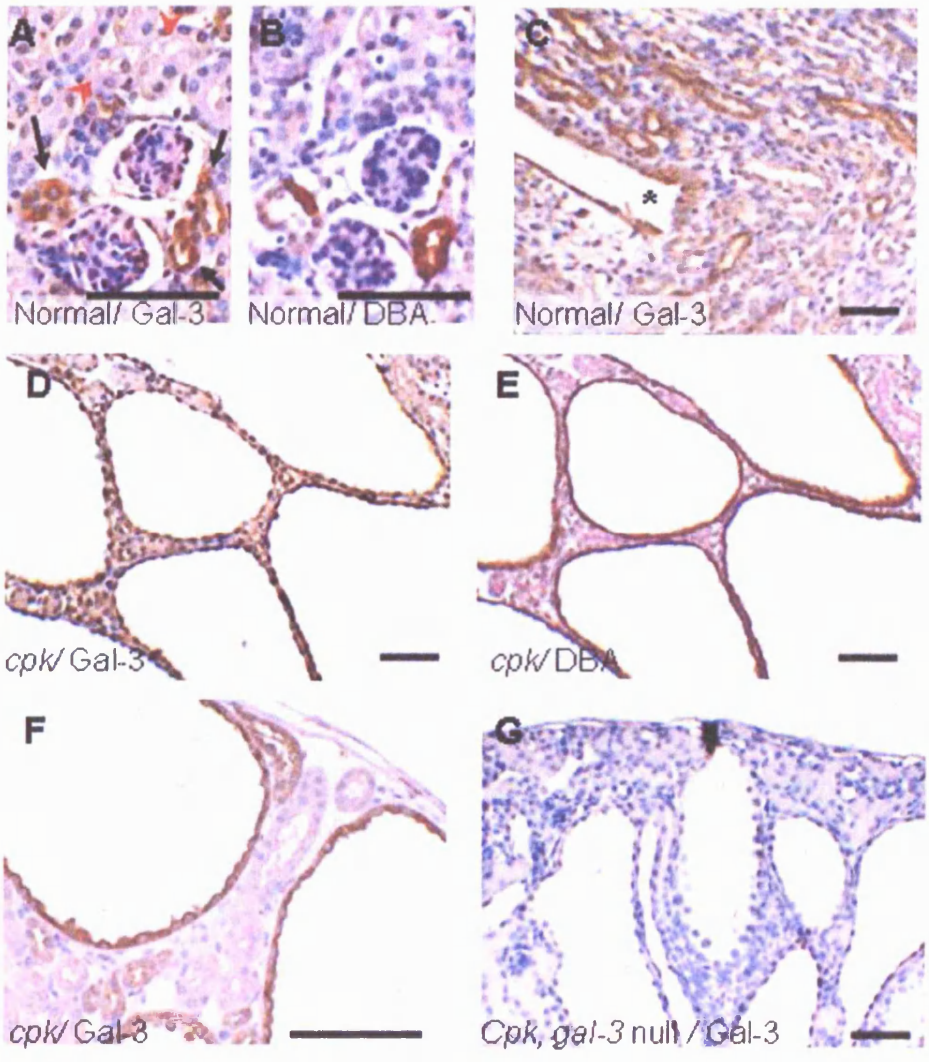

Figure 10.2. Expression of galectin-3 in normal adult kidneys.

A to D below show the expression of galectin-3 in normal adult mouse kidneys, of different magnitude (A with the lowest magnification and D with the highest). A strong cytoplasmic expression can be seen in all figures. Galectin-3 was detected in the collecting tubules and in the urothelium (* in A). Galectin-3 was expressed cytoplasmically in the majority of cells that express the protein, except a small subtype that express the protein apically (white arrow in C). Negative control of anti-galectin-3 antibodies was carried out using pre-immune rabbit antibodies in figure 10.3E. Only anti-galectin-3 antibodies were applied and no nuclear markers were use. Scale bars = 20 mm

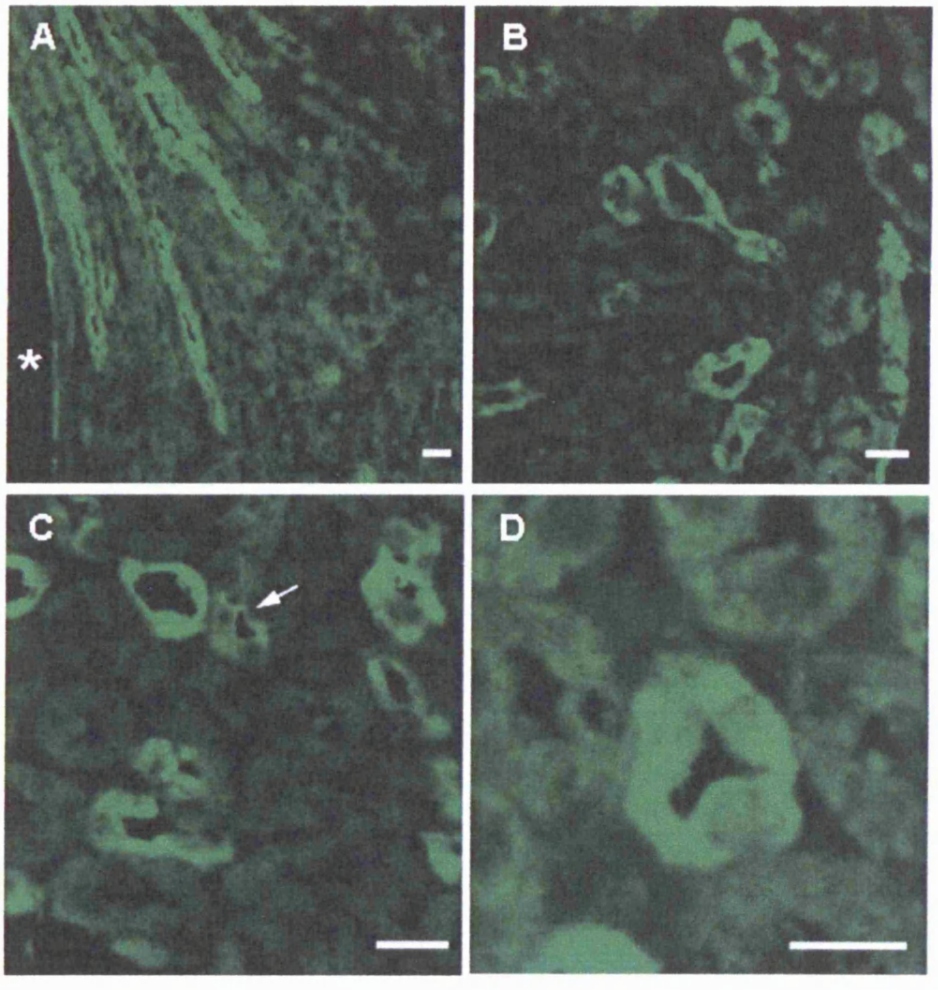

Figure 10.3. Expression of galectin-3 in 3 week old *cpk* kidneys and cyst fluid.

Fluorescent immunohistochemistry of *cpk* kidneys (A – E) and western blot analysis of cyst fluid (F). A – E show galectin-3 expression in different samples and of various magnifications. No nuclear immunostain was carried out in these samples. Majority of cystic epithelial cells express galectin-3 in the cytoplasmic domain, though a subset of cells expressed the protein apically only (white arrow in C). E is a negative control using pre-immune rabbit IgG on a *cpk* sample. Scale bars = 10 mm.

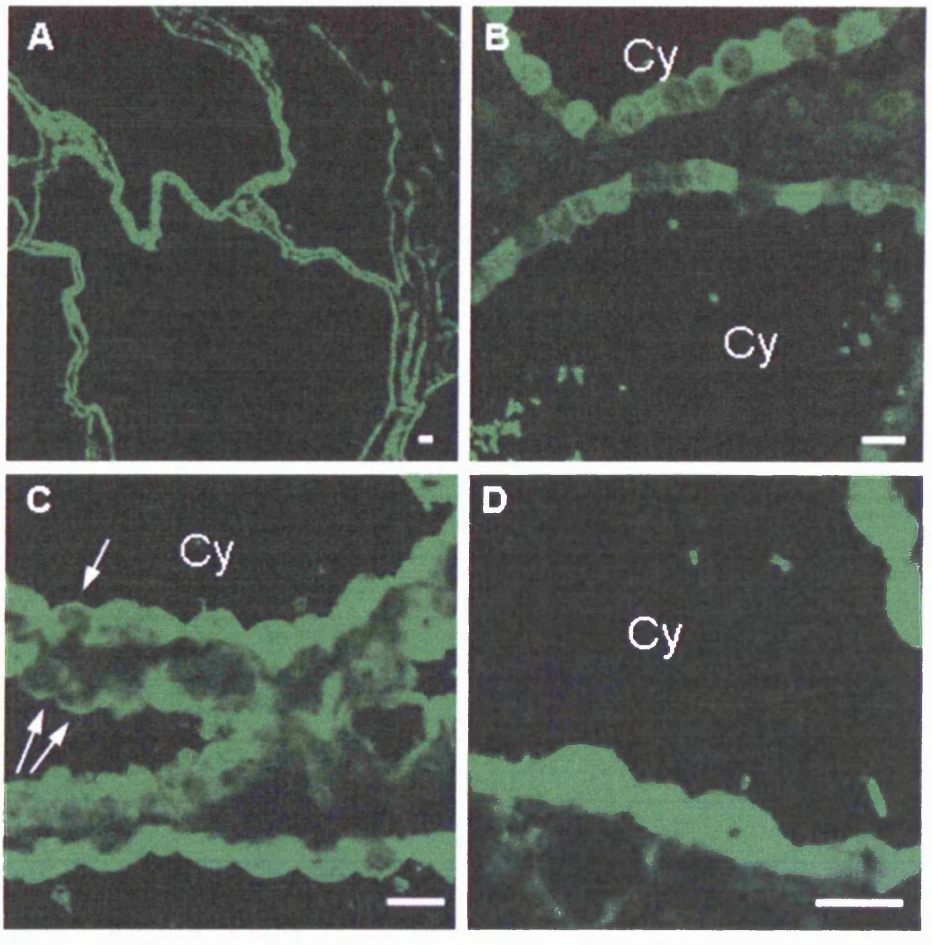

Figure 10.3. (continue)

Western blot analysis (F) of the cyst fluid of two different samples (1 and 2). These samples were undiluted prior to loading, thus of unknown concentration. Negative control using pre-immune antibodies (3) and a positive control using recombinant galectin-3 (4) is also shown in F. All samples and controls were run in the same blot thus the positive control was used as a size marker. Lane 1 and 2 contained positive protein bands (both monomer and dimer galectin-3) at the same positions to that of the positive control (lane 4).

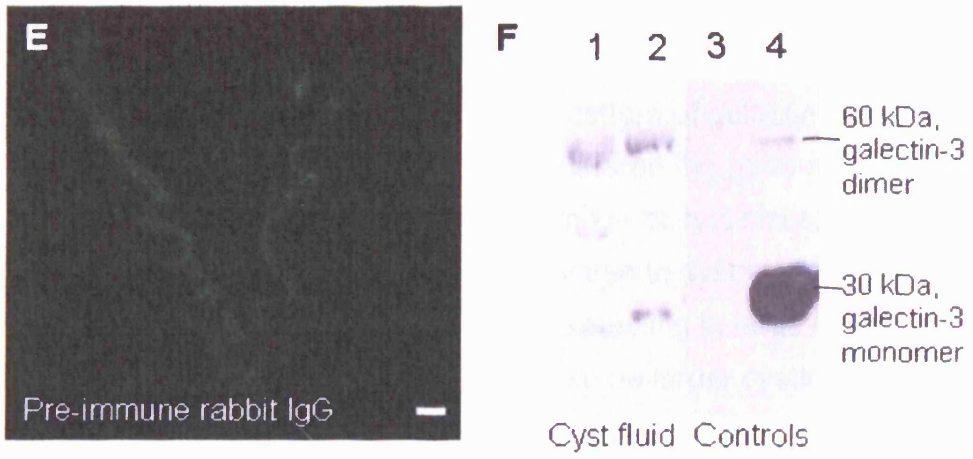

Figure 10.3. (continue)

Western blot analysis (F) of the cyst fluid of two different samples (1 and 2). These samples were undiluted prior to loading, thus of unknown concentration. Negative control using pre-immune antibodies (3) and a positive control using recombinant galectin-3 (4) is also shown in F. All samples and controls were run in the same blot thus the positive control was used as a size marker. Lane 1 and 2 contained positive protein bands (both monomer and dimer galectin-3) at the same positions to that of the positive control (lane 4).

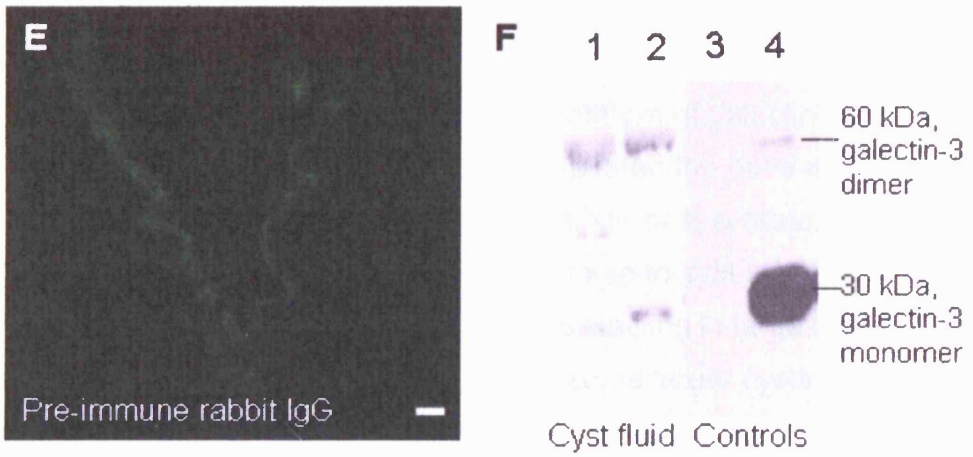

Expression of other collecting duct markers in cystic kidneys compared with galectin-3.

Galectin-3 upregulation in cysts might simply represent non-specific re-expression of early ureteric markers as these epithelia dedifferentiate towards a more embryonic phenotype. Hence, we investigated expression of other developmental markers, including ret, aquaporin-2 and calbindin. Strikingly similar expression patterns were observed for galectin-3, ret and aquaporin-2 in normal kidneys, with positive immunoreactivity restricted to collecting ducts (Fig. 10.4). Calbindin expression was more widespread, including some distal tubule segments (Fig. 10.4D). The distribution pattern of galectin-3 was unique in cystic kidneys: none of the other markers reiterated the pattern of prominent galectin-3 immunoreactivity across the whole range of cyst sizes; ret and calbindin immunostaining, for example, was inverse to cyst size (i.e. strong signal in tubules and small cysts, but little or no staining in large cysts); aquaporin-2 immunoreactivity was detected in some larger cysts but it was not as widely expressed in all cysts as galectin-3 was (Fig.10. 4G).

Figure 10.4. Expression of different collecting tubule markers in normal and cystic kidneys.

All samples from 3 week old mice. A-D: phenotypically-normal kidneys; E-H: cystic kidneys. Immunostaining is for galectin-3 (gal-3), ret (ret) aquaporin-2 (aq-2) and calbindin d28k (calb). All counterstained with PAS. A – C, Similar distribution of immunoreactive galectin-3, ret and aquaporin-2 in collecting ducts (arrowed) in normal kidneys. D, more widespread calbindin expression in distal tubules as well as collecting ducts. E, prominent cytoplasmic galectin-3 expression in collecting ducts/cyst of all sizes, from small undilated tubules through to large cysts. F, ret immunoreactivity in smaller tubules (arrowed) but reduced signal in larger cysts, with some having virtually no staining (*). G, aquaporin-2 was expressed in some cysts (arrowed), although others were negative (*). H, intense calbindin immunostaining of tubules and small cysts but reduced intensity in larger cysts (*). Scale bars = 50 mm.

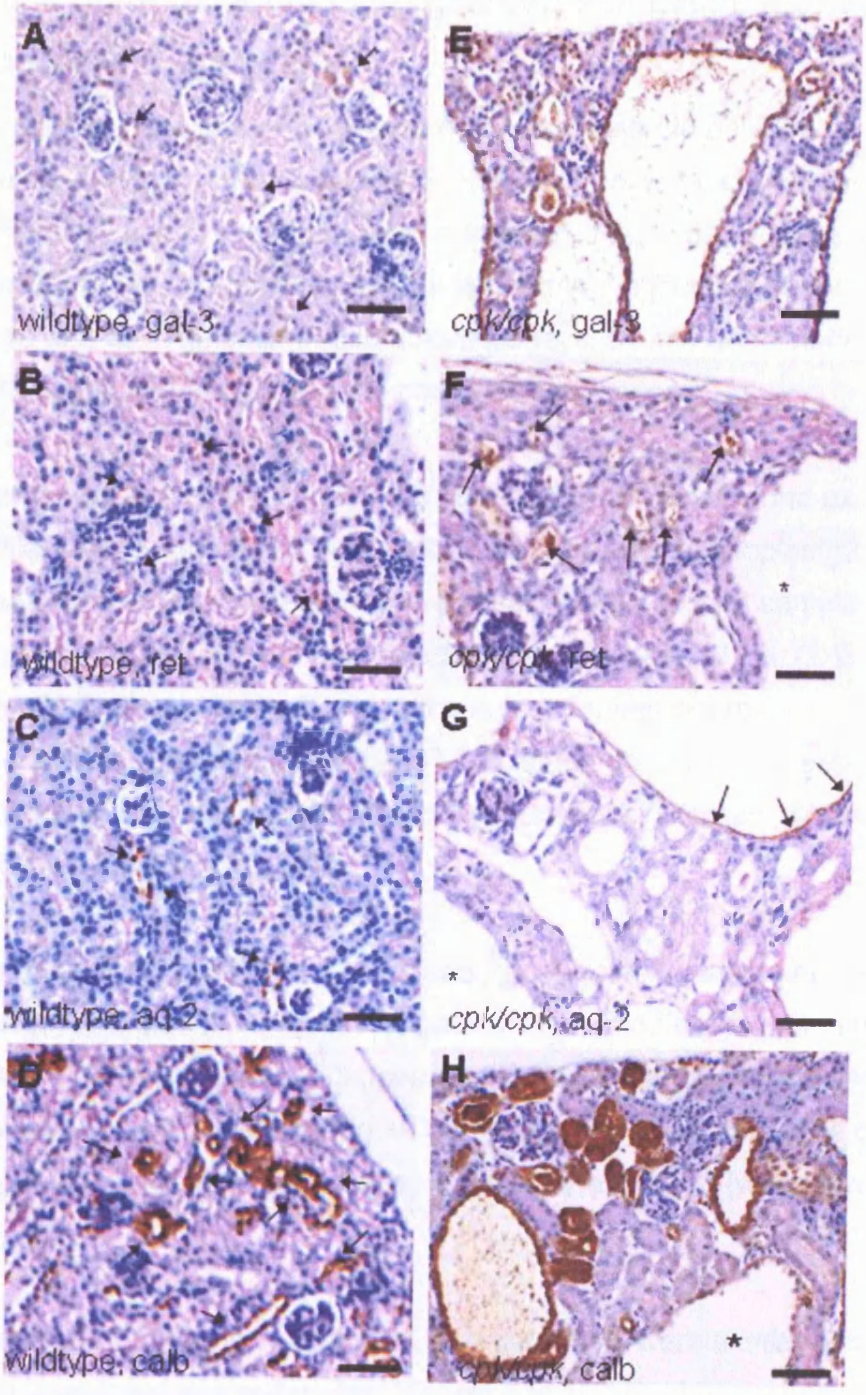
A
wildtype, gal-3
E
cpk/cpk, gal-3
B
wildtype, ret
F
cpk/cpk, ret
C
wildtype, aq-2
G
cpk/cpk, aq-2
D
wildtype, calb
H
cpk/cpk, calb

Expression of galectin-1 and galectin-9 in cystic kidneys compared with galectin-3

Both galectin-1 and galectin-9 are normally expressed in developing and mature kidneys; galectin-1 is predominantly located in the connective tissues and galectin-9 is expressed mainly in the proximal tubules (Hughes, 2004). Expression of the two galectins was examined in the kidneys of normal and *cpk* mice, as well as in galectin-3 null mutant kidneys, by immunohistochemistry using the light microscope and the confocal microscope.

In both normal and cystic kidneys (fig 10.5), galectin-1 was found exclusively in interstitial cells between epithelial cells, exhibiting strong cytoplasmic expression. No epithelial cells in both normal and *cpk* kidney samples were found positively stained with anti-galectin-1 antibody (fig 10.5A, C, E and G). As for galectin-9, it was mainly found in the apical domain of proximal tubules in both normal and cystic epithelia (fig.10.6B), although it was expressed in the rare collecting tubule epithelial cells in the cytoplasmic domain (black arrows in fig 10.5B, D, F and H).

Co-immunostaining using antibodies against galectin-3 (rabbit anti-galectin-3 antibodies) and galectin-9 (goat anti-galectin-9 antibodies) revealed that the expression of the two galectin-3 appeared to overlap each other in the apical domain of non-cystic samples (fig 10.6A – F); while the expressions of galectin-3 and galectin-9 in cystic samples were mutually exclusive (white arrows in fig 10.6G – I).

The expression patterns of galectin-1 and galectin-9 were similar in both galectin-3 wildtype and null mutant kidneys (fig 10.5E – H) compared with galectin-3 wildtypes.

Figure 10.5. Expression of galectin-1 and galectin-9 in normal and cystic kidneys.

A – D are three week old normal kidneys and E – H are 3 weeks old *cpk* kidneys. Samples were immunostained with antibodies against galectin-1 (A, C, E, G) or galectin-9 (arrowed in B, D, F, H). The genotypes of each samples are indicated on the left. Galectin-3 null mutant samples are in C, D, G and H, which have the same expression pattern as galectin-3 widetype samples. Scale bars = 30 mm

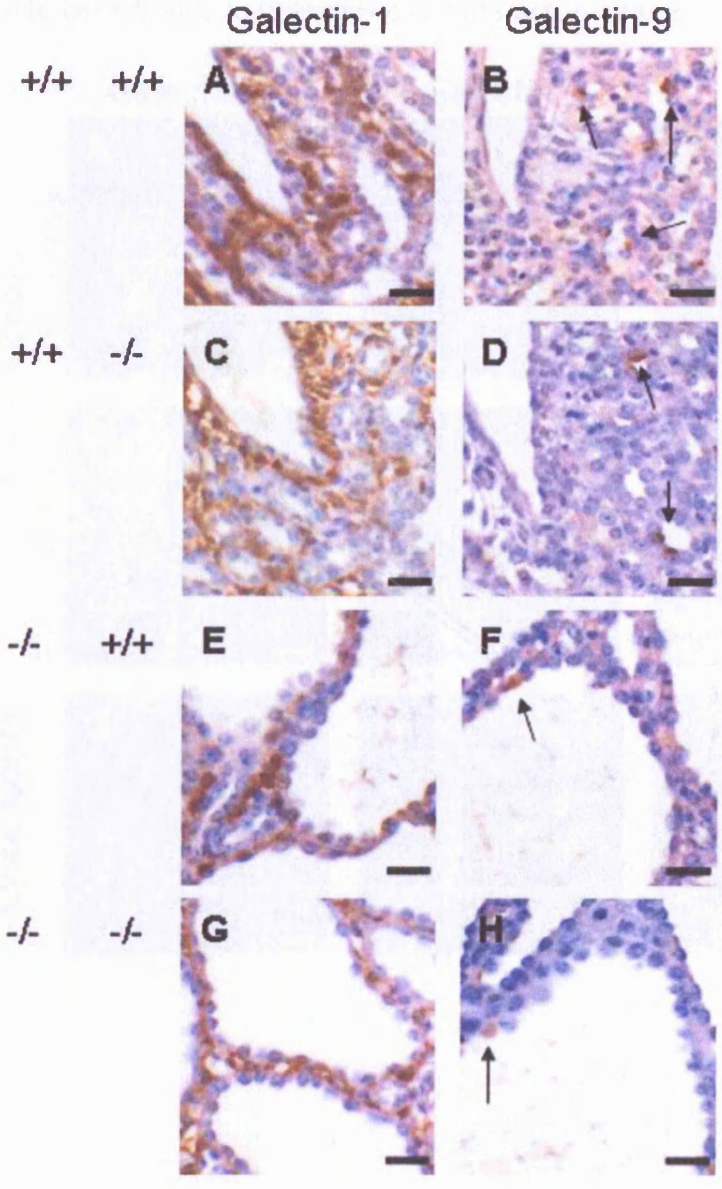

Figure 10.6. Co-localisation of galectin-3 and galectin-9 in normal and cystic kidneys.

A – F are 3 week old normal kidneys and G – I are 3 week old *cpk* kidneys. All samples were immunostained with antibodies against both galectin-3 and galectin-9 and examined using a confocal microscopy. Co-localisation of the two galectins in normal collecting ducts were observed in the cortex and the medulla (C and F). In cystic kidneys, most epithelial cells expressed galectin-3 (G) with a few cells that did not express it (white arrows in G – I), galectin-9 was instead expressed in these cells that lack galectin-3. Scale bars = 20 mm

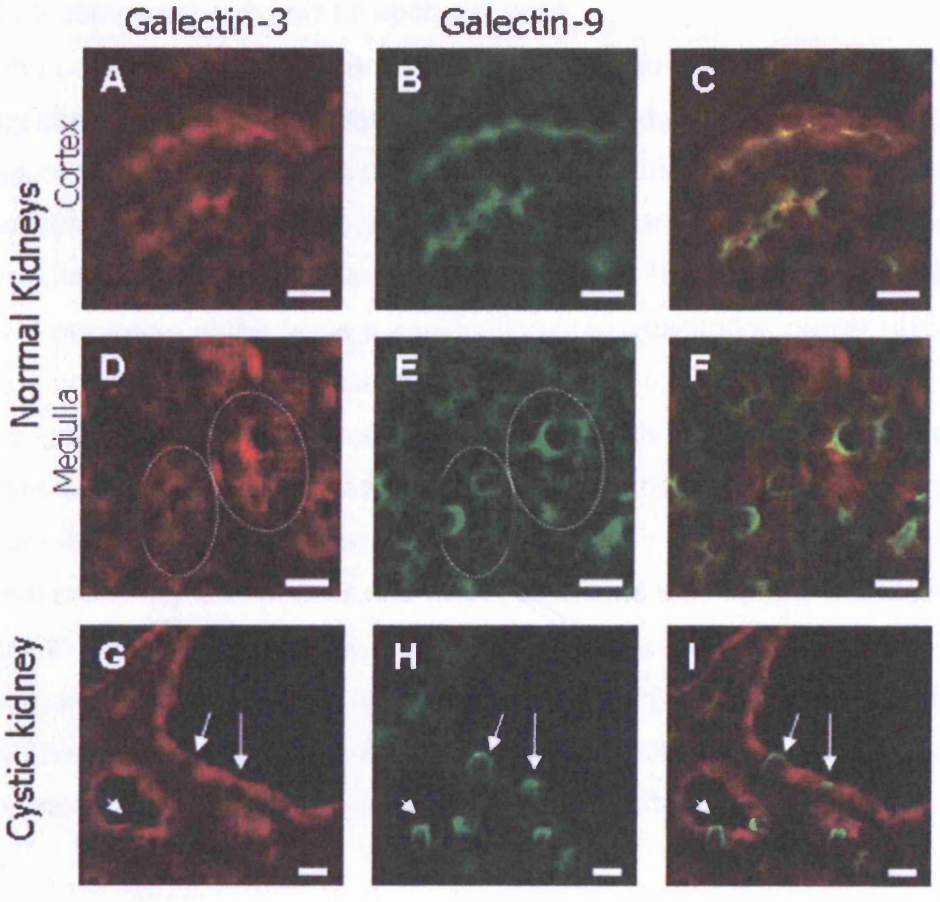

Semi-quantification of galectin-3 expression in cystic and normal kidneys.

Attempts were made to quantify the level of galectin-3 expression in normal tubule epithelia and in *cpk* cystic epithelia. Using immuno-blotting, my predecessor Dr. Tanya Johnson detected that the total amount of galectin-3 protein expressed in cystic kidneys was much higher than in normal kidneys. However, she did not show that individual cystic epithelial cells expressed more galectin-3 compared with normal epithelial cells.

Using the Leica Confocal Software (LCS) and immunofluorescence, the intensity of galectin-3 immuno-staining was measured and quantified. Six samples of normal and five of cystic kidneys were immuno-stained for galectin-3 and accessed using the confocal microscope. All samples were processed at the same time to ensure consistency. Approximately 15 normal tubules/cysts were photographed at the same magnification (x40), excitation power (843 voltage) and offset (2%). Representative images are shown in figure 10.7. At least 20 normal tubules/cysts were examined for each sample and their staining intensities were quantified and compared. Refer to Chapter 9: Methods, figure 9.2 for an illustration of staining quantification.

In normal collecting tubular cells, the mean amplitude was 92 and the maximum was 200. In cystic epithelial cells, the mean amplitude was 94 and the maximum was 222 (fig 10.8). The differences in mean and maximum amplitude between normal and cystic sample was biologically non-significant, (p-values 0.87 for mean amplitude and 0.10 for maximum amplitude).

Figure 10.7. Representative images of kidney sections used for semi-quantification.

All samples were processed together to ensure equal exposure to anti-galectin-3 antibodies and other reagents; in addition, the images were taken using the same setting. Thus comparison of immuno-staining intensity can be compared. The four images below were randomly selected. A and B were sections taken from normal kidneys whereas C and D were from *cpk* kidneys. Note the different staining intensity between sections and also within the same section (white arrows in D). Cy = cysts and scale bars = 40 μm.

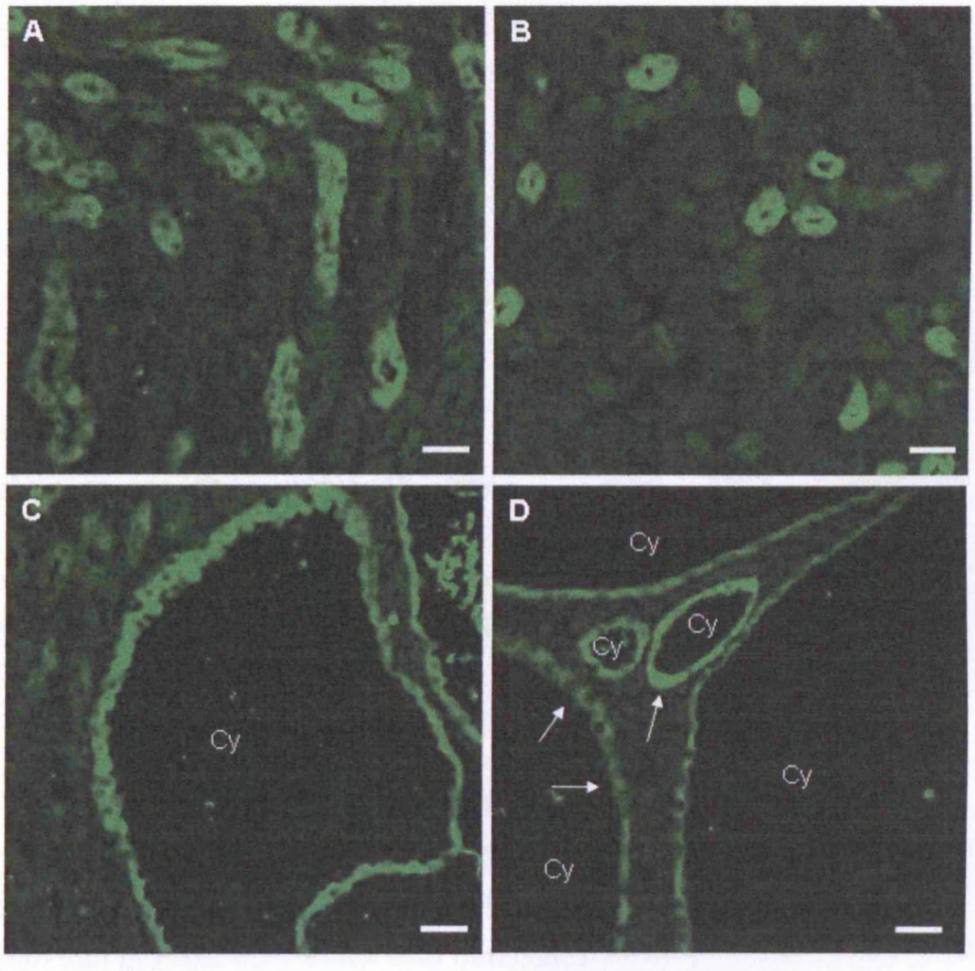

Figure 10.8. Comparison of the mean and maximum level of galectin-3 expression in normal tubular cells and cystic epithelial cells.

A is a summary of the mean amplitude (mean staining intensity) comparing normal and cystic epithelia whereas B is a summary of the maximum amplitude (highest staining intensity).

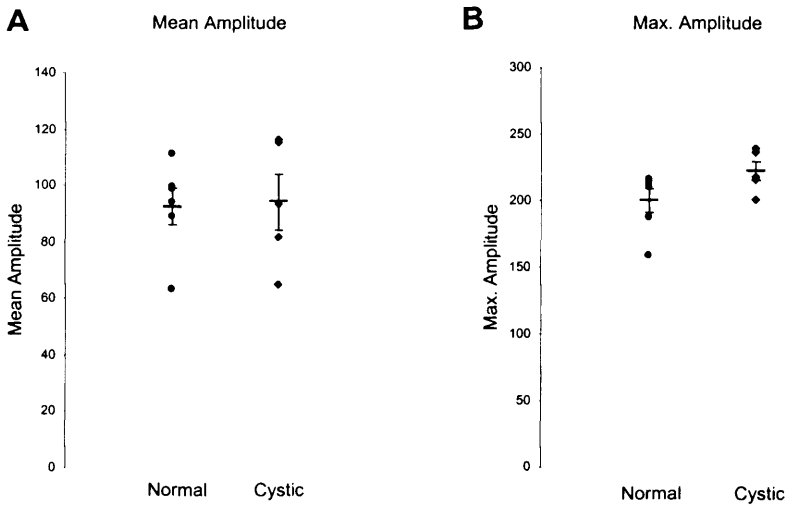

Mean	92.3	94.1	**Mean**	199.9	222.4
SE	6.57	9.85	**SE**	9.21	7.20
Lower ci	79.4	74.8	**Lower ci**	181.8	208.2
Upper ci	105.2	113.4	**Upper ci**	217.9	236.5
n	6	5	**n**	6	5

It is important to acknowledge that this protocol did not measure the total protein expression as it only allows the measurement of cytoplasmic galectin-3 expression, ignoring the secreted protein. It was shown that galectin-3 was secreted into the cyst fluid which was detected by immuno-blotting (fig 10.3F).

High level of galectin-3 expression in renal cystic epithelia of various PKD samples.

The focus of this expression study is on the *cpk* model as this was the chosen model for the study of ARPKD development. However, the phenotypes of *cpk* animals depend on the background of the animals, implying the presence of important modifier genes (ref, Guay-Woodford and Woo et al 1997). Therefore *cpk* samples from three different backgrounds (C57BL/6j, Balb/c and DBA) were examined. Various otherPKD kidney samples of different PKD mouse models and human samples were examined for the expression of galectin-3. These samples include *pkd2*, *bpk* and *orpk* mutant mouse; human samples included ARPKD and ADPKD samples. All mouse samples were of 3 week of age except *orpk* which was 1 week old, as this mutant dies before Day14.

Examination of galectin-3 expression in *cpk* mice of different backgrounds.

Galectin-3 expression in cpk models on different backgrounds were compared. It was previously shown that galectin-3 was widely expressed in *cpk* mouse in the B57BL/6j background, its natural and the most characterised background. Kidneys from 3 week old *cpk* mice on the Balb/c background were assessed. Renal cytogenesis in this background is very similar to that of C57BL/6j background: the 3 week old *cpk* Balb/c kidney was almost entirely filled with collecting duct cysts. Immunohistochemistry of the *cpk* Balb/c kidney revealed that the majority of cysts expressed galectin-3 cytoplasmically (figure 10.9B).

The 3 week old *cpk* kidney in DBA background did not exhibit renal cystic lesion. Immunohistochemistry analysis showed that galectin-3 was expressed in the collecting tubules in the cortex and the medulla of the kidney. No renal cysts were found in these samples. The expression pattern of galectin-3 was very similar to that of normal kidney (fig 10.9C).

Examination of galectin-3 expression in different PKD models showed that galectin-3 was expressed in the cystic epithelial of all samples.

Immunohistrochemistry examination of the 3 week old samples of the *pkd2* and *bpk* mutant showed that, similar to *cpk* kidney, galectin-3 was widely expressed in cystic epithelia (fig 10.10A – D).

The *orpk* samples obtained was on the FVB background, and at one week did not have a gross renal cystic presentation. Immunohistorchemistry showed that galectin-3 was expressed in the few cysts present in the *orpk* kidney (fig 10.10 E and F).

Lastly, examination of human samples: ARPKD and ADPKD, revealed that galectin-3 was also cytoplasmically expressed in these cystic epithelial cells (fig 10.10 G-J).

In both *orpk* and ADPKD samples: not all cysts express galectin-3 as indicated with * in fig 10.10F and 10.10G, these cysts may not be derived from collecting tubules.

Figure 10.9. Expression of galectin-3 in *cpk* models on three different backgrounds (B57BL/6j, Balb/c and DBA).

All kidney samples were of three week old *cpk* null mutants. *cpk* mutants on both the B57BL/6j (A) and Balb/c (B) backgrounds were severely cystic at three weeks, however on the DBA (C) background, no cysts were present. Instead a small number of dilated tubules were found expressing galectin-3. Scale bars = 80 mm.

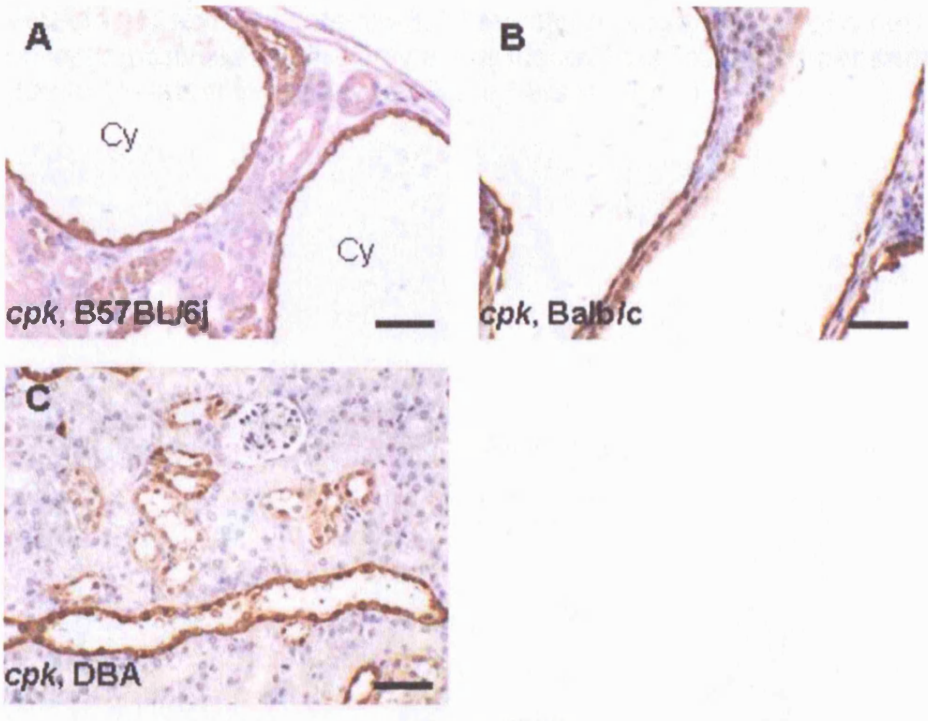

Figure 10.10. Expression of galectin-3 in cystic epithelia of various PKD models.

Galectin-3 expression on various PKD samples. A, C, E, G and H are of lower magnification. Galectin-3 expression was found in cystic epithelial cells of all samples examined. A and B are *PkD-2* heterozygote, which gives rise to PKD; C and D are from *bpk* model; E and F are from *orpk* model; G to J are human PKD samples (AD and AR). All samples expressed galectin-3 in the cystic epithelia. * in F and G indicate cyst that did not express galectin-3. They may represent cysts of a non-collecting tubules origin. Only a one kidney was examined per sample due to limitation in resources. Scale bars = 80 mm.

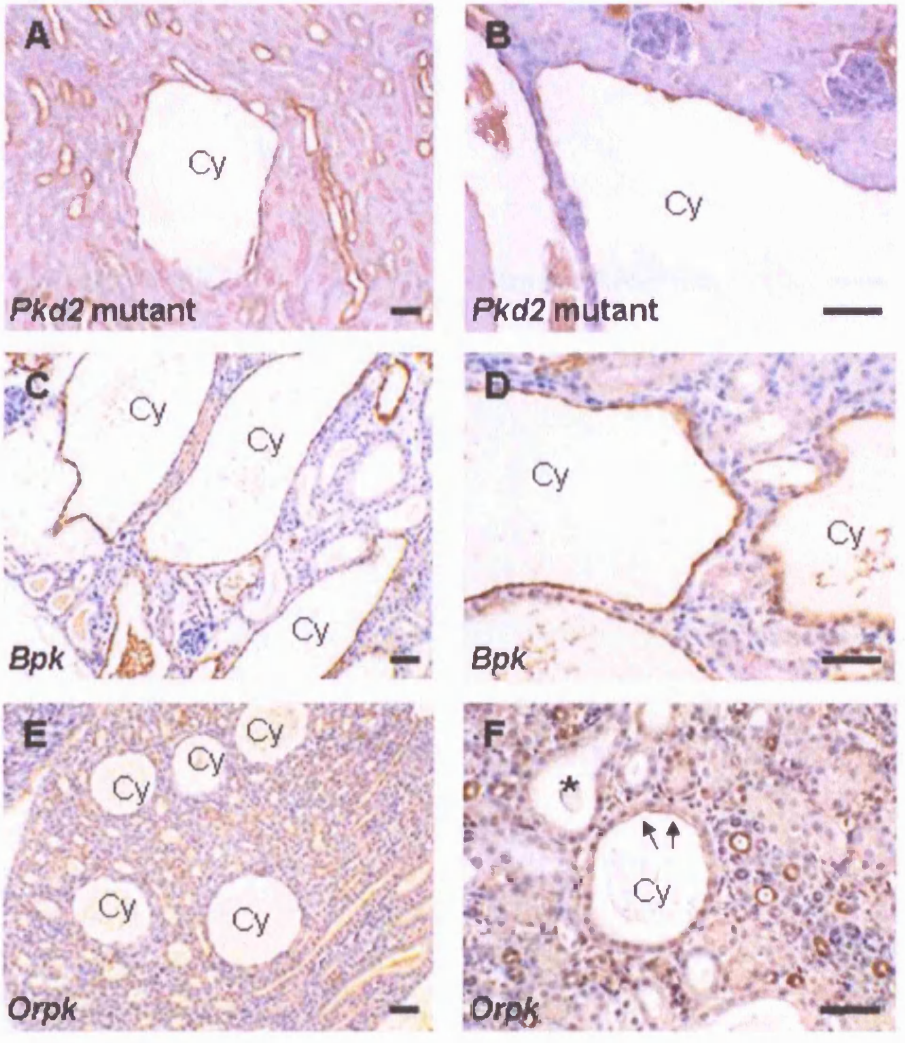

Figure 10.10 Continued.

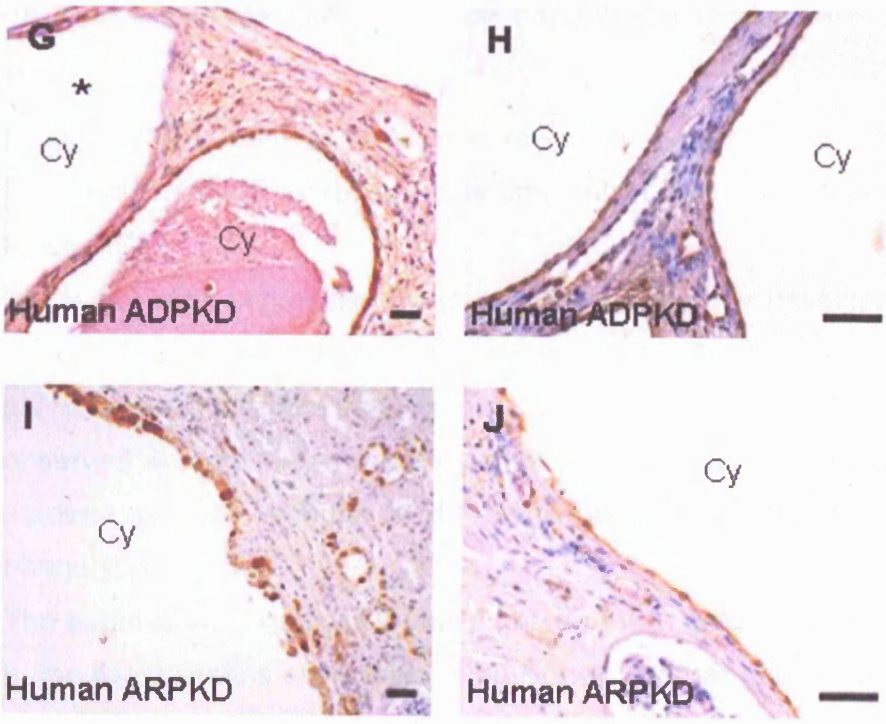

Summary of findings of galectin-3 expression on cystic epithelia:

- Galectin-3 was found to be widely expressed in renal cystic epithelia of *cpk* mutant mice. It exhibited a predominantly cytoplasmic expression in these cells.
- The expression of galectin-3 was compared with other developmental collecting tubule proteins (ret, aquaporin-2 and calbindin) and found galectin-3 was different from the others and the wide expression observed was not simply a non-specific re-expression of early ureteric markers as these epithelia dedifferentiate towards a more embryonic phenotype.
- The expression of galectin-3 was compared with galectin-1 and galectin-9, the two galectins expressed in the kidney. Neither galectin-1 nor -9 have the same expression pattern of galectin-3 in cystic epithelia. Assessment in *galectin-3* null mutant kidneys found that two galectins were not widely expressed in the cystic epithelial cells: galectin-1 was absent and galectin-9 was only expressed in a small number of cystic epithelial cells; therefore it was unlikely that they could compensate for the lack of galectin-3 in these samples.
- Lastly, the expression of galectin-3 was assessed in a limited number of other PKD samples and found that in all samples examined (*Pkd2, Bpk, Orpk,* human ADPKD and human ADPKD kidney samples), galectin-3 was widely expressed in the cystic epithelia.

Next the function of galectin-3 was investigated *in vivo* by introducing *galectin-3* null mutant allele to the *cpk* mutant. The effects of the lack of galectin-3 in cystogenesis were examined.

EFFECTS OF GALECTIN-3 MUTATION ON CYSTOGENESIS *IN VIVO*

Previous findings of the widespread expression of galectin-3 in cystic epithelia did not show that protein is able to modulate cystogenesis. Previous *in vitro* study using *cpk* suspension cultures showed that the addition of galectin-3 to the culture medium significantly reduced the number of cysts formed after 24 hours (Johnson, 2001). To further investigate the effect of galectin-3 on cyst growth, we examined the *cpk* mouse model, to determine the effect of reducing the expression of galectin-3 in these mice.

The effect of galectin-3 on renal cyst development was investigated *in vivo* by generating double mutant, *galectin-3* and *cpk* null. *Galectin-3* null mutant mice (129Sv background) were bred with *cpk* heterozygous (C57BL/6j), then the F1 double heterozygous (Galectin-3 +/-, *cpk* +/-) were genotyped by PCR. They were crossed to generate F2 which had 9 possible genotypic outcomes following the Mendelian's Laws of Inheritance according to either the *cpk* or the *galectin-3* genotypes (see fig. 10.11 and 10.12 below). 24 litters were generated in the F2 generation, yielding a total of 266 animals. No post-natal death was recorded in these samples. All animals were sacrificed at 1 week, when renal cysts were still developing and there was an adequate level of renal activity. The absolute kidney to body weight ratio (K/B ratio) was calculated and used as an indicator of the severity of cystogenesis in the kidneys. This is based on the fact that cyst growth results in kidney enlargement, hence, the more severe the cystic kidney disease, the heavier the kidney.

Western blotting was used to quantify the amount of galectin-3 in these 1 week old cystic samples with various *galectin-3* genotypes. However, no galectin-3 protein bands were detected in all samples due to the very low amount of galectin-3 presence in 1 week old kidneys.

Frequency test (chi-square) on the ratio of the genotype outcome.

Frequency test was carried out in the initial 8 litters collected, a total of 93 samples. The number of samples in each genotype group is summarised in table 10.1 and 10.2 below. Chi-square test was performed on these samples to determine if the ratio of the genotype outcome was as expected, following the Mendelian's Laws of Inheritance.

The transmissions of *cpk* and *galectin-3* loci were analysed separately as well as clustered into nine groups (various *galectin-3* and *cpk* genotypes) The chi-square values of the three tests carried were 0.26, 0.39 and 0.69 (see table 10.1 and 10.2) which is above the 0.05 significant value, therefore, there were no significant difference between the actual and the expected frequency.

Table 10.1. Frequency test 1 and 2.

Genotype	Observed number	Observed frequency %	Expected Number	Expected frequency %	Chi-square test
Cpk +/+	30	32	23.25	25	
Cpk +/-	43	46	46.5	50	
Cpk -/-	20	22	23.25	25	
Total:	**93**	**100**	**93**	**100**	**0.26**
gal-3 +/+	21	23	23.25	25	
gal-3 +/-	53	57	46.5	50	
gal-3 -/-	19	20	23.25	25	
Total:	**93**	**100**	**93**	**100**	**0.39**

Table 10.2. Frequency test 3

Genotype	Observed number	Observed frequency %	Expected Number	Expected frequency %	Chi-square test
cpk+/+, gal-3 +/+	7	7.53	6	6.25	
cpk+/+, gal-3 +/-	15	16.13	12	12.5	
cpk+/+, gal-3 -/-	8	8.60	6	6.25	
cpk+/-, gal-3 +/+	10	10.75	12	12.5	
cpk+/-, gal-3 +/-	26	27.96	23	25	
cpk+/-, gal-3 -/-	7	7.53	12	12.5	
cpk-/-, gal-3 +/+	4	4.30	6	6.25	
cpk-/-, gal-3 +/-	12	12.90	12	12.5	
cpk-/-, gal-3 -/-	4	4.30	6	6.25	
Total:	**93**	**100**	**93**	**100**	**0.69**

After the confirmation that both loci were inherited as expected, galectin-3 genotyping was performed only in cystic animals. This was to save resources and time. *cpk* locus was confirmed using the PCR genotyping method.

Inter- and intra-litter variability did not affect the kidney/body weight ratio, as assessed by Multi-level modelling

Multi-level modelling was employed to confirm that there was no variation in the K/B ratio between animals in the same litter and between animals of different litters. Hence all animals were analysed together as one group, without adjusting to its litter of origin.

Reduced galectin-3 gene expression accelerated cystogenesis

61 animals were phenotypically and genotypically confirmed to be cystic, out of which there were 15 *galectin-3* wildtypes, 35 *galectin-3* heterozygotes and 11 *galectin-3* null mutants.

In terms of kidney weight, non-cystic kidneys weighed on average 0.025g (left kidney only); mean kidney weight of cystic *galectin-3* wildtype was 0.046g and that of both cystic *galectin-3* heterozygotes and *galectin-3* null mutants was 0.065g. Compared with cystic *galectin-3* wildtype, cystic *galectin-3* heterozygotes and *galectin-3* null mutants had an 41% increase (p-value = 0.023 and 0.076) in single kidney weight (fig. 10.11).

No significant difference was found in body weight when comparing cystic (mean body weight = 3.86g) to non-cystic samples (mean body weight = 4.15g), t-test determined a p-value of 0.062. The mean body weight of all animals was 4.05g. Among cystic animals, galectin-3 genotypes did not affect the body weight of the animals (fig.10.12).

Non-cystic animals at 1 week had a mean K/B ratio of 0.60%; that of cystic animals with a normal expression of galectin-3 rose up to 1.18%. This K/B ratio in cystic *galectin-3* heterozygotes and cystic *galectin-3* null mutants increased to 1.69% and 1.72% respectively (fig. 10.13). *Galectin-3* heterozygotes and *galectin-3* null mutants had an increase in K/B ratio of 43% (p-value = 0.030) and 46% (p-value = 0.016) compared with cystic *galectin-3* wildtype animals, as determined using t-test (table 10.3).

Figure 10.11. Summary of kidney weight.

Mean kidney weights of different genotypes. Significant difference was indicated by *. c.i. represents 95% confidence interval.

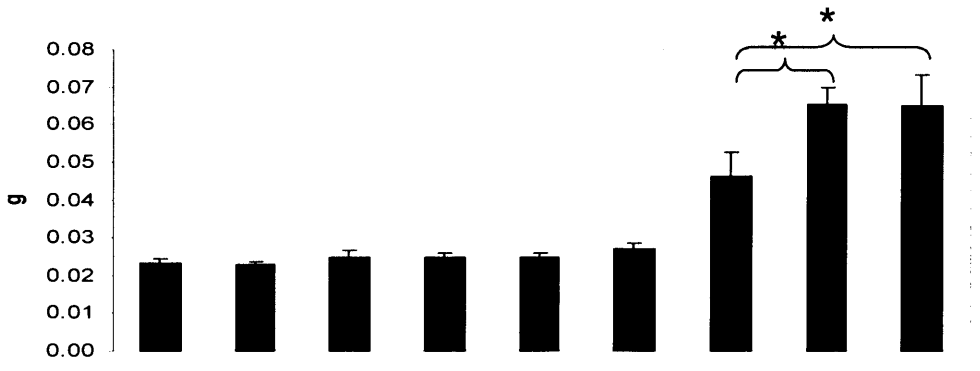

cpk	+/+	+/+	+/+	+/-	+/-	+/-	-/-	-/-	-/-
Gal-3	+/+	+/-	-/-	+/+	+/-	-/-	+/+	+/-	-/-
Mean (g)	0.023	0.023	0.025	0.025	0.025	0.027	0.046	0.065	0.065
Lower ci	0.021	0.022	0.021	0.023	0.023	0.024	0.034	0.056	0.049
Upper ci	0.026	0.024	0.029	0.027	0.027	0.030	0.058	0.074	0.081
n	7	15	8	10	26	7	15	35	11

Figure 10.12. Summary of body weight

Mean kidney weights of different genotypes. No significantly differences were found.

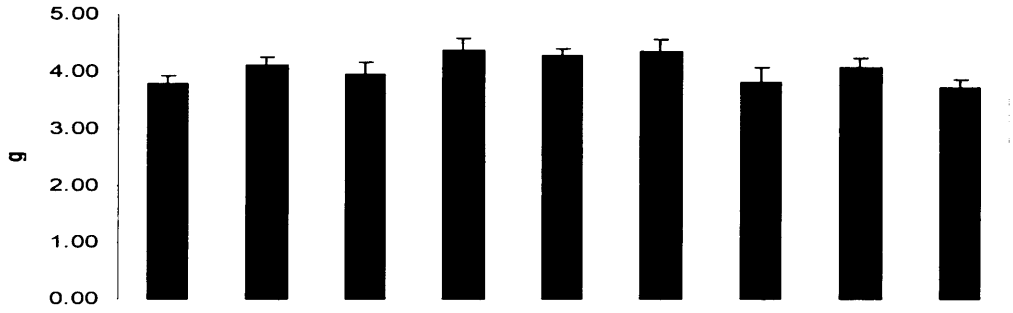

cpk	+/+	+/+	+/+	+/-	+/-	+/-	-/-	-/-	-/-
Gal-3	+/+	+/-	-/-	+/+	+/-	-/-	+/+	+/-	-/-
Mean (g)	3.786	4.123	3.963	4.370	4.288	4.350	3.803	4.067	3.718
Lower ci	3.525	3.853	3.589	3.966	4.061	3.957	3.293	3.734	3.420
Upper ci	4.046	4.394	4.336	4.774	4.516	4.743	4.314	4.400	4.017
n	7	15	8	10	26	7	15	35	11

Figure 10.13. Summary of kidney/body weight (K/B) ratio.

Mean K/B ratio of different genotypes. Significant difference was indicated by *.

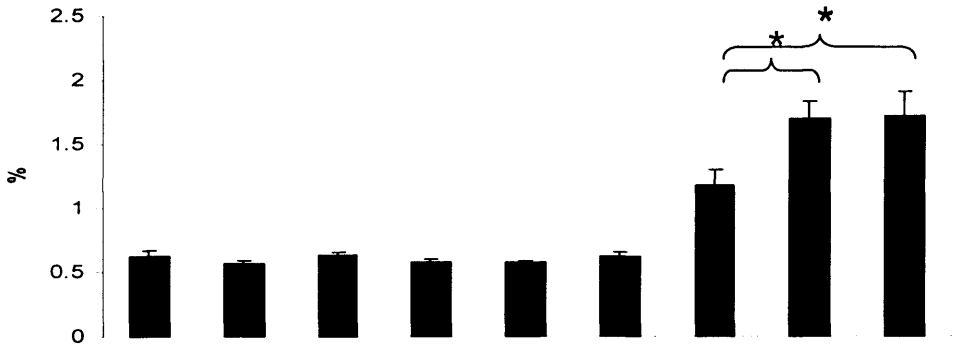

cpk	+/+	+/+	+/+	+/-	+/-	+/-	-/-	-/-	-/-
Gal-3	+/+	+/-	-/-	+/+	+/-	-/-	+/+	+/-	-/-
Mean (%)	0.621	0.566	0.628	0.576	0.579	0.624	1.179	1.695	1.723
Lower ci	0.532	0.525	0.565	0.533	0.549	0.554	0.944	1.418	1.364
Upper ci	0.709	0.608	0.692	0.620	0.609	0.695	1.415	1.971	2.083
n	7	15	8	10	26	7	15	35	11

Table 10.3. Summary of K/B ratio of *cpk* animals with various galectin-3 genotypes.

The p-values were obtained in comparison with cpk -/- gal-3 +/+.

Genotype	**No.**	**Mean K/B ratio**	**Increase compared with *Gal-3* +/+**	**95% c.i.**	**p-value**
Gal-3 +/+	15	1.18%	----------	0.94%, 1,42%	----------
Gal-3 +/-	35	1.69%	43%	1.42%, 1.97%	0.030
Gal-3 -/-	11	1.72%	46%	1.36%, 2.08%	0.016

Comparison of proliferation and apoptosis in cystic samples with various *galectin-3* genotypes

Galectin-3 was known to affect cell proliferation and apoptosis (Inohara *et al.*, 1998;Yu *et al.*, 2002). It was interesting to note the similarity of outcome between *galectin-3* heterozygotes and *galectin-3* null mutants. The levels of proliferation and apoptosis were assessed in the cystic sample with three different *galectin-3* genotypes, in the hopes that these tests may provide an explanation for this phenomenon.

Proliferative and apoptotic Index were determined in the 1 week old cystic animals generated. 8 cystic samples were randomly selected from each *galectin-3* genotypes: Gal-3 +/+ Gal-3 +/- and Gal-3 -/-, hence, a total of 24 samples were assessed. Not all samples assessed due to the labour intensive nature of these tests and 8 samples per groups were sufficient for an adequate statistical analysis.

Proliferative cells were identified by immunohistochemistry using biotin labelled antibody against PCNA, proliferating cell nuclear antigen (fig. 10.14A). Apoptotic cells were detected using the *In Situ* Cell Death Detection kit, Fluorescein, which is based on the TUNEL technology (fig.10.14B).

Figure 10.14. Immunostaining of proliferating cells and apoptotic cells in 3 week old *cpk* kidneys.

Proliferating cells were stained brown using anti-PCNA antibodies (A); whereas cells undergoing apoptosis was identified using the TUNEL method which gave a fluorescent green signal (arrow in B). A was co-stained with haematoxylin and B with propidium iodide in order to visualise the nucleus of all cystic epithelial cells. Scale bars = 50 mm.

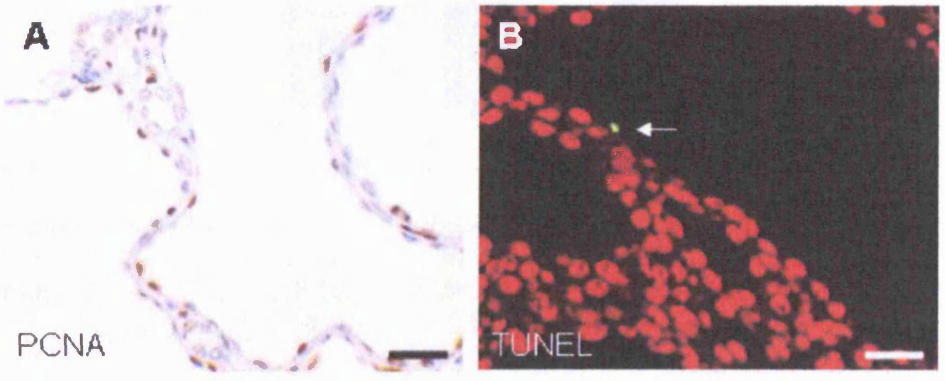

Proliferative index

Galectin-3 has been found to stimulate cell proliferation in fibroblasts and mesangial cells (Inohara *et al.*, 1998; Sasaki *et al.*, 1999). The effect of galectin-3 expression on proliferation in cystic kidney epithelial cells was investigated. Proliferating cells were identified using PCNA antibodies. Proliferative index (PI) was expressed as a percentage of PCNA positive cells over the total number of cystic epithelial cells counted.

PI for all cystic samples ranged from 44% to 96%. When the samples were sorted according to their *galectin-3* genotypes, it was found that *galectin-3* heterozygotes had a significantly higher PI of 88%, compared with *galectin-3* wildtypes 68% (p-value = 0.002) and *galectin-3* null mutants 78% (p-value = 0.038). No significant differences were found between *galectin-3* wildtypes and *galectin-3* null mutants. See figure 10.15.

Figure 10.15. Proliferative Index of cystic epithelial cells.

The percentage of PCNA positive cells over the total number of cystic epithelial cells counted. *Galectin-3* heterozygotes had significantly more proliferating cells.

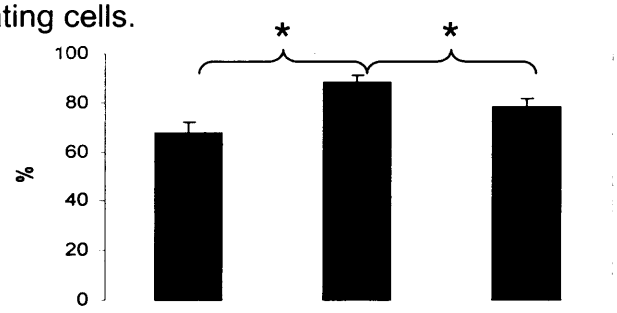

Genotype	*Gal-3 +/+*	*Gal-3 +/-*	*Gal-3 -/-*
MEAN			
Proliferative Index (PI)	67.75%	88.21%	78.13%
Lower ci	59.37	82.36	71.79
Upper ci	76.13	94.06	84.47
n	8	8	8

Apoptotic index

Apoptotic cells were detected using the *In Situ* Cell Death Detection kit, Fluorescein, which is based on the TUNEL technology. Apoptotic index was expressed as a percentage of apoptotic bodies over the total number of cystic epithelial cells counted (see fig.10.16).

Figure 10.16. Apoptotic Index of cystic epithelial cells.

Percentage of apoptotic bodies over the total number of cystic epithelial cells counted. No significant differences were found.

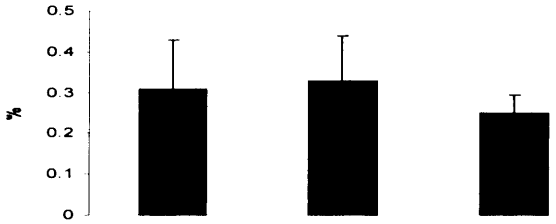

Genotype	*Gal-3 +/+*	*Gal-3 +/-*	*Gal-3 -/-*
MEAN			
Apoptotic Index (AI)	0.31%	0.33%	0.25%
Lower ci	0.07	0.11	0.16
Upper ci	0.55	0.55	0.34
n	8	8	8

Apoptosis was consistenly detected in cystic samples but at a low level. The AI ranged from 0% to 0.9% in all cystic samples examined with a mean AI across all samples of 0.030%. When samples were sorted to their *galectin-3* genotypes, no significant difference was found between each genotype.

Kidney morphology of cystic samples

Cystic kidney sections (randomly selected 8 samples from each of the three *galectin-3* genotypes) were prepared and were stained with haematoxylin and eosin and labelled with DBA to reveal their morphology and identify their collecting ducts origin. Brief analysis of these histological samples was carried out in which two sections from each samples were examined under a light microscope. Among these cystic animals, subtle differences between galectin-3 wildtype, heterozygotes and null mutants were observed in the cortical region, where the latter two had more cystic lesions (figure 10.17). The degree of cystic lesions in the cortex was examined and was given a score range from 1 to 5, the bigger the number the more cysts there were in that region. The score for *galectin-3* wildtype was 11/40, that of *galectin-3* heterozygotes was 24/40 and in *galectin-3* null mutants was 23/40. It appeared that *galectin-3* heterozygotes and null mutants had more cortical cysts compared with *galectin-3* wildtypes. This result concurs with the kidney/body weight ratio which revealed that *galectin-3* heterozygotes and null mutants had a more severe cystic disease. A more thorough examination of the histology was carried out on the pure background (C57BL/6j) as this set of samples came from a mixed genetic background (129Sv x C57BL/6j) which may affect the variability of the outcome.

Figure 10.17. Histology of cystic kidneys with various *galectin-3* genotypes.

Histology of *cpk* kidney at 1 week showing the cortex of the kidney. The three images were representative of their genotypes: A) *gal-3* wildtype, B) *gal-3* heterozygotes and C) *gal-3* null mutants. All sections were stained with haematoxylin, eosin and labelled with DBA, which is a marker for collecting tubules. Scale bars = 200 mm.

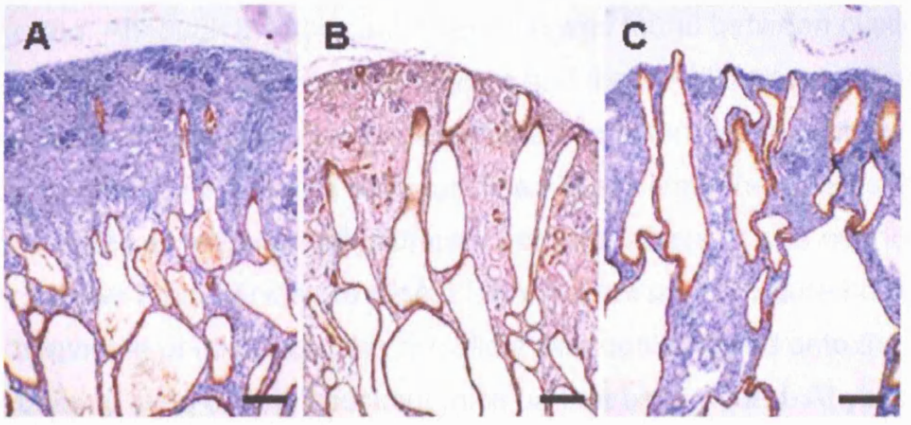

Effects of galectin-3 mutation on cystogenesis *in vivo*: analysis using double mutants on a pure background

The previous set of *in vivo* data was obtained from F2 animals with a mixed background. The *cpk* mutation arose spontaneously on the C57BL/6j background and the *galectin-3* mutants available at the time were on a 129Sv background. Although a significant difference was found between cystic animals with different *galectin-3* genotypes and that multilevel modelling analysis showed that there were no significant variation between litters from different parents, one must be cautious when interpreting the data as the control animals were genetically different from the others. It was due to this reason that we have decided to repeat the experiments on a pure background. At the beginning of this study, the *cpk* allele was backcrossed onto the 129Sv background to yield double knockout mice on that background. At year 3 of the study, *galectin-3* mutants on the C57BL/6j were obtained from the Consortium for Functional Glycomics; these mice were crossed with C57BL/6j *cpk* heterozygotes to yield double knockout on the C57BL/6j background.

Cytogenesis of *cpk galectin-3* null animals on 129Sv background (previously uncharacterised)

The *cpk* allele has previously backcrossed onto different backgrounds such as Balb/c, CAST, CD-1 and DBA, for the study of various phenotypic outcomes (Guay-Woodford *et al.*, 2000). In this study, the *cpk* null allele was backcrossed onto the 129Sv background for the first time as far as we are aware. The *cpk* null allele was backcrossed onto the 129Sv background for 10 generations. After which, the *cpk* heterozygotes (129Sv) were bred with galectin-3 null mutants (129Sv). F1 double heterozygotes were selected by genotyping using tail tips for DNA extraction and were used to generate F2, which contained the double mutants used for data analysis.

Sample collection, processing and assessment were performed as before. 34 litters were collected giving a total of 181 animals born, though only 171 were available for analysis due to early death.

A few unexpected factors occurred in this set of experiment, which affected the analysis of the results and the assessment of cystogenesis:

1) Ten animals died before day 7 a death rate of 5.5%. The cause of death was not known. The number of animals per litter was recorded at birth and the litters were checked daily and counted, and missing animals were noted. DNA was extracted from samples of the 7 post-natal deaths, but no samples were available for 3 samples. Table 10.4 shows a summary of these samples.

2) F2 generation did not follow the Mendelian's Law of Inheritance, as there were significantly less *galectin-3* null mutants. It is possible that *galectin-3* null mutants died *in utero*, therefore the samples obtained were not a representative of the true cystic *galectin-3* null mutants population;

3) Pancreatic cysts of various sizes occured in some *cpk* samples and the degree of severity did not correlate with *galectin-3* genotypes.

Details of these unexpected factors are explained below:

Premature death

Ten mice (5.5%) died before Day 7, when the samples were collected. DNA were available from 7 out of these 10 samples: 6 out of 7 were genotyped and shown to be *cpk* null mutants with various *galectin-3* genotypes and one was *cpk* +/+, *gal-3* -/- (see Table 10.4); half of these samples died at birth.

Table 10.4. Summary of animals that died before day 7.

10 animals died before day 7. 3 of them had no DNA available, the reminding 7 were genotyped and their genotypes are stated in the table below. No correlations were found between genotypes and the animals that died.

Sample	Age died (Day)	Genotypes
1	0	*cpk* -/-, *gal-3* +/+
2	2	*cpk* -/-, *gal-3* +/+
3	6	*cpk* -/-, *gal-3* +/-
4	0	*cpk* -/-, *gal-3* +/-
5	0	*cpk* -/-, *gal-3* +/-
6	0	*cpk* -/-, *gal-3* -/-
7	0	*cpk* +/+, *gal-3* -/-
8	1	No DNA
9	2	No DNA
10	2	No DNA

A significantly lower number of galectin-3 null mutants indicated by the frequency test (chi-square).

One hundred and seventy one samples (excluding the 10 that died before day 7) were analysed using the frequency test, chi-square, to determine if the samples follow the Mendelian's Law of Inheritance. When the samples were grouped into 9 groups according to the *cpk* and *galectin-3* loci, there was no significant difference between the observed frequency and the expected frequency, although the value, 0.079, was very close to being biologically significant (table 10.5). To inspect this further, the samples were grouped according to either their *cpk* genotype or *galectin-3* genotype; frequency tests (table 10.6) were preformed on this new grouping. Chi-square test on data grouped according to the *cpk* genotype gave a p-value of 0.239, indicating that the *cpk* allele was inherited as expected. However the test on data grouped by *galectin-3* genotype gave a p-value of 0.008, indicating that the *galectin-3* allele did not follow the expected pattern of inheritance. .

Table 10.5. Frequency test on sample on the 129Sv background grouped by their *cpk* and *galectin-3* genotypes.

Genotype	Observed number	Observed frequency %	Expected Number	Expected frequency %	Chi-square test
cpk+/+, gal-3 +/+	11	6.43	10.69	6.25	
cpk+/+, gal-3 +/-	23	13.45	21.38	12.5	
cpk+/+, gal-3 -/-	8	4.68	10.69	6.25	
cpk+/-, gal-3 +/+	19	11.11	21.38	12.5	
cpk+/-, gal-3 +/-	61	35.67	42.75	25	
cpk+/-, gal-3 -/-	15	8.77	21.38	12.5	
cpk-/-, gal-3 +/+	7	4.09	10.69	6.25	
cpk-/-, gal-3 +/-	21	12.28	21.38	12.5	
cpk-/-, gal-3 -/-	6	3.51	10.69	6.25	
Total:	171	100	171	100	**0.079**

Table 10.6. Frequency test on samples on 129Sv background grouped by either *cpk* or *galectin-3* genotypes.

Genotype	Observed number	Observed frequency %	Expected Number	Expected frequency %	Chi-square test
Cpk +/+	42	24.56	42.75	25	
Cpk +/-	95	55.56	85.5	50	
Cpk -/-	34	19.88	42.75	25	
Total:	**171**	**100**	**171**	**100**	**0.239**
gal-3 +/+	37	21.64	42.75	25	
gal-3 +/-	105	61.40	85.5	50	
gal-3 -/-	29	16.96	42.75	25	
Total:	**171**	**100**	**171**	**100**	0.008

It was suspected that there were less *galectin-3* null mutants than expected. To confirm this, frequency test was carried out where the data was grouped into two: *galectin-3* null mutants vs all others. The p-value obtained was 0.015, thus verifying that there were less *galectin-3* null mutants (table 10.7).

Table 10.7. Frequency test to confirm that there were less *galectin-3* null mutants.

Genotype	Observed number	Observed frequency %	Expected Number	Expected frequency %	Chi-square test
Gal-3 +/+ and *Gal-3* +/-	142	83.04	128.25	75	
Gal-3 -/-	29	16.96	42.75	25	
Total:	**171**	**100**	**171**	**100**	**0.015**

In conclusion from these frequency tests, there were significantly less galectin-3 null mutants than expected from Mendelian's Law of Inheritence among the F2 generation.

***Cpk* animals on the 129Sv developed pancreatic cysts of various sizes.**

Out of the 171 F2 samples generated at day 7, 34 cystic samples were collected. Among the cystic samples, there were 7 *galectin-3* wildtypes, 21 *galectin-3* heterozygotes and 6 *galectin-3* null mutants. 22 out of 34 cystic animals exhibited pancreatic lesions, 7 had very enlarged cystic pancreases, which were over double the size of the animal's stomach. The severity of pancreatic cysts was graded from 0 to 3, 0 = no pancreas lesion observed, 1 = gross dilation of pancreatic ducts, 2 = presence of multiple cysts in the pancreas and 3 = much enlarged cystic pancreas (fig. 10.19A). Among cystic animals, a mean pancreatic cysts score was generated for each *galectin-3* genotype. The mean pancreatic cysts score for *galectin-3* homozygotes was 1.43; *galectin-3* heterozygotes were 1.57 and that of *galectin-3* null mutants was 1.17. No significant difference was found between each genotype (fig. 10.18). Therefore, the severity of pancreatic cysts was not affected by *galectin-3* expression. No pancreatic cysts were observed in *cpk* mutants on the B57BL/6j background and the *cpk* B57BL/6j x *galectin-3* 129Sv mixed background.

Figure 10.18. The correlation between the severity of pancreatic cysts and *galectin-3* genotypes.

The severity of pancreatic cysts was scored and the scores were group according to *galectin-3* genotypes. No correlations were found between the severity of pancreatic cysts and *galectin-3* genotypes.

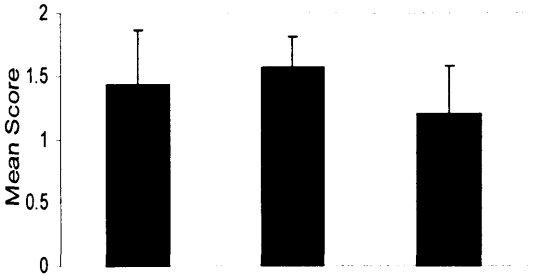

cpk	*-/-*	*-/-*	*-/-*
Gal-3	*+/+*	*+/-*	*-/-*
MEAN Pancreatic cyst score	1.43	1.57	1.17
Lower ci	0.59	1.11	0.57
Upper ci	2.27	2.03	1.77
n	7	21	6

Figure 10.19. Pancreatic cysts in *cpk* mutants on the 129Sv background

A grossly enlarged pancreas can be seen in A before it was dissected out and B was of the same pancreas after carefully dissected out and placed in 4% PFA. C and D are low power view of two different *cpk* pancreases. E is a high magnification of a normal pancreas, compared with F, a *cpk* mutant with presentation of pancreatic cysts in the ductal tubules. C to F were all stained with haematoxylin and eosin. Scale bars = 100 mm.

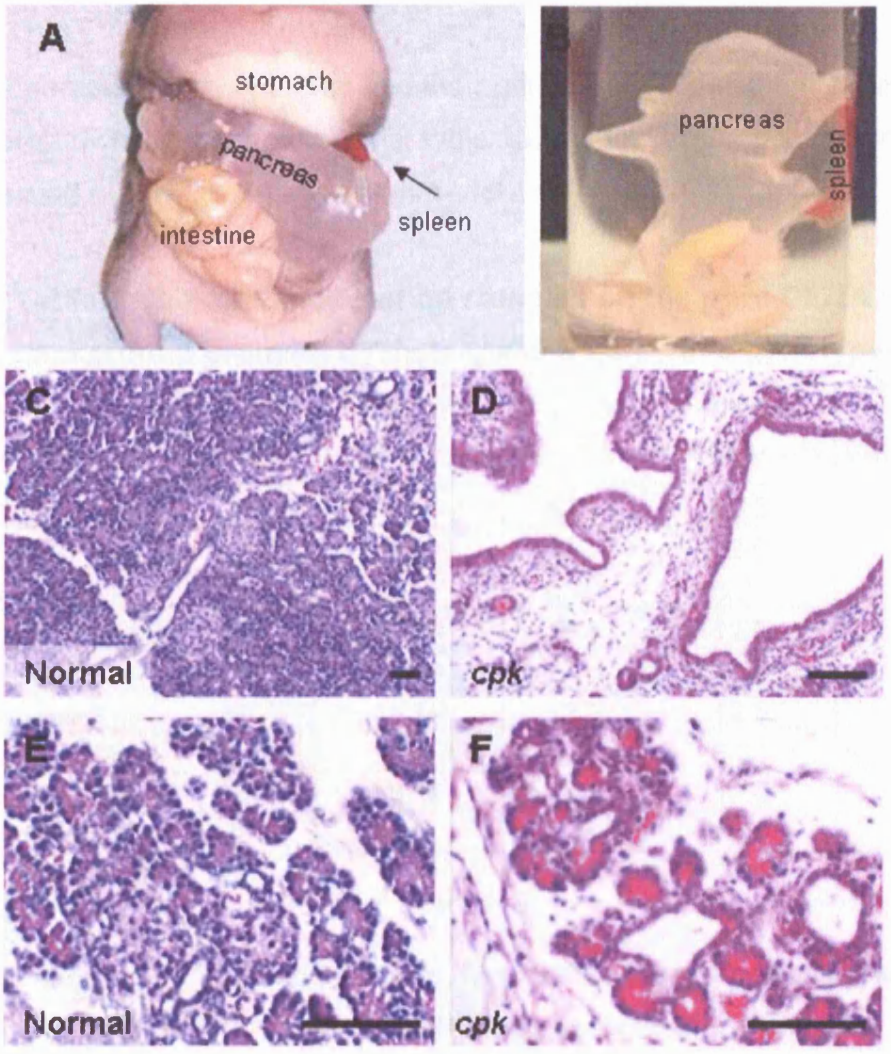

Cytogenesis of *cpk galectin-3* null animals on C57BL/6j background

Towards the end of my study, we successfully obtained *galectin-3* C57BL/6j null mutant mice from the Consortium for Functional Glycomics and bred them with *cpk* C57BL/6j heterozygotes to yield double heterozygotes animals; the offspring were then inter-crossed to yield F2 which contained *cpk* mice with various *galectin-3* genotypes on a pure C57BL/6j background.

108 F2 samples were collected and their genotypes followed the expected Mendel's law (see frequency test at table 10.8). Most of the sample collection was carried out by Dr. Eugenia Dahm-Vicker.

Table 10.8. Frequency test on samples on the pure C57BL/6j background grouped by their *cpk* and *galectin-3* genotypes.

Genotype	Observed number	Observed frequency %	Expected Number	Expected frequency %	Chi-square test
cpk+/+, gal-3 +/+	8	7.41	6.75	6.25	
cpk+/+, gal-3 +/-	9	8.33	13.5	12.5	
cpk+/+, gal-3 -/-	3	2.78	6.75	6.25	
cpk+/-, gal-3 +/+	19	17.59	13.5	12.5	
cpk+/-, gal-3 +/-	27	25.00	27	25	
cpk+/-, gal-3 -/-	17	15.74	13.5	12.5	
cpk-/-, gal-3 +/+	8	7.41	6.75	6.25	
cpk-/-, gal-3 +/-	11	10.19	13.5	12.5	
cpk-/-, gal-3 -/-	6	5.56	6.75	6.25	
Total:	108	100	108	100	**0.46**

25 were genotyped to be *cpk* mutants, from which 8 were *galectin-3* wildtype, 11 were *galectin-3* heterozygotes and 6 were *galectin-3* null mutants. The absolute kidney weights among cystic animals exhibited no significant difference (*galectin-3* wildtype 30mg, *galectin-3* heterozygotes 38mg and *galectin-3* null-mutant 34mg, p-value > 0.07), see figure 10.20. The K/B ratios were: *galectin-3* wildtype 0.79%, *galectin-3* heterozygotes 0.94% and *galectin-3* null-mutant 0.92%, although it appears that heterozygotes and null mutants had

greater K/B ratios no significance differences were found (p-values compared with wildtype are 0.10 and 0.12), see figure 10.21.

Figure 10.20. Summary of kidney weight

Mean kidney weight of cystic animals of different *galectin-3* genotypes. No significant differences were found.

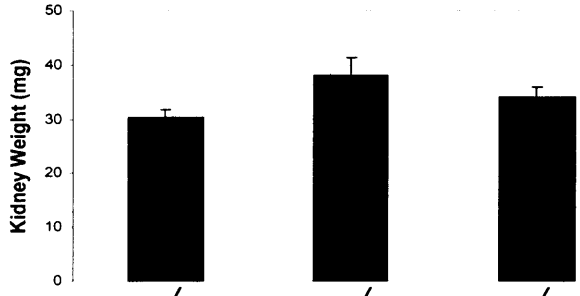

cpk	-/-	-/-	-/-
Gal-3	+/+	+/-	-/-
MEAN Kidney Weight (mg)	30.34	37.98	34.2
Lower ci	27.47	31.36	30.7
Upper ci	33.22	44.59	37.7
n	8	11	6
p-value compared with *gal-3* +/+	----------	0.07	0.11

Figure 10.21. Summary of kidney/body weight ratio

Mean K/B ratio of cystic animals of different *galectin-3* genotypes. No significant differences were found.

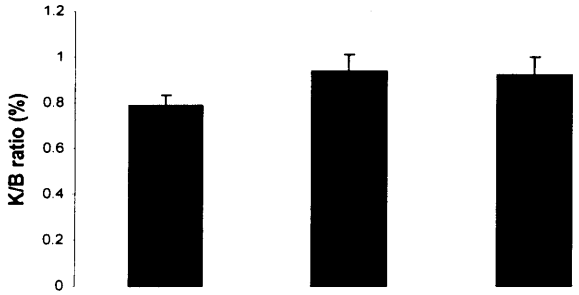

cpk	-/-	-/-	-/-
Gal-3	+/+	+/-	-/-
MEAN K/B ratio (%)	0.79	0.94	0.92
Lower ci	0.71	0.80	0.77
Upper ci	0.87	1.08	1.07
n	8	11	6
p-value compared with *gal-3* +/+	----------	0.10	0.12

Examination of kidney histology revealed that *galectin-3* null mutants had more cortical cysts.

Kidney histology of all cystic samples was examined; all cystic mice had prominent meduallary cysts but there was a qualitative impression of more cortical cysts in the *galectin-3* null-mutants. A scoring system (0 – 4) was developed to assess the degree of cyst growth (see figure 10.22). Utilising a twice-blinded approach (photographs and scoring), clear differences was detected: *galectin-3* null mutants had a cortical cyst score of 2.83, compared to 2.01 in *galectin-3* wildtypes (p-value = 0.01) and 1.92 in *galectin-3* heterozygous (p-value = 0.002), a highly significant difference.

Figure 10.22. Summary of cystic index indicating the degree of cyst growth in the cortex.

Mean cystic index reveals that *galectin-3* null mutants had significantly more cysts in the cortex. * *

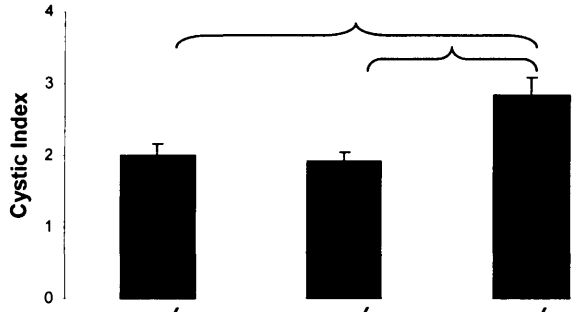

cpk	-/-	-/-	-/-
Gal-3	+/+	+/-	-/-
MEAN Cystic index score	2.01	1.92	2.83
Lower ci	1.71	1.69	2.33
Upper ci	2.31	2.15	3.33
n	8	11	6

Figure 10.23. Representation of different cortical cystic index score.

Below four pictures represent the four different cortical cystic score, A – score 4, B – score 3, C – score 2 and D – score 1. Scoring depends on the number and size of cysts in the cortical region. All sections were reacted with DBA and stained with haematoxylin and eosin. Three sections were taken per samples and all sections were scored by three blind observers to obtain a mean score per sample. Scale bars = 300 μm.

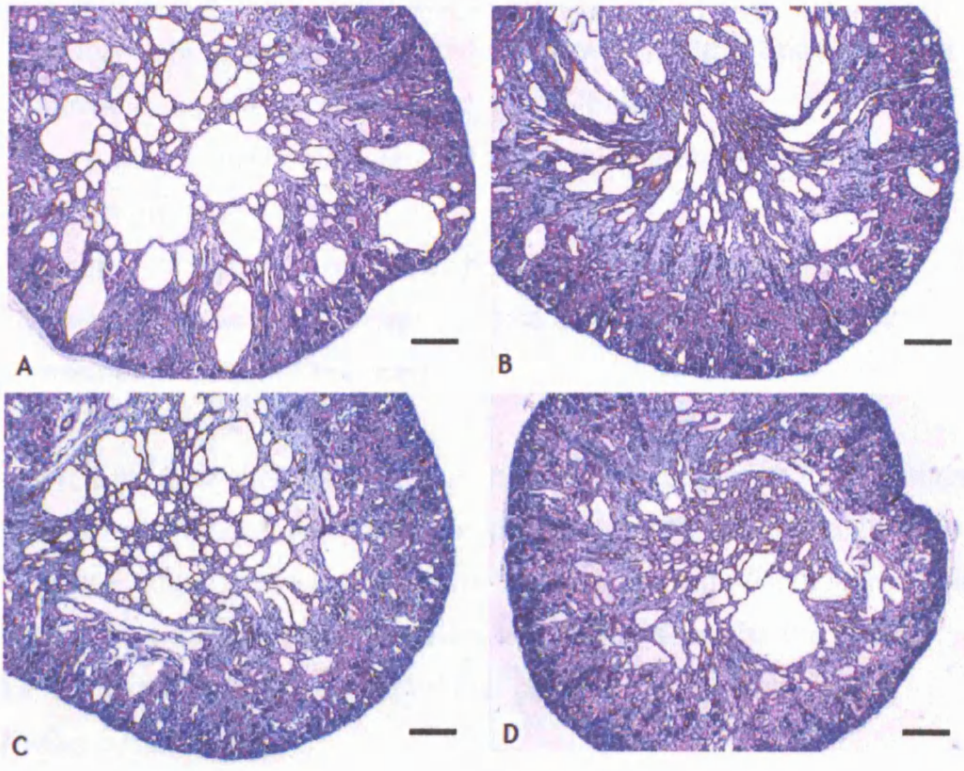

Summary of findings from the *in vivo* studies:

- *Galectin-3* null mutants and heterozygotes *cpk* mice had higher kidney/body weight ratio at Day 7 compared with *galectin-3* wildtypes *cpk* mice, amongst animals on mixed genetics background C57BL/6j x 129Sv.
- *Galectin-3* null mutant *cpk* mice had more cortical cysts compared with *Galectin-3* heterozygotes and *galectin-3* wildtype *cpk* mice amongst animals one pure genetics background C57BL/6j.
- There were significantly less *galectin-3* null mutant animals on the 129Sv Sv background.
- 22 out of 34 c*pk* mice on 129Sv background developed enlarged, multicystic pancreas. The appearance of pancreatic cysts did not correlate to *galectin-3* genotype.

From the results from the C57BL/6j pure background suggests that *galectin-3* null mutants had more cortical cysts compared with *galectin-3* wildtypes and heterozygotes. Although the cystic index did not show significant increase in cysts growth in *galectin-3* heterozygotes, the finding supports the results obtained using the mixed background that *galectin-3* null mutants had accelerated cystogenesis.

EXPRESSION OF GALECTIN-3 ON THE PRIMARY CILIUM OF RENAL EPITHELIAL CELLS

As mentioned earlier, research into the development of PKD has been focusing on an organelle called the primary cilium. Primary cilia can be found in most mammalian cells, it is derived from the mother centriole and it is a flagella-like structure that occurs singly in differentiated cells. Many important proteins that are associated with PKD are localised to this structure, e.g. PC-1, PC-2, fibrocystin, cystin. As galectin-3 was proposed to be important to the development of renal cysts, its localisation on the primary cilia was investigated.

Galectin-3 localisation on the primary cilium

Immunofluorescence was employed to detect the co-localisation of galectin-3 and acetylated tubulin, which identified ciliary structure. Confocal microscopy was used to detect the dual signals expressed by the two different antibodies. Various samples were tested: primary cultures of normal and *cpk* kidneys and IMCD monolayers (fig. 10.24); human ARPKD and ADPKD samples (fig 10.25); 3D cultured cysts from *cpk* kidneys (fig 10.26). Primary cilia developed in monolayer culture when the cells reached full confluency and were differentiated, and they were found in renal epithelial cells in the kidney samples.

Primary cilia were found in all monolayer cell cultures and human ARPKD and ADPKD kidneys examined. Galectin-3 was found localised to the organelle in all samples. The expression pattern varied slightly between primary cilia within the total cell population or kidney sample. Galectin-3 was mostly expressed at the shaft of the primary cilium in a discontinuous manner. Expression at the basal body and on the tip of the primary cilia was sometimes observed. No differences were found on the general expression pattern between cystic, non-cystic samples and of ARPDK and ADPKD samples.

Examination of 3D cysts was more difficult due to technical issues and no obvious co-localisation of galectin-3 was found on the primary cilium. These cells were only cultured for 24 hours (compared with 4 days for monolayer culture); the primary cilia were relatively shorter which may signify that the organelle was not fully developed. The immunocytochemistry of these samples were carried out in suspension and then fixed to poly-L-lysine coated slides for examination. Although the fixation was adequate to hold the cysts in place, it was not strong enough to prevent small movement of the cysts. Therefore no high resolution lens was used for those samples as they require direct contact with the cover slip via the oil interphase, which in turns disturbed the stability of the cysts.

Figure 10.24. Galectin-3 localisation on the primary cilia of cultured cells.

Galectin-3 localisation on the primary cilia of diverse cultured cells: First row (A – C) is a primary culture of normal kidney epithelial cells; second and third rows are from primary culture of *cpk* kidney epithelial cells and the last row is from IMCD cells, which is an established kidney epithelial cell line. Each row shows the same picture with just galectin-3 expression (green), acetylated a-tubulin expression (red). Co-localisation can be seen in the last column (merged) in yellow. In all samples examined, galectin-3 was localised on the primary cilia. Scale bars = 5 mm.

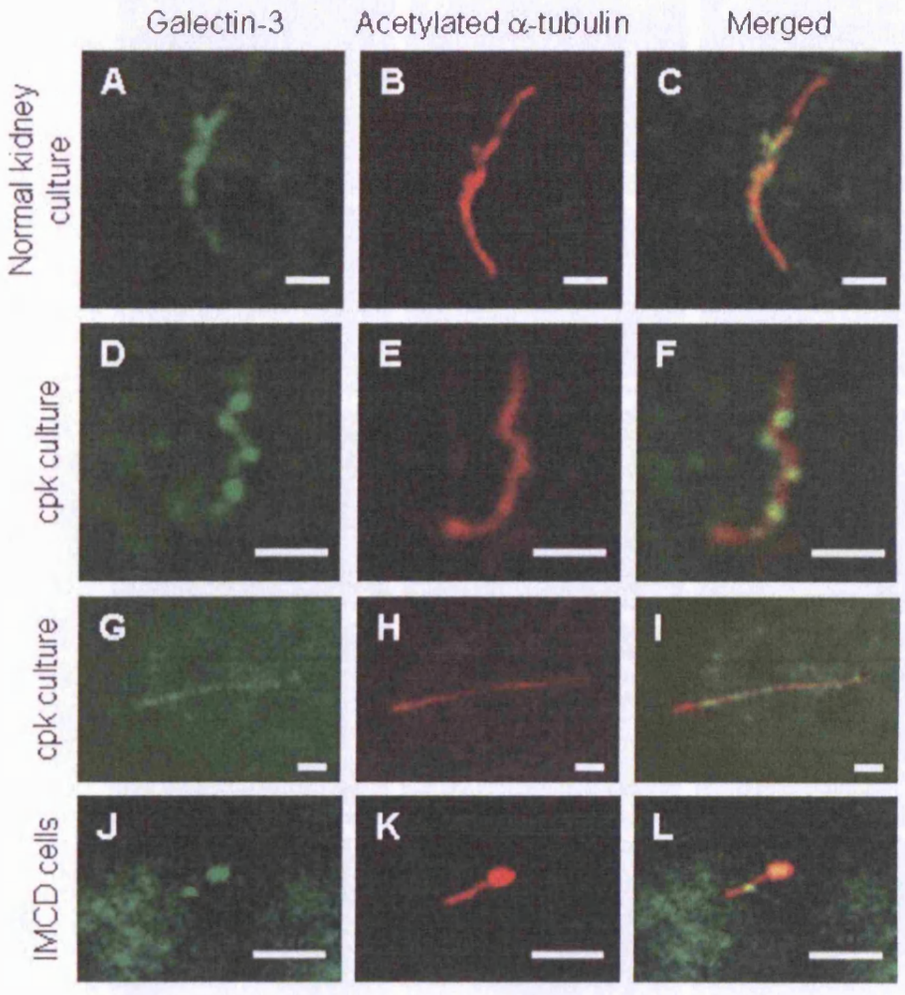

Figure 10.25. Galectin-3 on the primary cilia of kidney sections.

Galectin-3 localisation in kidney samples. First (A-C) and second (D-F) rows are normal mouse kidney collecting tubules and *cpk* cystic epithelia; third (G-I) and forth (J-L) rows are cystic epithelia of human ARPKD and ADPKD samples. Galectin-3 expression in green, acetylated tubulin in red and co-localisation of the two proteins are shown in yellow (merged column). Galectin-3 was detected in primary cilia of all samples examined. Negative control (M-O) using *cpk, gal-3* null mutant shows no galectin-3 expression. Scale bars = 5 mm.

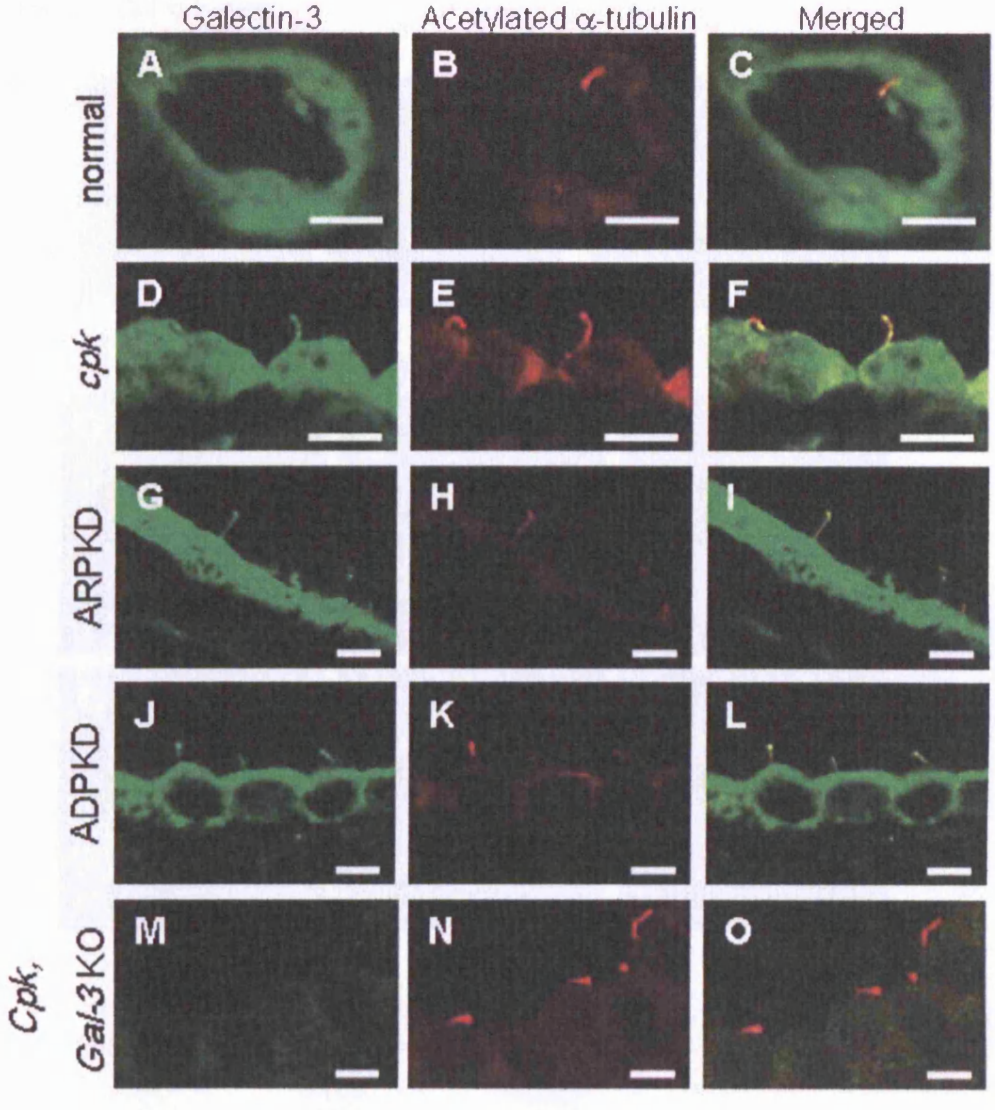

Figure 10.26. Primary cilia on 3D cultured cysts.

Primary culture of 3D cyst from *cpk* kidneys. A and B are of the same cyst taken with a light microscopy with and without fluorescence showing galectin-3 expression. C – F are of the same cyst: C is an enlarged portion of F (dashed box), showing a number of very short primary cilia on the outside of the cyst (white arrows). G – I showed the same cell from a cyst with a cilium on the outside (white arrows). Galectin-3 expression in green, acetylated a-tubulin in red and co-localisation of the two proteins are shown in yellow (merged column). Very subtle galectin-3 expression was seen in I (white arrow), however, it was not a common observation because of technical issues. Scale bars A-C = 5 mm, D-F = 50 mm, G-I = 2 mm.

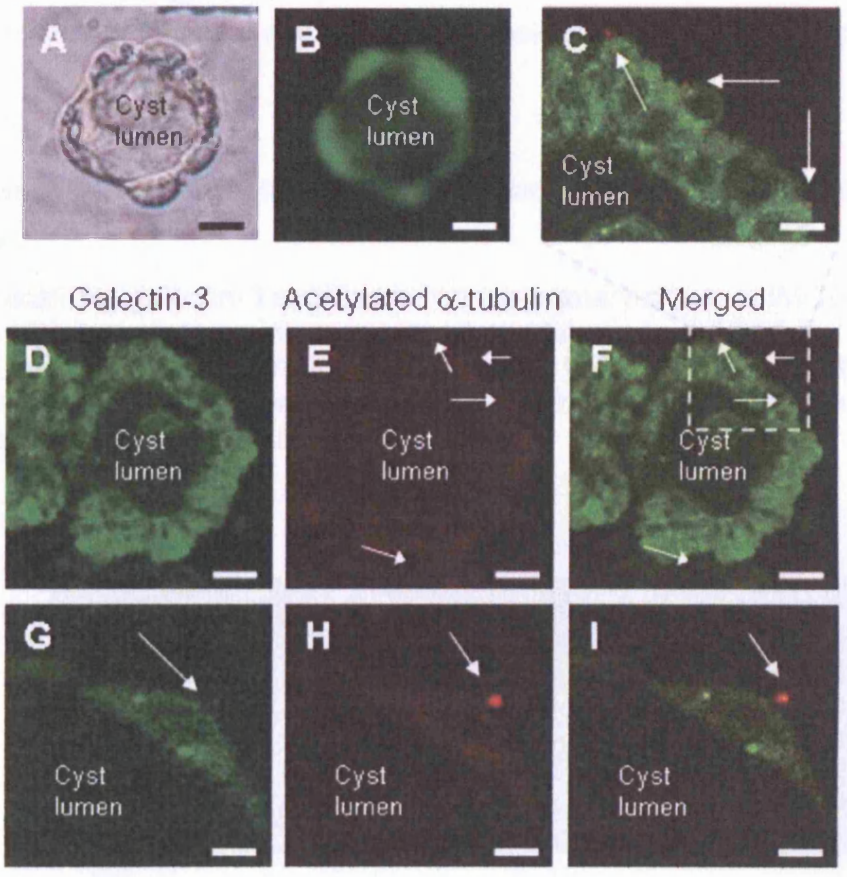

Galectin-3 localisation on the outside of the primary cilia.

Galectin-3 is a secreted protein and it was found in cyst fluid (fig 10.3F). Its localisation on the outside of the primary cilia was assessed on IMCD cells. A stable cell line was used instead of a primary culture due to the technical difficulty of this experiment. Immuno-detection of extracellular galectin-3 was performed on non-permeablised cells. The live cells were cooled down to 4 °C and immunostaining of galectin-3 was carried out in this condition, as fixatives might cause slight permeablisation. Protocol detail is in chapter 8: Methods.

Figure 10.27 clearly shows that galectin-3 is localised to the outside of primary cilia.

Figure 10.27. Extracellular galectin-3 localisation on the primary cilia.

Extracellular galectin-3 expression on the primary cilium of IMCD cells. Galectin-3 expression in green, acetylated tubulin in red and co-localisation of the two proteins are shown in yellow (merged). D-F: negative control using pre-immune rabbit antibodies instead of anti-galectin-3 antibodies. Scale bars = 3 mm.

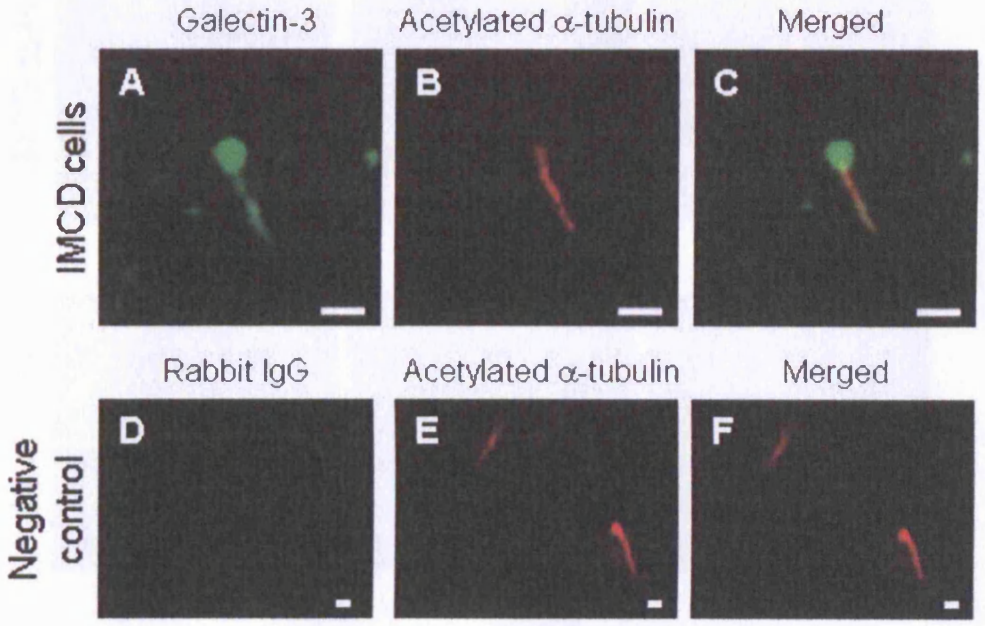

Galectin-3 localisation on the centrosome of IMCD cells

While assessing galectin-3 localisation on the primary cilia of IMCD cells, galectin-3 was occasionally found localised at the spindle poles of dividing cells (fig.10.28A – C). It was speculated that the protein was expressed on the centrosome. To confirm this observation, anti-γ tubulin antibodies were used. It is specifically expressed in the centrioles, and was therefore used as a marker for centrosome. As observed in figure 10.28A – F, galectin-3 was found around the centrioles, hence in the peri-centriolar material.

Figure 10.28. Expression of galectin-3 in the centrosome.

Expression of galectin-3 on the centrosome of IMCD cells. All samples were immunostained with anti-galectin-3 antibodies (green); A – C were immunostained with anti-acetylated tubulin (red) and D – F were immunostained with anti-g-tubulin (red). A – C indicate a dividing cell, which the acetylated a-tubulin was a marker for the chromosomal material. Galectin-3 was expressed in the spindle pole of dividing cells (C) and to the peri-centriolar material (F). Scale bars A-C = 5 mm, D-F = 0.1 mm.

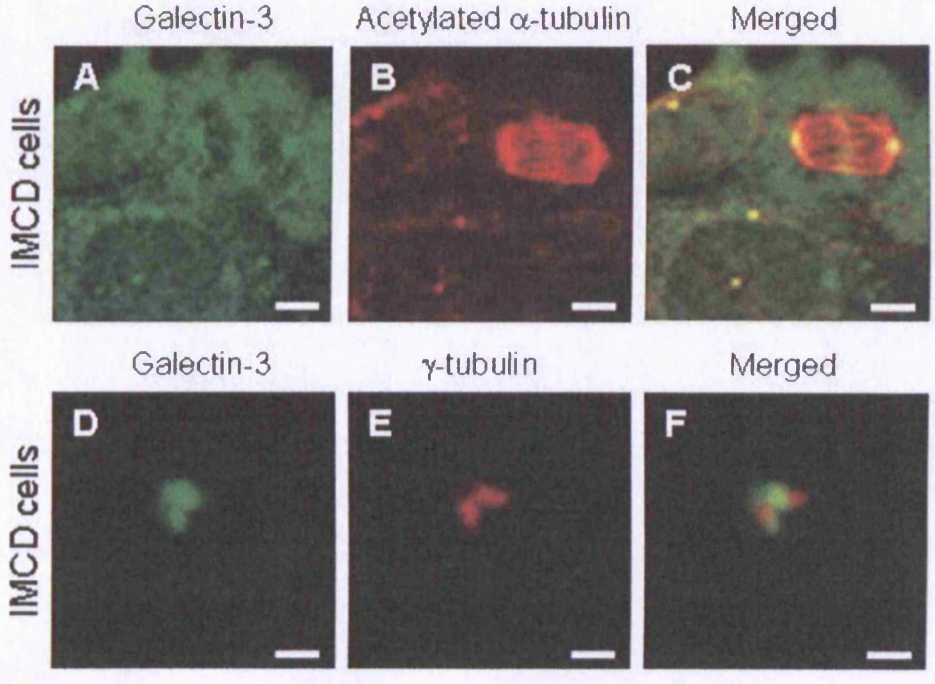

Comparison of primary cilia in galectin-3 wildtype and galectin-3 knockout cystic kidneys.

The primary ciliary structures of *galectin-3* wildtypes and *galectin-3* knockout cystic kidneys were examined. At least three samples were examined in each group. Assessments were done using confocal microscopy and scanning electro-microscopy. Neither assessment showed any observable differences in appearance between the two groups of samples (fig 10.29).

Figure 10.29. Primary cilia in *galectin-3* wildtype and knockout cystic kidneys.

Primary cilia in cystic galectin-3 wildtype and knockout samples. A, C and E are from *cpk* -/-, *gal-3* +/+ kidneys; B, D and F are from *cpk* -/-, *gal-3* -/- kidneys. A and B are confocal images immunostained for galectin-3 (green) and acetylated a-tubulin (red), which identify the structure of primary cilia. C – F are scanning electro-microscope images. Comparison of these images shows that there are no obvious structural different between galectin-3 wildtype and null mutant samples. Scale bars = 5 mm.

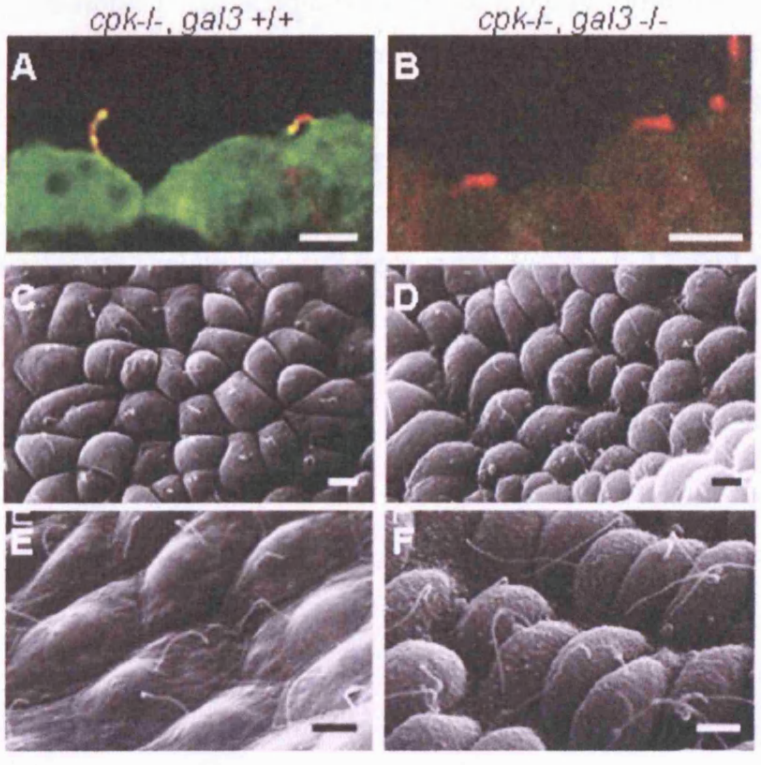

Galectin-3 may be a lipid raft protein

Cystin is present in the lipid raft of IMCD cells (Yang *et al.*, 2004); galectin-4 is a well established lipid raft associated protein in intestinal epithelial cells (Danielsen and Hansen, 2006). Therefore I hypothesised that galectin-3 could also be found in the lipid raft compartment of renal epithelial cells.
Lipid raft extraction was carried out using IMCD cells to determine if galectin-3 was in the raft fraction. Lipid rafts were extracted in cold 0.1% Triton; proteins associated with the rafts were insoluble under this condition. The cell homogenates were then mixed and adjusted to a density gradient solution and centrifuged at 200,000 x g for four hours. Afterwards the content containing fractionated cell components was divided into ten fractions and western blot analysis was carried out. Antibodies against galectin-3 and caveolin-1 were used; the latter is a marker for lipid rafts. Further details of this process can be found in Chapter 9: Methods.

Referring to figure 10.30, fractions 3 to 5 were most enriched with raft proteins, as indicated by caveolin-1. Galectin-3 was found in these three fractions in relatively high concentration, although it was also found in high concentration in fraction 9 and 10, which were the cytoplasmic proteins fractions. This result suggests that galectin-3 is a raft-associated protein at least in IMCD cells.

Attempts were made to isolate lipid raft from cystic kidney but failed due to technical difficulty.

Figure 10.30. Western blot analysis showing that galectin-3 was associated with the lipid raft fraction.

Western blot analysis showed that galectin-3 (30kDa) is found together with caveolin-1 (22kDa) in fraction 3 to 5. Marker was loaded in fraction 1. Galectin-3 was found in all fractions from 3 to 10, although the highest concentration was in factions 3, 9 and 10. It was expected to see galectin-3 in the last two fractions as galectin-3 is a cytoplasmic protein. The high concentration of the protein in fraction 3, 4 and 5 indicate that it is a lipid raft-associated protein. Caveolin-1 was used as a raft-marker and also to confirm that the fractionation was a success as no caveolin-1 was found in the non-raft fractions (9 and 10). The sizes of marker were indicated on the left.

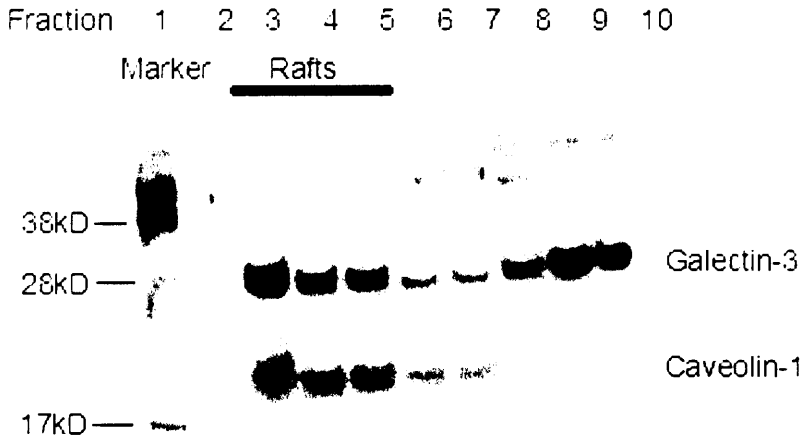

Attempt to repeat the perfusion study which triggers calcium influx in ciliated renal epithelial cells

A few studies have successfully shown that the bending of primary cilia, either by direct contact or by introducing flow on the surface of the cell, leads to calcium influx (Praetorius and Spring, 2003; Nauli *et al.*, 2003; Liu *et al.*, 2005; Shiba *et al.*, 2005).

Therefore I performed experiments to determine whether altering *galectin-3* concentration had a functional effect on the mechanical response of primary cilia to calcium influx. Firstly I attempted to set up a perfusion study so I could pass a constant flow rate over cultured cells which would then bend the primary cilia and triggers a calcium influx response. Then I would repeat the experiment with *galectin-3* null cells (taken from the medulla of *galectin-3* null kidneys); and compare the response rate and the strength of calcium influx with that of normal renal epithelial cells. Finally, I planned to repeat the experiment with primary cultures of *cpk* renal epithelial cells, with the addition of galectin-3 in medium and determine if the exogenous galectin-3 alter the rate and strength of response of calcium influx compared with cells treated with media alone.

In order to carry out this experiment, one must be able to achieve the appropriate flow rate. Previous experiments on the bending of primary cilia were carried out under a flow rate of 8 μl sec^{-1} for a period of 10 minutes in a custom built perfusion chamber (16mm long x 3 mm deep and 3 mm wide) (Praetorius and Spring, 2001). No equipments were available in my laboratory for this flow rate experiment, therefore two different research groups were contacted and after several trials, I could not achieve the desired flow rate due to the absence of the custom built perfusion chamber. Instead, our attention changed to finding a way to physically bend the organelle. To do that, a very fine instrument is required that can tap the tip of the cilia without contacting the cell surface. Atomic force microscope (AFM) is able to provide that; it is sometimes described as a scanning machine that uses a very fine tip at the

end of its cantilever to scan the surface of any samples, including live biological cells, and gives a image based on the topograph of the sample (Trache and Meininger, 2005).

Examination of the primary cilia using an atomic force microscope.

AFM was used in an attempt to examine and to manipulate the structure of the primary cilium. It is a highly sensitive device that is used to assess the topography of substances, both biological or non-biological. It can also be used to give quantitative analysis of the samples, e.g. the presence of microvilli on cell surface and the degree of roughness of the surface (Poole *et al.*, 2004).

AFM is based on the use of a scanning cantilever with a tip that is in contact with the sample; for my experiments the idea was to develop a system in which the tip can be used to bend the primary cilium in live cell; and incorporate the AFM imaging system with fluorescent microscopy to assess calcium influx in cells upon stimulation of the primary cilium. My collaborator Professor Horton already had an AFM machine that was intergrated with a fluorescent microscope.

To test the system, quick-dried IMCD cells were used as a sample and primary cilia were detected and imaged using the AFM (fig 10.31 and 10.32). As it was planned for the system to run on live cells, it was important to be able to detect the primary cilium in liquid phase. AFM was used to image IMCD cells in PBS (fig 10.31). Although it was successful in imaging the wet sample, we were unable to get a good image of the primary cilia. Several attempts were made, but due to the sensitivity of the cantilever to temperature change and the lack of rigidity of wet cells, it was difficult to achieve a stable engagement between the tip of the cantilever and the cilia. The difference in cell morphology between dried and wet cells can be compared (fig. 10.31). The latter were fuller with a

smoother appearance of the cell surface. The problem with the sensitivity of the cantilever to temperature is being investigated. It can be eliminated by using a specially designed chamber that controls the temperature and humidity of the samples. This chamber is currently being optimised for use; preliminary results showed that the primary cilia in liquid phase could be imaged using this chamber (personal communication with Dr. Haupt).

Referring to figure 10.31 and 10.32: in each frame, two images were produced, a height image (left) and an amplitude image (right). The former is a topographical image; the latter refers to the alternating voltage that is applied to the piezo (an adjustable platform where the sample was placed). A voltage is applied to the piezo to adjust its height in response to the heights of the sample, so that the amplitude of the cantilever oscillation remains constant. In other words, the signal was created by the changes on the surface of the sample: the bigger the change the greater the voltage. Therefore the contrast in the image reflects the changes on the sample.

Presence of primary cilia was confirmed by immunofluorescence which showed that the organelle was fully developed in confluent IMCD culture prior to AFM imaging (Fig 10.31B). Primary cilia were detected on dried IMCD cells. AFM image showed that it is a hair-like structure on the surface of IMCD cells; the tip of the cilia was fatter than its stalk, as observed using the confocal microscope. In addition, a bulky structure which appeared to be the basal body was detected in the AFM images (fig 10.32K and O). The primary cilia were between 2 and 4 μm in these dried IMCD cells. The shortened length compared to the average 5 μm observed indicated that the samples had shrunk, possibly by drying.

Figure 10.31. AFM imaging of dried and wet IMCD cells.

A) phase contrast image of the cantilever over IMCD cells. B) An exact same frame as A, immunofluorescent image of IMCD cells showing fully developed primary cilia labelled with acetylated a-tubulin (green). C – F) AFM imaging of dried (C, D) and wet (E, F) IMCD cells. C and E are height images; and D and F are amplitude image

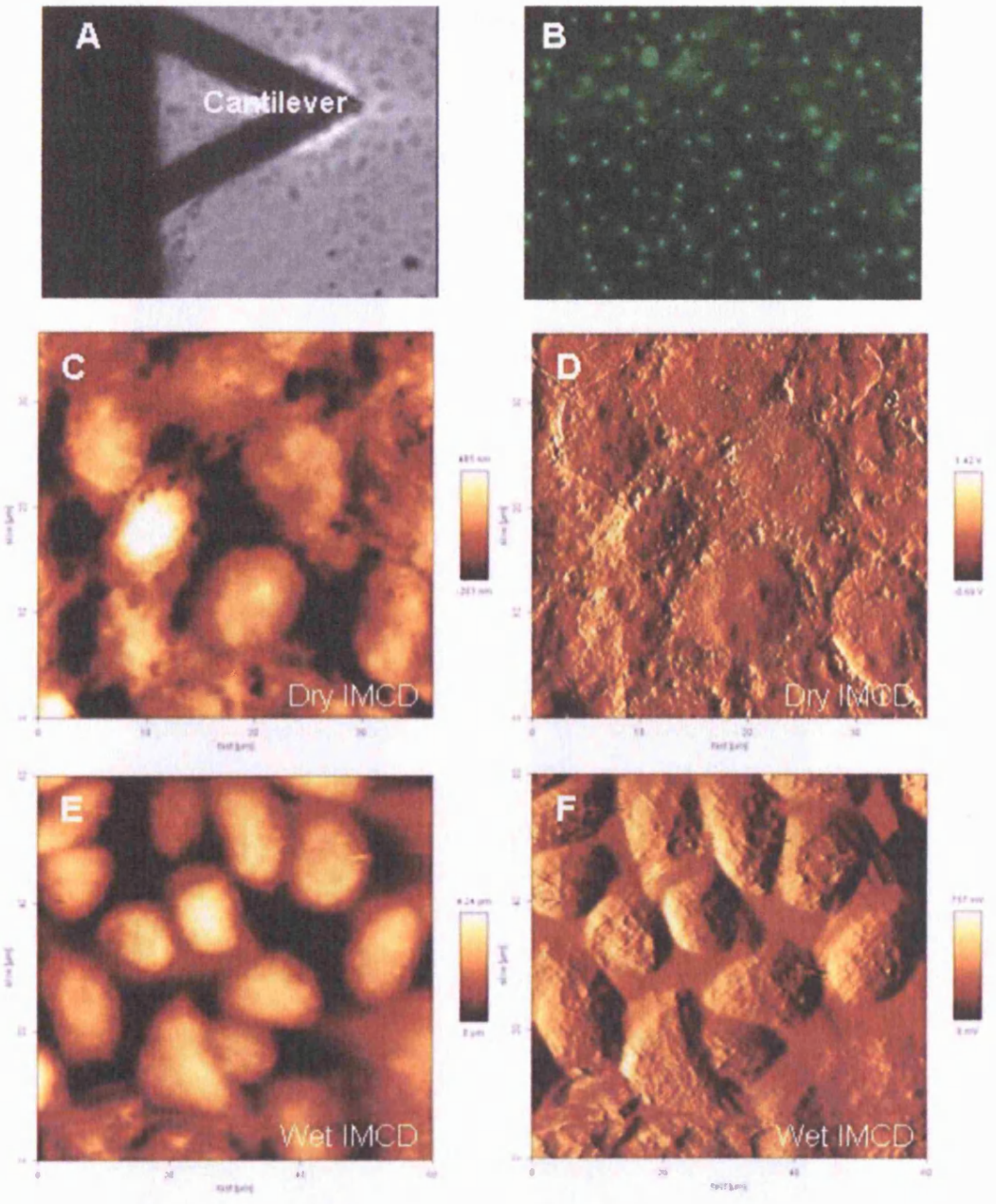

Figure 10.32. AFM imaging of primary cilia in dried IMCD cells.

All images on the left are height images, whereas those on the right are amplitude images. Each cell was represented in four images (A – D, E – H, I – L and M – P), thus four different primary cilia were shown. White boxes in B, F, J and N are where the primary cilia were and was subsequently enlarged in the following images. White circles in height images C, G, K and O indicated the basal bodies of each primary cilia, revealing a shape of the two centrioles.

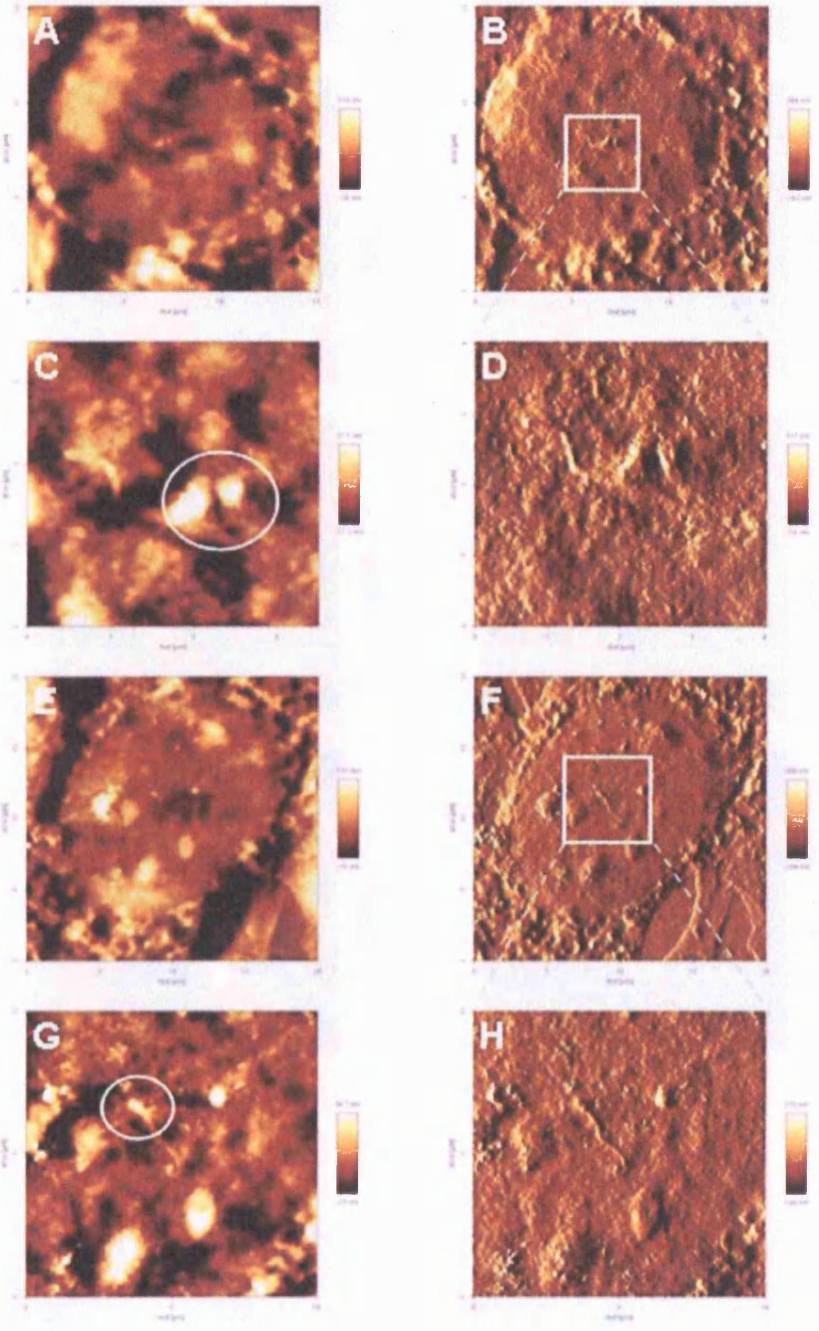

Figure 10.32 continued.

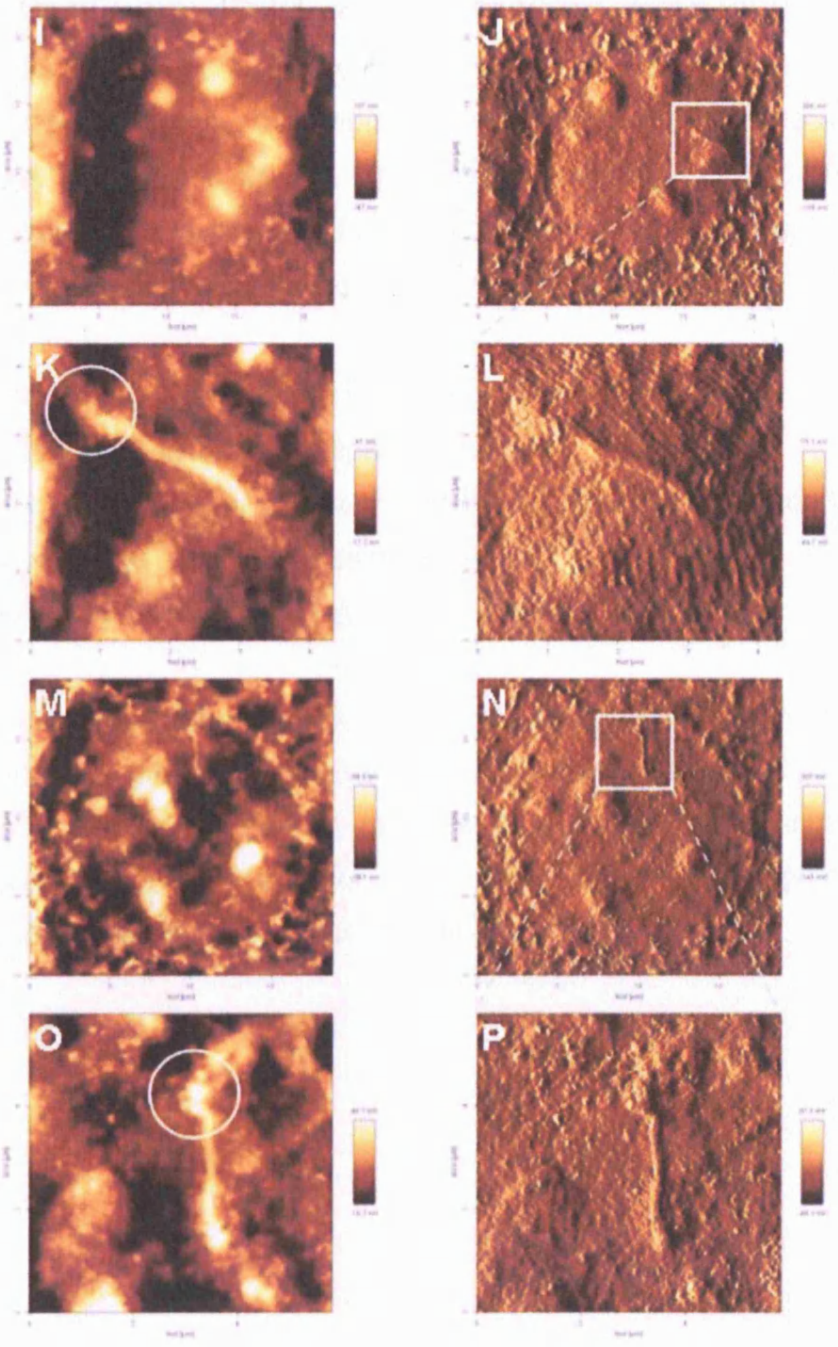

Summary of findings from the studies on primary cilia:

- Galectin-3 was expressed on renal primary cilia of cystic and non-cystic kidney samples (*cpk,* human AD-, ARPKD and normal mouse kidneys) and in cells cultures (*cpk* primary cultures and IMCD cells).
- The protein was found on the outside of the organelle, although some of the protein may also be expressed intracellularly in the primary cilium.
- Galectin-3 was expressed in the centrosome of IMCD cells.
- Galectin-3 was found in the lipid raft fraction.
- Although no functional data were presented, efforts were made to carry out the calcium influx study using AFM.
- Successfully detected primary cilia on dried IMCD cultures.

So far, I have described the wide expression of galectin-3 in cystic kidney epithelial cells; *galectin-3* null mutants had accelerated cystogenesis and that galectin-3 is localised to the primary cilia. This following section describes the work continued from my predecessor, Dr. Johnson, into the role of galectin-3 in the effect of paclitaxel in suppressing cyst growth.

THE EFFECT OF PACLITAXEL ON THE CYSTOGENESIS OF *CPK* MICE.

It was previously reported that paclitaxel, a drug that amongst other actions stabilises microtubules, has a very significant effect on the development of renal cystic disease in *cpk* mice in that it greatly prolongs the lifespan of these animals (Woo et al 1997). The effect of paclitaxel on the expression patterns of galectin-3 in normal and *cpk* mice was investigated by Dr. Tanya Johnson. Like the original study carried out by Woo et al, *cpk* mice were treated with a single dose (150 μg) of paclitaxel at day 10 and the animal were sacrificed at day 21 for analyses. Immunohistochemistry was used to determine that in paclitaxel treated cystic kidney epithelial cells, galectin-3 was expressed apically instead of the cytoplasmic expression in untreated cystic kidneys. In addition, Dr. Johnson demonstrated, using *in vitro* 3D cyst culture system, that paclitaxel treated cyst culture had more galectin-3 protein in the medium compared with vehicle treated (DMSO) culture, as detected with immunoblotting, indicating that paclitaxel enhanced the secretion of galectin-3.

In this thesis, the samples obtained by Dr. Johnson were reanalysed for the galectin-3 expression pattern and primary cilia were examined. In addition, a new set of paclitaxel treatment was carried out on *cpk* mice; again a single administration of 150 μg at day 10 and the animals were sacrificed at day 11, a much earlier time-point compared with at day 21 in previous experiment. Kidneys from these animals were dissected out and their galectin-3 expression pattern was examined by immunohistochemistry.

The *in vitro* cyst culture was also repeated: paclitaxel (50 μM) and galectin-3 (30 μg/ml) reduced the number of cyst formed in culture when added separately (Woo *et al.* 1994). Also, paclitaxel enhanced the secretion of

galectin-3 (Johnson, 2001). The increased extracellular level of galectin-3 may in turn reduce cystogenesis. I was interested to determine if the two reagents act on different pathways or if they have a synergistic effect on each other. In both cases, one would expect to see a greater reduction in cystogenesis when the two reagents were added. To test that, the two reagents were added together to the culture medium.

Expression pattern of galectin-3 in paclitaxel treated *cpk* kidneys.

Cpk mice were treated with a single dose of 150 μg paclitaxel in DMSO at day 10 and kidneys were collected at day 11 (one day after treatment) and day 21; the latter were samples prepared by Dr. Johnson. Immunohistochemistry was performed on these kidney samples.

Galectin-3 expression was relocalised to the apical surface of cystic kidneys in paclitaxel treated *cpk* kidneys, compared with a pre-dominantly cytoplasmic expression in vehicle (DMSO) treated and untreated samples (fig. 10.33). The presence of primary cilia was also examined in these samples; paclitaxel is a well known microtubule stabiliser, therefore it was of interest to see if it acts on cystic epithelial cells by structurally changing the primary cilium. In addition, galectin-3 was localised to the primary cilia in normal and *cpk* kidneys; thus the localisation of galectin-3 on the organelle was also assessed in these samples.

Anti-galectin-3 antibodies were used to assess the localisation of galectin-3 in paclitaxel treated samples; and anti-acetylated α-tubulin antibodies were used to assess the presence of primary cilia.
As previously described in *cpk* kidney, the majority of cystic epithelial cells expressed galectin-3 in the cytoplasmic domain. In paclitaxel treated samples (both day 21 and day 11), galectin-3 was found predominantly in the apical

domain. This observation was more prominent in the day 11 samples. Primary cilia were present in all samples (treated and untreated), no difference were observed using the confocal microscope. Galectin-3 was found on the primary cilia of treated and untreated samples (fig 10.33). Therefore, paclitaxel had no effect on the structure of primary cilia and on galectin-3 localisation to the organelle *in vivo*.

Figure 10.33. Galectin-3 and primary cilia expression in paclitaxel treated and untreated *cpk* kidneys.

Galectin-3 and primary cilia expression on *cpk* kidney samples: untreated and single dose paclitaxel treated. Galectin-3 protein was expressed in green and primary cilia was expressed in red. Colocalisation of galectin-3 on the cilia was shown in yellow. Only the merged pictures are shown. In untreated kidney, galectin-3 was widely expressed in the cytoplasmic domain of the cystic epithelia; whereas in paclitaxel treated samples, either at day 21 or 11, a predominantly apical expression of galectin-3 was detected. Scale bars = 10 mm.

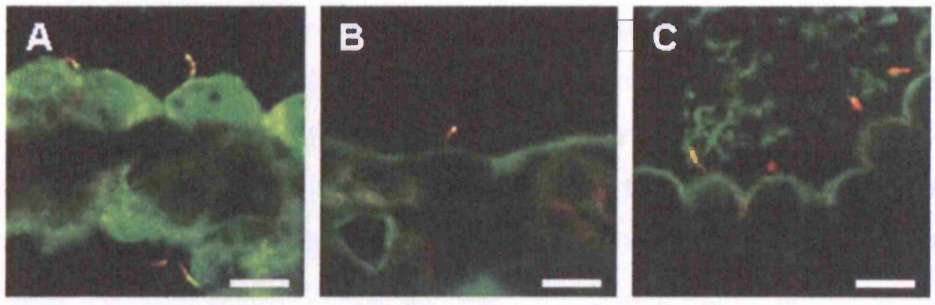

Untreated | Paclitaxel treated day 21 | Paclitaxel treated day 11

The effect of paclitaxel and galectin-3 on cystogenesis of *in vitro* cyst cultures.

3 week old *cpk* kidneys were partially digested and the cells were used to prepare primary cultures in suspension. Cystogenesis was measured by the number of cysts formed and the mean cyst size after 24 hours in culture.

The number of cysts formed after 24 hours in different conditions is summarised in the figure 10.34. Control was where the medium had no additional galectin-3 or paclitaxel added and it was used as a standard point (100%). All other values were measured against the control in a form of percentage. Compared with control, the addition of galectin-3, paclitaxel or both together significantly reduced the number of cysts formed by 21%, 52% and 62% respectively. Paclitaxel had a greater effect in reducing cyst formation then galectin-3 (p-value = 0.019). By adding the two reagents together, there were no significant differences when compared with adding paclitaxel alone (p-value = 0.438), although a significant difference is seen when comparing adding both reagents together versus galectin-3 only. This may suggest that either the two reagents work on the same pathway or a maximum effect was already achieved, therefore no cumulative effects were observed.

Mean cyst size were also calculated for all samples and they are summarised in figure 10.35. These values were compared. No significant differences were found between them; hence the addition of galectin-3, paclitaxel or both did not affect the size of cyst formed after 24 hours in suspension culture.

These results suggest that both galectin-3 and paclitaxel affect cytogenesis perhaps not by restricting cyst growth as the size of cysts were not affected; rather the reagents may act by inhibiting the formation of cysts at the beginning, hence a reduced number of cysts formed in culture.

Figure 10.34. Addition of paclitaxel and galectin-3 to *in vitro* cyst culture: effect on cyst number.

Treatment with paclitaxel and galectin-3 sigificantly reduced the number of cyst formed after 24 hours, compared with control. No significant difference was found between adding paclitaxel alone and adding both paclitaxel and galectin-3 together. Hence no cumulative effects were detected.

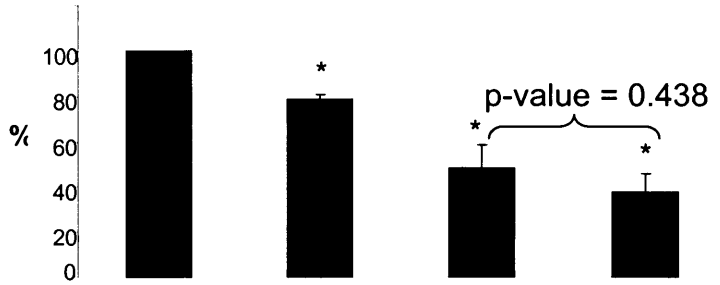

	Control	+ Gal-3	+ Paclitaxel	+ Gal-3 and Paclitaxel
MEAN cyst number (%)	100	79	48	38
Upper ci	NA	82	68	54
Lower ci	NA	75	28	21
p-value compared with control	NA	0.000004	0.001	0.00006
n	5	5	5	5

Figure 10.35. Addition of paclitaxel and galectin-3 to *in vitro* cyst culture: effect on cyst size.

Treatment with paclitaxel and galectin-3 had no significant effects on cyst size.

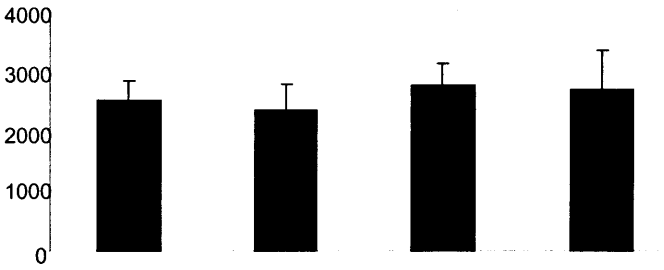

	Control	+ Gal-3	+ Paclitaxel	+ Gal-3 and Paclitaxel
MEAN cyst size (%)	2502	2757	2341	2671
Upper ci	2815	3113	2773	3327
Lower ci	2188	2400	1909	2015
p-value compared with control	NA	0.32	0.57	0.66
n	5	5	5	5

Summary of findings from the paclitaxel treated *cpk* mice:

- Paclitaxel treated *cpk* animals exhibited relocalisation of galectin-3 in the cystic epithelia, from cytoplasmic expression to apical expression. The change in expression was observed in *cpk* animals at one day and 11 days after treatment.
- Addition of galectin-3 and paclitaxel separately to *cpk* cyst cultures reduced the number of cysts formed after 24 hours but did not affect the size of cysts.
- Addition of galectin-3 and paclitaxel together did not have an enhanced effect on cyst number compared with adding paclitaxel alone, hence there are not cumulative effects.

CHAPTER 11: DISCUSSION

Autosomal Recessive Polycystic Kidney Disease (ARPKD) is an inherited disease that causes cyst formation in kidneys as well as ductal malformation in the liver. Clinically, the disease presents in new born patients or in young children. Advances in medical care and pre-natal diagnosis have dramatically reduced the neonatal mortality rate, though this may be partly due to increased number of abortions before this stage. Approximately 50% of surviving individuals progress to end-stage renal disease (ESRD) within the first decade of life. They represent 5% - 8% of all individuals requiring renal replacement therapy in childhood (dialysis and/or kidney transplantation) (Sweeney, Jr. and Avner, 2006).

In 2002, several groups (Xiong *et al.*, 2002; Ward *et al.*, 2002; Onuchic *et al.*, 2002) successfully identified mutations in *PKHD1* as causative for ARPKD in humans. It is one of the largest disease causing genes to date in the human genome (Onuchic *et al.,* 2002), with a complicated transcription profile that is predicted to have multiple variants of the transcribed protein – fibrocystin. The *PKHD1* gene consists of at least 86 exons (12,222 bp) with a longest continuous open reading frame of 67 exons, spanning approximately 472kb of genomic DNA. The combination of the large size of this gene and the variability of the disease has made the investigation of the pathophysiology and the molecular mechanisms of the disease very difficult. ARPKD belongs to a group of polycystic kidney diseases (PKD) which share many similarities especially the characterisation of their renal cystic epithelia. Thus studies of other PKD may provide vital information about cystogenesis of renal cysts in ARPKD.

Galectin-3 was previously implicated in cystogenesis in an *in vitro* model using Madin Darby canine kidney (MDCK) cells and partial digestion of cystic

kidneys taken from the *cpk* model, a phenotypic ARPKD mouse model. In these experiments, addition of galectin-3 retards cystogenesis by restricting cyst growth either in size (MDCK cells) or in number (*cpk* primary culture). The experiments in this thesis were designed to further evaluate the effect of this protein on the development of renal cysts. Based on the studies on *in vitro* cyst cultures, the hypothesis is that galectin-3 retards cystogenesis.

I investigated the role of galectin-3 in the development of ARPKD using the *cpk* mouse model. Kidney cyst development in this model closely resembles that of human ARPKD. Also studies were carried out in kidney epithelial cell lines and in kidney samples from other PKD models. Through this study, I was able to identify the importance of galectin-3 in reducing renal cyst growth *in vitro* and *in vivo*; galectin-3 was also found on the primary cilium, an organelle that has a very important functional role in the pathogenesis of PKD. Additionally, I have begun to investigate a new technique (Atomic Force Microscopy - AFM) that may be used to study the primary cilia. I believe that this study of galectin-3 on the development of ARPKD has added valuable information on cystogenesis on a molecular level.

GALECTIN-3 WAS FOUND WIDELY EXPRESSED IN THE CYSTIC EPITHELIA OF *CPK* MICE AND OTHER PKD MODELS.

The expression of galectin-3 in cystic kidneys was first detected by my supervisor, Dr. Winyard; he found that galectin-3 protein is expressed in the dysplastic kidneys and in human ARPKD samples (Winyard *et al.*, 1997). Later Dr. Johnson (a previous PhD student studying this project), using *in situ* hybridisation, described an up-regulation of galectin-3 mRNA in the *cpk* cystic epithelial cells compared with epithelial cells in normal kidneys.

In this thesis, I confirmed that galectin-3 protein was detected, using immunohistochemistry, in the majority of cystic epithelial cells of *cpk* samples. The protein was predominantly expressed in the cytoplasm. The protein was also detected in cyst fluid by western blot, suggesting that the protein was secreted.

One of the early concepts about PKD is that epithelial cells dedifferentiate towards embryonic state. Hence, the wide expression of galectin-3 in cystic kidneys can merely be caused by the dedifferentiation of epithelial cells to a more embryonic phenotype. Therefore, the expression patterns of other collecting tubules proteins expressed during development (ret, aquaporin-2 and calbindin d28) were examined using immunohistochemistry on 3 week old *cpk* kidneys. As described in results, none of these markers reiterated the expression pattern of galectin-3 which was detected across a whole range of cyst sizes; hence, galectin-3 expression in cystic epithelial cells is unlikely to be due solely to the dedifferentiation of these cells.

The expression of galectin-1 and galectin-9, two other prominent galectins found in the kidneys, were also investigated. This was carried out in order to determine if they are also over-expressed in cystic epithelia and if they may compensate for the lack of galectin-3 in the null mutants. One common feature between galectins is the presence of a common carbohydrate-recognition domain (CRD); many of the functions of galectins are brought about by the CRD and some galectins do share the same functions (the role of galectin-1 and -3 in pre-mRNA splicing (Park *et al.*, 2001).

Neither galectin-1 nor galectin-9 had the same expression pattern as galectin-3. Galectin-1 protein was not detected in any epithelial cells in the kidneys (normal and cystic) and galectin-9 was only detected in a small subset of collecting tubule epithelial cells in both normal and cystic kidneys. The expression pattern of these galectins remained the same in galectin-3 null

mutants; hence, they do not appear to compensate for the lack of galectin-3 in these animals. As we did not examine all known galectins, it is possible that other ones are expressed in the collecting tubules and could be up-regulated in *galectin-3* null mutants. Very recently, galectin-7 was found in hamster kidney (Saussez *et al.,* 2006). Results from null mutants suggest that galectin-3 role during normal development is redundant although a 11% reduction in the number of nephrons was observed in *galectin-3* null mutant mice (Bichara *et al.*, 2006) and its function is perhaps more important in response to cell damage. Several galectins are expressed as part of the immune system or as repair mechanisms: galectin-3 in activated macrophages, galectin-3 and -7 in re-epithelialisation and galectin-11 in infected gastrointestinal tissue (Dunphy *et al.*, 2000; Cao *et al.*, 2002; Sharma *et al.*, 2004).

The *in situ* hybridisation assessing the expression of galectin-3 mRNA, work carried out by Dr. Johnson, appeared to show that galectin-3 is up-regulated in cystic epithelial cells compared with normal collecting tubule epithelial cells. This was reflected by the more intense signal in the *cpk* samples. Although it showed a positive result, the method used was not quantitative, however, hence one cannot conclude that galectin-3 expression is definitely upregulated in cystic epithelial cell compared with normal. Previous western blot analysis shows that the protein is upregulated in the whole organ but that may not reflect an upregulation in individual cells due to a higher presence of collecting tubules as cysts in cystic kidneys. This problem may be corrected by using a marker that is only expressed in collecting tubules, such as DBA (dolichos bifloros agglutinin). In theory, the most direct way to quantify the level of protein expression would be to use western immunoblot of epithelial cells; however, they cannot be readily isolated from the kidneys in sufficient quantity.

I attempted to quantify the expression level of galectin-3 by measuring the immunostaining intensity, using a confocal microscope with same settings to

image all samples, which were examined with Leica software that quantified staining intensity. Several 3 week old normal and *cpk* kidneys were assessed and a mean level of cytoplasmic expression of the protein was determined. Although no significant difference was found, I cannot conclude that the protein expression level was the same in normal and cystic samples. This is because galectin-3 was detected in cyst fluid, which added to the total amount of protein expressed in the cystic kidney. The quantifying method used only measured cytoplasmic expression of galectin-3 and not the total amount of protein expressed or subcellular distribution. Due to lack of confirmation that the protein is upregulated, the expression galectin-3 in cystic samples was described as widely expressed rather than up-regulated. Although I did not manage to show a specific up-regulation of galectin-3 expression in individual cystic epithelial cells, the expression of galectin-3 is more prominent across all range of cysts when compared with the expression pattern of other collecting tubule markers.

The expression of galectin-3 was examined in other PKD samples: *cpk* mutants on balbc and DBA backgrounds; *Pkd2*$^{ws25/-}$, a genotypic ADPKD model; *Bpk and Orpk*, both are ARPKD models; and human samples of ADPKD and ARPKD. Galectin-3 protein was found widely expressed in all these samples, suggesting that the role of galectin-3 in cystogenesis is not restricted to the *cpk* model.

What is the role of galectin-3 in the cystic epithelia?

Setting aside my original hypothesis, the expression of galectin-3 in cystic epithelia may represent one of three phenomenons:

1) Galectin-3 may enhance cyst development; the protein may play a role in the progression of cyst expansion by modulating proliferation and cell adhesion. Overexpressions of proteins such as EGFR and P2X(7), and

the second messenger cAMP in cystic epithelia lead to cyst development. Moreover, antagonists against these proteins appear to reduce cystogenesis (Sweeney, Jr. and Avner, 1998; Hillman *et al.*, 2004; Torres *et al.*, 2004b; Wilson *et al.*, 2006), therefore it may be logical to think that galectin-3 acts in the same way.

2) Galectin-3 may suppress cyst development. The protein may be expressed as a response to the distressed cells, thus its expression may ameliorate the condition. Galectin-3 is known to be expressed in various cell types in the immune system as part of the immune responses, where it participates in the activation and differentiation of immune cells (Chen *et al.*, 2005). Here, the protein is expressed in response to pathophysiological changes and it acts as a defence mechanism. MDCK cell culture in 3D Matrigel revealed that exogenous galectin-3 inhibits the enlargement of these MDCK cysts (Bao and Hughes, 1995), supporting the theory that the expression of galectin-3 in cystic epithelia suppresses cystogenesis. Examples of the protective role of galectin-3 can be found in glomerulopathy. Galectin-3 is not normally expressed at the glomerular/ mesangial level, but is overexpressed in diabetic individuals. *Galectin-3* null mutant mice developed accelerated diabetic glomerulopathy, suggesting that the lectin exerts a protective effect over tissue injury *in vivo* (Pugliese *et al.*, 2001). In addition, *galectin-3* null mutant mice show accelerated AGE (advanced glycation end products) – induced glomerular injury (Iacobini *et al.*, 2004).

3) It plays no part in cystogenesis. Galectin-3 null mutant mice show only minor differences in body function and development. The same redundancy may apply to its role in cystogenesis. Its expression may be a reponse to the changes in the environment. It is known that galectin-3 expression is induced during metabolic acidosis (Schwaderer *et al.*, 2006), so it may be altered because of this.

Based on the MDCK work carried out by Bao et al, I hypothesised that galectin-3 does play a role in cystogenesis and that it retards cyst development in kidneys.

Previous *in vitro* work shows that, in agreement with out hypothesis, addition of galectin-3 to culture medium retards cystogenesis. We hypothesised that a reduction of galectin-3 would have an opposite effect, thus *galectin-3* null mice would have accelerated cyst growth (fig.11.1).

Figure 11.1. Diagrammatic illustration on the hypothesis of the role of galectin-3 on cyst development.

Hypothesis of the role of galectin-3 during renal cyst development. Addition of galectin-3 (left) retards cysts growth, which was supported by the *in vitro* data: exogenous galectin-3 reduced the number of cyst form in the *cpk* 3D cyst culture (Johnson 2001). Reduction of galectin-3 enhances cysts development, as observed in the *in vivo* data: *galectin-3* null mutant had accelerated cyst growth in one week old *cpk* mice. *Galectin-3* null mutants had accelerated cyst growth *in vivo*.

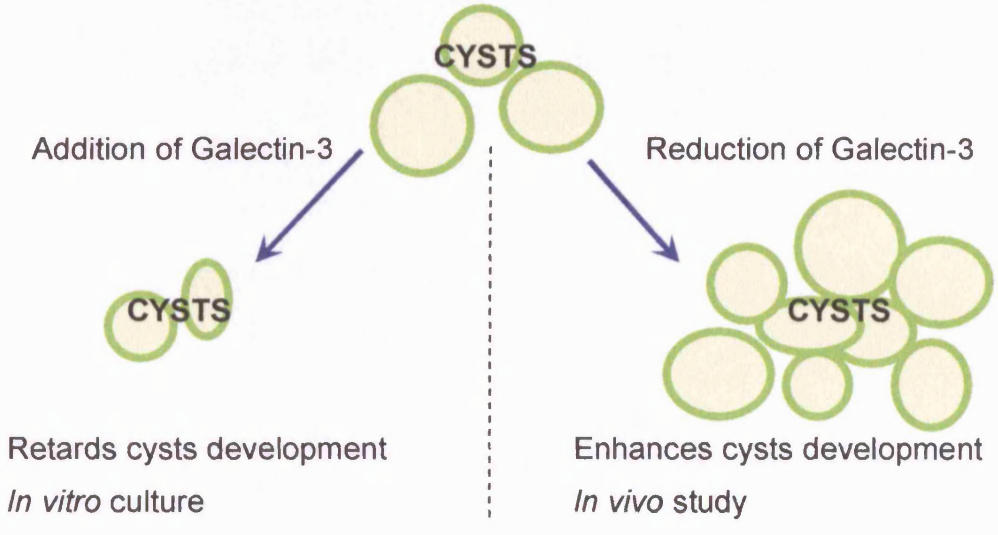

We hypothesised that cytogenesis is enhanced in *galectin-3* null mice, therefore we decided to assess these animals at Day 7. *Cpk* mutants were bred with *galectin-3* null mutants to generate cystic animals with the three different *galectin-3* genotypes. Cystogenesis in these animals at Day 7 were determined and compared using the kidney/body weight (K/B) ratio. The experiment was initially carried out on a mixed C57BL/6j x 129Sv backgrounds, due to the availability of *galectin-3* null mutants on 129Sv at the start of this study. Nearer the end of the study, the *galectin-3* null mutants on C57BL/6j became available. Thus double mutants were obtained on both the pure 129Sv by repeated backcrosses and C57BL/6j backgrounds.

STUDY OF THE DOUBLE MUTANTS ON A MIXED GENETIC BACKGROUND.

From the first set of experiments (on mixed background): in results cystic animals, *galectin-3* null mutants (K/B ratio: 1.72%) and heterozygotes (K/B ratio: 1.69%) were significantly more cystic compared with wildtypes (K/B ratio: 1.18%). Suggesting that a reduction in *galectin-3* expression caused accelerated cyst growth in *cpk* kidneys. This result supported the hypothesis that galectin-3 retards cystogenesis, therefore when galectin-3 is removed from cysts, the rate of cystogenesis was much greater.

The similarity in K/B ratio between *galectin-3* heterozygotes and *galectin-3* null mutant cystic mice.

Galectin-3 heterozygotes and null mutants shared a very similar K/B ratio. They exhibited a 43% and 46% increase in K/B ratio respectively compared with *galectin-3* wildtypes. According to the hypothesis, one would expect either only the null mutants had accelerated cystogenesis or that there would be a significant difference between the null mutants and the heterozygotes; the former would be the most cystic group, hence the degree of cystogenesis would increase in proportion to the reduction of *galectin-3* expression. But why did the heterozygotes had the same outcome as the null mutants?

It was recently found that *galectin-3* null mutant mice had 10% fewer glomeruli (Bichara *et al.*, 2006). This may contribute to the reduction in cystogenesis in null mutants. Less glomeruli means less nephrons and less collecting tubules, which are the origins for cyst growth. Therefore, a reduction in the number of glomeruli may lead to less cysts being developed. The lower than expected K/B ratio in null mutants observed may be explained by this phenomenon. However, the multi-functions of galectin-3 may mean that the level of the protein and its location may affect cyst growth differently.

Therefore, it is important to investigate the difference in cellular activity between *galectin-3* heterozygotes and *galectin-3* null mutants.

I performed proliferation and apoptosis studies on the cystic epithelial cells by immunohistochemistry. Proliferative index (PI) and apoptotic index (AI) were generated by counting the number of positively immunostained cystic epithelial cells over the number of total epithelial cells. Results from blinded counts showed that *galectin-3* heterozygotes had a significantly higher rate of proliferation compared with *galectin-3* wildtypes and *galectin-3* null mutants; whereas no significant differences were found between the wildtypes and null mutants. No differences were found in the apoptotic index amongst all *galectin-3* genotypes.

The PI values obtained here are much higher than those previously reported: 10.5% in human ARPKD samples (Nadasdy *et al.*, 1995). This may be due to several factors:
1) Different samples: *cpk* is a rapidly progressive form of PKD where affected individuals reaches end stage renal failure at around week 4 of age; therefore a higher rate of proliferation was obtained compared with samples taken from human ARPKD.
2) Different methods: although PCNA was used for the previous study in human ARPKD, the experimental procedure was different in term of incubation time, in particular in the detection step which generated the positive signal; the longer the incubation period, the stronger the signal.
3) Different investigators: there are various degree of "brownness" of the positively stained nuclei. The various degrees of intensity may reflect the stages of cells in the cell cycle. PCNA is not immediately degraded after mitosis, therefore cells that have just completed the cell cycle may still be positively stained although the level of protein expression is much lower. For this experiment, I counted all positively stained nuclei irrespective of their staining intensity.

Galectin-3 is implicated in regulating cell cycle, both proliferation and apoptosis. However, the exact mechanisms for these functions are unclear, making the interpretation of the results obtained here very difficult. Apoptosis was not affected by the expression of galectin-3 at least not in the cystic epithelia, although there may be a difference in tissues surrounding the epithelia. In terms of the effect on proliferation, it was surprising to find out that only *galectin-3* heterozygotes had a higher rate of proliferation. The higher proliferation rate in heterozygotes might contribute to the greater than expected cyst development in this group compared with *galectin-3* null mutants. The PI result suggests that lack of galectin-3 reduced proliferation in cystic epithelial cells, thus suppressed cyst growth. Therefore the level of galectin-3 may be important in inducing proliferation, in which a low level is required to induce proliferation. It is clear from the results that null mutants had the same level of cysts growth as heterozygotes, thus proliferation does not solely govern cyst expansion. Galectin-3 may act on other cellular process such as altering adhesion, which in turns regulate cystogenesis.

It is difficult to elucidate a hypothesis of what galectin-3 roles is on the proliferation of cystic epithelia. Firstly, one should evaluate the level of galectin-3 protein expression in *galectin-3* heterozygotes cystic epithelia compared with that of *galectin-3* wildtypes, in order to assess the difference in the quantity of galectin-3 expressed. I attempted that using western blotting but no signal was detected at one week old kidneys as the expression was not high enough. And if the concentration of galectin-3 is important, then one could investigate the effect of differing the concentration of galectin-3 *in vitro* using a cystic renal epithelia cell line, e.g. primary culture of *cpk* monolayer, and how that may effect the rate of proliferation and cystogenesis. Another factor affecting the outcome may be sub-cellular localisation; extracellular galectin-3 may have a different role than cytoplasmic and nuclear galectin-3. Therefore it is perhaps important to investigate the localisation of galectin-3 in

the *galectin-3* heterozygotes and null mutants and relate it to the rate of proliferation and degree of cystogenesis.

The mixed genetic background of the animals.

Although the animals on the mixed background presented a significant difference in the K/B ratio among cystic animals with different *galectin-3* genotype, one may see this result as preliminary due to the mixed background, hence a genetic confounder may affect the experiment. Nonetheless, the differences were significant and they represent a vast 41% increase in K/B ratio in *galectin-3* heterozygote and *galectin-3* null mutants when compared with *galectin-3* wildtypes. It was always the intention to backcross the double mutants onto a pure genetic background for detailed analyses, however that required at least 6 backcrosses, to yield a relatively pure genetic background with less than 2% difference. The *cpk* allele was eventually backcrossed 10 generations onto the 129Sv background, which gave a less than 0.2% difference in genetic background. This backcrossing work alone took over 2 years; which is why the double heterozygotes (*cpk* +/- and *gal3* +/-) on the mixed background were interbred to yield offspring in order to obtain samples for my preliminary analysis.
Nearer the end of the study, we obtained *galectin-3* null mutants on C57BL/6j and they were bred with *cpk* mice.

Study of the double mutants on the 129Sv genetic background.

The *cpk* null allele was successfully bred onto the 129Sv background and the experiment yielding *cpk* animals with various *galectin-3* genotypes was repeated, generating 34 litters and 181 animals. *Cpk* mutants have not been previously characterised on this particular background. A few unexpected factors lead to the termination of analysis of these data:

1) 181 animals were born, out of which 10 (5.5%) died before day 7. Such early death was not observed in the previous set of experiments (mixed background) and rarely seen in *cpk* animals on its natural C57BL/6j background.
2) The F2 generation did not follow Mendelian's Law of Inheritance, because there were significantly less *galectin-3* null mutants. This implies that the samples obtained may be skewed as the samples did not include the true *galectin-3* null mutant population.
3) Very large pancreatic cysts were seen in some cystic samples and the degree of pancreatic lesion did not correlate with *galectin-3* genotypes. The size of the pancreatic cysts greatly increased the body weight of the affected samples and thus skewed the K/B ratio.

These outcomes are likely to be caused by specific alleles on the 129Sv background. They have greatly affected the assessment of the effect of *galectin-3* expression on cystogenesis. The expression of certain alleles may lead to *in utero* death of *galectin-3* null mutant, or it may affect implantation of null mutants as the protein is implicated in that process (Colnot *et al.*, 1998). Animals that died before day 7 did not correlate with the *galectin-3* genotypes although most samples genotyped were *cpk* -/- (6 out of 7). This may reflect a correlation with an allele or a group of alleles that affect the survival of the *cpk* animals; death could be due to lack of kidney function or most likely the gross pancreatic lesions.

Development of the pancreas is sometimes affected in PKD models. Pancreatic cysts are found in *orpk* and *Pkd2* mice (Cano *et al.*, 2004); dilated pancreatic ducts are found in *orpk* mice. However the severity of pancreatic lesion was mild in comparison to that observed in *cpk* animals on 129Sv.

Due to the lack of correlation of *galectin-3* genotypes to the death rate and pancreatic cyst, these samples were not analysed further. Instead attention

was turned to the same experiments but on the pure C57BL/6j. One may still use this *cpk* model on 129Sv in future for the study of underlying genes that govern the different phenotypic outcomes, in particular the occurrence and severity of pancreatic cysts. This model can also be used to study the role of cystin (protein encoded by *cpk*) in the development of pancreatic lesions.

Study of the double mutants on a pure, B57BL/6j, genetic background.

Nearer the end of the study, *galectin-3* mutants on C57/6j were imported and the *in vivo* analysis of double mutants on this background has begun. Double heterozygous (*cpk+/-, gal-3+/-*) were generated and crossed to yield 108 offspring for analysis. No significant difference of K/B ratio was found but analysis of the cortical region of the cystic kidney samples showed that *galectin-3* null mutants had a significantly higher cortical cystic index, which reflects the size and number of cysts as observed in histological sections, compared with *galectin-3* heterozygotes and *galectin-3* wildtypes; representing a ~40% increase (p-value < 0.05). No differences were found between *galectin-3* heterozygotes and wildtypes. The K/B ratio of *gal-3* +/+ is 0.79%, and *gal-3* +/- is 0.94% and *gal-3* -/- is 0.92%. Compared with *gal-3* +/+ the p-values were 0.10 and 0.12 in respect to *gal-3* +/- and *gal-3* -/-. They were relatively close to being biologically significant, suggesting that there may be a tendency of having higher K/B ratios. Unfortunately I did not have the time to measure apoptosis and proliferation in these mice. It is perhaps a good idea to collect more samples in order to see if that would affect the K/B ratio of different *galectin-3* genotypes and the changes on the p-values.

This set of results support previous findings on the mixed background that *galectin-3* null mutants were more cystic. Therefore I am confident to conclude that *cpk* mice that lack galectin-3 have accelerated cystogenesis and galectin-3 suppresses cyst growth *in vivo*.

GALECTIN-3 WAS EXPRESSED ON THE PRIMARY CILIUM OF RENAL EPITHELIAL CELLS

In the past few years, the primary cilium has emerged to play a very important role in the development of PKD. Many proteins associated with the disease were found to locate on this organelle, such as PC-1, PC-2, cystin, OFD-1 and polaris. As I proposed that galectin-3 is important to the development of renal cysts, I was interested to see if the protein was also expressed on this organelle. As predicted, the protein was found on the primary cilium in all samples tested: IMCD cells, primary culture of normal mice and *cpk* mice kidney epithelial cells, kidney sections of normal and *cpk* samples, human ARPKD and ADPKD samples. The expression pattern of galectin-3 on the primary cilia on each samples varied from cilium to cilium, even within the same colony, from punctuate expression along the shaft of the cilia to sole expression at the end/bulb of the cilia. Galectin-3 location on the primary cilia may reflect different developmental or functional state of the organelle, or that it is localised to the cargos of the intraflagellar transport (IFT) system which moves up and down the shaft of the cilia.

Other PKD causing proteins, PC-1, PC-2, polaris and cystin were previously shown to be expressed all along the cilia (Yoder *et al.*, 2002a), with an expression pattern similar to that of galectin-3; whereas inversin functional site is restricted to the base of the cilia (Shiba *et al.*, 2005). It is difficult to suggest a function of a protein based on its location, in particular when the size of the organelle is so small. Using the confocal microscope, it is very difficult to identify the sub-location of the protein on either the membrane of the cilia, or associated with the microtubule network. Immunocytochemistry on non-permeablised IMCD cells was carried out and it revealed that at least

some galectin-3 was on the outside of the primary cilia. A better way to examine this would be to use scanning immuno-electron microscopy.

The primary cilium has been shown to act as a mechano-sensor which induces calcium influx into the cell (Nauli *et al.* 2003, Praetorius and Spring, 2001). I attempted to repeat the calcium influx study, however I was unable to obtain the low flow rate required to bend the primary cilium. A specially designed flow chamber was absent in my experiments. Therefore the use of AFM was explored as it may be applied to bend the primary cilium.
AFM is able to produce detailed topographs and give quantitative measurement of substances in the nanometer range. So far, I have been able to obtain topographs of quick dried primary cilia in IMCD cells, showing that it is possible to detect and give an accurate quantitative picture of the organelle using the cantilever of the AFM. Preliminary testing revealed that the organelle could also be detected in solution, which is a more fragile state. The use of AFM depends on a good contact between the cantilever and the cell surface; liquid phase is a less rigid environment and it exhibits a force against the cantilever thus disrupting the engagement it has with the primary cilia, which itself is unstable in liquid. The ultimate goal is to detect and manipulate the primary cilia of live cells (fig. 11.2). The cantilever of the AFM can used to bend the primary cilium. And by incorporating the AFM with a fluorescent microscope, one would be able to investigate the effect of calcium influx upon manipulation of the primary cilia with the cantilever. Such integration of AFM and fluorescent microscope are being carried out by my collaborator Prof. Horton.

Also I believe that in order to investigate the subtle differences between galectin-3 null mutant primary cilia and normal primary cilia, an alternative technique must be used that can provide a more detailed analysis particularly of its structure. It was partly this belief that encouraged me to explore the application of AFM in the study of the organelle.

Figure 11.2. Illustration of calcium influx triggered by the cantilever of AFM.

Two renal epithelial cells are represented with the primary cilia at the top of the cells. The cell on the left is under stable condition whereas the one on the right is in contact with the cantilever of the AFM: the cantilever physically bends the primary cilium thus triggers calcium influx into the cells. Under fluorescent microscope, calcium influx can be detect by the green signal. The signal is produced by a fluorescent dye, Fura-2, which reacts to free intracellular calcium.

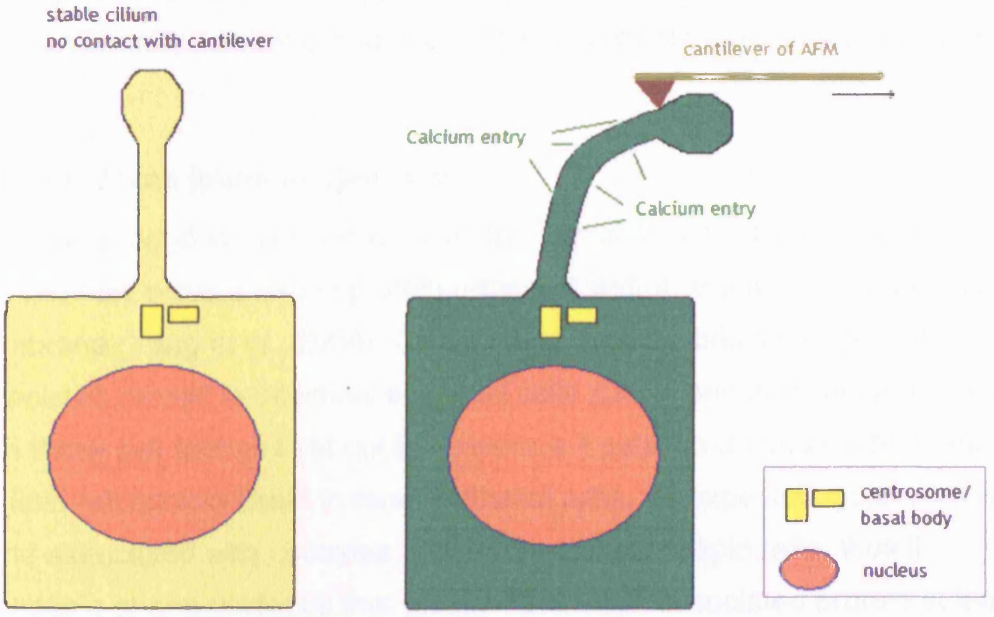

Possible roles for galectin-3 in the primary cilium

This study shows for the first time that galectin-3 is expressed on the primary cilium, and no investigations have been conducted to look into the functions of lectins and glycoproteins on this organelle. It is certain that galectin-3 exhibtis a diverse cellular functions depending on its binding ligands. Many PKD associated proteins have been identified to be located at the primary cilium, they have a diverse range of actions from calcium channel to the assembly of the organelle. Many of these proteins are highly glycosylated:

there are 64 potential N-glycosylation sites in fibrocystin, 60 in PC-1 and 5 in PC-2. Both fibrocystin and PC-1 have very large extracellular domains which contains many of these glycosylation sites, which are potential sites for galectin-3 interaction. Immuno-staining revealed that galectin-3 is expressed on the outside of the primary cilia, where it can potentially interact with the PKD glycoproteins.

Galectin-3 may modulate the function of PC-1 and other PKD proteins by forming a lattice thus clustering these proteins on the ciliary surface. The ability of protein clustering is similar to the role of lipid rafts on the membrane.

Galectin-3 was found in lipid rafts

Cystin was found to be in the lipid raft fraction of IMCD cells; suggesting that lipid raft may serve a role in protein transport and/or retention on the ciliary membrane (Yang *et al.,* 2004). Galectin-4 is a well established lipid raft associated protein in intestinal epithelial cells (Danielsen and Hansen, 2003). With these two factors I set out to determine if galectin-3 can also be found in the lipid raft compartment in renal epithelial cells. As expected, galectin-3 was found associated with caveolae, which is a marker of lipid rafts, thus it provides a strong evidence that galectin-3 is a raft associated protein at least in IMCD cells. Attempts were made to extract lipid raft from *cpk* kidney but failed due to technical difficulties, although the precise reason was unknown.

Lipid rafts are implicated in several biological functions, including cell signalling, polarisation, protein secretion and endocytosis (Brown and London, 1998). The function of these microdomains in cell polarisation is of most interest. Protein polarisation is disrupted in cystic epithelial cells; primary cilia are thought to play a role in cell differentiation which is partly marked by protein targeting to either the apical or the basolateral domains; N-glycans, which are potential ligands for galectin-3, can mediate apical targeting of

proteins, a process that may involve lipid rafts (Benting *et al.*, 1999; Rodriguez-Boulan and Gonzalez, 1999; Pang *et al.*, 2004). Also, findings of galectin-3 in the lipid rafts may provide clues to how galectin-3 is secreted from cells, a process that is yet unidentified (Hughes, 1999).

Galectin-4 is a major component of lipid raft in intestinal epithelial cells, it acts as a stabiliser for other more loosely raft-associated proteins (Danielsen and Hansen, 2003). Both galectin-4 and galectin-3 have an ability to self-polymerise (Yang *et al.*, 1998; Braccia *et al.*, 2003; Partridge *et al.*, 2004), forming a lattice which results in a "gluing" effect that keeps the glycoproteins and glycolipids in place. Lipid rafts are microdomains on the cell surface, they are commonly perceived as the more ordered domains within the lipid bi-layer that are rich in cholesterol and glycosphingolipids. Glycosphingolipids contain a high degree of acyl chain which raises the melting temperature of lipid. This results in a more stabilised lipid phase, where proteins is able to cluster together in order to induce reaction such as initiation of signalling pathway.

Studies on the role of galectin-3 in clustering cell surface receptors (namely EGFR and TGF-β–R, both are glycosylated and are found in lipid rafts) suggest that it may be a raft associated protein (Schwartz *et al.*, 2005; Pike *et al.*, 2005). It was found that galectin-3 is able to cross-link Mgat5-modified N-glycans on the cell surface resulting in the formation of galectin-3/glycoprotein clusters. Mgat5 promotes the substitution of N-glycan with poly N-acetyllactosamine, the preferred ligand for galectin-3. This cross-linking action retains receptors on the surface against loss via endocytosis. Mgat5 deficient mice had a delayed reaction in response to EGF, IGF (Insulin growth factor), FGF (fibroblast growth factor); Scatchard analysis revealed sixfold fewer EGFR at the cell surface or Mgat5 -/- cells, although total EGFR amounts were not different between mutant and wildtype cell lysates. Suggesting that suppressing the interaction of galectin-3 with EGFR leads to less EGFR retained on the cell surface. Mga5-/- cells also exhibits a threefold decrease

in sensitivity to TGF-β (Partridge *et al.*, 2004). Galectin-3 can also modulate TCR (T-cell receptor) clustering. It interacts with TCR at the cell surface of normal cells but not in Mgat5 deficient cells; the galectin-3/TCR lattice may contain galectin-1, which is shown to modulate T-cell activation *in vitro* (Fuertes *et al.*, 2004; Toscano *et al.*, 2006). The lectin/TCR lattice restricts TCR recruitment to the site of antigen presentation thus modulating the immune response of T-cells. This process is inhibited by lactose thus suggesting that the CRD of galectin-3 is responsible for the interaction (Demetriou *et al.*, 2001). Conflicting results show that galectin-3 is not in the lipid raft of differentiated MDCK cells. The study suggests that galectin-3 is involved in a non-raft dependent apical protein sorting (Delacour *et al.*, 2006).

Whether or not galectin-3 is in lipid raft, its ability to cluster proteins on the cell surface is perhaps most important. In terms of its role on the primary cilia; it may act by clustering and retaining PKD proteins on the surface thus facilitating adequate response to external stimulation. Galectin-3 localisation to lipid rafts remains speculative. The primary cilia have a high concentration of receptors, it may therefore contain a high proportion of lipid rafts, which provide a more ordered lipid bilayer to stabilise the position of these receptors. Apart from cystin, the polycystin complex may also be found in lipid rafts. The constituents of the complex PC-1, E-cadherin and β-catenin associate together with a cholesterol-containing signalling microdomain in human kidney epithelia (Roitbak *et al.*, 2005). The relationships between lipid raft, primary cilium and cytogenesis remain to be determined.

Figure 11.3. Illustration of galectin-3 forming a lattice and clustering PKD proteins on cell surface.

A hypothetical function of galectin-3 on the cell surface. A lipid bilayer membrane was shown where three glycosylated PKD proteins (blue) were found within. Galectin-3 (red) binds directly to the N-glycan (green) and also self-associates to form a lattice containing the PKD protein.

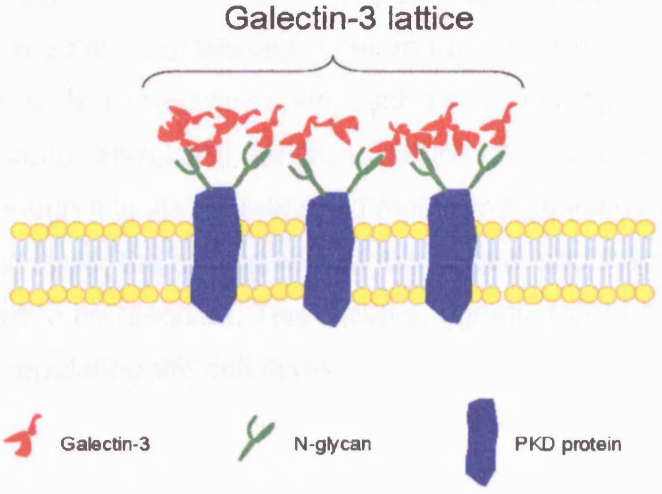

Galectin-3 was expressed on the centrosome of IMCD cells

Immunocytochemistry of IMCD monolayers showed that galectin-3 was expressed on the pericentriolar material (PCM), area around the centrioles, of the centrosome and at the spindle poles of dividing cells. The centrosome is regarded as the microtubule organising centre as well as a regulator of the cell cycle. It is also the precursor of the primary cilium. This is the first time that a galectin was shown localised to this important organelle.

The link between the centrosome and PKD

Several ciliary proteins associated to PKD are found to localised to the centrosome: OFD1(Romio *et al.*, 2004), BBS4 (Kim *et al.*, 2004), BBS6 (Kim *et al.*, 2005), Nek8 (Quarmby and Mahjoub, 2005), all are found in the basal body of the primary cilium. PC-L, a protein closely related to PC-2, is found in centrosome of unciliated cells (Bui-Xuan *et al.*, 2006) whereas PC-2 is

proposed to form a complex with intraflagellar transport (IFT) proteins and centrosome protein pericentrin (Pcnt) that is required for the assembly of primary cilia (Jurczyk *et al.*, 2004). The primary cilium is derived from the mother centriole near the end stage of cell differentiation when the centrosome migrates close to the apical surface (Rieder *et al.*, 2001). The roles of PKD proteins in centrosome are unclear; however, they may participate in regulation of the cell cycle and/or the formation of the primary cilia. There may be shared functions, such as organising microtubules, between the centrosome and the cilium, which are carried out by this group of proteins. Although it is well established that some galectins are capable of regulating cell cycle, the mechanism of this control and their subcellular targets are yet to be resolved. This result suggests a possible target for galectin-3 in regulating the cell cycle.

GALECTIN-3 WAS RELOCALISED IN CYSTIC EPITHELIAL CELLS AFTER TREATMENT WITH PACLITAXEL

Results from the examination of paclitaxel treated kidneys revealed that the reagent relocalises the expression of galectin-3 from cytoplasmic to apical. *In vitro* studies done by Dr. Tanya Johnson showed that paclitaxel enhanced the secretion of galectin-3 to the medium. The renal primary cilia from treated *cpk* samples were examined using confocal microscopy: no differences were found on the appearance of the primary cilia; the localisation of galectin-3 remained on paclitaxel treated primary cilia.

Paclitaxel (50 μM) and galectin-3 (30 μg/ml) reduced the number of cyst formed in culture when added separately (Woo et al 94, Johnson's Thesis 2001). Here I carried out *in vitro* experiments where the two reagents were added together and found that there was no significant cumulative effect. The two reagents may therefore work in the same pathway in reducing cytogenesis. However, one can argue that the concentration of paclitaxel used was high enough to saturate the effect that galectin-3 might impose, or that paclitaxel altered the physiology of the cells to a point that galectin-3 could no longer influence the cells. Paclitaxel may encourage the secretion of galectin-3.

Linking the paclitaxel data to other work in this thesis: galectin-3 was found localised to the outside of the primary cilia, together with the fact that paclitaxel did not appear to alter the structure of the organelle. I hypothesized that the increased concentration of galectin-3 in cyst fluid caused by paclitaxel modulates cytogenesis by binding to the outside of the primary cilia, thus stabilising the protein receptors on the outside of the cilia.

Previous studies of the effect of paclitaxel on other PKD animal models found that the reagent is not effective on *orpk* mice (Sommardahl *et al.*, 1997), *pcy* mice and Han:SPRD-cy rats (Martinez *et al.*, 1997). Although *in vitro* culture of Han:SPRD-cy derived cysts showed a positive effect in inhibiting cytogenesis (Pey *et al.*, 1999). In Chapter 6, I examined the dosages used for each models and found that all other models used a dosage that was at most, half the dosage used in the *cpk* mice. Hence, the inefficiency observed could be due to this reduced dosage. If my hypothesis is true, that part of the effect of paclitaxel is due to an increased concentration of galectin-3 in cysts fluid, which stabilises protein receptors on the outside of the primary cilia, then paclitaxel might not have any effect on models that do not have structurally normal cilia. I know from this study and from various published data that *cpk* mice develop primary cilia that are structurally indistinguishable to normal cilia. On the other hand, the majority of cystic cells in *orpk* mice either lack the expression of primary cilium or express shortened cilia (Brown and Murcia, 2003); in this case, according to the hypothesis, paclitaxel would have no effect on cystogenesis in *orpk* mice. The expression of primary cilia in *pcy* mice and Han:SPRD-cy rats have not been published.

CHAPTER 12: CONCLUSION

Taking all these results together, I am confident that galectin-3 plays a role in inhibiting cyst growth in *cpk* animals, and I speculate that its effect may extend to other PKD models. The results obtained in this thesis: the wide expression of galectin-3 on cystic epithelia of several PKD models; lack of galectin-3 in *cpk* models led to an accelerated cystogenesis *in vivo*; the presence of galectin-3 in primary cilia. All these point towards the significance of this lectin in cyst development. The *in vivo* data in particular, together with previous *in vitro* data showing that addition of exogenous galectin-3 reduces cyst formation, support the hypothesis that galectin-3 acts by suppressing cyst growth.

The finding that galectin-3 was on the outside of the primary cilia; the presence of galectin-3 in cyst fluid; and that paclitaxel treated *in vitro* cysts secreted more galectin-3. All these suggest that galectin-3 may work on the outside of the primary cilium. Preliminary data revealed that galectin-3 was found in the lipid raft fraction of IMCD cells, provokes the idea that galectin-3 function on the cell surface by forming a lattice, which stabilises and retains receptors on the cell surface against endocystosis. Referring back to the *in vivo* data; among *cpk* animals *galectin-3* heterozygotes had the same K/B ratio as *galectin-3* null mutants. This reflected a similar degree of cyst growth between the two groups of samples. If the role of galectin-3 depends on the formation of a functional lattice, one may expect the concentration of galectin-3 to be critical in the formation of lattice with an adequate size. *Galectin-3* heterozygotes may have a reduced level of secreted galectin-3, thus are unable to create a significant lattice to cluster PKD proteins on the cell surface.

It is sometimes thought that if a protein is widely expressed in diseased tissues, it contributes to the pathophysiology. Specifically in PKD, several

proteins that are upregulated in the cystic epithelia are implicated in the worsening of the disease: EGFR, P2X(7), cAMP. However, in the case of galectin-3, I am proposing that it has a beneficial effect on the disease. Its expression in cystic epithelia acts as an inhibitory factor on cyst development but it is insufficient to prevent cysts completely. The protective effect of galectin-3 against disease progression is apparent in a few other renal diseases. Diabetic glomerulopathy is one such example; Galectin-3 null mutant mice developed accelerated glomerulopathy, the lectin would otherwise be up-regulated in diabetic individuals (Pugliese *et al.*, 2001a) glomerular lesion caused by the accumulation of AGEs (advanced glycation end-products) is also protected by galectin-3. Aging *galectin-3* knockout mice develop more pronounced changes in renal function and structure than wildtype mice. This changes is associated with the higher accumulation of AGEs, suggesting that galectin-3 may be a AGE receptor that assists in the clearing of AGEs (Iacobini *et al.*, 2005). The protein was found to be markedly up-regulated in both ischaemic (bilateral renal pedicles clamped for 40 minutes) and toxic types (folic acid) of acute renal failure (ARF) in rats. Upregulation of galectin-3 mRNA was observed as early as 2 hours after injury. In the ischaemic ARF, the mRNA level extended by 6.2-fold at 48 hours, and then decreased by 28 days after injury. In toxin induced ARF, increased levels continued until at least 7 days post injury (Nishiyama *et al.*, 2000).

Galectin-3 posses multiple functions, many of those mimic the pathophysiology of PKD: alteration in cell adhesion, alteration of proliferation and apoptosis, importance of primary cilia in the renal cyst development. And galectin-3 can potentially interact with the highly glycosylated PC-1, fibrocystin and perhaps other glycosylated PKD proteins. Therefore it is no surprise that galectin-3 may modulate their functions and cystogenesis. This thesis has provided many novel findings and it shows the importance of galectin-3 in the development of renal cysts. The fact that galectin-3 is able to

inhibit cyst growth raises the possibility of developing the lectin into a therapeutic treatment against PKD.

CHAPTER 13: FUTURE WORK

Detailed examination of *galectin-3* null mutant *cpk* mice

Detailed examination of the cystic kidney samples on the pure 129Sv and C57BL/6j backgrounds: proliferative and apoptotic indexes, would provide further insight into the role of galectin-3 in ameliorating the disease. It is important to find out the physiological changes associated with the lack of galectin-3, which leads to the accelerated cyst growth. This may provide insight to the mechanism of how galectin-3 modulates cyst growth.

To further investigate the hypothesis that galectin-3 form lattice on cell surface and retains protein receptors, in particular PKD proteins, on the primary cilium. One can examine the precise localisation of several PKD proteins on the primary cilium in *galectin-3* wildtype and *galectin-3* knockout samples, as well as the location of galectin-3 on the ciliary membrane. The association of galectin-3 and PKD proteins to lipid raft in kidney epithelial cells also needs to be confirmed.

Examination of *galectin-3* null primary cilia

One of the most established functions of primary cilia is its role in initiating calcium influx in response to mechanical force that bends the organelle. I began searching for ways to replicate the experiment in triggering calcium influx in IMCD cells, however, without the appropriate equipment, it was impossible to achieve the required flow rate. Instead I look at AFM (atomic force microscopy) in bending the primary cilium, thus initiating the calcium response. Progress was slower than expected, but I did determine that the AFM is able to detect the primary cilium. To test the physiology effect, one must carry out the experiment in live cells, which poses the biggest challenge. However, examination of live cells using AFM is not a new technique and a

tailor-made biological chamber (which controls the temperature and humidity of samples) is already available. The challenge lies in optimising the process to yield results. The AFM is already integrated to a confocal microscope; again the challenge here depends on development of an effective imaging protocol. The strategy of the experiment would be to culture *galectin-3* null mutant kidney epithelial cells in monolayer, prior to testing the cells would be equilibrate with Fura-2 (a fluorescent dye that binds to free intracellular calcium and causes an emission between 300 and 400 nm). Using the cantilever on the AFM to physically bend the primary cilia, and calcium influx can be measured and timed using the confocal microscope. This result could then be compared to that of wildtype cells to assess any differences in the strength and duration of the reaction. Finally, I would repeat the experiment with the addition of galectin-3 in medium and determine if exogenous galectin-3 alter the rate and strength of response of calcium influx compared with cells treated with media alone.

The AFM can also be used to give an accurate assessment of the size and surface structure of *galectin-3* null mutant primary cilia in comparison to wildtype cilia.

Galectin-3 binding ligands on the primary cilia and *cpk* cells

It is important to determine which proteins galectin-3 interacts with on the primary cilia, specifically PC-1, PC-2, fibrocystin, polaris, inversin, kinesins and dyenin. Co-immunoprecipitation can be done with these specific proteins using IMCD cells. In addition, one should assess the differences in the constituent of galectin-3 ligands in *cpk* cells and wildtype cells, which is also a good way to search for novel ligands of galectin-3. This may be determined by affinity chromatography. The technique was successfully used to identify macrophage surface glycoproteins that bind galectin-3 (Dong *et al.,* 1997). Primary culture of *cpk* kidney epithelial cells and IMCD cells will be used for protein extraction. These protein lysates will be used as substrates to run

through a column containing either galectin-3 or specific antibodies against the lectin. Proteins that interact with galectin-3 will be selected and eluted. It can then be separated by 1D or 2D SDS-PAGE and visualised by silver staining. Individual protein bands will be excised and in-gel tryptic digestion will be preformed. The released peptides will be extracted from the gel and analysed by mass spectrometry. Data analysis will be carried out using specific softwares to identify "pulled-down" proteins.

Treatment of *cpk* mice with recombinant galectin-3 protein

The hypothesis is that galectin-3 has a beneficial effect in delaying cystogenesis and it raises a possibility of using the lectin as a therapeutic drug. To ultimately prove the application of galectin-3 as a therapeutic drug, one must show that the administration of the lectin to diseased animals delays the progression of the disease. Recombinant galectin-3 can be made using *E.coli* (the protein is not glycosylated) and it would be administered to *cpk* litters, some treated with vehicle only as control. Treatment with recombinant galectin-3 was tested in nude mice bearing orthotopically implanted tumours derived from breast cancer cell line. Toxicity, pharmacokinetic and organ biodistribution studies were performed. The maximum tolerated dose of galectin-3 in adult nude mice was >125mg/kg without obvious adverse effects. The elimination half-life when administered via the intramuscular route was found to be 3 hours in the serum and 4.3 hours in the cellular fraction of the blood. Organ biodistribution studies revealed that galectin-3 localised in the liver, kidneys and spleen but not in the heart or lungs. The published data showed that mice with tumours were injected with galectin-3 via the intramuscular route, twice a day of 125 μg (5mg/kg) with an approximately 6-8 hours interval for 90 days. This dosage was able to reduce the growth of the tumour compared with vehicle-treated mice (John *et al.*, 2003). *Cpk* mice would be treated much earlier, as they do not survive to adulthood. The treatment might start before day 7, the dosage should be much less than 125mg/kg.

This thesis represents a very exciting new research area in the field of ARPKD research. There are clearly much more work to be done in order to determine the mechanism of galectin-3 in modulating cystogenesis and to enhance out understanding of the disease. Many of the proposed work are based on the *cpk* model, however if it does prove that galectin-3 can retards cyst growth in these animals, the next step woud be to verify its effects in other PKD models, especially in the genotypic models to the human ARPKD and ADPKD disease such as *pcy* mice.

REFERENCES

Abedin,M.J., Kashio,Y., Seki,M., Nakamura,K., Hirashima,M. (2003). Potential roles of galectins in myeloid differentiation into three different lineages. J Leukoc.Biol. *73*, 650-656.

Akahani,S., Nangia-Makker,P., Inohara,H., Kim,H.R., Raz,A. (1997). Galectin-3: a novel antiapoptotic molecule with a functional BH1 (NWGR) domain of Bcl-2 family. Cancer Res. *57*, 5272-5276.

Al Awqati,Q. (2003). Terminal differentiation of intercalated cells: the role of hensin. Annu.Rev.Physiol *65*, 567-583.

Al Awqati,Q., Oliver,J.A. (2002). Stem cells in the kidney. Kidney Int. *61*, 387-395.

Alexandre,J., Batteux,F., Nicco,C., Chereau,C., Laurent,A., Guillevin,L., Weill,B., Goldwasser,F. (2006). Accumulation of hydrogen peroxide is an early and crucial step for paclitaxel-induced cancer cell death both *in vitro* and *in vivo*. Int.J Cancer. *119*, 41-48.

Alieva,I.B., Vorobjev,I.A. (2004). Vertebrate primary cilia: a sensory part of centrosomal complex in tissue cells, but a "sleeping beauty" in cultured cells? Cell Biol.Int. *28*, 139-150.

Amos,L.A., Lowe,J. (1999). How Taxol stabilises microtubule structure. Chem.Biol. *6*, R65-R69.

Andre,N., Braguer,D., Brasseur,G., Goncalves,A., Lemesle-Meunier,D., Guise,S., Jordan,M.A., Briand,C. (2000). Paclitaxel induces release of cytochrome c from mitochondria isolated from human neuroblastoma cells'. Cancer Res. *60*, 5349-5353.

Ansley,S.J., Badano,J.L., Blacque,O.E., Hill,J., Hoskins,B.E., Leitch,C.C., Kim,J.C., Ross,A.J., Eichers,E.R., Teslovich,T.M., Mah,A.K., Johnsen,R.C., Cavender,J.C., Lewis,R.A., Leroux,M.R., Beales,P.L., Katsanis,N. (2003). Basal body dysfunction is a likely cause of pleiotropic Bardet-Biedl syndrome. Nature. *425*, 628-633.

Aukema,H.M., Housini,I. (2001). Dietary soy protein effects on disease and IGF-I in male and female Han:SPRD-cy rats. Kidney Int. *59*, 52-61.

Avner,E.D., Sweeney,W.E., Jr., Nelson,W.J. (1992). Abnormal sodium pump distribution during renal tubulogenesis in congenital murine polycystic kidney disease. Proc.Natl.Acad.Sci.U.S.A *89*, 7447-7451.

Badano,J.L., Mitsuma,N., Beales,P.L., Katsanic,N. (2006). The ciliopathies: an emerging class of human genetic disorders. Annu.Rev.Genomics.Hum.Genet.

Bao,Q., Hughes,R.C. (1995). Galectin-3 expression and effects on cyst enlargement and tubulogenesis in kidney epithelial MDCK cells cultured in three-dimensional matrices *in vitro*. J.Cell Sci. *108*, 2791-2800.

Bao,Q., Hughes,R.C. (1999). Galectin-3 and polarized growth within collagen gels of wild-type and ricin-resistant MDCK renal epithelial cells. Glycobiology *9*, 489-495.

Barboni,E.A., Bawumia,S., Henrick,K., Hughes,R.C. (2000). Molecular modeling and mutagenesis studies of the N-terminal domains of galectin-3: evidence for participation with the C-terminal carbohydrate recognition domain in oligosaccharide binding. Glycobiology *10*, 1201-1208.

Bard,J.B. (1992). The development of the mouse kidney--embryogenesis writ small. Curr.Opin.Genet.Dev. *2*, 589-595.

Bard,J.B. (2002). Growth and death in the developing mammalian kidney: signals, receptors and conversations. Bioessays *24*, 72-82.

Barondes,S.H., Castronovo,V., Cooper,D.N., Cummings,R.D., Drickamer,K., Feizi,T., Gitt,M.A., Hirabayashi,J., Hughes,C., Kasai,K. (1994). Galectins: a family of animal beta-galactoside-binding lectins. Cell *76*, 597-598.

Bastani,B., Purcell,H., Hemken,P., Trigg,D., Gluck,S. (1991). Expression and distribution of renal vacuolar proton-translocating adenosine triphosphatase in response to chronic acid and alkali loads in the rat. J Clin.Invest. *88*, 126-136.

Basu,A., Haldar,S. (1998). Microtubule-damaging drugs triggered bcl2 phosphorylation-requirement of phosphorylation on both serine-70 and serine-87 residues of bcl2 protein. Int.J Oncol. *13*, 659-664.

Belibi,F.A., Reif,G., Wallace,D.P., Yamaguchi,T., Olsen,L., Li,H., Helmkamp,G.M., Jr., Grantham,J.J. (2004). Cyclic AMP promotes growth and secretion in human polycystic kidney epithelial cells. Kidney Int. *66*, 964-973.

Benting,J.H., Rietveld,A.G., Simons,K. (1999). N-Glycans mediate the apical sorting of a GPI-anchored, raft-associated protein in Madin-Darby canine kidney cells. J Cell Biol. *146*, 313-320.

Bichara,M., Attmane-Elakeb,A., Brown,D., Essig,M., Karim,Z., Muffat-Joly,M., Micheli,L., Eude-Le Parco,I., Cluzeaud,F., Peuchmaur,M., Bonvalet,J.P., Poirier,F., Farman,N. (2006). Exploring the role of galectin 3 in kidney function: a genetic approach. Glycobiology *16*, 36-45.

Bidon-Wagner,N., Le Pennec,J.P. (2004). Human galectin-8 isoforms and cancer. Glycoconj.J *19*, 557-563.

Birdsall,B., Feeney,J., Burdett,I.D., Bawumia,S., Barboni,E.A., Hughes,R.C. (2001). NMR solution studies of hamster galectin-3 and electron microscopic visualization of surface-adsorbed complexes: evidence for interactions between the N- and C-terminal domains. Biochemistry *40*, 4859-4866.

Blagosklonny,M.V., Chuman,Y., Bergan,R.C., Fojo,T. (1999). Mitogen-activated protein kinase pathway is dispensable for microtubule-active drug-induced Raf-1/Bcl-2 phosphorylation and apoptosis in leukemia cells. Leukemia. *13*, 1028-1036.

Bohn,H., Kraus,W., Winckler,W. (1983). Purification and characterization of two new soluble placental tissue proteins (PP13 and PP17). Oncodev.Biol.Med *4*, 343-350.

Braccia,A., Villani,M., Immerdal,L., Niels-Christiansen,L.L., Nystrom,B.T., Hansen,G.H., Danielsen,E.M. (2003). Microvillar membrane microdomains exist at physiological temperature. Role of galectin-4 as lipid raft stabilizer revealed by "superrafts". J Biol.Chem. *278*, 15679-15684.

Brichese,L., Barboule,N., Heliez,C., Valette,A. (2002). Bcl-2 phosphorylation and proteasome-dependent degradation induced by paclitaxel treatment: consequences on sensitivity of isolated mitochondria to Bid. Exp.Cell Res. *278*, 101-111.

Brown,D.A., London,E. (1998). Functions of lipid rafts in biological membranes. Annu.Rev.Cell Dev.Biol. *14:111-36.*, 111-136.

Brown,N.E., Murcia,N.S. (2003). Delayed cystogenesis and increased ciliogenesis associated with the re-expression of polaris in Tg737 mutant mice. Kidney Int. *63*, 1220-1229.

Bui-Xuan,E.F., Li,Q., Chen,X.Z., Boucher,C.A., Sandford,R., Zhou,J., Basora,N. (2006). More than colocalizing with polycystin-1, polycystin-L is in the centrosome. Am.J.Physiol Renal Physiol *291*, F395-F406.

Bullock,S.L., Johnson,T.M., Bao,Q., Hughes,R.C., Winyard,P.J.D., Woolf,A.S. (2001). Galectin-3 modulates ureteric bud branching in organ culture of the developing mouse kidney. J.Am.Soc.Nephrol. *12*, 515-523.

Califice,S., Castronovo,V., Van Den,B.F. (2004). Galectin-3 and cancer (Review). Int.J.Oncol. *25*, 983-992.

Calvet,J.P. (2003). Ciliary signaling goes down the tubes. Nat.Genet. *33*, 113-114.

Cano,D.A., Murcia,N.S., Pazour,G.J., Hebrok,M. (2004). *Orpk* mouse model of polycystic kidney disease reveals essential role of primary cilia in pancreatic tissue organization. Development *131*, 3457-3467.

Cao,Z., Said,N., Amin,S., Wu,H.K., Bruce,A., Garate,M., Hsu,D.K., Kuwabara,I., Liu,F.T., Panjwani,N. (2002). Galectins-3 and -7, but not galectin-1, play a role in re-epithelialization of wounds. J Biol.Chem. *277*, 42299-42305.

Cao,Z., Said,N., Wu,H.K., Kuwabara,I., Liu,F.T., Panjwani,N. (2003). Galectin-7 as a potential mediator of corneal epithelial cell migration. Arch.Ophthalmol. *121*, 82-86.

Carre,M., Carles,G., Andre,N., Douillard,S., Ciccolini,J., Briand,C., Braguer,D. (2002). Involvement of microtubules and mitochondria in the antagonism of arsenic trioxide on paclitaxel-induced apoptosis. Biochem.Pharmacol. *63*, 1831-1842.

Cecchinelli,B., Lavra,L., Rinaldo,C., Iacovelli,S., Gurtner,A., Gasbarri,A., Ulivieri,A., Del Prete,F., Trovato,M., Piaggio,G., Bartolazzi,A., Soddu,S., Sciacchitano,S. (2006). Repression of the antiapoptotic molecule galectin-3 by homeodomain-interacting

protein kinase 2-activated p53 is required for p53-induced apoptosis. Mol.Cell Biol. *26*, 4746-4757.

Charras,G.T., Lehenkari,P.P., Horton,M.A. (2001). Atomic force microscopy can be used to mechanically stimulate osteoblasts and evaluate cellular strain distributions. Ultramicroscopy *86,* 85-95.

Chen,H.Y., Liu,F.T., Yang,R.Y. (2005). Roles of galectin-3 in immune responses. Arch.Immunol.Ther.Exp.(Warsz.) *53*, 497-504.

Cherayil,B.J., Chaitovitz,S., Wong,C., Pillai,S. (1990). Molecular cloning of a human macrophage lectin specific for galactose. Proc.Natl.Acad.Sci.U.S.A *87*, 7324-7328.

Chiariotti,L., Salvatore,P., Frunzio,R., Bruni,C.B. (2004). Galectin genes: regulation of expression. Glycoconj.J *19*, 441-449.

Coffman,T.M. (2002). Another cystic mystery solved. Nature Genetics *30*, 247-248.

Colnot,C., Fowlis,D., Ripoche,M.A., Bouchaert,I., Poirier,F. (1998). Embryonic implantation in *galectin 1/galectin 3* double mutant mice. Dev.Dyn. *211*, 306-313.

Cooper,D.N., Barondes,S.H. (1999). God must love galectins; he made so many of them. Glycobiology *9*, 979-984.

Danielsen,E.M., Hansen,G.H. (2003). Lipid rafts in epithelial brush borders: atypical membrane microdomains with specialized functions. Biochim.Biophys.Acta *1617*, 1-9.

Danielsen,E.M., Hansen,G.H. (2006). Lipid raft organization and function in brush borders of epithelial cells. Mol.Membr.Biol. *23*, 71-79.

Danielsen,E.M., van Deurs,B. (1997). Galectin-4 and small intestinal brush border enzymes form clusters. Mol.Biol.Cell *8*, 2241-2251.

Delacour,D., Cramm-Behrens,C.I., Drobecq,H., Le Bivic,A., Naim,H.Y., Jacob,R. (2006). Requirement for galectin-3 in apical protein sorting. Curr.Biol. *16*, 408-414.

Delmas,P., Nomura,H., Li,X., Lakkis,M., Luo,Y., Segal,Y., Fernandez-Fernandez,J.M., Harris,P., Frischauf,A.M., Brown,D.A., Zhou,J. (2002). Constitutive activation of G-proteins by polycystin-1 is antagonized by polycystin-2. J.Biol.Chem. *277*, 11276-11283.

Demetriou,M., Granovsky,M., Quaggin,S., Dennis,J.W. (2001). Negative regulation of T-cell activation and autoimmunity by Mgat5 N-glycosylation. Nature *409*, 733-739.

Dufrene,Y.F. (2001). Application of atomic force microscopy to microbial surfaces: from reconstituted cell surface layers to living cells. Micron *32*, 153-165.

Dunphy,J.L., Balic,A., Barcham,G.J., Horvath,A.J., Nash,A.D., Meeusen,E.N. (2000). Isolation and characterization of a novel inducible mammalian galectin. J Biol.Chem. *275*, 32106-32113.

Dunphy,J.L., Barcham,G.J., Bischof,R.J., Young,A.R., Nash,A., Meeusen,E.N. (2002). Isolation and characterization of a novel eosinophil-specific galectin released into the lungs in response to allergen challenge. J Biol.Chem. *277*, 14916-14924.

Dyer,K.D., Rosenberg,H.F. (2001). Transcriptional regulation of galectin-10 (eosinophil Charcot-Leyden crystal protein): a GC box (-44 to -50) controls butyric acid induction of gene expression. Life Sci. *69*, 201-212.

Fasshauer,M., Klein,J., Lossner,U., Paschke,R. (2002). Negative regulation of adipose-expressed galectin-12 by isoproterenol, tumour necrosis factor alpha, insulin and dexamethasone. Eur.J Endocrinol. *147*, 553-559.

Fischer,E., Legue,E., Doyen,A., Nato,F., Nicolas,J., Torres,V., Yaniv,M., Pontoglio,M. (2006). Defective planar cell polarity in polycystic kidney disease. Nat.Genet. *38*, 21-23.

Fliegauf,M., Frohlich,C., Horvath,J., Olbrich,H., Hildebrandt,F., Omran,H. (2003). Identification of the human CYS1 gene and candidate gene analysis in Boichis disease. Pediatr.Nephrol. *18*, 498-505.

Fliegauf,M., Horvath,J., von Schnakenburg,C., Olbrich,H., Muller,D., Thumfart,J., Schermer,B., Pazour,G.J., Neumann, H.P., Zentgraf,H., Benzing,T., Omran,H., (2006). Nephrocystin specifically localizes to the transition zone of renal and respiratory cilia and photorecepter connecting cilia. J.Am.Soc.Nephrol. *17*, 2424-2433.

Foggensteiner,L., Bevan,A.P., Thomas,R., Coleman,N., Boulter,C., Bradley,J., Ibraghimov-Beskrovnaya,O., Klinger,K., Sandford,R. (2000). Cellular and subcellular distribution of polycystin-2, the protein product of the *Pkd-2* gene. J.Am.Soc.Nephrol. *11*, 814-827.

Forman,J.R., Qamar,S., Paci,E., Sandford,R.N., Clarke,J. (2005). The remarkable mechanical strength of polycystin-1 supports a direct role in mechanotransduction. J.Mol.Biol. *349*, 861-871.

Fowlis,D., Colnot,C., Ripoche,M.A., Poirier,F. (1995). Galectin-3 is expressed in the notochord, developing bones, and skin of the postimplantation mouse embryo. Dev.Dyn. *203*, 241-251.

Francois,C., van Velthoven,R., De Lathouwer,O., Moreno,C., Peltier,A., Kaltner,H., Salmon,I., Gabius,H.J., Danguy,A., Decaestecker,C., Kiss,R. (1999). Galectin-1 and galectin-3 binding pattern expression in renal cell carcinomas. Am.J.Clin.Pathol. *112*, 194-203.

Fuertes,M.B., Molinero,L.L., Toscano,M.A., Ilarregui,J.M., Rubinstein,N., Fainboim,L., Zwirner,N.W., Rabinovich,G.A. (2004). Regulated expression of galectin-1 during T-cell activation involves Lck and Fyn kinases and signaling

through MEK1/ERK, p38 MAP kinase and p70S6 kinase. Mol.Cell Biochem. *267*, 177-185.

Fukumori,T., Takenaka,Y., Yoshii,T., Kim,H.R., Hogan,V., Inohara,H., Kagawa,S., Raz,A. (2003). CD29 and CD7 mediate galectin-3-induced type II T-cell apoptosis. Cancer Res. *63*, 8302-8311.

Furtak,V., Hatcher,F., Ochieng,J. (2001). Galectin-3 mediates the endocytosis of beta-1 integrins by breast carcinoma cells. Biochem.Biophys.Res.Commun. *289*, 845-850.

Furu,L., Onuchic,L.F., Gharavi,A., Hou,X., Esquivel,E.L., Nagasawa,Y., Bergmann,C., Senderek,J., Avner,E., Zerres,K., Germino,G.G., Guay-Woodford,L.M., Somlo,S. (2003). Milder presentation of recessive polycystic kidney disease requires presence of amino acid substitution mutations. J.Am.Soc.Nephrol. *14*, 2004-2014.

Gattone,V.H., Maser,R.L., Tian,C., Rosenberg,J.M., Branden,M.G. (1999). Developmental expression of urine concentration-associated genes and their altered expression in murine infantile-type polycystic kidney disease. Dev.Genet. *24*, 309-318.

Gattone,V.H., Wang,X., Harris,P.C., Torres,V.E. (2003). Inhibition of renal cystic disease development and progression by a vasopressin V2 receptor antagonist. Nat.Med. *9*, 1323-1326.

Geng,L., Segal,Y., Peissel,B., Deng,N., Pei,Y., Carone,F., Rennke,H.G., Glucksmann-Kuis,A.M., Scheneider,M.C., Ericsson,M., Reeders,S.T., Zhou,J. (1996). J.Clin.Invest. *98*, 2674-2682.

Geng,L., Burrow,C.R., Li,H.P., Wilson,P.D. (2000). Modification of the composition of polycystin-1 multiprotein complexes by calcium and tyrosine phosphorylation. Biochem.Biophy.Acta. *1535,* 21-35.

Giannakakou,P., Sackett,D.L., Kang,Y.K., Zhan,Z., Buters,J.T., Fojo,T., Poruchynsky,M.S. (1997). Paclitaxel-resistant human ovarian cancer cells have mutant beta-tubulins that exhibit impaired paclitaxel-driven polymerization. J Biol.Chem. *272*, 17118-17125.

Gitt,M.A., Colnot,C., Poirier,F., Nani,K.J., Barondes,S.H., Leffler,H. (1998). Galectin-4 and galectin-6 are two closely related lectins expressed in mouse gastrointestinal tract. J Biol.Chem. *273*, 2954-2960.

Gitt,M.A., Massa,S.M., Leffler,H., Barondes,S.H. (1992). Isolation and expression of a gene encoding L-14-II, a new human soluble lactose-binding lectin. J Biol.Chem. *267*, 10601-10606.

Gitt,M.A., Wiser,M.F., Leffler,H., Herrmann,J., Xia,Y.R., Massa,S.M., Cooper,D.N., Lusis,A.J., Barondes,S.H. (1995). Sequence and mapping of galectin-5, a beta-galactoside-binding lectin, found in rat erythrocytes. J Biol.Chem. *270*, 5032-5038.

Gomes,D.A., Leite,M.F., Bennett,A.M., Nathanson,M.H. (2006). Calcium signaling in the nucleus. Can.J Physiol Pharmacol. *84*, 325-332.

Gonzalez-Perrett,S., Kim,K., Ibarra,C., Damiano,A.E., Zotta,E., Batelli,M., Harris,P.C., Reisin,I.L., Arnaout,M.A., Cantiello,H.F. (2001). Polycystin-2, the protein mutated in autosomal dominant polycystic kidney disease (ADPKD), is a Ca2+-permeable nonselective cation channel. Proc.Natl.Acad.Sci.U.S.A *98*, 1182-1187.

Grantham,J.J. (1993). Polycystic kidney disease: hereditary and acquired. Adv.Intern.Med. *38*, 409-420.

Gray,C.A., Adelson,D.L., Bazer,F.W., Burghardt,R.C., Meeusen,E.N., Spencer,T.E. (2004). Discovery and characterization of an epithelial-specific galectin in the endometrium that forms crystals in the trophectoderm. Proc.Natl.Acad.Sci.U.S.A *101*, 7982-7987.

Gray,C.A., Dunlap,K.A., Burghardt,R.C., Spencer,T.E. (2005). Galectin-15 in ovine uteroplacental tissues. Reproduction. *130*, 231-240.

Gross,A., McDonnell,J.M., Korsmeyer,S.J. (1999). BCL-2 family members and the mitochondria in apoptosis. Genes Dev. *13,* 1899-1911

Guay-Woodford,L.M. (2002). Autosomal recessive polycystic kidney disease (ARPKD): new insights from the identification of the ARPKD gene, PKHD1. Pediatr.Res. *52*, 830-831.

Guay-Woodford,L.M. (2003). Murine models of polycystic kidney disease: molecular and therapeutic insights. Am.J.Physiol Renal Physiol *285*, F1034-F1049.

Guay-Woodford,L.M., Desmond,R.A. (2003). Autosomal recessive polycystic kidney disease: the clinical experience in North America. Pediatrics *111*, 1072-1080

Guay-Woodford,L.M., Green,W.J., Lindsey,J.R., Beier,D.R. (2000). Germline and somatic loss of function of the mouse *cpk* gene causes biliary ductal pathology that is genetically modulated. Hum.Mol.Genet. *9*, 769-778.

Hadari,Y.R., Paz,K., Dekel,R., Mestrovic,T., Accili,D., Zick,Y. (1995). Galectin-8. A new rat lectin, related to galectin-4. J Biol.Chem. *270*, 3447-3453.

Harris,P.C. (2002). Molecular basis of polycystic kidney disease: PKD1, PKD2 and PKHD1. Curr.Opin.Nephrol.Hypertens. *11*, 309-314.

Harris,P.C., Rossetti,S. (2004). Molecular genetics of autosomal recessive polycystic kidney disease. Mol.Genet.Metab *81*, 75-85.

Hayashi,M., Yamaji,Y., Monkawa,T., Yoshida,T., Tsuganezawa,H., Sasamura,H., Kitajima,W., Sasaki,S., Ishibashi,K., Maurmo,F., Saruta,T. (1997). Expression and localization of the water channels in human autosomal dominant polycystic kidney disease. Nephron *75*, 321-326.

Herrmann,J., Turck,C.W., Atchison,R.E., Huflejt,M.E., Poulter,L., Gitt,M.A., Burlingame,A.L., Barondes,S.H., Leffler,H. (1993). Primary structure of the soluble lactose binding lectin L-29 from rat and dog and interaction of its non-collagenous proline-, glycine-, tyrosine-rich sequence with bacterial and tissue collagenase. J.Biol.Chem. *268*, 26704-26711.

Hikita,C., Takito,J., Vijayakumar,S., Al-Awqati,Q. (1999). Only multimeric hensin located in the extracellular matrix can induce apical endocytosis and reverse the polarity of intercalated cells. J.Biol.Chem. *274*, 17671-17676.

Hikita,C., Vijayakumar,S., Takito,J., Erdjument-Bromage,H., Tempst,P., Al Awqati,Q. (2000). Induction of terminal differentiation in epithelial cells requires polymerization of hensin by galectin 3. J.Cell Biol. *151*, 1235-1246.

Hillman,K.A., Woolf,A.S., Johnson,T.M., Wade,A., Unwin,R.J., Winyard,P.J.D. (2004). The P2X7 ATP receptor modulates renal cyst development *in vitro*. Biochem.Biophys.Res.Commun. *322*, 434-439.

Hirabayashi,J., Hashidate,T., Arata,Y., Nishi,N., Nakamura,T., Hirashima,M., Urashima,T., Oka,T., Futai,M., Muller,W.E., Yagi,F., Kasai,K. (2002). Oligosaccharide specificity of galectins: a search by frontal affinity chromatography. Biochim.Biophys.Acta *1572*, 232-254.

Ho,M.K., Springer,T.A. (1982). Mac-2, a novel 32,000 Mr mouse macrophage subpopulation-specific antigen defined by monoclonal antibodies. J Immunol. *128*, 1221-1228.

Hogan,M.C., Griffin,M.D., Rossetti,S., Torres,V.E., Ward,C.J., Harris,P.C. (2003). PKHDL1, a homolog of the autosomal recessive polycystic kidney disease gene, encodes a receptor with inducible T lymphocyte expression. Hum.Mol.Genet. *12*, 685-698.

Horiguchi,N., Arimoto,K., Mizutani,A., Endo-Ichikawa,Y., Nakada,H., Taketani,S. (2003). Galectin-1 induces cell adhesion to the extracellular matrix and apoptosis of non-adherent human colon cancer Colo201 cells. J Biochem.(Tokyo) *134*, 869-874.

Hotta,K., Funahashi,T., Matsukawa,Y., Takahashi,M., Nishizawa,H., Kishida,K., Matsuda,M., Kuriyama,H., Kihara,S., Nakamura,T., Tochino,Y., Bodkin,N.L., Hansen,B.C., Matsuzawa,Y. (2001). Galectin-12, an Adipose-expressed Galectin-like Molecule Possessing Apoptosis-inducing Activity. J Biol.Chem. *276*, 34089-34097.

Hou,X., Mrug,M., Yoder,B.K., Lefkowitz,E.J., Kremmidiotis,G., D'Eustachio,P., Beier,D.R., Guay-Woodford,L.M. (2002). Cystin, a novel cilia-associated protein, is disrupted in the *cpk* mouse model of polycystic kidney disease. J.Clin.Invest *109*, 533-540.

Hsu,D.K., Zuberi,R.I., Liu,F.T. (1992). Biochemical and biophysical characterization of human recombinant IgE-binding protein, an S-type animal lectin. J.Biol.Chem. *267*, 14167-14174.

Huan,Y., van Adelsberg,J. (1999). Polycystin-1, the *PKD1* gene product, is in a complex containing E-cadherin and the catenins. J.Clin.Inv. *104,* 1459-1468.

Huangfu,D., Liu,A., Rakeman,A.S., Murcia,N.S., Niswander,L., Anderson,K.V. (2003). Hedgehog signalling in the mouse requires intraflagellar transport proteins. Nature. *426*, 83-87.

Hughes,J., Ward,C.J., Peral,B. (1995). The polycystic kidney disease 1 (*PKD1)* gene encodes a novel protein with multiple cell recognition domains. Nat Genet. *10,* 151-160.

Hughes,R.C. (1999). Secretion of the galectin family of mammalian carbohydrate-binding proteins. Biochim.Biophys.Acta *1473*, 172-185.

Hughes,R.C. (2004). Galectins in kidney development. Glycoconj.J *19*, 621-629.

Iacobini,C., Amadio,L., Oddi,G., Ricci,C., Barsotti,P., Missori,S., Sorcini,M., Di Mario,U., Pricci,F., Pugliese,G. (2003). Role of galectin-3 in diabetic nephropathy. J.Am.Soc.Nephrol. *14*, S264-S270.

Iacobini,C., Menini,S., Oddi,G., Ricci,C., Amadio,L., Pricci,F., Olivieri,A., Sorcini,M., Di Mario,U., Pesce,C., Pugliese,G. (2004). Galectin-3/AGE-receptor 3 knockout mice show accelerated AGE-induced glomerular injury: evidence for a protective role of galectin-3 as an AGE receptor. FASEB J. *18*, 1773-1775.

Iacobini,C., Oddi,G., Menini,S., Amadio,L., Ricci,C., Di Pippo,C., Sorcini,M., Pricci,F., Pugliese,F., Pugliese,G. (2005). Development of age-dependent glomerular lesions in galectin-3/AGE-receptor-3 knockout mice. Am.J.Physiol Renal Physiol *289*, F611-F621.

Inohara,H., Akahani,S., Raz,A. (1998). Galectin-3 stimulates cell proliferation. Exp.Cell Res. *245*, 294-302.

Ishikawa,H., Kubo,A., Tsukita,S., Tsukita,S. (2005). Odf2-deficient mother centrioles lack distal/subdistal appendages and the ability to generate primary cilia. Nat.Cell Biol. *7*, 517-524.

Iurisci,I., Tinari,N., Natoli,C., Angelucci,D., Cianchetti,E., Iacobelli,S. (2000). Concentrations of galectin-3 in the sera of normal controls and cancer patients. Clin.Cancer Res. *6*, 1389-1393.

Jaffrezou,J.P., Dumontet,C., Derry,W.B., Duran,G., Chen,G., Tsuchiya,E., Wilson,L., Jordan,M.A., Sikic,B.I. (1995). Novel mechanism of resistance to paclitaxel (Taxol) in human K562 leukemia cells by combined selection with PSC 833. Oncol.Res. *7*, 517-527.

Jensen,C.G., Davison,E.A., Bowser,S.S., Rieder,C.L. (1987). Primary cilia cycle in PtK1 cells: effects of colcemid and taxol on cilia formation and resorption. Cell Motil.Cytoskeleton. *7*, 187-197.

John,C.M., Leffler,H., Kahl-Knutsson,B., Svensson,I., Jarvis,G.A. (2003). Truncated galectin-3 inhibits tumour growth and metastasis in orthotopic nude mouse model of human breast cancer. Clin.Cancer Res. *9*, 2374-2383.

Johnson,T.M. (2001). The biology of galectin-3 in normal and cystic renal development. PhD thesis, University College London.

Joly,D., Morel,V., Hummel,A., Ruello,A., Nusbaum,P., Patey,N., Noel,L.H., Rousselle,P., Knebelmann,B. (2003). Beta4 integrin and laminin 5 are aberrantly expressed in polycystic kidney disease: role in increased cell adhesion and migration. Am.J.Pathol. *163*, 1791-1800.

Jurczyk,A., Gromley,A., Redick,S., San Agustin,J., Witman,G., Pazour,G.J., Peters,D.J., Doxsey,S. (2004). Pericentrin forms a complex with intraflagellar transport proteins and polycystin-2 and is required for primary cilia assembly. J.Cell Biol. *166*, 637-643.

Kadrofske,M.M., Openo,K.P., Wang,J.L. (1998). The human LGALS3 (galectin-3) gene: determination of the gene structure and functional characterization of the promoter. Arch.Biochem.Biophys. *349*, 7-20.

Kashio,Y., Nakamura,K., Abedin,M.J., Seki,M., Nishi,N., Yoshida,N., Nakamura,T., Hirashima,M. (2003). Galectin-9 induces apoptosis through the calcium-calpain-caspase-1 pathway. J Immunol. *170*, 3631-3636.

Kavallaris,M., Kuo,D.Y., Burkhart,C.A., Regl,D.L., Norris,M.D., Haber,M., Horwitz,S.B. (1997). Taxol-resistant epithelial ovarian tumours are associated with altered expression of specific beta-tubulin isotypes. J Clin.Invest. *100*, 1282-1293.

Kemper,M.J, Neuhaus,T.J., Timmermann,K., Hueneke,B., Laube,G., Harps,E., Mueller-Wiefel,D.E. (2001). Antenatal oligohydramnios of renal origin: postnatal therpeutic and prognostic challenges. Clin.Nephrol. *56(6)*, S9-12.

Kim,J., Kim,Y.H., Cha,J.H., Tisher,C.C., Madsen,K.M. (1999). Intercalated cell subtypes in connecting tubule and cortical collecting duct of rat and mouse. J Am Soc.Nephrol. *10*, 1-12.

Kim,J.C., Badano,J.L., Sibold,S., Esmail,M.A., Hill,J., Hoskins,B.E., Leitch,C.C., Venner,K., Ansley,S.J., Ross,A.J., Leroux,M.R., Katsanis,N., Beales,P.L. (2004). The Bardet-Biedl protein BBS4 targets cargo to the pericentriolar region and is required for microtubule anchoring and cell cycle progression. Nat.Genet. *36*, 462-470.

Kim,J.C., Ou,Y.Y., Badano,J.L., Esmail,M.A., Leitch,C.C., Fiedrich,E., Beales,P.L., Archibald,J.M., Katsanis,N., Rattner,J.B., Leroux,M.R. (2005). MKKS/BBS6, a divergent chaperonin-like protein linked to the obesity disorder Bardet-Biedl syndrome, is a novel centrosomal component required for cytokinesis. J Cell Sci. *118*, 1007-1020.

Kopper,L., Timar,J. (2006). Genomics of renal cell cancer-- does it provide breakthrough? Pathol.Oncol.Res. *12*, 5-11.

Kuklinski,S., Probstmeier,R. (1998). Homophilic binding properties of galectin-3: involvement of the carbohydrate recognition domain. J.Neurochem. *70*, 814-823.

Kuure,S., Vuolteenaho,R., Vainio,S. (2000). Kidney morphogenesis: cellular and molecular regulation. Mech.Dev. *92*, 31-45.

Kuwabara,I., Kuwabara,Y., Yang,R.Y., Schuler,M., Green,D.R., Zuraw,B.L., Hsu,D.K., Liu,F.T. (2002). Galectin-7 (PIG1) exhibits pro-apoptotic function through JNK activation and mitochondrial cytochrome c release. J Biol.Chem. *277*, 3487-3497.

Lagana,A., Goetz,J.G., Cheung,P., Raz,A., Dennis,J.W., Nabi,I.R. (2006). Galectin binding to Mgat5-modified N-glycans regulates fibronectin matrix remodeling in tumour cells. Mol.Cell Biol. *26*, 3181-3193.

Leal-Pinto,E., Tao,W., Rappaport,J., Richardson,M., Barbara,A.K., Abramson.R.G. (1997). Molecular cloning and functional reconstitution of a urate tranporter/channel. J.Bio.Chem. *272*, 617-625.

Leal-Pinto,E., Cohen,B.E., Lipkowitz,M.S., Abramson,R.G. (2002). Functional analysis and molecular model of the human urate transporter/channel, hUAT. Am J Physiol Renal Physiol *283*, F150-F163.

Lechner,M.S., Dressler,G.R. (1997). The molecular basis of embryonic kidney development. Mech.Dev. *62*, 105-120.

Lensch,M., Lohr,M., Russwurm,R., Vidal,M., Kaltner,H., Andre,S., Gabius,H.J. (2006). Unique sequence and expression profiles of rat galectins-5 and -9 as a result of species-specific gene divergence. Int.J Biochem.Cell Biol. *38*, 1741-1758.

Levy,Y., Arbel-Goren,R., Hadari,Y.R., Eshhar,S., Ronen,D., Elhanany,E., Geiger,B., Zick,Y. (2001). Galectin-8 functions as a matricellular modulator of cell adhesion. J Biol.Chem. *276*, 31285-31295.

Lin,F., Hiesberger,T., Cordes,K., Sinclair,A.M., Goldstein,L.S., Somlo,S., Igarashi,P. (2003). Kidney-specific inactivation of the KIF3A subunit of kinesin-II inhibits renal ciliogenesis and produces polycystic kidney disease. Proc.Natl.Acad.Sci.U.S.A *100*, 5286-5291.

Lin,H.M., Pestell,R.G., Raz,A., Kim,H.R. (2002). Galectin-3 enhances cyclin D(1) promoter activity through SP1 and a cAMP-responsive element in human breast epithelial cells. Oncogene *21*, 8001-8010.

Lipkowitz,M.S., Leal-Pinto,E., Cohen,B.E., Abramson,R.G. (2004). Galectin 9 is the sugar-regulated urate transporter/channel UAT. Glycoconj.J *19*, 491-498.

Liu,F.T., Hsu,D.K., Zuberi,R.I., Hill,P.N., Shenhav,A., Kuwabara,I., Chen,S.S. (1996). Modulation of functional properties of galectin-3 by monoclonal antibodies binding to the non-lectin domains. Biochemistry *35*, 6073-6079.

Liu,F.T., Patterson,R.J., Wang,J.L. (2002). Intracellular functions of galectins. Biochim.Biophys.Acta *1572*, 263-273.

Liu,W., Murcia,N.S., Duan,Y., Weinbaum,S., Yoder,B.K., Schwiebert,E., Satlin,L.M. (2005). Mechanoregulation of intracellular Ca2+ concentration is attenuated in collecting duct of monocilium-impaired orpk mice. Am.J.Physiol Renal Physiol *289*, F978-F988.

Lutz,M.S., Burk, R.D. (2006). Primary cilium formation requires von hippel-lindau gene function in renal-derived cells. Cancer.Res. *66*, 6903-6907.

Madsen,P., Rasmussen,H.H., Flint,T., Gromov,P., Kruse,T.A., Honore,B., Vorum,H., Celis,J.E. (1995). Cloning, expression, and chromosome mapping of human galectin-7. J Biol.Chem. *270*, 5823-5829.

Maeda,N., Kawada,N., Seki,S., Arakawa,T., Ikeda,K., Iwao,H., Okuyama,H., Hirabayashi,J., Kasai,K., Yoshizato,K. (2003). Stimulation of proliferation of rat hepatic stellate cells by galectin-1 and galectin-3 through different intracellular signaling pathways. J.Biol.Chem. *278*, 18938-18944.

Magnaldo,T., Fowlis,D., Darmon,M. (1998). Galectin-7, a marker of all types of stratified epithelia. Differentiation *63*, 159-168.

Mai,W., Chen,D., Ding,T., Kim,I., Park,S., Cho,S.Y., Chu,J.S., Liang,D., Wang,N., Wu,D., Li,S., Zhao,P., Zent,R., Wu,G. (2005). Inhibition of Pkhd1 impairs tubulomorphogenesis of cultured IMCD cells. Mol.Biol.Cell. *16*, 4398-4409.

Maiche,A.G., Jekunen,A.P., Kaleva-Kerola,J., Blanco,S.G. (2000). High response rate with a lower dose of paclitaxel in combination with cisplatin in heavily pretreated patients with advanced breast carcinoma. Cancer *88*, 1863-1868.

Malhas,A.N., Abuknesha,R.A., Price,R.G. (2002). Interaction of the leucine-rich repeats of polycystin-1 with extracellular matrix proteins: possible role in cell proliferation. J.Am.Soc.Nephrol. *13*, 19-26.

Martinez,J.R., Cowley,B.D., Gattone,V.H., Nagao,S., Yamaguchi,T., Kaneta,S., Takahashi,H., Grantham,J.J. (1997). The effect of paclitaxel on the progression of polycystic kidney disease in rodents. Am.J.Kidney Dis. *29*, 435-444.

Matarrese,P., Fusco,O., Tinari,N., Natoli,C., Liu,F.T., Semeraro,M.L., Malorni,W., Iacobelli,S. (2000). Galectin-3 overexpression protects from apoptosis by improving cell adhesion properties. Int.J.Cancer *85*, 545-554.

Mazurek,N., Conklin,J., Byrd,J.C., Raz,A., Bresalier,R.S. (2000). Phosphorylation of the beta-galactoside-binding protein galectin-3 modulates binding to its ligands. J.Biol.Chem. *275*, 36311-36315.

Mehul,B., Bawumia,S., Martin,S.R., Hughes,R.C. (1994). Structure of baby hamster kidney carbohydrate-binding protein CBP30, an S-type animal lectin. J.Biol.Chem. *269*, 18250-18258.

Menon,R.P., Hughes,R.C. (1999). Determinants in the N-terminal domains of galectin-3 for secretion by a novel pathway circumventing the endoplasmic reticulum-Golgi complex. Eur.J.Biochem. *264*, 569-576.

Mochizuki,T., Wu,G., Hayashi,T., Xenophontos,S.L., Veldhuisen,B., Saris,J.J., Reynolds,D.M., Cai,Y., Gabow,P.A., Pierides,A., Kimberling,W.J., Breuning,M.H., Deltas,C.C., Peters,D.J., Somlo,S. (1996). PKD2, a gene for polycystic kidney disease that encodes an integral membrane protein. Science. *272*, 1339-1342.

Morgan,D., Eley,L., Sayer,J., Strachan,T., Yates,L.M., Craighead,A.S., Goodship,J.A. (2002). Expression analyses and interaction with the anaphase promoting complex protein Apc2 suggest a role for inversin in primary cilia and involvement in the cell cycle. Hum.Mol.Genet. *11*, 3345-3350.

Moriki,T., Kuwabara,I., Liu,F.T., Maruyama,I.N. (1999). Protein domain mapping by lambda phage display: the minimal lactose-binding domain of galectin-3. Biochem.Biophys.Res.Commun. *265*, 291-296.

Moutsatsos,I.K., Wade,M., Schindler,M., Wang,J.L. (1987). Endogenous lectins from cultured cells: nuclear localization of carbohydrate-binding protein 35 in proliferating 3T3 fibroblasts. Proc.Natl.Acad.Sci.U.S.A *84*, 6452-6456.

Moy,G.W., Mendoza,L.M., Schulz,J.R., Swanson,W.J., Glabe,C.G., Vacquier,V.D. (1996). The sea urchin sperm receptor for egg jelly is a modular protein with extensive homology to the human polycystic kidney disease protein, PKD1. J Cell Biol. *133*, 809-817.

Moyer,J.H., Lee-Tischler,M.J., Kwon,H.Y., Schrick,J.J., Avner,E.D., Sweeney,W.E., Godfrey,V.L., Cacheiro,N.L., Wilkinson,J.E., Woychik,R.P. (1994). Candidate gene associated with a mutation causing recessive polycystic kidney disease in mice. Science. *264*, 1329-1333.

Muller,U., Brandli,A.W. (1999). Cell adhesion molecules and extracellular-matrix constituents in kidney development and disease. J Cell Sci. *112 (Pt 22)*, 3855-3867.

Murcia,N.S., Richards,W.G., Yoder,B.K., Mucenski,M.L., Dunlap,J.R., Woychik,R.P. (2000). The Oak Ridge Polycystic Kidney (orpk) disease gene is required for left-right axis determination. Development *127*, 2347-2355.

Murcia,N.S., Sweeney,W.E., Jr., Avner,E.D. (1999). New insights into the molecular pathophysiology of polycystic kidney disease. Kidney Int. *55*, 1187-1197.

Murcia,N.S., Woychik,R.P., Avner,E.D. (1998). The molecular biology of polycystic kidney disease. Pediatr.Nephrol. *12*, 721-726.

Musch,A. (2004). Microtubule organization and function in epithelial cells. Traffic. *5*, 1-9.

Nadasdy,T., Lajoie,G., Laszik,Z., Blick,K.E., Molnar-Nadasdy,G., Silva,F.G. (1998). Cell proliferation in the developing human kidney. Pediatr.Dev.Pathol. *1*, 49-55.

Nadasdy,T., Laszik,Z., Lajoie,G., Blick,K.E., Wheeler,D.E., Silva,F.G. (1995). Proliferative activity of cyst epithelium in human renal cystic diseases. J.Am.Soc.Nephrol. *5*, 1462-1468.

Nagano,J., Kitamura,K., Hujer,K.M., Ward,C.J., Bram,R.J., Hopfer,U., Tomita,K., Huang,C., Miller,R.T. (2005). Fibrocystin interacts with CAML, a protein involved in Ca^{2+} signaling. Biochem.Biophys.Res.Commun. *338*, 880-889.

Nagasawa,Y., Matthiesen,S., Onuchic,L.F., Hou,X., Bergmann,C., Esquivel,E., Senderek,J., Ren,Z., Zeltner,R., Furu,L., Avner,E., Moser,M., Somlo,S., Guay-Woodford,L., Buttner,R., Zerres,K., Germino,G.G. (2002). Identification and characterization of Pkhd1, the mouse orthologue of the human ARPKD gene. J.Am.Soc.Nephrol. *13*, 2246-2258.

Nakamura,T., Ushiyama,C., Suzuki,S., Ebihara,I., Shimada,N., Koide,H. (2000). Elevation of serum levels of metalloproteinase-1, tissue inhibitor of metalloproteinase-1 and type IV collagen, and plasma levels of metalloproteinase-9 in polycystic kidney disease. Am.J.Nephrol. *20*, 32-36.

Nakayama,K., Nakayama,K., Negishi,I., Kuida,K., Sawa,H., Loh,D.Y. (1994). Targeted disruption of Bcl-2 alpha beta in mice: occurrence of gray hair, polycystic kidney disease, and lymphocytopenia. Proc.Natl.Acad.Sci.U.S.A *91*, 3700-3704.

Nauli,S.M., Alenghat,F.J., Luo,Y., Williams,E., Vassilev,P., Li,X., Elia,A.E., Lu,W., Brown,E.M., Quinn,S.J., Ingber,D.E., Zhou,J. (2003). Polycystins 1 and 2 mediate mechanosensation in the primary cilium of kidney cells. Nat.Genet. *33*, 129-137.

Nauli,S.M., Zhou,J. (2004). Polycystins and mechanosensation in renal and nodal cilia. Bioessays *26*, 844-856.

Nauta,J., Ozawa,Y., Sweeney,W.E., Rutledge,J.C., Avner,E.D. (1993). Renal and biliary adnormalities in a new murine model of autosomal recessive polycystic kidney disease. Pediatric Nephrology *7*, 163-172.

Nicolaou,K.C., Yang,Z., Liu,J.J., Ueno,H., Nantermet,P.G., Guy,R.K., Claiborne,C.F., Renaud,J., Couladouros,E.A., Paulvannan,K., . (1994). Total synthesis of taxol. Nature *367*, 630-634.

Nio,J., Takahashi-Iwanaga,H., Morimatsu,M., Kon,Y., Iwanaga,T. (2006). Immunohistochemical and *in situ* hybridization analysis of galectin-3, a beta-galactoside binding lectin, in the urinary system of adult mice. Histochem.Cell Biol. *126*, 45-56.

Nishiyama,J., Kobayashi,S., Ishida,A., Nakabayashi,I., Tajima,O., Miura,S., Katayama,M., Nogami,H. (2000). Up-regulation of galectin-3 in acute renal failure of the rat. Am.J.Pathol. *157*, 815-823.

Nogales,E. (2000). Structural insights into microtubule function. Annu.Rev.Biochem. *69:277-302.*, 277-302.

Nonaka,S., Tanaka,Y., Okada,Y., Takeda,S., Harada,A., Kanai,Y., Kido,M., Hirokawa,N. (1998). Randomization of left-right asymmetry due to loss of nodal cilia generating leftward flow of extraembryonic fluid in mice lacking KIF3B motor protein. Cell *95*, 829-837.

Novack,D.V., Korsmeyer,S.J. (1994). Bcl-2 protein expression during murine development. Am J Pathol. *145*, 61-73.

O'Driscoll,L., Linehan,R., Liang,Y.H., Joyce,H., Oglesby,I., Clynes,M. (2002). Galectin-3 expression alters adhesion, motility and invasion in a lung cell line (DLKP), *in vitro*. Anticancer Res. *22*, 3117-3125.

Obermuller,N., Morente,N., Kranzlin,B., Gretz,N.,Witzgall,R. (2001). A possible role for metalloproteinases in renal cysts development. Am J Physiol Renal Physiol. *280*, F540-550.

Ochieng,J., Furtak,V., Lukyanov,P. (2004). Extracellular functions of galectin-3. Glycoconj.J. *19*, 527-535.

Ochieng,J., Leite-Browning,M.L., Warfield,P. (1998). Regulation of cellular adhesion to extracellular matrix proteins by galectin-3. Biochem.Biophys.Res.Commun. *246*, 788-791.

Ogborn,M.R., Bankovic-Calic,N., Shoesmith,C., Buist,R., Peeling,J. (1998). Soy protein modification of rat polycystic kidney disease. Am.J.Physiol *274*, F541-F549.

Oishi,I., Kawakami,Y., Raya,A., Callol-Massot,C., Belmonte,J.C. (2006). Regulation of primary cilia formation and left-right patterning in zebrafish by a noncanonical Wnt signaling mediator, duboraya. Nat.Genet.

Oka,T., Murakami,S., Arata,Y., Hirabayashi,J., Kasai,K., Wada,Y., Futai,M. (1999). Identification and cloning of rat galectin-2: expression is predominantly in epithelial cells of the stomach. Arch.Biochem.Biophys. *361*, 195-201.

Okada,Y., Nonaka,S., Tanaka,Y., Saijoh,Y., Hamada,H., Hirokawa,N. (1999). Abnormal nodal flow precedes situs inversus in iv and inv mice. Mol.Cell. *4*, 459-468.

Olbrich,H., Fliegauf,M., Hoefele,J., Kispert,A., Otto,E., Volz,A., Wolf,M.T., Sasmaz,G., Trauer,U., Reinhardt,R., Sudbrak,R., Antignac,C., Gretz,N., Walz,G., Schermer,B., Benzing,T., Hildebrandt,F., Omran,H. (2003). Mutations in a novel gene, NPHP3, cause adolescent nephronophthisis, tapeto-retinal degeneration and hepatic fibrosis. Nat.Genet. *34*, 355-356.

Ong,A.C., Wheatley,D.N. (2003). Polycystic kidney disease--the ciliary connection. Lancet *361*, 774-776.

Onuchic,L.F., Furu,L., Nagasawa,Y., Hou,X., Eggermann,T., Ren,Z., Bergmann,C., Senderek,J., Esquivel,E., Zeltner,R., Rudnik-Schoneborn,S., Mrug,M., Sweeney,W., Avner,E.D., Zerres,K., Guay-Woodford,L.M., Somlo,S., Germino,G.G. (2002). PKHD1, the polycystic kidney and hepatic disease 1 gene, encodes a novel large

protein containing multiple immunoglobulin-like plexin-transcription-factor domains and parallel beta-helix 1 repeats. Am.J.Hum.Genet. *70*, 1305-1317.

Orr,G.A., Verdier-Pinard,P., McDaid,H., Horwitz,S.B. (2003). Mechanisms of Taxol resistance related to microtubules. Oncogene. *%20;22*, 7280-7295.

Ostrom,L., Tang,M.J., Gruss,P., Dressler,G.R. (2000). Reduced Pax2 gene dosage increases apoptosis and slows the progression of renal cystic disease. Dev.Biol. *219*, 250-258.

Otto,E.A., Schermer,B., Obara,T., O'Toole,J.F., Hiller,K.S., Mueller,A.M., Ruf,R.G., Hoefele,J., Beekmann,F., Landau,D., Foreman,J.W., Goodship,J.A., Strachan,T., Kispert,A., Wolf,M.T., Gagnadoux,M.F., Nivet,H., Antignac,C., Walz,G., Drummond,I.A., Benzing,T., Hildebrandt,F. (2003). Mutations in INVS encoding inversin cause nephronophthisis type 2, linking renal cystic disease to the function of primary cilia and left-right axis determination. Nat.Genet. *34*, 413-420.

Panda,D., Miller,H.P., Banerjee,A., Luduena,R.F., Wilson,L. (1994). Microtubule dynamics *in vitro* are regulated by the tubulin isotype composition. Proc.Natl.Acad.Sci.U.S.A. *91*, 11358-11362.

Pang,S., Urquhart,P., Hooper,N.M. (2004). N-glycans, not the GPI anchor, mediate the apical targeting of a naturally glycosylated, GPI-anchored protein in polarised epithelial cells. J Cell Sci. *117*, 5079-5086.

Park,J.W., Voss,P.G., Grabski,S., Wang,J.L., Patterson,R.J. (2001). Association of galectin-1 and galectin-3 with Gemin4 in complexes containing the SMN protein. Nucleic Acids Res. *29*, 3595-3602.

Paron,I., Scaloni,A., Pines,A., Bachi,A., Liu,F.T., Puppin,C., Pandolfi,M., Ledda,L., Di Loreto,C., Damante,G., Tell,G. (2003). Nuclear localization of Galectin-3 in transformed thyroid cells: a role in transcriptional regulation. Biochem.Biophys.Res.Commun. *302*, 545-553.

Partridge,E.A., Le Roy,C., Di Guglielmo,G.M., Pawling,J., Cheung,P., Granovsky,M., Nabi,I.R., Wrana,J.L., Dennis,J.W. (2004). Regulation of cytokine receptors by Golgi N-glycan processing and endocytosis. Science *306*, 120-124.

Patterson,R.J., Wang,W., Wang,J.L. (2004). Understanding the biochemical activities of galectin-1 and galectin-3 in the nucleus. Glycoconj.J *19*, 499-506.

Pazour,G.J. (2004). Intraflagellar transport and cilia-dependent renal disease: the ciliary hypothesis of polycystic kidney disease. J.Am.Soc.Nephrol. *15*, 2528-2536.

Pazour,G.J., Dickert,B.L., Vucica,Y., Seeley,E.S., Rosenbaum,J.L., Witman,G.B., Cole,D.G. (2000). Chlamydomonas IFT88 and its mouse homologue, polycystic kidney disease gene tg737, are required for assembly of cilia and flagella. J.Cell Biol. *151*, 709-718.

Pennekamp,P., Karcher,C., Fischer,A., Schweickert,A., Skryabin,B., Horst,J., Blum,M., Dworniczak,B. (2002). The ion channel polycystin-2 is required for left-right axis determination in mice. Curr.Biol. *12*, 938-943.

Pey,R., Bach,J., Schieren,G., Gretz,N., Hafner,M. (1999). A new *in vitro* bioassay for cyst formation by renal cells from an autosomal dominant rat model of polycystic kidney disease. *In vitro* Cell Dev.Biol.Anim *35*, 571-579.

Pike,L.J., Han,X., Gross,R.W. (2005). Epidermal growth factor receptors are localized to lipid rafts that contain a balance of inner and outer leaflet lipids: a shotgun lipidomics study. J Biol.Chem. *280*, 26796-26804.

Poirier,F., Timmons,P.M., Chan,C.T.J., Guenet,J.L., Rigby,P.W.J. (1992). Expression of the L14 lectin during mouse embryogenesis suggests roles during pre- and post-implantation development. Devel. *115*, 143-155.

Poole,K., Meder,D., Simons,K., Muller,D. (2004). The effect of raft lipid depletion on microvilli formation in MDCK cells, visualized by atomic force microscopy. FEBS Lett. *565*, 53-58.

Potter,E.L. (1964). Facial characteristics of infants with bilateral renal agenesis. Am.J.Obstetrical Gyneocology. *51*, 885-888

Praetorius,H.A., Praetorius,J., Nielsen,S., Frokiaer,J., Spring,K.R. (2004). Beta1-integrins in the primary cilium of MDCK cells potentiate fibronectin-induced Ca2+ signaling. Am.J.Physiol Renal Physiol *287*, F969-F978.

Praetorius,H.A., Spring,K.R. (2001). Bending the MDCK cell primary cilium increases intracellular calcium. J Membr.Biol. *184*, 71-79.

Praetorius,H.A., Spring,K.R. (2003). The renal cell primary cilium functions as a flow sensor. Curr.Opin.Nephrol.Hypertens. *12*, 517-520.

Praetorius,H.A., Spring,K.R. (2005). A physiological view of the primary cilium. Annu.Rev.Physiol *67*, 515-529.

Pugliese,G., Pricci,F., Iacobini,C., Leto,G., Amadio,L., Barsotti,P., Frigeri,L., Hsu,D.K., Vlassara,H., Liu,F.T., Di Mario,U. (2001). Accelerated diabetic glomerulopathy in galectin-3/AGE receptor 3 knockout mice. FASEB J *15*, 2471-2479.

Pugliese,G., Pricci,F., Leto,G., Amadio,L., Iacobini,C., Romeo,G., Lenti,L., Sale,P., Gradini,R., Liu,F.T., Di Mario,U. (2000). The diabetic milieu modulates the advanced glycation end product-receptor complex in the mesangium by inducing or upregulating galectin-3 expression. Diabetes *49*, 1249-1257.

Qian,F., Germino,F.J., Cai,Y., Zhang,X., Somlo,S., Germino,G.G. (1997). PKD1 interacts with PKD2 through a probable coiled-coil domain. Nat.Genet. *16*, 179-183.

Quarmby,L.M., Mahjoub,M.R. (2005). Caught Nek-ing: cilia and centrioles. J.Cell Sci. *118*, 5161-5169.

Quarmby,L.M., Parker,J.D. (2005). Cilia and the cell cycle? J.Cell Biol. *169*, 707-710.

Raimond,J., Zimonjic,D.B., Mignon,C., Mattei,M., Popescu,N.C., Monsigny,M., Legrand,A. (1997). Mapping of the galectin-3 gene (LGALS3) to human chromosome 14 at region 14q21-22. Mamm.Genome *8*, 706-707.

Ranganathan,S., Benetatos,C.A., Colarusso,P.J., Dexter,D.W., Hudes,G.R. (1998). Altered beta-tubulin isotype expression in paclitaxel-resistant human prostate carcinoma cells. Br.J Cancer. *77*, 562-566.

Rankin,C.A., Suzuki,K., Itoh,Y., Ziemer,D.M., Grantham,J.J., Calvet,J.P., Nagase,H. (1996). Matrix metalloproteinases and TIMPS in cultured C57BL/6J-*cpk* kidney tubules. Kidney Int. *50*, 835-844.

Rauchman,M.I., Nigam,S.K., Delpire,E., Gullans,S.R. (1993). An Osmotically tolerant inner medullary collecting duct cell line from an SV40 transgenic mouse. Am.J Physiol. *265*, 416-424.

Raz,A., Meromsky,L., Zvibel,I., Lotan,R. (1987). Transformation-related changes in the expression of endogenous cell lectins. Int.J Cancer *39*, 353-360.

Raz,A., Zhu,D.G., Hogan,V., Shah,N., Raz,T., Karkash,R., Pazerini,G., Carmi,P. (1990). Evidence for the role of 34-kDa galactoside-binding lectin in transformation and metastasis. Int.J Cancer *46*, 871-877.

Resh,M.D. (2004). Membrane targeting of lipid modified signal transduction proteins. Subcell.Biochem. *37*, 217-232.

Richards,W.G., Sweeney,W.E., Yoder,B.K., Wilkinson,J.E., Woychik,R.P., Avner,E.D. (1998). Epidermal growth factor receptor activity mediates renal cyst formation in polycystic kidney disease. J.Clin.Invest *101*, 935-939.

Rieder,C.L., Faruki,S., Khodjakov,A. (2001). The centrosome in vertebrates: more than a microtubule-organizing center. Trends Cell Biol. *11*, 413-419.

Rodriguez-Boulan,E., Gonzalez,A. (1999). Glycans in post-Golgi apical targeting: sorting signals or structural props? Trends Cell Biol. *9*, 291-294.

Roff,C.F., Wang,J.L. (1983). Endogenous lectins from cultured cells. Isolation and characterization of carbohydrate-binding proteins from 3T3 fibroblasts. J Biol.Chem. *258*, 10657-10663.

Rohatgi,R., Greenberg,A., Burrow,C.R., Wilson,P.D., Satlin,L.M. (2003). Na transport in autosomal recessive polycystic kidney disease (ARPKD) cyst lining epithelial cells. J.Am.Soc.Nephrol. *14*, 827-836.

Roitbak,T., Surviladze,Z., Tikkanen,R., Wandinger-Ness,A. (2005). A polycystin multiprotein complex constitutes a cholesterol-containing signalling microdomain in human kidney epithelia. Biochem.J. *392*, 29-38.

Romio,L., Fry,A.M., Winyard,P.J.D., Malcolm,S., Woolf,A.S., Feather,S.A. (2004). OFD1 is a centrosomal/basal body protein expressed during mesenchymal-epithelial transition in human nephrogenesis. J.Am.Soc.Nephrol. *15*, 2556-2568.

Rosenberg,I.M., Iyer,R., Cherayil,B., Chiodino,C., Pillai,S. (1993). Structure of the murine Mac-2 gene. Splice variants encode proteins lacking functional signal peptides. J.Biol.Chem. *268*, 12393-12400.

Russell,E.S., McFarland,E.C. (1977). Cystic kidneys. Mouse Newsletter, *56*, 40-43

Saal,I., Nagy,N., Lensch,M., Lohr,M., Manning,J.C., Decaestecker,C., Andre,S., Kiss,R., Salmon,I., Gabius,H.J. (2005). Human galectin-2: expression profiling by RT-PCR/immunohistochemistry and its introduction as a histochemical tool for ligand localization. Histol.Histopathol. *20*, 1191-1208.

Sakakura,Y., Hirabayashi,J., Oda,Y., Ohyama,Y., Kasai,K. (1990). Structure of chicken 16-kDa beta-galactoside-binding lectin. Complete amino acid sequence, cloning of cDNA, and production of recombinant lectin. J Biol.Chem. *265*, 21573-21579.

Sano,H., Hsu,D.K., Apgar,J.R., Yu,L., Sharma,B.B., Kuwabara,I., Izui,S., Liu,F.T. (2003). Critical role of galectin-3 in phagocytosis by macrophages. J.Clin.Invest *112*, 389-397.

Sasaki,S., Bao,Q., Hughes,R.C. (1999). Galectin-3 modulates rat mesangial cell proliferation and matrix synthesis during experimental glomerulonephritis induced by anti-Thy1.1 antibodies. J.Pathol. *187*, 481-489.

Sato,M., Nishi,N., Shoji,H., Kumagai,M., Imaizumi,T., Hata,Y., Hirashima,M., Suzuki,S., Nakamura,T. (2002). Quantification of galectin-7 and its localization in adult mouse tissues. J Biochem.(Tokyo) *131*, 255-260.

Saussez,S., Lorfevre,F., Nonclercq,D., Laurent,G., Andre,A., Journe,F., Kiss,R., Toubeau,G., Gabius,H. (2006) Towards functional glycomics by localisation of binding sites for tissue lectins: lectin histochemiscal reactivity for galectins during diethylstilbestrol-induced kidney tumourigenesis in male Syrin hamster. Histochem.Cell.Biol. *126*, 57-69.

Schwaderer,A.L., Vijayakumar,S., Al Awqati,Q., Schwartz,G.J. (2006). Galectin-3 expression is induced in renal beta-intercalated cells during metabolic acidosis. Am J Physiol Renal Physiol *290*, F148-F158.

Schwartz,E.A., Reaven,E., Topper,J.N., Tsao,P.S. (2005). Transforming growth factor-beta receptors localize to caveolae and regulate endothelial nitric oxide synthase in normal human endothelial cells. Biochem.J. *390*, 199-206.

Sharma,U.C., Pokharel,S., van Brakel,T.J., van Berlo,J.H., Cleutjens,J.P., Schroen,B., Andre,S., Crijns,H.J., Gabius,H.J., Maessen,J., Pinto,Y.M. (2004). Galectin-3 marks activated macrophages in failure-prone hypertrophied hearts and contributes to cardiac dysfunction. Circulation *110*, 3121-3128.

Sharp,A.M., Messiaen,L.M., Page,G., Antignac,C., Gubler,M.C., Onuchic,L.F., Somlo,S., Germino,G.G., Guay-Woodford,L.M. (2005). Comprehensive genomic analysis of PKHD1 mutations in ARPKD cohorts. J Med Genet. *42*, 336-349.

Shiba,D., Takamatsu,T., Yokoyama,T. (2005). Primary cilia of inv/inv mouse renal epithelial cells sense physiological fluid flow: bending of primary cilia and Ca2+ influx. Cell Struct.Funct. *30*, 93-100.

Simons,M., Gloy,J., Ganner,A., Bullerkotte,A., Bashkurov,M., Kronig,C., Schermer,B., Benzing,T., Cabello,O.A., Jenny, A., Mlodzik,M., Polok,B., Driever,W., Obara,T., Walz,G. (2005). Nat.Genet. *37*, 537-543.

Sommardahl,C.S., Woychik,R.P., Sweeney,W.E., Avner,E.D., Wilkinson,J.E. (1997). Efficacy of taxol in the orpk mouse model of polycystic kidney disease. Pediatr.Nephrol. *11*, 728-733.

Stierstorfer,B., Kaltner,H., Neumuller,C., Sinowatz,F., Gabius,H.J. (2000). Temporal and spatial regulation of expression of two galectins during kidney development of the chicken. Histochem.J *32*, 325-336.

Sturm,A., Lensch,M., Andre,S., Kaltner,H., Wiedenmann,B., Rosewicz,S., Dignass,A.U., Gabius,H.J. (2004). Human galectin-2: novel inducer of T cell apoptosis with distinct profile of caspase activation. J Immunol. *173*, 3825-3837.

Sweeney,W.E., Jr., Avner,E.D. (1998). Functional activity of epidermal growth factor receptors in autosomal recessive polycystic kidney disease. Am.J.Physiol *275*, F387-F394.

Sweeney,W.E., Jr., Avner,E.D. (2006). Molecular and cellular pathophysiology of autosomal recessive polycystic kidney disease (ARPKD). Cell Tissue Res. ..

Sweeney,W.E., Futey,L., Frost,P., Avner,E.D. (1999). *In vitro* modulation of cyst formation by a novel tyrosine kinase inhibitor. Kidney Int. *56*, 406-413.

Takenaka,Y., Fukumori,T., Raz,A. (2004). Galectin-3 and metastasis. Glycoconj.J. *19*, 543-549.

Tanner,G.A., Tanner,J.A. (2000). Citrate therapy for polycystic kidney disease in rats. Kidney Int. *58*, 1859-1869.

Tao,Y., Kim,J., Faubel,S., Wu,J.C., Falk,S.A., Schrier,R.W., Edelstein,C.L. (2005). Caspase inhibition reduces tubular apoptosis and proliferation and slows disease progression in polycystic kidney disease. Proc.Natl.Acad.Sci.U.S.A *102*, 6954-6959.

Taulman,P.D., Haycraft,C.J., Balkovetz,D.F., Yoder,B.K. (2001). Polaris, a protein involved in left-right axis patterning, localizes to basal bodies and cilia. Mol.Biol.Cell. *12*, 589-599.

Than,N.G., Pick,E., Bellyei,S., Szigeti,A., Burger,O., Berente,Z., Janaky,T., Boronkai,A., Kliman,H., Meiri,H., Bohn,H., Than,G.N., Sumegi,B. (2004). Functional analyses of placental protein 13/galectin-13. Eur.J Biochem. *271*, 1065-1078.

Timmons,P.M., Colnot,C., Cail,I., Poirier,F., Magnaldo,T. (1999). Expression of galectin-7 during epithelial development coincides with the onset of stratification. Int.J Dev.Biol. *43*, 229-235.

Tomobe,K., Philbrick,D., Aukema,H.M., Clark,W.F., Ogborn,M.R., Parbtani,A., Takahashi,H., Holub,B.J. (1994). Early dietary protein restriction slows disease progression and lengthens survival in mice with polycystic kidney disease. J.Am.Soc.Nephrol. *5*, 1355-1360.

Torres,K., Horwitz,S.B. (1998). Mechanisms of Taxol-induced cell death are concentration dependent. Cancer Res. *58*, 3620-3626.

Torres,V.E., Sweeney,W.E., Jr., Wang,X., Qian,Q., Harris,P.C., Frost,P., Avner,E.D. (2004a). Epidermal growth factor receptor tyrosine kinase inhibition is not protective in PCK rats. Kidney Int. *66*, 1766-1773.

Torres,V.E., Wang,X., Qian,Q., Somlo,S., Harris,P.C., Gattone,V.H. (2004b). Effective treatment of an orthologous model of autosomal dominant polycystic kidney disease. Nat.Med. *10*, 363-364.

Toscano,M.A., Commodaro,A.G., Ilarregui,J.M., Bianco,G.A., Liberman,A., Serra,H.M., Hirabayashi,J., Rizzo,L.V., Rabinovich,G.A. (2006). Galectin-1 suppresses autoimmune retinal disease by promoting concomitant Th2- and T regulatory-mediated anti-inflammatory responses. J Immunol. *176*, 6323-6332.

Trache,A., Meininger,G.A. (2005). Atomic force-multi-optical imaging integrated microscope for monitoring molecular dynamics in live cells. J Biomed.Opt. *10*, 064023.

Valkova,N., Yunis,R., Mak,S.K., Kang,K., Kultz,D. (2005). Nek8 mutation causes overexpression of galectin-1, sorcin, and vimentin and accumulation of the major urinary protein in renal cysts of jck mice. Mol.Cell Proteomics. *4*, 1009-1018.

van Adelsberg,J. (1994). Murine polycystic kidney epithelial cell lines have increased integrin-mediated adhesion to collagen. Am.J.Physiol. *267*, 1082-1093.

Veis,D.J., Sorenson,C.M., Shutter,J.R., Korsmeyer,S.J. (1993). Bcl-2-deficient mice demonstrate fulminant lymphoid apoptosis, polycystic kidneys, and hypopigmented hair. Cell *75*, 229-240.

Voss,P.G., Tsay,Y.G., Wang,J.L. (1994). Galectin-3: differential accumulation of distinct mRNAs in serum-stimulated mouse 3T3 fibroblasts. Glycoconj.J. *11*, 353-362.

Wada,J., Ota,K., Kumar,A., Wallner,E.I., Kanwar,Y.S. (1997). Developmental regulation, expression, and apoptotic potential of galectin-9, a beta-galactoside binding lectin. J Clin.Invest *99*, 2452-2461.

Wang,J.L., Gray,R.M., Haudek,K.C., Patterson,R.J. (2004). Nucleocytoplasmic lectins. Biochim.Biophys.Acta *1673*, 75-93.

Wang,T.H., Wang,H.S., Ichijo,H., Giannakakou,P., Foster,J.S., Fojo,T., Wimalasena,J. (1998). Microtubule-interfering agents activate c-Jun N-terminal kinase/stress-activated protein kinase through both Ras and apoptosis signal-regulating kinase pathways. J Biol.Chem. *273*, 4928-4936.

Ward,C.J., Turley,H.T., Ong,A.C.M., Comley,M., Biddolph,S., Chetty,R., Ratcliffe,P.J., Gatter,K., Harris,P.C. (1996). Proc.Natl.Acad.Sci. *93*, 1524-1528.

Ward,C.J., Hogan,M.C., Rossetti,S., Walker,D., Sneddon,T., Wang,X., Kubly,V., Cunningham,J.M., Bacallao,R., Ishibashi,M., Milliner,D.S., Torres,V.E., Harris,P.C. (2002). The gene mutated in autosomal recessive polycystic kidney disease encodes a large, receptor-like protein. Nat.Genet. *30*, 259-269.

Ward,C.J., Yuan,D., Masyuk,T.V., Wang,X., Punyashthiti,R., Whelan,S., Bacallao,R., Torra,R., Larusso,N.F., Torres,V.E., Harris,P.C. (2003). Cellular and subcellular localization of the ARPKD protein; fibrocystin is expressed on primary cilia. Hum.Mol.Genet. *12*, 2703-2710.

Warfield,P.R., Makker,P.N., Raz,A., Ochieng,J. (1997). Adhesion of human breast carcinoma to extracellular matrix proteins is modulated by galectin-3. Invasion Metastasis *17*, 101-112.

Wasano,K., Hirakawa,Y., Yamamoto,T. (1990). Immunohistochemiscal localization of 14kDa galactoside-binding lectin in various organs of the rat. Kidney Int. *50*, 750-759.

Wheatley,D.N., Wang,A.M., Strugnell,G.E. (1996). Expression of primary cilia in mammalian cells. Cell Biol.Int. *20*, 73-81.

Wilson,P.D., Falkenstein,D. The pathology of human renal cystic disease. (1995). Tubulointestinal and cystic diseas of the kidney, current topics in pathology. Berlin, Germany: Springer-Verlag, *88*, 1-50.

Wilson,P.D., Geng,L., Li,X., Burrow,C.R. (1999). The PKD1 gene products, "polycystin-1," is a tyrosine-phosphorylated protein that colocalizes with alpha2beta1-integrin in focal clusters in adherent renal epithelia. Lab.Invest. *79*, 1311-1323.

Wilson,P.D. (2004a). Polycystic kidney disease. N.Engl.J.Med. *350*, 151-164.

Wilson,P.D. (2004b). Polycystic kidney disease: new understanding in the pathogenesis. Int.J.Biochem.Cell Biol. *36*, 1868-1873.

Wilson,S.J., Amsler,K., Hyink,D.P., Li,X., Lu,W., Zhou,J., Burrow,C.R., Wilson,P.D. (2006). Inhibition of HER-2(neu/ErbB2) restores normal function and structure to polycystic kidney disease (PKD) epithelia. Biochim.Biophys.Acta. *1762*, 647-655.

Winyard,P.J.D., Bao,Q., Hughes,R.C., Woolf,A.S. (1997). Epithelial galectin-3 during human nephrogenesis and childhood cystic diseases. J.Am.Soc.Nephrol. *8*, 1647-1657.

Winyard,P.J.D., Nauta,J., Lirenman,D.S., Hardman,P., Sams,V.R., Risdon,R.A., Woolf,A.S. (1996). Deregulation of cell survival in cystic and dysplastic renal development. Kidney Int. *49*, 135-146.

Wolf,M.T., Lee,J., Panther,F., Otto,E.A., Guan,K.L., Hildebrandt,F. (2005). Expression and phenotype analysis of the nephrocystin-1 and nephrocystin-4 homologs in Caenorhabditis elegans. J.Am.Soc.Nephrol. *16*, 676-687.

Woo,D. (1995). Apoptosis and loss of renal tissue in polycystic kidney diseases. N.Engl.J.Med. *333*, 18-25.

Woo,D.D., Miao,S.Y., Pelayo,J.C., Woolf,A.S. (1994). Taxol inhibits progression of congenital polycystic kidney disease. Nature *368*, 750-753.

Woo,D.D., Tabancay,A.P., Jr., Wang,C.J. (1997). Microtubule active taxanes inhibit polycystic kidney disease progression in *cpk* mice. Kidney Int. *51*, 1613-1618.

Wu,G., D'Agati,V., Cai,Y., Mackowitz,G., Park,J.H., Reynolds,D.M., Maeda,Y., Le,T.C., Hou,H.Jr., Kucherlapati,R., Edelmann,W., Somlo,S. (1998). Somatic Inactivation of *Pkd2* results in polycystic kidney disease. Cell. *93*, 177-188.

Xiong,H., Chen,Y., Yi,Y., Tsuchiya,K., Moeckel,G., Cheung,J., Liang,D., Tham,K., Xu,X., Chen,X.Z., Pei,Y., Zhao,Z.J., Wu,G. (2002). A novel gene encoding a TIG multiple domain protein is a positional candidate for autosomal recessive polycystic kidney disease. Genomics *80*, 96-104.

Yamaguchi,T., Hempson,S.J., Reif,G.A., Hedge,A.M., Wallace,D.P. (2006). Calcium restores a normal proliferation phenotype in human polycystic kidney disease epithelial cells. J.Am.Soc.Nephrol. *17*, 178-187.

Yamaguchi,T., Wallace,D.P., Magenheimer,B.S., Hempson,S.J., Grantham,J.J., Calvet,J.P. (2004). Calcium restriction allows cAMP activation of the B-Raf/ERK pathway, switching cells to a cAMP-dependent growth-stimulated phenotype. J.Biol.Chem. *279*, 40419-40430.

Yang,Q.S., Ying,K., Yuan,H.L., Chen,J.Z., Meng,X.F., Wang,Z., Xie,Y., Mao,Y.M. (2002). Cloning and expression of a novel human galectin cDNA, predominantly expressed in placenta(1). Biochim.Biophys.Acta *1574*, 407-411.

Yang,R.Y., Hill,P.N., Hsu,D.K., Liu,F.T. (1998). Role of the carboxyl-terminal lectin domain in self-association of galectin-3. Biochemistry *37*, 4086-4092.

Yang,R.Y., Hsu,D.K., Yu,L., Ni,J., Liu,F.T. (2001). Cell cycle regulation by galectin-12, a new member of the galectin superfamily. J Biol.Chem. *276*, 20252-20260.

Yang,Z., Tao,B., Gao,Z., Guay-Woodford,L.M. (2004) The novel cystoprotein, cystin, targets to primary apical cilia via lipid raft-mediated mechanisms. (Abstract). J Am Soc. Nephrol. *15*, 652A

Yen,H.J., Tayeh,MK., Mullins,R.F., Stone,E.M., Sheffield,V.C., Slusarski,D.C. (2006). Bardet-Biedl syndrome genes are important in retrograde intracellular trafficking and Kupffer's vesicle cilia function. Hum.Mol.Genet. *15*, 667-677.

Yoder,B.K., Hou,X., Guay-Woodford,L.M. (2002a). The polycystic kidney disease proteins, polycystin-1, polycystin-2, polaris, and cystin, are co-localized in renal cilia. J.Am.Soc.Nephrol. *13*, 2508-2516.

Yoder,B.K., Tousson,A., Millican,L., Wu,J.H., Bugg,C.E.Jr., Schafer,J.A., Balkovetz,D.F. (2002b). Polaris, a protein disrupted in orpk mutant mice, is required for assembly of renal cilium. Am J Physiol Renal Physiol. *282*, 541-552.

Young,A.N., Amin,M.B., Moreno,C.S., Lim,S.D., Cohen,C., Petros,J.A., Marshall,F.F., Neish,A.S. (2001). Expression profiling of renal epithelial neoplasms: a method for tumour classification and discovery of diagnostic molecular markers. Am.J.Pathol. *158*, 1639-1651.

Yu,F., Finley,R.L., Jr., Raz,A., Kim,H.R. (2002). Galectin-3 translocates to the perinuclear membranes and inhibits cytochrome c release from the mitochondria. A role for synexin in galectin-3 translocation. J.Biol.Chem. *277*, 15819-15827.

Yvon,A.M., Wadsworth,P., Jordan,M.A. (1999). Taxol suppresses dynamics of individual microtubules in living human tumour cells. Mol.Biol.Cell. *10*, 947-959.

Zhang,M.Z., Mai,W., Li,C., Cho,S.Y., Hao,C., Moeckel,G., Zhao,R., Kim,I., Wang,J., Xiong,H., Wang,H., Sato,Y., Wu,Y., Nakanuma,Y., Lilova,M., Pei,Y., Harris,R.C., Li,S., Coffey,R.J., Sun,L., Wu,D., Chen,X.Z., Breyer,M.D., Zhao,Z.J., McKanna,J.A., Wu,G. (2004). PKHD1 protein encoded by the gene for autosomal recessive polycystic kidney disease associates with basal bodies and primary cilia in renal epithelial cells. Proc.Natl.Acad.Sci.U.S.A *101*, 2311-2316.

Zang,Q., Murcia,N.S., Chitterden,L.R., Richards,W.G., Michaud,E.J., Woychik,R.P., Yoder,B.K. (2003). Loss of the Tg737 protein results in skeletal patterning defects. Dev.Dyn. *227*, 78-90.

Zhu,W., Sano,H., Nagai,R., Fukuhara,K., Miyazaki,A., Horiuchi,S. (2001). The role of galectin-3 in endocytosis of advanced glycation end products and modified low density lipoproteins. Biochem.Biophys.Res.Commun. *280*, 1183-1188.

Zerres,K., Muecher,G., Becker,J., Steinkamm,C., Rudnik-Schoneborn,S., Heikkila,P., Rapola,J., Salonen,R., Germino,G.G., Onuchic,L., Somlo,S., Avner,E.D., Harman,L.A., Stockwin,J.M., Guay-Woodford,L.M (1998). Prenatal diagnosis of autosomal recessive polycystic kidney disease (ARPKD): molecular genetics, clinical experience, and fetal morphology. Am.J.Med.Genet. *76(2)*, 137-144.